RETROGRADE NEUROTROPHIN TRANSPORT IN BASAL FOREBRIAN NEURONS

THE EFFECTS OF AGING AND ALZHEIMER'S DISEASE ON RETROGRADE NEUROTROPHIN TRANSPORT IN BASAL FOREBRAIN CHOLINERGIC NEURONS

By ARMAN SHEKARI, Hons B.Sc.

A Thesis Submitted to the School of Graduate Studies in Partial Fulfilment of the Requirements for the Degree of Doctor of Philosophy (Ph.D.)

Descriptive Note

McMaster University DOCTOR OF PHILOSOPHY (2021) Hamilton, Ontario

(Neuroscience Graduate Program)

TITLE: The Effects of Aging and Alzheimer's Disease on Retrograde Neurotrophin Transport in Basal Forebrain Cholinergic Neurons

AUTHOR: Arman Shekari, Hons. B.Sc.

SUPERVISOR: Professor Margaret Fahnestock

NUMBER OF PAGES: viii, 166

Lay Abstract

During aging and Alzheimer's disease (AD), the connections between neurons, a type of brain cell, break down, causing memory loss. This breakdown begins in a brain area called the basal forebrain. Basal forebrain neurons rely upon the transport of nutrients along their connections with other neurons, called axons, for proper function. This transport process becomes impaired in AD. Our goal was to understand why this happens. First, we determined that axonal transport was impaired with age and in basal forebrain neurons of mice genetically predisposed to develop AD. We recreated these impairments by increasing the levels of harmful molecules called reactive oxidative species (ROS). ROS levels increase with age and become abnormally high during AD. We found that increased ROS impair axonal transport and contribute to the breakdown of basal forebrain neurons. Our work suggests that reducing ROS will help prevent the breakdown of basal forebrain neurons in AD.

Abstract

Basal forebrain cholinergic neurons (BFCNs) are critical for learning and memory. Profound and early BFCN degeneration is a hallmark of aging and Alzheimer's disease (AD). BFCNs depend for their survival on the retrograde axonal transport of neurotrophins, proteins critical for neuronal function. Neurotrophins like brain derived neurotrophic factor (BDNF) and pro-nerve growth factor (proNGF) are retrogradely transported to BFCNs from their synaptic targets. In AD, neurotrophin levels are increased within BFCN target areas and reduced in the basal forebrain, implicating dysfunctional neurotrophin transport in AD pathogenesis. However, neurotrophin transport within this highly susceptible neuronal population is currently poorly understood.

We began by establishing protocols for the accurate quantification of axonal transport in BFCNs using microfluidic culture. We then determined the effect of age on neurotrophin transport. BFCNs were left in culture for up to 3 weeks to model aging *in vitro*. BFCNs initially displayed robust neurotrophin transport, which diminished with *in vitro* age. We observed that the levels of proNGF receptor tropomyosin-related kinase-A (TrkA) were reduced in aged neurons. Additionally, neurotrophin transport in BFCNs derived from 3xTg-AD mice, an AD model, was also impaired.

Next, we sought to determine a mechanism for these transport deficits. First, we determined that proNGF transport was solely contingent upon the levels of TrkA. We then found that elevation of oxidative stress, an established AD contributor, significantly reduced both TrkA levels and proNGF retrograde transport. TrkA levels are partially regulated by protein tyrosine phosphatase-1B (PTP1B), an enzyme whose activity is reduced by oxidation. PTP1B antagonism significantly reduced TrkA levels and proNGF retrograde transport in BFCNs. Treatment of BFCNs with PTP1B-activating antioxidants rescued TrkA levels, proNGF transport, and proNGF-mediated axonal degeneration.

Our results suggest that oxidative stress contributes to BFCN degeneration in aging and AD by impairing retrograde neurotrophin transport via oxidative PTP1B-mediated TrkA loss.

Acknowledgements

First and foremost, I would like to thank my supervisor, Margaret Fahnestock for the incredible support and guidance she has provided me over the last 5 years. Through Margaret I have learned so much about what it truly means to be a good scientist. She has instilled within me a deep appreciation for detail and precision, something I was lacking at the beginning of my studies. Her boundless curiosity, seemingly endless wisdom, incredible work ethic, and unwavering perseverance, have served as inspiration to me from the very start of my time working with her. Margaret has also been one of my biggest advocates during my graduate studies – even with her incredibly busy schedule, she always found time to support me during the tougher times. I am so grateful for all she has done for me.

I would also like to express my appreciation for my supervisory committee members, Judy West-Mays and Bhagwati Gupta. Their expertise in molecular biology has been instrumental to the success of my work. I would especially like to thank them for their unwavering support during the beginning of my project when I was initially troubleshooting my experimental system. I would have not been able to navigate the many early technical challenges I encountered without their support.

I also thank our collaborator, Chengbiao Wu, for allowing me to complete a 6-week placement in their lab at the University of California, San Diego at the start of my graduate studies. The methodological knowledge I gained during my time there was instrumental for the establishment of many of my protocols. I will also never forget the perfect San Diego weather in the middle of January.

I thank my fellow lab members, Erika Kropf, Crystal Mahadeo, Mona Abdolahi, Wei Song, and Bernadeta Michalski for all of their incredible feedback and support over the years. I would especially like to thank Bernadeta, our lab manager, for her incredible technical knowledge and always being willing to lend me a much-needed hand. I am so grateful to have worked especially closely with Erika over the last year, who is taking over my project – I am so proud of what she has accomplished and cannot wait to see where she takes this work. I also thank all of the extremely bright and talented undergraduate students I have had the pleasure of working with: Gary Liao, Ahmed Draia, Nisha Sanwalka, Rie Montgomery, Haolin Ye, Esra Rakab, and Nikko Pfaff. Working with my undergraduates has solidified in me a love of teaching that I hope to carry forward throughout my career.

Finally, I thank from the very bottom of heart my support system back home. First and foremost, my parents, Reza and Sima, for everything they have done for me. I cannot put into words how grateful I am for them. I also could not have gotten through this journey without the love and support from my sister, Mitra. My best friend since elementary school, Dov Derin, for his advice, companionship, and support, especially during the tougher times. Last but not least, I thank my girlfriend, Sahar, for constantly inspiring me and pushing me to be a better person every day.

Table of Contents

Declaration of Academic Achievement

This thesis includes three published or submitted manuscripts which explore retrograde neurotrophin transport in basal forebrain cholinergic neurons in the context of aging and Alzheimer's Disease. A list of these manuscripts and my contributions to each are outlined below. This thesis also includes a chapter of unpublished work.

Chapter 1: Introduction

Author: Arman Shekari

Chapter 2: Manuscript

Shekari, A., & Fahnestock, M. (2021). Retrograde axonal transport of neurotrophins in basal forebrain cholinergic neurons. Methods in Molecular Biology, 1-34 (accepted). I established all the protocols outlined in this chapter and prepared the report.

Chapter 3: Manuscript

Shekari, A., & Fahnestock, M. (2019). Retrograde axonal transport of BDNF and proNGF diminishes with age in basal forebrain cholinergic neurons. Neurobiology of Aging, 84, 131–140. https://doi.org/10.1016/j.neurobiolaging.2019.07.018. I designed the experiments, collected and analyzed all of the data in this chapter, and prepared the manuscript.

Chapter 4: Unpublished Work

Comments: The chapter assesses retrograde neurotrophin transport in basal forebrain neurons derived from triple transgenic (3xTg-AD) mice, the most commonly used animal model of Alzheimer's Disease. I would like to thank Dr. Boris Sakic for providing the 3xTg-AD mice that were used in this work. This section also assesses the role of Rab proteins, critical regulators of intracellular trafficking, in neurotrophin transport to determine the mechanistic underpinnings of the transport impairments outlined in the previous chapter. I designed the experiments, collected and analyzed all of the data in this chapter, and prepared the report.

Chapter 5: Manuscript

Shekari, A., Wu, C., & Fahnestock, M. (2021). Oxidative Stress Reduces proNGF transport in basal forebrain cholinergic neurons. (Submitted)

Comments: This project was done in collaboration with Dr. Chengbiao Wu who generously donated mutant proNGF plasmids and provided training that was critical to the completion of this work. I designed the experiments, collected and analyzed all of the data in this chapter, and prepared the manuscript.

Preface

Dear reader,

This document has been written in a "sandwich" format, meaning the chapters are written in the style of academic journal articles. The first chapter serves as an introduction and includes background information pertinent to all the subsequent chapters. Each chapter also includes its own, shorter, and more focused, introductory section.

Chapters 2, 3, and 5 are reproduced *verbatim* from published, accepted, or submitted articles. Copyright information for these chapters is included on the first page of each chapter. All figures, references, and appendices pertaining to each chapter are either embedded or included at the end of that chapter to facilitate reading flow.

Part of the introduction of Chapter 4 is reproduced (with minor changes) from one of my published reviews: Shekari A, Fahnestock M. Cholinergic neurodegeneration in Alzheimer disease mouse models. Handb Clin Neurol. 2021;182:191-209. doi: 10.1016/B978-0-12-819973-2.00013-7.

1. Introduction: Aging and Alzheimer's Disease, the Basal Forebrain, Neurotrophins, and Retrograde Axonal Transport

1.1 The Aging Brain and Alzheimer's Disease

Aging is often associated with cognitive decline in the general population (Yankner et al., 2008). While some cognitive functions including long term memory and emotion cognition are largely retained with aging, other functions including working memory, spatial memory, and information processing speed are significantly impaired in aged humans and animals (Lai et al., 1995; Petersen et al., 1992; Yankner et al., 2008). Age-related cognitive decline coincides with gradual neurodegeneration in areas associated with cognition including the neocortex, hippocampus, and basal forebrain. Neurodegeneration in these areas is accompanied by synaptic dysfunction including deficits in long term potentiation induction and calcium buffering capacity (Barnes, 1979, 2000; Porter et al., 1997). Dendritic spine density, white matter density, and synapse number are reduced in an age-related manner throughout these areas in aged humans and rodents (Ballinger et al., 2016; Bartzokis et al., 2003; Buell & Coleman, 1979; Conover et al., 1995; Geinisman et al., 1986; Yankner et al., 2008). Age-related neurodegeneration concomitant with cognitive dysfunction is significantly more rapid in onset and extreme in manifestation in neurodegenerative disorders like Alzheimer's Disease (AD).

AD is a neurodegenerative disorder that is characterized symptomatically by progressive learning and memory deficits (Belarbi et al., 2009; Bondi et al., 2017). The single greatest risk factor for developing AD is age (Bondi et al., 2017). Classical pathologic hallmarks of AD include deposits throughout the neocortex of aggregated amyloid-β (Aβ) and tau proteins known as plaques and neurofibrillary tangles, respectively (Bierer et al., 1995). As the disease progresses, widespread synaptic dysfunction and neuronal atrophy occur throughout the brain, resulting in severe cognitive deficits, mood instability, and eventually death. Aβ plaques consist of Aβ peptide aggregates that originate from the amyloidogenic processing of amyloid precursor protein (APP). Aβ peptides associate to form neurotoxic oligomers that further aggregate into insoluble extracellular plaques as the disorder progresses (Sengupta et al., 2016). Aβ peptides propagate throughout the entirety of the neocortex and hippocampus in a prion-like fashion in AD (Rasmussen et al., 2017). However, the distribution of Aβ pathology throughout the AD brain varies widely between individuals (Braak & Braak, 1991).

Neurofibrillary tangles occur alongside Aβ plaques in the AD brain and consist of aggregates of the microtubule-stabilizing protein tau. Tau is a phosphoprotein whose phosphorylation state determines its microtubule binding affinity. Tau phosphorylation normally is a dynamic and highly regulated process critical for the cytoskeletal plasticity inherent to neuronal projections (Johnson, 2004). In AD, tau becomes hyperphosphorylated, chronically detaches from microtubules, and forms intracellular aggregates (Goedert & Spillantini, 2011). Dissociation of tau from microtubules triggers microtubule disassembly which disrupts axonal transport and overall neuronal cytoskeletal integrity (Noble et al., 2013). Dissociated, hyperphosphorylated tau proteins aggregate together forming toxic, soluble oligomers which further aggregate and eventually develop into neurofibrillary tangles (Ballatore et al., 2007; Goedert & Spillantini, 2011). Unlike plaque pathology, tangle pathology progression throughout the brain occurs in a characteristic spatiotemporal fashion in AD, beginning within the trans-entorhinal layer and eventually spreading throughout the entirety of the neocortex and

hippocampus (Braak & Braak, 1991; Braak & Del Tredici, 2018). Interestingly, tangle burden throughout the brain is a much better correlate of cognitive decline in AD patients compared to plaque burden (Bondareff et al., 1989; Braak & Braak, 1991; Gómez-Isla et al., 1997). The predictable spread of tau pathology in AD suggests that tau can propagate trans-neuronally, utilizing the synaptic connections between neurons to spread throughout the brain (DeVos et al., 2018; Thal et al., 2014).

The study of AD has largely been focused on the cellular and molecular biology of Aβ over the past 40 years. This focus has not translated into a single efficacious treatment for the disorder. Continual failures of human clinical trials targeting Aβ have called the amyloid hypothesis into question. (Gold, 2017; Hardy & De Strooper, 2017; Mullane & Williams, 2018). Alternative contributors to AD pathogenesis, many of which focus on understanding the link between aging and AD, have been brought into focus as a result of these failures (Xia et al., 2018). One potential contributor underlying both aging and AD is oxidative stress. The intrinsically high metabolic rate of neurons coupled with their postmitotic nature suggests that the generation of reactive oxygen species (ROS) throughout the lifespan may be especially damaging to these cells (Tönnies & Trushina, 2017). ROS accumulation concomitant with oxidative damage is observed in the aging brain and is exacerbated in AD, suggesting that mechanisms contributing to excess oxidative damage contribute to age-related neurodegeneration (Ahmad et al., 2017; Chakrabarti et al., 2011; Driver et al., 2000; Tönnies & Trushina, 2017; Tramutola et al., 2017). Another contributing factor potentially linking aging and AD is neurotrophin system dysfunction. Neurotrophins encompass a class of signaling molecules critical for the survival and proper function of neurons and their synaptic circuits (Bothwell, 2014). Factors relating to neurotrophin signaling including their synthesis, receptor levels, and trafficking are impaired both in aging in the absence of dementia and in AD (Budni et al., 2015; Miranda et al., 2019; Tapia-Arancibia et al., 2008). An area of the brain where these topics potentially intersect is the basal forebrain, one of the earliest and most severely affected brain areas in age-related neurodegeneration (Grothe et al., 2012; Schmitz et al., 2016).

1.2 The Basal Forebrain

The basal forebrain is located at the ventral rostrocaudal extent of the brain, in front of and below the striatum. It consists of multiple structures including the diagonal band of Broca (DB), nucleus basalis of Meynert (NbM), and the medial septal nucleus (MSN) (Figure 1) (Woolf, 1991). Most cell bodies within the basal forebrain produce the neurotransmitter acetylcholine (ACh), making the basal forebrain the major cholinergic output in the central nervous system (CNS) (M. G. Baxter & Chiba, 1999). Axons from MSN and DB project upwards to the hippocampus via the septohippocampal tract (Hara et al., 2017). Ascending projections from the NbM terminate widely throughout the cortex (Ballinger et al., 2016; Woolf, 1991). Basal forebrain projections are extremely long and diffuse; a single basal forebrain neuron can contain over 1000 axonal arbors, and the total axonal length contributed by a single human basal forebrain neuron is predicted to be around 100 meters, making these neurons some of the largest in the brain (Wu et al.,

2014). The long and numerous projections of BFCNs throughout the neocortex and hippocampus are critical for learning, memory, and attention.

Basal forebrain cholinergic neuron (BFCN) projections modulate hippocampal circuit dynamics that underlie learning and memory (Ballinger et al., 2016; M. G. Baxter & Chiba, 1999). ACh levels are consistently elevated in the hippocampus following spatial memory tasks (Mitsushima et al., 2013; Roland et al., 2014). Local pharmacological antagonism of cholinergic signaling in the hippocampus of rodents significantly impairs performance on memory tasks (Bierer et al., 1995; Wallenstein & Vago, 2001). Elevated ACh levels concurrently strengthen excitatory and inhibitory synapses in CA1 hippocampal neurons via metabotropic ACh receptor (mAChR)-mediated delivery of α-amino-3-hydroxy-5-methyl-4-isoxazolepropionic acid (AMPA) receptors to synapses and activation of nicotinic ACh receptors (nAChR), respectively (Mitsushima et al., 2013). However, nAChR-mediated cholinergic signaling can also promote LTP at hippocampal synapses via stabilization of GluA1 receptors on dendritic spines (Halff et al., 2014). The consequence of cholinergic signaling within the hippocampus is highly contingent on timing; signals received before CA3 input to CA1 trigger long term potentiation at CA1 synapses while signals received after input trigger short term depression (Gu et al., 2012). These findings suggest that the cholinergic innervation of the hippocampus is critical for the regulation of learning-induced synaptic plasticity at both excitatory and inhibitory synapses in the hippocampus.

Cholinergic signaling throughout the neocortex is critical for the mediation of attention, a prerequisite to learning and memory. Ascending NbM cholinergic projections terminating in the prefrontal cortex (PFC) play a role in cue detection during goal-oriented tasks (Gritton et al., 2016; Howe et al., 2013). ACh is transiently released during cue detection, and optogenetic inhibition of BFCNs within the NbM during cued appetitive tasks significantly increases the incidence of missed cues and impairs task performance in mice (Gritton et al., 2016). Cortical cholinergic signaling is also critical for discrimination between task relevant and irrelevant stimuli through the promotion of inhibitory post synaptic potentials (IPSCs) in parvalbumin-positive cortical interneurons within the sensory cortex (Chen et al., 2015; Kalmbach & Waters, 2014). The IPSCs generated following cholinergic signaling desynchronize cortical firing and allow for the fine discernment of sensory information during task completion in rodents (Ballinger et al., 2016; Runfeldt et al., 2014).

In sum, the basal forebrain acts as both an attention-modulating hub and synaptic plasticity regulator through its diffuse cholinergic projections throughout the neocortex and hippocampus. The degeneration of these projections is a hallmark of age-related neurodegenerative disorders and is thought to contribute to the cognitive impairments that accompany these conditions.

1.3 BFCNs in Aging and AD

Basal forebrain neurodegeneration is commonly observed in the aging brain. BFCN nuclear size and overall BFCN numbers are decreased in aged rats (Altavista et al., 1990). The length of cholinergic fibers projecting to the hippocampus from the basal

forebrain is reduced with age (Ypsilanti et al., 2008). These deficits have behavioral consequences, as loss of cholinergic innervation to the hippocampus has been shown to underlie age-related cognitive decline (Ypsilanti et al., 2008). Both aged rats and LHX7 knockout mice that fail to develop forebrain cholinergic neurons show learning and memory impairments (Fragkouli et al., 2005; Gustilo et al., 1999).

Cholinergic deficits also correlate strongly with the cognitive decline seen in AD (Köppen et al., 2016; Ypsilanti et al., 2008). In fact, cholinergic impairment was the first neurochemical deficit identified in the AD brain (Bartus et al., 1982; A. K. L. Liu et al., 2015). The NbM has been shown to be uniquely susceptible to Alzheimer's-related neurodegeneration. Significant degeneration of NbM cholinergic neurons is considered a hallmark of AD (Baker-Nigh et al., 2015; Ballinger et al., 2016; Hampel et al., 2018; A. K. L. Liu et al., 2015). Synaptic loss in BFCNs correlates strongly with dementia severity in AD (Ballinger et al., 2016; H. Ferreira-Vieira et al., 2016; Whitehouse et al., 1982). Reductions in the levels of ACh and activity of choline acetyltransferase (ChAT) have been observed in the NbM of AD patients compared to age-matched controls (Bartus et al., 1982; Coyle et al., 1983; Davies, 1979; Whitehouse et al., 1982). Degeneration of NbM cholinergic neurons in AD leads to reductions in ACh levels in synaptically upstream brain regions like the hippocampus and cortex (Ballinger et al., 2016; Bartus et al., 1982; Davies, 1979). The susceptibility of the basal forebrain to AD-related neurodegeneration results in up to 95% of these neurons degenerating by the end-stages of the disease (Baker-Nigh et al., 2015; Schmitz et al., 2016). This body of evidence led to the formation of the cholinergic hypothesis of AD. The cholinergic hypothesis posited that the cognitive decline seen in AD is due to dysfunctional cholinergic signaling stemming from the atrophy of the basal forebrain (Bartus et al., 1982; Contestabile, 2011; Hampel et al., 2018). While it is now understood that the cognitive decline seen in AD is more multifaceted in terms of neurotransmitter systems involved and brain regions affected, acetylcholinesterase inhibitors are still the predominant approved pharmaceuticals prescribed to AD patients (Danysz & Parsons, 2003; McGleenon et al., 2001). Recent research has suggested that basal forebrain degeneration predicts and precedes the degeneration of the transentorhinal cortex, challenging the long-held belief that AD pathology is cortical in its origin (Schmitz et al., 2016). Understanding how and why BFCNs degenerate in AD is therefore an important step in understanding the early-stage pathology of the disorder.

A factor that may explain the vulnerability of BFCNs to age-related neurodegeneration is their lack of neurotrophin synthesis. Neurotrophins like brain-derived neurotrophic factor (BDNF) and nerve growth factor (NGF) are critical for a wide variety of cellular processes including apoptotic suppression, differentiation, activity-dependent plasticity, and maintenance of synaptic connectivity (Bothwell, 2014). BFCNs are completely reliant on their synaptic targets in the cortex and hippocampus for retrograde neurotrophic support for the survival of their synaptic circuits (Lu et al., 2014; Seiler & Schwab, 1984). Retrograde axonal transport is diminished in aged rat BFCNs, possibly explaining their vulnerability to age-related neurodegeneration (Bearer et al., 2018; Cooper et al., 1994; de Lacalle et al., 1996). However, the mechanisms underlying this age-related transport impairment are currently poorly understood.

1.4 Neurotrophic Support and the Basal Forebrain

Neurotrophins are a family of extracellular signaling molecules that are critical for neuronal survival, maintenance, and function. NGF, BDNF, neurotrophin-3 (NT-3), and neurotrophin-4 (NT-4) make up the currently known neurotrophins found in mammals (Bothwell, 2014). NGF was the first neurotrophin characterized and is known for its key role in the development and organization of the nervous system and for its regulation of apoptosis (Levi-Montalcini, 1987; Levi-Montalcini & Cohen, 1956). NGF biosynthesis and activity has been extensively studied in the mouse submandibular gland due to its extremely high concentration in this tissue (Cohen, 1960; Fahnestock, 1991). While NGF has been widely studied in the context of the peripheral nervous system (PNS), its expression is also observed widely throughout the brain, with the highest levels observed within the cortex and hippocampus (Shelton & Reichardt, 1986). BDNF was the next neurotrophin discovered and is critical for the regulation of neuronal excitability and synaptic plasticity (Barde et al., 1982). The study of BDNF, in contrast to NGF, has been primarily focused on its effects on central neurons. However, BDNF, like NGF, is expressed both centrally and peripherally and plays a critical role in the development and maintenance of both central and peripheral circuits (Bothwell, 2014; Kowiański et al., 2018; McGregor & English, 2019). NT-3 was discovered next and has been extensively studied in the context of sympathetic and enteric nervous system development (Chalazonitis, 2004; Glebova & Ginty, 2005; Kuruvilla et al., 2004; Maisonpierre et al., 1990). NT-4 (sometimes referred to as neurotrophin-5) was discovered shortly after NT-3 and is involved in heart rate and breathing regulation, but has been less studied in comparison to other neurotrophins, possibly because of its lower levels of expression (Berkemeier et al., 1991; Ibáñez, 1996; Ip et al., 1992, 1993).

NGF and BDNF are initially translated as precursor "pro" proteins that are later processed to their mature forms (Sun et al., 2013). NGF is initially synthesized from four different mRNA species alternatively spliced from two promoters into 34kD and 27kD prepro species which undergo signal sequence removal at the endoplasmic reticulum (ER) to yield 32kD and 25kD proNGF products (Edwards et al., 1986, 1988; Selby et al., 1987). Cleavage of proNGF at both its amino and carboxyl-terminal ends can occur via the proteases furin or other proprotein convertases, kallikreins, plasmin or matrix metalloprotease-7 (MMP-7) to yield a 13.2kD product referred to as either mature NGF or β-NGF (Bresnahan et al., 1990; Fahnestock, 1991; R. Lee et al., 2001; Seidah, Benjannet, Pareek, Savaria, et al., 1996). The diversity of BDNF mRNA transcripts is much greater than that of NGF, with 17 distinct transcripts identified in humans and 11 in rodents (Pruunsild et al., 2007). The expression of these transcripts is tightly regulated in a cell-type specific manner, with transcript IV accounting for approximately 50% of the BDNF expression in the cortex (Fahnestock, 2011; Pruunsild et al., 2007; Timmusk et al., 1993). BDNF is produced as an initial prepropeptide within the ER that undergoes cleavage of its signal sequence to produce a ~35kD proBDNF product (Seidah, Benjannet, Pareek, Chrétien, et al., 1996). Cleavage of proBDNF can occur via the proteases furin or other proprotein convertases, matrix metalloproteases such as MMP-3,

MMP-7 and MMP-9, or plasmin to produce a 14kD species referred to as mature BDNF. ProBDNF can also be cleaved by proprotein convertase subtilisin/kexin Type 6, also known as subtilisin/kexin isozyme 1 (PCSK6/SKI-1), to produce a 28kD species referred to as truncated BDNF, whose biological significance is currently unknown (Jung et al., 2005; Krystosek & Seeds, 1981; R. Lee et al., 2001; Mowla et al., 2001; Seidah, Benjannet, Pareek, Chrétien, et al., 1996). While the cleavage of neurotrophins to their mature forms is well documented, both NGF and BDNF are capable of secretion as their uncleaved pro forms, suggesting inherent biological activity unique from their mature forms (Fahnestock, Yu, & Coughlin, 2004; Hasan et al., 2003; Mowla et al., 1999; Nagappan et al., 2009). The biological activity of pro-neurotrophins was initially unclear, but it is now understood that pro-neurotrophins are capable of facilitating intracellular signaling independently of their mature counterparts (Clewes et al., 2008; Fahnestock, Yu, Michalski, et al., 2004; Ioannou & Fahnestock, 2017; Koshimizu et al., 2009, 2010). In fact, it has been demonstrated that proNGF is the only detectable form of NGF in the brain in both humans and rodents (Fahnestock et al., 2001). Based on this information and the fact that proNGF is not cleaved upon binding and internalization (Masoudi et al., 2009), BFCNs are most likely transporting proNGF as opposed to mature NGF from their synaptic targets.

Neurotrophins exert their biological activity by binding to tropomyosin related kinases (Trks). NGF preferentially binds to TrkA, BDNF and NT-4 preferentially bind TrkB, and NT-3 preferentially binds TrkC (Deinhardt & Chao, 2014). Binding of neurotrophins to Trks promotes neuronal survival and differentiation via the activation of P13K-AKT and Ras-MEK-MAPK intracellular pathways (Kaplan & Miller, 2000). All neurotrophins and their pro forms also bind to the pan-neurotrophin $p75^{NTR}$ receptor. Proneurotrophins bind to $p75^{NTR}$ with a higher affinity compared to Trk receptors (Bothwell, 2014; Clewes et al., 2008; Fayard et al., 2005). When $p75^{NTR}$ is solely expressed on neuronal membranes, apoptosis occurs via activation of sphingomyelinase/ceramide, c-Jun N-terminal kinase (JNK), c-Jun phosphorylation and caspases 3, 6, and 9 (Bhakar et al., 2003; Ioannou & Fahnestock, 2017; Volosin et al., 2006). Neurite retraction and long-term depression (LTD) are also triggered by $p75^{NTR}$ via activation of the JNK and RhoA/ROCK pathways (Sun et al., 2012). A visual summary of these pathways is provided in Figure 2. When $p75^{NTR}$ is co-expressed with TrkA, TrkA binding and survival signaling are promoted (Davies et al., 1993; Epa et al., 2004; Hamanoue et al., 1999). As a result of this synergy between TrkA signaling and $p75^{NTR}$, the activity of proNGF is contingent on the receptor complement of its target cell; lack of TrkA expression renders proNGF apoptotic, while expression of TrkA alone or TrkA in the presence of $p75^{NTR}$ renders proNGF neurotrophic (Fahnestock & Shekari, 2019; Ioannou & Fahnestock, 2017; Masoudi et al., 2009).

Both NGF and BDNF promote the differentiation of cultured murine embryonic BFCNs (Hartikka & Hefti, 1988; Hatanaka et al., 1988). NGF and BDNF also regulate the cholinergic output of cultured BFCNs (Alderson et al., 1990; Latina et al., 2017; Rylett & Williams, 1994; Sanchez-Ortiz et al., 2012). TrkB expression in murine BFCNs along with NGF and BDNF expression in BFCN targets are observed as early as embryonic day 10, suggesting that neurotrophin signaling is critical for the development

of BFCN synaptic circuity (Elliott et al., 2001; Formaggio et al., 2010; Katoh-Semba et al., 2002; Large et al., 1986). Embryonic BFCNs do not express TrkA; TrkA expression is first observed at post-natal day 4 and increases until post-natal day 21, followed by a plateau during adulthood (Conover et al., 1995; Li et al., 1995). Lack of embryonic TrkA expression in BFCNs may reflect the differing roles of NGF and BDNF; unlike NGF, BDNF is not necessarily a survival factor, but regulates synaptic function and plasticity (Rauskolb et al., 2010). BFCNs may rely on BDNF for the establishment of their diffuse synaptic circuits during development, and NGF for the maintenance and pruning of these circuits postnatally. Interestingly, TrkA expression can be induced in embryonic cultured BFCNs via exogenous NGF administration, suggesting that this culture system could be used to study BDNF and NGF transport *in vitro* (Kojima et al., 1995).

1.5 Axonal Transport and Neurotrophins

The retrograde axonal transport of neurotrophins like proNGF and BDNF by BFCNs is critical to the survival and function of their synaptic circuits due to their lack of neurotrophin synthesis. The extremely long and diffuse nature of BFCN projections suggests that BFCNs are extremely dependent on mechanisms like retrograde axonal transport that maintain these projections. Retrograde axonal transport occurs along microtubules, polarized tubulin polymers that span the entire length of the axon (Maday et al., 2014). Microtubules are organized in parallel radial arrays within axons, forming unipolar filaments with plus ends proximal to the axon tip and minus ends proximal to the cell body (Rao & Baas, 2018). Retrograde transport is often referred to as "minus-end directed" transport because of this organization. Retrograde transport is carried out by the motor protein dynein (Figure 3). Dynein is a large protein consisting of many polypeptide domains classified as heavy, intermediate, light intermediate, or light chains depending on their molecular weight (Roberts et al., 2013). These polypeptide chains associate together via their N-terminal tail domains to form binding sites for both cargo and dynein adapter proteins (Maday et al., 2014). The function of dynein is heavily regulated by its adapter proteins. Adapter proteins including $p150^{glued}$ and dynactin are critical for the binding of dynein to microtubules and the binding of cargo itself, including NGF, to dynein, respectively. (Maday et al., 2014; Moughamian et al., 2013; Villarin et al., 2016).

The anterograde transport of receptors and organelles to the distal axon tip is critical for retrograde transport. The anterograde transport of mitochondria is especially critical, as motor protein procession along microtubules is an ATP-driven process (Sheng, 2014). The kinesin superfamily of plus-end directed molecular motors are responsible for anterograde axonal transport along microtubules (Figure 3) (Maday et al., 2014). While only a single cytoplasmic dynein is responsible for facilitating the entirety of retrograde transport, 15 subfamilies of kinesin proteins have been characterized that carry out anterograde transport in both a cell type-specific and cellular domain-specific manner (Hirokawa et al., 2009). Kinesin motors are much smaller compared to dynein, consisting of up to two 115-130 kDa heavy chains and two 62-70 kDa light chains which associate together to form various binding domains (Hirokawa, 1998). For comparison, a single dynein heavy chain can be 530 kDa in size (Hirokawa, 1998). Kinesins, much like

adapter proteins for proper function. For example, the trafficking kinesin protein (TRAK) family act as adapters that attach mitochondria to kinesin (Y. Chen & Sheng, 2013; van Spronsen et al., 2013).TRAK proteins bind to Miro, a protein expressed on the outer mitochondrial membrane, tethering mitochondria to the kinesin complex and allowing for their anterograde transport (MacAskill et al., 2009; MacAskill & Kittler, 2010).

The anterograde transport of Trk and $p75^{NTR}$ receptors to the distal axon is required for retrograde axonal transport of neurotrophins. Trk receptors physically associate with sortilin-1 at the Golgi apparatus, a type-I membrane glycoprotein that regulates receptor sorting (Vaegter et al., 2011). While the exact role of sortilin-1 in Trk trafficking is currently unclear, its association with Trk receptors at the Golgi apparatus suggests that Trk receptors, like the majority of membrane proteins, are delivered to distal axons via the secretory pathway (Scott-Solomon & Kuruvilla, 2018). Axonal delivery of Trk receptors like TrkA and TrkB are carried out by the kinesin motors KIF1A and Kinesin-1, respectively (Arimura et al., 2009; Tanaka et al., 2016). The kinesin adapter protein huntingtin associated protein (HAP) 1 is critical for TrkA trafficking, and its downregulation reduces neurite outgrowth and TrkA levels in neurons (Rong, 2006; Yang et al., 2012). Other adapters including collapsing response mediator protein (CRMP-2) and c-Jun NH_2-terminal kinase-interacting protein (JIP) 1 and 3 directly link TrkB to kinesin-1 and are critical for its anterograde trafficking to axons (Arimura et al., 2009; Huang et al., 2011; Sun et al., 2017). While much less is known about the anterograde transport of $p75^{NTR}$, both kinesin-1 and kinesin-3 have been shown to be responsible for its anterograde trafficking (Jaulin et al., 2007; Xue et al., 2010). Anterograde trafficking of neurotrophin receptors like TrkA, TrkB, and $p75^{NTR}$ by BFCNs is likely critical for their survival and proper function due to their reliance on retrograde neurotrophic support.

While neurotrophin trafficking is not well understood in BFCNs, it has been extensively studied in the context of NGF-TrkA transport in dorsal root ganglion neurons (DRGs), spinal projection neurons capable of growing long axonal projections in culture (De Nadai et al., 2016; Harrington & Ginty, 2013; Senger & Campenot, 1997). Multiple hypotheses have been proposed to explain retrograde neurotrophin trafficking in these neurons. The wave propagation hypothesis posits that NGF itself is not retrogradely trafficked to the cell body. Under this model, NGF binding to TrkA at distal axons triggers a wave of TrkA phosphorylation that propagates down the length of the axon, rapidly reaching the soma (Ginty, 2002; Senger & Campenot, 1997). Observations of phosphorylated TrkA at the soma upon axonal administration of NGF prior to the detection of somal NGF support this model (Senger & Campenot, 1997). The signaling endosome hypothesis stands in contrast to the wave propagation model and argues for the retrograde trafficking of NGF to the soma. Under this model, NGF is internalized at distal axons upon TrkA binding and is trafficked to the soma within an endosome (Barford et al., 2017; Delcroix et al., 2003; Grimes et al., 1996; Harrington & Ginty, 2013; C. Wu et al., 2009). The signaling endosome hypothesis represents the more widely accepted model of NGF-TrkA trafficking. The retrograde propagation of phosphorylated TrkA, while very rapid, is still well within the reported range of the retrograde motor protein dynein (Brokaw, 1991; Ginty, 2002). Additionally, NGF colocalizes with phosphorylated

TrkA within axons following axonal NGF administration (Ehlers et al., 1995; Tsui-Pierchala & Ginty, 1999). Observations of phosphorylated TrkA within vesicle-like structures in axons using immunoelectron microscopy further support the signaling endosome hypothesis (Bhattacharyya et al., 2002).

NGF-TrkA signaling endosome biogenesis begins at the axon terminal upon NGF binding to TrkA. Phosphorylation of TrkA tyrosine residues following binding triggers the activation of multiple signaling pathways including the P13K-AKT, Ras-MAPK, and PLCγ pathways (Kaplan & Miller, 2000). Activation of these pathways not only promotes survival at distal axons, but also mediates the internalization and formation of the NGF-TrkA signaling endosome. While the mode of internalization is still controversial, it is clear that the activation of PLCγ contributes to endosome formation through the recruitment of endocytic machinery such as dynamin-1 to sites of TrkA activation on the plasma membrane (Bodmer et al., 2011). Following internalization, the signaling endosome must be dissociated from the dense actin network present at the distal axon tip before retrograde trafficking can begin. Dissociation from the actin network is regulated by the recruitment of actin-modulatory proteins Rac1 and cofilin via activation of P13K by TrkA (Harrington et al., 2011; Kuruvilla et al., 2000). Persistent cytosolic exposure of phosphorylated TrkA residues following NGF binding is a consequence of endosome formation, allowing for the activation of TrkA-mediated survival pathways throughout the duration of transport. Constitutive TrkA activation during retrograde transport suggests that the trafficking of the NGF-TrkA endosome plays a role in axonal maintenance and is not solely a mechanism to deliver NGF to the soma (Crerar et al., 2019).

In AD, proNGF accumulates in BFCN target tissue and is reduced in the basal forebrain (Fahnestock et al., 2001; Scott et al., 1995). The buildup of NGF-immunoreactive material in BFCN targets in AD suggests that retrograde neurotrophin transport by BFCNs is impaired in the disorder (Scott et al., 1995). Significant age-related increases in proNGF levels are also seen in basal forebrain target areas of 3xTg-AD mice, an AD model employing the expression of humanized amyloid and tau transgenes (discussed further in Chapter 4) (Perez et al., 2011). Additionally, the retrograde axonal transport of NGF by basal forebrain neurons is significantly impaired in Ts65Dn mice, an AD model where Aβ overexpression is achieved via trisomy of the 16th murine chromosome which houses the APP locus (Cooper et al., 2001; Salehi et al., 2006). TrkA receptor levels and levels of downstream NGF signaling proteins are also decreased in aged rat BFCNs (Niewiadomska et al., 2002; Parikh et al., 2013; Williams et al., 2007, 2006). The observations of probable neurotrophin transport disruption both in aging in the absence of dementia and in AD suggests that the reliance of BFCNs on neurotrophin transport may contribute to their susceptibility to age-related neurodegeneration. Neurotrophin transport deficits are not NGF-specific, as Aβ-dependent BDNF retrograde transport deficits have been observed in cultured cortical neurons (Poon et al., 2011). Furthermore, both NGF and BDNF levels are increased in basal forebrain targets areas in APP23 mice, an AD model overexpressing a mutant, humanized APP isoform associated with AD (Schulte-Herbrüggen et al., 2008). However, retrograde axonal transport in BFCNs is currently poorly understood.

1.6 Reactive Oxygen Species in Aging and AD

ProNGF accumulation in BFCN targets suggests that axonal transport disruptions play an important role in the age-related neurodegeneration of these neurons. One factor linking aging and axonal transport disruptions is oxidative stress. The brain is highly susceptible to oxidative damage due to the high metabolic rate of neurons. Neurons are extremely metabolically demanding cells due to their generation of action potentials; the rectification of membrane potential following a single action potential requires between 4-8 billion molecules of ATP through the activity of the ATP-dependent Na/K pump (Chamberlain & Sheng, 2019). The relatively large size of basal forebrain neurons may make them especially vulnerable to ROS-induced damage, as mitochondrial mass scales directly with neuronal size (Chamberlain & Sheng, 2019; Misgeld & Schwarz, 2017). The reliance of BFCNs on axonal transport, a mitochondria-dependent process by virtue of reliance of dynein and kinesin motors on ATP for procession, may also contribute to the increased vulnerability of these cells to age-induced oxidative damage (Sheng, 2014).

The main source of ROS in neurons is mitochondria, where ROS are generated as naturally occurring by-products of oxidative phosphorylation (Balaban et al., 2005; Quinlan et al., 2013). The primary oxidative ion generated by mitochondria is the superoxide anion O_2^-. O_2^- is a potent electron donor that has the potential to oxidize proteins, lipids, and DNA, causing oxidative damage by altering their structure and function (Leuner et al., 2007, 2012; Venditti et al., 2013). O_2^- mediated oxidation also leads to the formation of other reactive oxygen species (ROS) including peroxynitrite and hydroxyperoxyl that are more reactive than superoxide and subsequently more damaging to cells (Cho et al., 2009; Guix et al., 2012; Leuner et al., 2007). Peroxynitrite is particularly damaging to neurons and is a longstanding contributor to AD pathogenesis (Smith et al., 1997; Torreilles et al., 1999). Oxidative damage triggered by nitrogen containing radicals like peroxynitrite is often referred to as nitrative stress and is a subset of oxidative stress. While the overproduction of ROS are harmful, low levels of ROS production are important for cellular function, as they act as second messengers in a variety of signaling cascades, many of which regulate ROS levels through negative feedback (Lubos et al., 2011; Nissanka & Moraes, 2018; A. R. Simon et al., 1998).

Increases in neuronal oxidative damage are commonly observed in the aging brain. The accumulation of protein carbonyls, nitrotyrosine, and hydroxynoneal (HNE) protein-adducts, markers of excessive protein oxidation, exist in significantly higher concentrations in the aging brain (Chakrabarti et al., 2011; Halliwell, 2006). Lipid oxidation products including thiobarbituric acid reactive substances (TBARS) and 4-hydroxynoneal (4-HNE) accumulate in the brain as a direct function of age (Chakrabarti et al., 2011; Sen et al., 2006). The progressive accumulation of the canonical oxidative DNA damage marker 8-oxo-2'-deoxyguanosine (oxo^8dG) has also been demonstrated in aged brain tissue (Chakrabarti et al., 2011; Mecocci et al., 1997). Increases in mitochondrial ROS production have been observed in both whole brain homogenates and in subregions like the cortex and hippocampus with age (Driver et al., 2000; Lores-Arnaiz et al., 2016; Navarro et al., 2008).

Increased ROS load is also a contributing factor to AD pathogenesis (Ahmad et al., 2017; Leutner et al., 2005; Mosconi, 2013; Tönnies & Trushina, 2017; Tramutola et al., 2017). Almost all cellular macromolecules are found in their oxidized form in post-mortem AD brain tissue (Kish et al., 1992; Mecocci et al., 1994; Subbarao et al., 1990). Mitochondria, while being the predominant source of ROS in neurons, are themselves especially sensitive to ROS levels and become far less efficient in energy metabolism under high levels of ROS load (Bhatti et al., 2017). This loss of efficiency is thought to underlie the inefficient metabolism of glucose in the AD brain (Mosconi, 2013).

Increased ROS accumulation has been shown to impact axonal transport. ROS-mediated reductions of Ca^{2+} levels via JNK reduce axonal mitochondrial motility (Liao et al., 2017). Anterograde axonal transport of mitochondria and lysosomes is irreversibly reduced following tert-butyl hydroperoxide-induced ROS accumulation in cultured DRGs (Isonaka et al., 2011). Reduction of ROS load with pharmacological agents like N(G)-Nitro-L-arginine methyl ester (L-NAME), an inhibitor of nitric oxide synthesis, has been shown to ameliorate axonal transport deficits (Stykel et al., 2018).

1.7 Microfluidics and Studying Aging *In Vitro*

Axonal transport is commonly studied using *in vitro* systems. However, initial characterizations of axonal transport were done *in vivo* in the context of peripheral nerve regeneration in rodents (Weiss & Hiscoe, 1948). Seminal work in the early 1960s by Droz and Leblond utilizing autoradiography following the injection of radio-labelled molecules into the rodent sciatic nerve laid the foundation for the *in vivo* characterization of axonal transport (Droz & Leblond, 1962). NGF is commonly labelled with radioactive iodine (I^{125}) to study its transport *in vivo* (Hendry et al., 1974; Seiler & Schwab, 1984; Wayne & Heaton, 1988; Zhou et al., 2016). Recent advances in functional magnetic resonance imaging in conjunction with central manganese administration have allowed for the non-invasive monitoring of axonal transport in live animals (Bertrand et al., 2013). This technique has been recently used to demonstrate basal forebrain retrograde transport deficits in both aging and AD animal models (Bearer et al., 2018). However, this technique can only be used to study general axonal transport.

To properly assess axonal transport *in vitro*, neuronal cell bodies and axon terminals must be separated. Initially, Campenot chambers were used to achieve this (Campenot, 1977). These devices consist of a modular Teflon segment connected to 3 individual chambers sealed to a collagen-coated culture dish. Studies of axonal transport in these chambers are limited to peripheral neurons like DRGs, as CNS neurons are not robust enough to grow axons of sufficient length through the barriers of Campenot chambers. Recently, microfluidic chambers have been developed to achieve this same neuronal separation for CNS neurons (Taylor et al., 2005). These chambers contain microgrooves that are connected to a main channel that houses neuronal cell bodies. Axons grow through these microgrooves and emerge into another channel that maintains fluidic isolation from the channel that houses the cell bodies. These chambers allow for direction-specific axonal transport to be assayed in CNS neurons. However, the small and

enclosed nature of the axonal compartment of these chambers makes harvesting axon extensions for analysis very difficult, limiting their use to mainly microscopic analysis.

To model aging in BFCNs *in vitro*, cells can be maintained in culture and assayed at different time points. Embryonic BFCNs are difficult to maintain in culture, even more so in microfluidic chambers. With these limitations in mind, culturing BFCNs from aged animals is not viable. Aging *in vitro* is not a perfect analog of *in vivo* aging, but it is commonly used in both primary neuron and stem cell cultures to examine age-sensitive phenomena (Campos et al., 2014; Martin et al., 2008; Palomer et al., 2016; Sodero et al., 2011; Uday Bhanu et al., 2010). To confirm an aging phenotype, cells can be stained with senescence-associated beta galactosidase (SaβG), a well-validated marker of aging in humans, primates, and rodents both *in vivo* and *in vitro* (Dimri et al., 1995; Kurz et al., 2000; Mishima et al., 1999; Uday Bhanu et al., 2010).

1.8 Summary

In sum, BFCNs are critical for cognition, and their degeneration is a hallmark of general aging and AD. The reliance of these neurons on retrograde axonal transport for neurotrophic support may underlie their susceptibility to age-related neurodegeneration. This notion is supported by observations of neurotrophin accumulation in BFCN target areas and downregulation of neurotrophin receptors like TrkA in aging and AD. However, retrograde axonal transport in BFCNs is currently poorly understood. This is likely because BFCNs are very difficult to maintain in culture, making the study of axonal transport in a controlled *in vitro* system difficult. **The goal of this work is to establish a microfluidic culture system for the detailed characterization of BFCN neurotrophin transport *in vitro*.**

Additionally, mechanisms explaining age-related neurotrophin transport deficits in these neurons are absent from the literature. The large size of BFCNs coupled with their reliance on mitochondria-driven axonal transport likely renders BFCNs particularly susceptible to ROS-induced damage. Axonal transport disruptions mediated by ROS accumulation are well-documented in the literature and may contribute to the impairment of both retrograde neurotrophin transport and the anterograde transport of their receptors. **Using a microfluidic culture system, we aim to determine if mechanisms relating to oxidative stress contribute to the age-related impairment of retrograde neurotrophin transport in BFCNs.**

Hypothesis: oxidative stress impairs retrograde neurotrophin transport in BFCNs. Specific aims are listed below:

- To establish a microfluidic culture system for the study of retrograde neurotrophin transport in BFCNs,
- To test the validity of this system by determining if age-related and AD-related, neurotrophin transport deficits are recapitulated in this system
- To determine the effect of oxidative stress on neurotrophin transport in this system.

References

Ahmad, W., Ijaz, B., Shabbiri, K., Ahmed, F., & Rehman, S. (2017). Oxidative toxicity in diabetes and Alzheimer's disease: Mechanisms behind ROS/ RNS generation. *Journal of Biomedical Science*, *24*(1), 76. https://doi.org/10.1186/s12929-017-0379-z

Alderson, R. F., Alterman, A. L., Barde, Y. A., & Lindsay, R. M. (1990). Brain-derived neurotrophic factor increases survival and differentiated functions of rat septal cholinergic neurons in culture. *Neuron*, *5*(3), 297–306. https://doi.org/0896-6273(90)90166-D [pii]

Altavista, M. C., Rossi, P., Bentivoglio, A. R., Crociani, P., & Albanese, A. (1990). Aging is associated with a diffuse impairment of forebrain cholinergic neurons. *Brain Research*, *508*(1), 51–59. https://doi.org/10.1016/0006-8993(90)91116-X

Arimura, N., Kimura, T., Nakamuta, S., Taya, S., Funahashi, Y., Hattori, A., Shimada, A., Ménager, C., Kawabata, S., Fujii, K., Iwamatsu, A., Segal, R. A., Fukuda, M., & Kaibuchi, K. (2009). Anterograde Transport of TrkB in Axons Is Mediated by Direct Interaction with Slp1 and Rab27. *Developmental Cell*, *16*(5), 675–686. https://doi.org/10.1016/j.devcel.2009.03.005

Baker-Nigh, A., Vahedi, S., Davis, E. G., Weintraub, S., Bigio, E. H., Klein, W. L., & Geula, C. (2015). Neuronal amyloid-β accumulation within cholinergic basal forebrain in ageing and Alzheimer's disease. *Brain*, *138*(6), 1722–1737. https://doi.org/10.1093/brain/awv024

Balaban, R. S., Nemoto, S., & Finkel, T. (2005). Mitochondria, Oxidants, and Aging. *Cell*, *120*(4), 483–495. https://doi.org/10.1016/j.cell.2005.02.001

Ballatore, C., Lee, V. M. Y., & Trojanowski, J. Q. (2007). Tau-mediated neurodegeneration in Alzheimer's disease and related disorders. *Nature Reviews Neuroscience*, *8*(9), 663–672. https://doi.org/10.1038/nrn2194

Ballinger, E. C., Ananth, M., Talmage, D. A., & Role, L. W. (2016). Basal Forebrain Cholinergic Circuits and Signaling in Cognition and Cognitive Decline. *Neuron*, *91*(6), 1199–1218. https://doi.org/10.1016/j.neuron.2016.09.006

Barde, Y. A., Edgar, D., & Thoenen, H. (1982). Purification of a new neurotrophic factor from mammalian brain. *Hoppe-Seyler's Zeitschrift Fur Physiologische Chemie*, *363*(11), 1295–1296. https://doi.org/10.1002/j.1460-2075.1982.tb01207.x

Barford, K., Deppmann, C., & Winckler, B. (2017). The neurotrophin receptor signaling endosome: Where trafficking meets signaling. *Developmental Neurobiology*, *77*(4), 405–418. https://doi.org/10.1002/dneu.22427

Barnes, C. (1979). Memory deficits associated with senescence: A neurophysiological and behavioral study in the rat. *Journal of Comparative and Physiological Psychology*, *93*(1), 74–104. https://doi.org/10.1037/h0077579

Barnes, C. (2000). LTP induction threshold change in old rats at the perforant pathway and granule cell synapse. *Neurobiology of Aging*, *21*(5), 613–620. https://doi.org/10.1016/S0197-4580(00)00163-9

Bartus, R., Dean, R., Beer, B., & Lippa, A. (1982). The cholinergic hypothesis of geriatric memory dysfunction. *Science*, *217*(4558), 408–414. https://doi.org/10.1126/science.7046051

Bartzokis, G., Cummings, J. L., Sultzer, D., Henderson, V. W., Nuechterlein, K. H., & Mintz, J. (2003). White Matter Structural Integrity in Healthy Aging Adults and Patients With Alzheimer Disease. *Archives of Neurology*, *60*(3), 393. https://doi.org/10.1001/archneur.60.3.393

Baxter, M. G., & Chiba, A. A. (1999). Cognitive functions of the basal forebrain. *Current Opinion in Neurobiology*, *9*(2), 178–183. https://doi.org/10.1016/S0959-4388(99)80024-5

Bearer, E. L., Manifold-Wheeler, B. C., Medina, C. S., Gonzales, A. G., Chaves, F. L., & Jacobs, R. E. (2018). Alterations of functional circuitry in aging brain and the impact of mutated APP expression. *Neurobiology of Aging*, *70*, 276–290. https://doi.org/10.1016/j.neurobiolaging.2018.06.018

Belarbi, K., Schindowski, K., Burnouf, S., Caillierez, R., Grosjean, M.-E., Demeyer, D., Hamdane, M., Sergeant, N., Blum, D., & Buée, L. (2009). Early Tau pathology involving the septo-hippocampal pathway in a Tau transgenic model: Relevance to Alzheimer's disease. *Current Alzheimer Research*, *6*(2), 152–157. https://doi.org/10.2174/156720509787602843

Berkemeier, L. R., Winslow, J. W., Kaplan, D. R., Nikolics, K., Goeddel, D. V., & Rosenthal, A. (1991). Neurotrophin-5: A novel neurotrophic factor that activates trk and trkB. *Neuron*, *7*(5), 857–866. https://doi.org/10.1016/0896-6273(91)90287-A

Bertrand, A., Khan, U., Hoang, D. M., Novikov, D. S., Krishnamurthy, P., Rajamohamed Sait, H. B., Little, B. W., Sigurdsson, E. M., & Wadghiri, Y. Z. (2013). Non-invasive, in vivo monitoring of neuronal transport impairment in a mouse model of tauopathy using MEMRI. *NeuroImage*, *64*, 693–702. https://doi.org/10.1016/j.neuroimage.2012.08.065

Bhakar, A. L., Howell, J. L., Paul, C. E., Salehi, A. H., Becker, E. B. E., Said, F., Bonni, A., & Barker, P. A. (2003). Apoptosis induced by p75NTR overexpression requires Jun kinase-dependent phosphorylation of Bad. *The Journal of Neuroscience: The Official Journal of the Society for Neuroscience*, *23*(36), 11373–11381.

Bhattacharyya, A., Watson, F. L., Pomeroy, S. L., Zhang, Y. Z., Stiles, C. D., & Segal, R. A. (2002). High-resolution imaging demonstrates dynein-based vesicular transport of activated trk receptors. *Journal of Neurobiology*, *51*(4), 302–312. https://doi.org/10.1002/neu.10062

Bhatti, J. S., Bhatti, G. K., & Reddy, P. H. (2017). Mitochondrial dysfunction and oxidative stress in metabolic disorders—A step towards mitochondria based therapeutic strategies. *Biochimica et Biophysica Acta (BBA) - Molecular Basis of Disease*, *1863*(5), 1066–1077. https://doi.org/10.1016/j.bbadis.2016.11.010

Bierer, L. M., Haroutunian, V., Gabriel, S., Knott, P. J., Carlin, L. S., Purohit, D. P., Perl, D. P., Schmeidler, J., Kanof, P., & Davis, K. L. (1995). Neurochemical correlates of dementia severity in Alzheimer's disease: Relative importance of the

cholinergic deficits. *Journal of Neurochemistry*, *64*(2), 749–760. https://doi.org/10.1046/j.1471-4159.1995.64020749.x

Bodmer, D., Ascaño, M., & Kuruvilla, R. (2011). Isoform-Specific Dephosphorylation of Dynamin1 by Calcineurin Couples Neurotrophin Receptor Endocytosis to Axonal Growth. *Neuron*, *70*(6), 1085–1099. https://doi.org/10.1016/j.neuron.2011.04.025

Bondareff, W., Mountjoy, C., Roth, M., & Hauser, D. (1989). Neurofibrillary degeneration and neuronal loss in alzheimer's disease. *Neurobiology of Aging*, *10*(6), 709–715. https://doi.org/10.1016/0197-4580(89)90007-9

Bondi, M. W., Edmonds, E. C., & Salmon, D. P. (2017). Alzheimer's Disease: Past, Present, and Future. *Journal of the International Neuropsychological Society*, *23*(9–10), 818–831. https://doi.org/10.1017/S135561771700100X

Bothwell, M. (2014). NGF, BDNF, NT3, and NT4. In *Handbook of Experimental Pharmacology* (pp. 3–15). https://doi.org/10.1007/978-3-642-45106-5_1

Braak, H., & Braak, E. (1991). Neuropathological stageing of Alzheimer-related changes. *Acta Neuropathologica*, *82*(4), 239–259. https://doi.org/10.1007/BF00308809

Braak, H., & Del Tredici, K. (2018). Spreading of Tau Pathology in Sporadic Alzheimer's Disease Along Cortico-cortical Top-Down Connections. *Cerebral Cortex*, *28*(9), 3372–3384. https://doi.org/10.1093/cercor/bhy152

Bresnahan, P. A., Leduc, R., Thomas, L., Thorner, J., Gibson, H. L., Brake, A. J., Barr, P. J., & Thomas, G. (1990). Human fur gene encodes a yeast KEX2-like endoprotease that cleaves pro-beta-NGF in vivo. *The Journal of Cell Biology*, *111*(6), 2851–2859. https://doi.org/10.1083/jcb.111.6.2851

Brokaw, C. J. (1991). Microtubule sliding in swimming sperm flagella: Direct and indirect measurements on sea urchin and tunicate spermatozoa [published erratum appears in J Cell Biol 1991 Nov;115(4):1204]. *The Journal of Cell Biology*, *114*(6), 1201–1215. https://doi.org/10.1083/jcb.114.6.1201

Budni, J., Bellettini-Santos, T., Mina, F., Lima Garcez, M., & Ioppi Zugno, A. (2015). The involvement of BDNF, NGF and GDNF in aging and Alzheimer's disease. *Aging and Disease*, *6*(5), 331. https://doi.org/10.14336/AD.2015.0825

Buell, S., & Coleman, P. (1979). Dendritic growth in the aged human brain and failure of growth in senile dementia. *Science*, *206*(4420), 854–856. https://doi.org/10.1126/science.493989

Campenot, R. B. (1977). Local control of neurite development by nerve growth factor. *Proceedings of the National Academy of Sciences of the United States of America*, *74*(10), 4516–4519. https://doi.org/10.1073/pnas.74.10.4516

Campos, P. B., Paulsen, B. S., & Rehen, S. K. (2014). Accelerating neuronal aging in in vitro model brain disorders: A focus on reactive oxygen species. *Frontiers in Aging Neuroscience*, *6*, 292. https://doi.org/10.3389/fnagi.2014.00292

Chakrabarti, S., Munshi, S., Banerjee, K., Thakurta, I. G., Sinha, M., & Bagh, M. B. (2011). Mitochondrial Dysfunction during Brain Aging: Role of Oxidative Stress and Modulation by Antioxidant Supplementation. *Aging and Disease*, *2*(3), 242–256.

Chalazonitis, A. (2004). Neurotrophin-3 in the development of the enteric nervous system. In *Progress in Brain Research* (pp. 243–263). https://doi.org/10.1016/S0079-6123(03)46016-0

Chamberlain, K. A., & Sheng, Z. (2019). Mechanisms for the maintenance and regulation of axonal energy supply. *Journal of Neuroscience Research*, *97*(8), 897–913. https://doi.org/10.1002/jnr.24411

Chen, Sugihara, H., & Sur, M. (2015). An acetylcholine-activated microcircuit drives temporal dynamics of cortical activity. *Nature Neuroscience*, *18*(6), 892–902. https://doi.org/10.1038/nn.4002

Chen, Y., & Sheng, Z.-H. (2013). Kinesin-1–syntaphilin coupling mediates activity-dependent regulation of axonal mitochondrial transport. *The Journal of Cell Biology*, *202*(2), 351–364. https://doi.org/10.1083/jcb.201302040

Cho, D.-H., Nakamura, T., Fang, J., Cieplak, P., Godzik, A., Gu, Z., & Lipton, S. A. (2009). S-Nitrosylation of Drp1 Mediates β-Amyloid-Related Mitochondrial Fission and Neuronal Injury. *Science*, *324*(5923), 102–105. https://doi.org/10.1126/science.1171091

Clewes, O., Fahey, M. S., Tyler, S. J., Watson, J. J., Seok, H., Catania, C., Cho, K., Dawbarn, D., & Allen, S. J. (2008). Human ProNGF: Biological effects and binding profiles at TrkA, P75NTRand sortilin. *Journal of Neurochemistry*, *107*(4), 1124–1135. https://doi.org/10.1111/j.1471-4159.2008.05698.x

Cohen, S. (1960). PURIFICATION OF A NERVE-GROWTH PROMOTING PROTEIN FROM THE MOUSE SALIVARY GLAND AND ITS NEURO-CYTOTOXIC ANTISERUM. *Proceedings of the National Academy of Sciences*, *46*(3), 302–311. https://doi.org/10.1073/pnas.46.3.302

Conover, J. C., Erickson, J. T., Katz, D. M., Bianchi, L. M., Poueymirou, W. T., McClain, J., Pan, L., Helgren, M., Ip, N. Y., Boland, P., Friedman, B., Wiegand, S., Vejsada, R., Kato, A. C., DeChiara, T. M., & Yancopoulos, G. D. (1995). Neuronal deficits, not involving motor neurons, in mice lacking BDNF and/or NT4. *Nature*, *375*(6528), 235–238. https://doi.org/10.1038/375235a0

Contestabile, A. (2011). The history of the cholinergic hypothesis. *Behavioural Brain Research*, *221*(2), 334–340. https://doi.org/10.1016/j.bbr.2009.12.044

Cooper, J. D., Lindholm, D., & Sofroniew, M. V. (1994). Reduced transport of [125I]nerve growth factor by cholinergic neurons and down-regulated trka expression in the medial septum of aged rats. *Neuroscience*, *62*(3), 625–629. https://doi.org/10.1016/0306-4522(94)90462-6

Cooper, J. D., Salehi, A., Delcroix, J.-D., Howe, C. L., Belichenko, P. V., Chua-Couzens, J., Kilbridge, J. F., Carlson, E. J., Epstein, C. J., & Mobley, W. C. (2001). Failed retrograde transport of NGF in a mouse model of Down's syndrome: Reversal of cholinergic neurodegenerative phenotypes following NGF infusion. *Proceedings of the National Academy of Sciences*, *98*(18), 10439–10444. https://doi.org/10.1073/pnas.181219298

Coyle, J., Price, D., & DeLong, M. (1983). Alzheimer's disease: A disorder of cortical cholinergic innervation. *Science*, *219*(4589), 1184–1190. https://doi.org/10.1126/science.6338589

Crerar, H., Scott-Solomon, E., Bodkin-Clarke, C., Andreassi, C., Hazbon, M., Logie, E., Cano-Jaimez, M., Gaspari, M., Kuruvilla, R., & Riccio, A. (2019). Regulation of NGF Signaling by an Axonal Untranslated mRNA. *Neuron*, *102*(3), 553-563.e8. https://doi.org/10.1016/j.neuron.2019.02.011

Danysz, W., & Parsons, C. G. (2003). The NMDA receptor antagonist memantine as a symptomatological and neuroprotective treatment for Alzheimer's disease: Preclinical evidence. *International Journal of Geriatric Psychiatry*, *18*(S1), S23–S32. https://doi.org/10.1002/gps.938

Davies. (1979). Neurotransmitter-related enzymes in senile dementia of the alzheimer type. *Brain Research*, *171*(2), 319–327. https://doi.org/10.1016/0006-8993(79)90336-6

Davies, A. M., Lee, K.-F., & Jaenisch, R. (1993). P75-Deficient trigeminal sensory neurons have an altered response to NGF but not to other neurotrophins. *Neuron*, *11*(4), 565–574. https://doi.org/10.1016/0896-6273(93)90069-4

de Lacalle, S., Cooper, J. D., Svendsen, C. N., Dunnett, S. B., & Sofroniew, M. V. (1996). Reduced retrograde labelling with fluorescent tracer accompanies neuronal atrophy of basal forebrain cholinergic neurons in aged rats. *Neuroscience*, *75*(1), 19–27. https://doi.org/10.1016/0306-4522(96)00239-4

De Nadai, T., Marchetti, L., Di Rienzo, C., Calvello, M., Signore, G., Di Matteo, P., Gobbo, F., Turturro, S., Meucci, S., Viegi, A., Beltram, F., Luin, S., & Cattaneo, A. (2016). Precursor and mature NGF live tracking: One versus many at a time in the axons. *Scientific Reports*, *6*(1), 20272. https://doi.org/10.1038/srep20272

Deinhardt, K., & Chao, M. V. (2014). Trk Receptors. In *Handbook of Experimental Pharmacology* (pp. 103–119). https://doi.org/10.1007/978-3-642-45106-5_5

Delcroix, J.-D., Valletta, J. S., Wu, C., Hunt, S. J., Kowal, A. S., & Mobley, W. C. (2003). NGF Signaling in Sensory Neurons. *Neuron*, *39*(1), 69–84. https://doi.org/10.1016/S0896-6273(03)00397-0

DeVos, S. L., Corjuc, B. T., Oakley, D. H., Nobuhara, C. K., Bannon, R. N., Chase, A., Commins, C., Gonzalez, J. A., Dooley, P. M., Frosch, M. P., & Hyman, B. T. (2018). Synaptic Tau Seeding Precedes Tau Pathology in Human Alzheimer's Disease Brain. *Frontiers in Neuroscience*, *12*. https://doi.org/10.3389/fnins.2018.00267

Dimri, G. P., Lee, X., Basile, G., Acosta, M., Scott, G., Roskelley, C., Medrano, E. E., Linskens, M., Rubelj, I., & Pereira-Smith, O. (1995). A biomarker that identifies senescent human cells in culture and in aging skin in vivo. *Proceedings of the National Academy of Sciences*, *92*(20), 9363–9367. https://doi.org/10.1073/pnas.92.20.9363

Driver, A. S., Kodavanti, P. R. S., & Mundy, W. R. (2000). Age-related changes in reactive oxygen species production in rat brain homogenates. *Neurotoxicology and Teratology*, *22*(2), 175–181. https://doi.org/10.1016/S0892-0362(99)00069-0

Droz, B., & Leblond, C. P. (1962). Migration of Proteins along the Axons of the Sciatic Nerve. *Science*, *137*(3535), 1047–1048. https://doi.org/10.1126/science.137.3535.1047

Edwards, R. H., Selby, M. J., Mobley, W. C., Weinrich, S. L., Hruby, D. E., & Rutter, W. J. (1988). Processing and secretion of nerve growth factor: Expression in mammalian cells with a vaccinia virus vector. *Molecular and Cellular Biology*, *8*(6), 2456–2464. https://doi.org/10.1128/MCB.8.6.2456

Edwards, R. H., Selby, M. J., & Rutter, W. J. (1986). Differential RNA splicing predicts two distinct nerve growth factor precursors. *Nature*, *319*(6056), 784–787. https://doi.org/10.1038/319784a0

Ehlers, M. D., Kaplan, D. R., Price, D. L., & Koliatsos, V. E. (1995). NGF-stimulated retrograde transport of trkA in the mammalian nervous system. *The Journal of Cell Biology*, *130*(1), 149–156. https://doi.org/10.1083/jcb.130.1.149

Elliott, R. C., Black, I. B., & Dreyfus, C. F. (2001). Differential regulation of p75 and trkB mRNA expression after depolarizing stimuli or BDNF treatment in basal forebrain neuron cultures. *Journal of Neuroscience Research*, *66*(1), 83–88. https://doi.org/10.1002/jnr.1199

Epa, W. R., Markovska, K., & Barrett, G. L. (2004). The p75 neurotrophin receptor enhances TrkA signalling by binding to Shc and augmenting its phosphorylation. *Journal of Neurochemistry*, *89*(2), 344–353. https://doi.org/10.1111/j.1471-4159.2004.02344.x

Fahnestock, M. (1991). Structure and Biosynthesis of Nerve Growth Factor. In *Current Topics in Microbiology and Immunology* (pp. 1–26). https://doi.org/10.1007/978-3-642-75747-1_1

Fahnestock, M. (2011). Brain-derived neurotrophic factor: The link between amyloid-β and memory loss. *Future Neurology*, *6*(5), 627–639. https://doi.org/10.2217/fnl.11.44

Fahnestock, M., & Shekari, A. (2019). ProNGF and neurodegeneration in Alzheimer's disease. In *Frontiers in Neuroscience* (Vol. 13, Issue FEB). https://doi.org/10.3389/fnins.2019.00129

Fahnestock, M., Yu, G., & Coughlin, M. D. (2004). ProNGF: a neurotrophic or an apoptotic molecule? In *Progress in Brain Research* (pp. 101–110). https://doi.org/10.1016/S0079-6123(03)46007-X

Fahnestock, Michalski, B., Xu, B., & Coughlin, M. (2001). The precursor pro-nerve growth factor is the predominant form of nerve growth factor in brain and is increased in Alzheimer's disease. *Molecular and Cellular Neuroscience*, *18*(2), 210–220. https://doi.org/10.1006/mcne.2001.1016

Fahnestock, Yu, G., Michalski, B., Mathew, S., Colquhoun, A., Ross, G., & Coughlin, M. (2004). The nerve growth factor precursor proNGF exhibits neurotrophic activity but is less active than mature nerve growth factor. *Journal of Neurochemistry*, *89*(3), 581–592. https://doi.org/10.1111/j.1471-4159.2004.02360.x

Fayard, B., Loeffler, S., Weis, J., Vögelin, E., & Krüttgen, A. (2005). The secreted brain-derived neurotrophic factor precursor pro-BDNF binds to TrkB and p75NTR but not to TrkA or TrkC. *Journal of Neuroscience Research*, *80*(1), 18–28. https://doi.org/10.1002/jnr.20432

Formaggio, E., Fazzini, F., Dalfini, A. C., Di Chio, M., Cantù, C., Decimo, I., Fiorini, Z., Fumagalli, G., & Chiamulera, C. (2010). Nicotine increases the expression of

neurotrophin receptor tyrosine kinase receptor A in basal forebrain cholinergic neurons. *Neuroscience*, *166*(2), 580–589. https://doi.org/10.1016/j.neuroscience.2009.12.073

Fragkouli, A., Hearn, C., Errington, M., Cooke, S., Grigoriou, M., Bliss, T., Stylianopoulou, F., & Pachnis, V. (2005). Loss of forebrain cholinergic neurons and impairment in spatial learning and memory in LHX7-deficient mice. *European Journal of Neuroscience*, *21*(11), 2923–2938. https://doi.org/10.1111/j.1460-9568.2005.04141.x

Geinisman, Y., de Toledo-Morrell, L., & Morrell, F. (1986). Loss of perforated synapses in the dentate gyrus: Morphological substrate of memory deficit in aged rats. *Proceedings of the National Academy of Sciences*, *83*(9), 3027–3031. https://doi.org/10.1073/pnas.83.9.3027

Ginty, D. (2002). Retrograde neurotrophin signaling: Trk-ing along the axon. *Current Opinion in Neurobiology*, *12*(3), 268–274. https://doi.org/10.1016/S0959-4388(02)00326-4

Glebova, N. O., & Ginty, D. D. (2005). GROWTH AND SURVIVAL SIGNALS CONTROLLING SYMPATHETIC NERVOUS SYSTEM DEVELOPMENT. *Annual Review of Neuroscience*, *28*(1), 191–222. https://doi.org/10.1146/annurev.neuro.28.061604.135659

Goedert, M., & Spillantini, M. G. (2011). Pathogenesis of the Tauopathies. *Journal of Molecular Neuroscience*, *45*(3), 425–431. https://doi.org/10.1007/s12031-011-9593-4

Gold, M. (2017). Phase II clinical trials of anti–amyloid β antibodies: When is enough, enough? In *Alzheimer's and Dementia: Translational Research and Clinical Interventions* (Vol. 3, Issue 3, pp. 402–409). https://doi.org/10.1016/j.trci.2017.04.005

Gómez-Isla, T., Hollister, R., West, H., Mui, S., Growdon, J. H., Petersen, R. C., Parisi, J. E., & Hyman, B. T. (1997). Neuronal loss correlates with but exceeds neurofibrillary tangles in Alzheimer's disease. *Annals of Neurology*, *41*(1), 17–24. https://doi.org/10.1002/ana.410410106

Grimes, M. L., Zhou, J., Beattie, E. C., Yuen, E. C., Hall, D. E., Valletta, J. S., Topp, K. S., LaVail, J. H., Bunnett, N. W., & Mobley, W. C. (1996). Endocytosis of activated trkA: Evidence that nerve growth factor induces formation of signaling endosomes. *Journal of Neuroscience*, *16*(24), 7950–7964. https://doi.org/10.1523/jneurosci.16-24-07950.1996

Gritton, H. J., Howe, W. M., Mallory, C. S., Hetrick, V. L., Berke, J. D., & Sarter, M. (2016). Cortical cholinergic signaling controls the detection of cues. *Proceedings of the National Academy of Sciences*, *113*(8), E1089–E1097. https://doi.org/10.1073/pnas.1516134113

Grothe, M., Heinsen, H., & Teipel, S. J. (2012). Atrophy of the Cholinergic Basal Forebrain Over the Adult Age Range and in Early Stages of Alzheimer's Disease. *Biological Psychiatry*, *71*(9), 805–813. https://doi.org/10.1016/j.biopsych.2011.06.019

Gu, Z., Lamb, P. W., & Yakel, J. L. (2012). Cholinergic Coordination of Presynaptic and Postsynaptic Activity Induces Timing-Dependent Hippocampal Synaptic Plasticity. *Journal of Neuroscience*, *32*(36), 12337–12348. https://doi.org/10.1523/JNEUROSCI.2129-12.2012

Guix, F. X., Wahle, T., Vennekens, K., Snellinx, A., Chávez-Gutiérrez, L., Ill-Raga, G., Ramos-Fernandez, E., Guardia-Laguarta, C., Lleó, A., Arimon, M., Berezovska, O., Muñoz, F. J., Dotti, C. G., & De Strooper, B. (2012). Modification of γ-secretase by nitrosative stress links neuronal ageing to sporadic Alzheimer's disease. *EMBO Molecular Medicine*, *4*(7), 660–673. https://doi.org/10.1002/emmm.201200243

Gustilo, M. C., Markowska, A. L., Breckler, S. J., Fleischman, C. A., Price, D. L., & Koliatsos, V. E. (1999). Evidence that nerve growth factor influences recent memory through structural changes in septohippocampal cholinergic neurons. *The Journal of Comparative Neurology*, *405*(4), 491–507. https://doi.org/10.1002/(SICI)1096-9861(19990322)405:4<491::AID-CNE4>3.0.CO;2-N

H. Ferreira-Vieira, T., M. Guimaraes, I., R. Silva, F., & M. Ribeiro, F. (2016). Alzheimer's disease: Targeting the Cholinergic System. *Current Neuropharmacology*, *14*(1), 101–115. https://doi.org/10.2174/1570159X13666150716165726

Halff, A. W., Gomez-Varela, D., John, D., & Berg, D. K. (2014). A Novel Mechanism for Nicotinic Potentiation of Glutamatergic Synapses. *Journal of Neuroscience*, *34*(6), 2051–2064. https://doi.org/10.1523/JNEUROSCI.2795-13.2014

Halliwell, B. (2006). Oxidative stress and neurodegeneration: Where are we now? *Journal of Neurochemistry*, *97*(6), 1634–1658. https://doi.org/10.1111/j.1471-4159.2006.03907.x

Hamanoue, M., Middleton, G., Wyatt, S., Jaffray, E., Hay, R. T., & Davies, A. M. (1999). P75-Mediated NF-κB Activation Enhances the Survival Response of Developing Sensory Neurons to Nerve Growth Factor. *Molecular and Cellular Neuroscience*, *14*(1), 28–40. https://doi.org/10.1006/mcne.1999.0770

Hampel, H., Mesulam, M.-M., Cuello, A. C., Farlow, M. R., Giacobini, E., Grossberg, G. T., Khachaturian, A. S., Vergallo, A., Cavedo, E., Snyder, P. J., & Khachaturian, Z. S. (2018). The cholinergic system in the pathophysiology and treatment of Alzheimer's disease. *Brain*, *141*(7), 1917–1933. https://doi.org/10.1093/brain/awy132

Hara, Y., Motoi, Y., Hikishima, K., Mizuma, H., Onoe, H., Matsumoto, S.-E., Elahi, M., Okano, H., Aoki, S., & Hattori, N. (2017). Involvement of the Septo-Hippocampal Cholinergic Pathway in Association with Septal Acetylcholinesterase Upregulation in a Mouse Model of Tauopathy. *Current Alzheimer Research*, *14*(1), 94–103. https://doi.org/10.2174/1567205013666160602235800

Hardy, J., & De Strooper, B. (2017). Alzheimer's disease: Where next for anti-amyloid therapies? *Brain*, *140*(4), 853–855. https://doi.org/10.1093/brain/awx059

Harrington, A. W., & Ginty, D. D. (2013). Long-distance retrograde neurotrophic factor signalling in neurons. *Nature Reviews Neuroscience*, *14*(3), 177–187. https://doi.org/10.1038/nrn3253

Harrington, A. W., St. Hillaire, C., Zweifel, L. S., Glebova, N. O., Philippidou, P., Halegoua, S., & Ginty, D. D. (2011). Recruitment of Actin Modifiers to TrkA Endosomes Governs Retrograde NGF Signaling and Survival. *Cell*, *146*(3), 421–434. https://doi.org/10.1016/j.cell.2011.07.008

Hartikka, J., & Hefti, F. (1988). Development of septal cholinergic neurons in culture: Plating density and glial cells modulate effects of NGF on survival, fiber growth, and expression of transmitter-specific enzymes. *The Journal of Neuroscience: The Official Journal of the Society for Neuroscience*, *8*(8), 2967–2985.

Hasan, W., Pedchenko, T., Krizsan-Agbas, D., Baum, L., & Smith, P. G. (2003). Sympathetic neurons synthesize and secrete pro-nerve growth factor protein. *Journal of Neurobiology*, *57*(1), 38–53. https://doi.org/10.1002/neu.10250

Hatanaka, H., Tsukui, H., & Nihonmatsu, I. (1988). Developmental change in the nerve growth factor action from induction of choline acetyltransferase to promotion of cell survival in cultured basal forebrain cholinergic neurons from postnatal rats. *Developmental Brain Research*, *39*(1), 85–95. https://doi.org/10.1016/0165-3806(88)90069-7

Hendry, I. A., Stockel, K., Thoenen, H., & Iversen, L. L. (1974). The retrograde axonal transport of nerve growth factor. *Brain Research*, *68*(1), 103–121. https://doi.org/10.1016/0006-8993(74)90536-8

Hirokawa, N. (1998). Kinesin and Dynein Superfamily Proteins and the Mechanism of Organelle Transport. *Science*, *279*(5350), 519–526. https://doi.org/10.1126/science.279.5350.519

Hirokawa, N., Noda, Y., Tanaka, Y., & Niwa, S. (2009). Kinesin superfamily motor proteins and intracellular transport. *Nature Reviews Molecular Cell Biology*, *10*(10), 682–696. https://doi.org/10.1038/nrm2774

Howe, W. M., Berry, A. S., Francois, J., Gilmour, G., Carp, J. M., Tricklebank, M., Lustig, C., & Sarter, M. (2013). Prefrontal Cholinergic Mechanisms Instigating Shifts from Monitoring for Cues to Cue-Guided Performance: Converging Electrochemical and fMRI Evidence from Rats and Humans. *Journal of Neuroscience*, *33*(20), 8742–8752. https://doi.org/10.1523/JNEUROSCI.5809-12.2013

Huang, S.-H., Duan, S., Sun, T., Wang, J., Zhao, L., Geng, Z., Yan, J., Sun, H.-J., & Chen, Z.-Y. (2011). JIP3 Mediates TrkB Axonal Anterograde Transport and Enhances BDNF Signaling by Directly Bridging TrkB with Kinesin-1. *Journal of Neuroscience*, *31*(29), 10602–10614. https://doi.org/10.1523/JNEUROSCI.0436-11.2011

Ibáñez, C. F. (1996). Neurotrophin-4: The odd one out in the neurotrophin family. *Neurochemical Research*, *21*(7), 787–793. https://doi.org/10.1007/BF02532301

Ioannou, M., & Fahnestock, M. (2017). ProNGF, but Not NGF, Switches from Neurotrophic to Apoptotic Activity in Response to Reductions in TrkA Receptor

Levels. *International Journal of Molecular Sciences*, *18*(3), 599. https://doi.org/10.3390/ijms18030599

Ip, N. Y., Ibanez, C. F., Nye, S. H., McClain, J., Jones, P. F., Gies, D. R., Belluscio, L., Le Beau, M. M., Espinosa, R., Squinto, S. P., Persson, H., & Yancopoulos, G. D. (1992). Mammalian neurotrophin-4: Structure, chromosomal localization, tissue distribution, and receptor specificity. *Proceedings of the National Academy of Sciences of the United States of America*, *89*(7), 3060–3064. https://doi.org/10.1073/pnas.89.7.3060

Ip, N. Y., Li, Y., Yancopoulos, G. D., & Lindsay, R. M. (1993). Cultured hippocampal neurons show responses to BDNF, NT-3, and NT-4, but not NGF. *Journal of Neuroscience*, *13*(8), 3394–3405.

Isonaka, R., Hiruma, H., & Kawakami, T. (2011). Inhibition of Axonal Transport Caused by tert-Butyl Hydroperoxide in Cultured Mouse Dorsal Root Ganglion Neurons. *Journal of Molecular Neuroscience*, *45*(2), 194–201. https://doi.org/10.1007/s12031-010-9457-3

Jaulin, F., Xue, X., Rodriguez-Boulan, E., & Kreitzer, G. (2007). Polarization-Dependent Selective Transport to the Apical Membrane by KIF5B in MDCK Cells. *Developmental Cell*, *13*(4), 511–522. https://doi.org/10.1016/j.devcel.2007.08.001

Johnson, G. V. W. (2004). Tau phosphorylation in neuronal cell function and dysfunction. *Journal of Cell Science*, *117*(24), 5721–5729. https://doi.org/10.1242/jcs.01558

Jung, J. H., Park, M. H., Choi, S. Y., & Koh, J. Y. (2005). Activation of the Trk signaling pathway by extracellular zinc. Role of metalloproteinases. *Journal of Biological Chemistry*. https://doi.org/10.1074/jbc.M403172200

Kalmbach, A., & Waters, J. (2014). Modulation of high- and low-frequency components of the cortical local field potential via nicotinic and muscarinic acetylcholine receptors in anesthetized mice. *Journal of Neurophysiology*. https://doi.org/10.1152/jn.00244.2013

Kaplan, D. R., & Miller, F. D. (2000). Neurotrophin signal transduction in the nervous system. In *Current Opinion in Neurobiology* (Vol. 10, Issue 3, pp. 381–391). https://doi.org/10.1016/S0959-4388(00)00092-1

Katoh-Semba, R., Takeuchi, I. K., Semba, R., & Kato, K. (2002). Distribution of Brain-Derived Neurotrophic Factor in Rats and Its Changes with Development in the Brain. *Journal of Neurochemistry*, *69*(1), 34–42. https://doi.org/10.1046/j.1471-4159.1997.69010034.x

Kish, S. J., Bergeron, C., Rajput, A., Dozic, S., Mastrogiacomo, F., Chang, L.-J., Wilson, J. M., DiStefano, L. M., & Nobrega, J. N. (1992). Brain Cytochrome Oxidase in Alzheimer's Disease. *Journal of Neurochemistry*, *59*(2), 776–779. https://doi.org/10.1111/j.1471-4159.1992.tb09439.x

Kojima, M., Ikeuchi, T., & Hatanaka, H. (1995). Role of nerve growth factor in the expression oftrkA mRNA in cultured embryonic rat basal forebrain cholinergic neurons. *Journal of Neuroscience Research*, *42*(6), 775–783. https://doi.org/10.1002/jnr.490420606

Köppen, J. R., Stuebing, S. L., Sieg, M. L., Blackwell, A. A., Blankenship, P. A., Cheatwood, J. L., & Wallace, D. G. (2016). Cholinergic deafferentation of the

hippocampus causes non-temporally graded retrograde amnesia in an odor discrimination task. *Behavioural Brain Research*, *299*, 97–104. https://doi.org/10.1016/j.bbr.2015.11.021

Koshimizu, H., Hazama, S., Hara, T., Ogura, A., & Kojima, M. (2010). Distinct signaling pathways of precursor BDNF and mature BDNF in cultured cerebellar granule neurons. *Neuroscience Letters*, *473*(3), 229–232. https://doi.org/10.1016/j.neulet.2010.02.055

Koshimizu, H., Kiyosue, K., Hara, T., Hazama, S., Suzuki, S., Uegaki, K., Nagappan, G., Zaitsev, E., Hirokawa, T., Tatsu, Y., Ogura, A., Lu, B., & Kojima, M. (2009). Multiple functions of precursor BDNF to CNS neurons: Negative regulation of neurite growth, spine formation and cell survival. *Molecular Brain*, *2*(1), 27–27. https://doi.org/10.1186/1756-6606-2-27

Kowiański, P., Lietzau, G., Czuba, E., Waśkow, M., Steliga, A., & Moryś, J. (2018). BDNF: A Key Factor with Multipotent Impact on Brain Signaling and Synaptic Plasticity. *Cellular and Molecular Neurobiology*, *38*(3), 579–593. https://doi.org/10.1007/s10571-017-0510-4

Krystosek, A., & Seeds, N. (1981). Plasminogen activator release at the neuronal growth cone. *Science*, *213*(4515), 1532–1534. https://doi.org/10.1126/science.7197054

Kuruvilla, R., Ye, H., & Ginty, D. D. (2000). Spatially and Functionally Distinct Roles of the PI3-K Effector Pathway during NGF Signaling in Sympathetic Neurons. *Neuron*, *27*(3), 499–512. https://doi.org/10.1016/S0896-6273(00)00061-1

Kuruvilla, R., Zweifel, L. S., Glebova, N. O., Lonze, B. E., Valdez, G., Ye, H., & Ginty, D. D. (2004). A Neurotrophin Signaling Cascade Coordinates Sympathetic Neuron Development through Differential Control of TrkA Trafficking and Retrograde Signaling. *Cell*, *118*(2), 243–255. https://doi.org/10.1016/j.cell.2004.06.021

Kurz, D. J., Decary, S., Hong, Y., & Erusalimsky, J. D. (2000). Senescence-associated (beta)-galactosidase reflects an increase in lysosomal mass during replicative ageing of human endothelial cells. *Journal of Cell Science*, *113 (Pt 2*, 3613–3622.

Lai, Z. C., Moss, M. B., Killiany, R. J., Rosene, D. L., & Herndon, J. G. (1995). Executive system dysfunction in the aged monkey: Spatial and object reversal learning. *Neurobiology of Aging*, *16*(6), 947–954. https://doi.org/10.1016/0197-4580(95)02014-4

Large, T., Bodary, S., Clegg, D., Weskamp, G., Otten, U., & Reichardt, L. (1986). Nerve growth factor gene expression in the developing rat brain. *Science*, *234*(4774), 352–355. https://doi.org/10.1126/science.3764415

Latina, V., Caioli, S., Zona, C., Ciotti, M. T., Amadoro, G., & Calissano, P. (2017). Impaired NGF/TrkA Signaling Causes Early AD-Linked Presynaptic Dysfunction in Cholinergic Primary Neurons. *Frontiers in Cellular Neuroscience*, *11*, 68. https://doi.org/10.3389/fncel.2017.00068

Lee, R., Kermani, P., Teng, K., & Hempstead, B. (2001). Regulation of Cell Survival by Secreted Proneurotrophins. *Science*, *294*(5548), 1945–1948. https://doi.org/10.1126/science.1065057

Leuner, K., Hauptmann, S., Abdel-Kader, R., Scherping, I., Keil, U., Strosznajder, J. B., Eckert, A., & Müller, W. E. (2007). Mitochondrial Dysfunction: The First Domino in Brain Aging and Alzheimer's Disease? *Antioxidants & Redox Signaling*, *9*(10), 1659–1676. https://doi.org/10.1089/ars.2007.1763

Leuner, K., Schütt, T., Kurz, C., Eckert, S. H., Schiller, C., Occhipinti, A., Mai, S., Jendrach, M., Eckert, G. P., Kruse, S. E., Palmiter, R. D., Brandt, U., Dröse, S., Wittig, I., Willem, M., Haass, C., Reichert, A. S., & Müller, W. E. (2012). Mitochondrion-Derived Reactive Oxygen Species Lead to Enhanced Amyloid Beta Formation. *Antioxidants & Redox Signaling*, *16*(12), 1421–1433. https://doi.org/10.1089/ars.2011.4173

Leutner, S., Schindowski, K., Frölich, L., Maurer, K., Kratzsch, T., Eckert, A., & Müller, W. E. (2005). Enhanced ROS-Generation in Lymphocytes from Alzheimer's Patients. *Pharmacopsychiatry*, *38*(6), 312–315. https://doi.org/10.1055/s-2005-916186

Levi-Montalcini, R. (1987). The nerve growth factor 35 years later. *Science*, *237*(4819), 1154–1162. https://doi.org/10.1126/science.3306916

Levi-Montalcini, R., & Cohen, S. (1956). IN VITRO AND IN VIVO EFFECTS OF A NERVE GROWTH-STIMULATING AGENT ISOLATED FROM SNAKE VENOM. *Proceedings of the National Academy of Sciences*, *42*(9), 695–699. https://doi.org/10.1073/pnas.42.9.695

Li, Y., Holtzman, D., Kromer, L., Kaplan, D., Chua-Couzens, J., Clary, D., Knusel, B., & Mobley, W. (1995). Regulation of TrkA and ChAT expression in developing rat basal forebrain: Evidence that both exogenous and endogenous NGF regulate differentiation of cholinergic neurons. *The Journal of Neuroscience*, *15*(4), 2888–2905. https://doi.org/10.1523/JNEUROSCI.15-04-02888.1995

Liao, P.-C., Tandarich, L. C., & Hollenbeck, P. J. (2017). ROS regulation of axonal mitochondrial transport is mediated by Ca2+ and JNK in Drosophila. *PLOS ONE*, *12*(5), e0178105. https://doi.org/10.1371/journal.pone.0178105

Liu, A. K. L., Chang, R. C.-C., Pearce, R. K. B., & Gentleman, S. M. (2015). Nucleus basalis of Meynert revisited: Anatomy, history and differential involvement in Alzheimer's and Parkinson's disease. *Acta Neuropathologica*, *129*(4), 527–540. https://doi.org/10.1007/s00401-015-1392-5

Lores-Arnaiz, S., Lombardi, P., Karadayian, A. G., Orgambide, F., Cicerchia, D., & Bustamante, J. (2016). Brain cortex mitochondrial bioenergetics in synaptosomes and non-synaptic mitochondria during aging. *Neurochemical Research*, *41*(1–2), 353–363. https://doi.org/10.1007/s11064-015-1817-5

Lu, B., Nagappan, G., & Lu, Y. (2014). BDNF and synaptic plasticity, cognitive function, and dysfunction. In *Handbook of experimental pharmacology* (Vol. 220). https://doi.org/10.1007/978-3-642-45106-5

Lubos, E., Kelly, N. J., Oldebeken, S. R., Leopold, J. A., Zhang, Y.-Y., Loscalzo, J., & Handy, D. E. (2011). Glutathione Peroxidase-1 Deficiency Augments Proinflammatory Cytokine-induced Redox Signaling and Human Endothelial Cell Activation. *Journal of Biological Chemistry*, *286*(41), 35407–35417. https://doi.org/10.1074/jbc.M110.205708

MacAskill, A. F., & Kittler, J. T. (2010). Control of mitochondrial transport and localization in neurons. In *Trends in Cell Biology* (Vol. 20, Issue 2, pp. 102–112). https://doi.org/10.1016/j.tcb.2009.11.002

MacAskill, A. F., Rinholm, J. E., Twelvetrees, A. E., Arancibia-Carcamo, I. L., Muir, J., Fransson, A., Aspenstrom, P., Attwell, D., & Kittler, J. T. (2009). Miro1 Is a Calcium Sensor for Glutamate Receptor-Dependent Localization of Mitochondria at Synapses. *Neuron*, *61*(4), 541–555. https://doi.org/10.1016/j.neuron.2009.01.030

Maday, S., Twelvetrees, A. E., Moughamian, A. J., & Holzbaur, E. L. F. (2014). Axonal Transport: Cargo-Specific Mechanisms of Motility and Regulation. *Neuron*, *84*(2), 292–309. https://doi.org/10.1016/j.neuron.2014.10.019

Maisonpierre, P., Belluscio, L., Squinto, S., Ip, N., Furth, M., Lindsay, R., & Yancopoulos, G. (1990). Neurotrophin-3: A neurotrophic factor related to NGF and BDNF. *Science*, *247*(4949), 1446–1451. https://doi.org/10.1126/science.2321006

Martin, M. G., Perga, S., Trovò, L., Rasola, A., Holm, P., Rantamäki, T., Harkany, T., Castrén, E., Chiara, F., & Dotti, C. G. (2008). Cholesterol Loss Enhances TrkB Signaling in Hippocampal Neurons Aging in Vitro. *Molecular Biology of the Cell*, *19*(5), 2101–2112. https://doi.org/10.1091/mbc.e07-09-0897

Masoudi, R., Ioannou, M. S., Coughlin, M. D., Pagadala, P., Neet, K. E., Clewes, O., Allen, S. J., Dawbarn, D., & Fahnestock, M. (2009). Biological Activity of Nerve Growth Factor Precursor Is Dependent upon Relative Levels of Its Receptors. *Journal of Biological Chemistry*, *284*(27), 18424–18433. https://doi.org/10.1074/jbc.M109.007104

McGleenon, Dynan, & Passmore. (2001). Acetylcholinesterase inhibitors in Alzheimer's disease. *British Journal of Clinical Pharmacology*, *48*(4), 471–480. https://doi.org/10.1046/j.1365-2125.1999.00026.x

McGregor, C. E., & English, A. W. (2019). The Role of BDNF in Peripheral Nerve Regeneration: Activity-Dependent Treatments and Val66Met. *Frontiers in Cellular Neuroscience*, *12*. https://doi.org/10.3389/fncel.2018.00522

Mecocci, P., Beal, M. F., Cecchetti, R., Polidori, M. C., Cherubini, A., Chionne, F., Avellini, L., Romano, G., & Senin, U. (1997). Mitochondrial membrane fluidity and oxidative damage to mitochondrial DNA in aged and AD human brain. *Molecular and Chemical Neuropathology*, *31*(1), 53–64. https://doi.org/10.1007/BF02815160

Mecocci, P., MacGarvey, U., & Beal, M. F. (1994). Oxidative damage to mitochondrial DNA is increased in Alzheimer's disease. *Annals of Neurology*, *36*(5), 747–751. https://doi.org/10.1002/ana.410360510

Miranda, M., Morici, J. F., Zanoni, M. B., & Bekinschtein, P. (2019). Brain-Derived Neurotrophic Factor: A Key Molecule for Memory in the Healthy and the Pathological Brain. *Frontiers in Cellular Neuroscience*, *13*. https://doi.org/10.3389/fncel.2019.00363

Misgeld, T., & Schwarz, T. L. (2017). Mitostasis in Neurons: Maintaining Mitochondria in an Extended Cellular Architecture. *Neuron*, *96*(3), 651–666. https://doi.org/10.1016/j.neuron.2017.09.055

Mishima, K., Handa, J. T., Aotaki-Keen, A., Lutty, G. A., Morse, L. S., & Hjelmeland, L. M. (1999). Senescence-associated beta-galactosidase histochemistry for the primate eye. *Investigative Ophthalmology & Visual Science*, *40*(7), 1590–1593.

Mitsushima, D., Sano, A., & Takahashi, T. (2013). A cholinergic trigger drives learning-induced plasticity at hippocampal synapses. *Nature Communications*, *4*(1), 2760. https://doi.org/10.1038/ncomms3760

Mosconi, L. (2013). Glucose metabolism in normal aging and Alzheimer's disease: Methodological and physiological considerations for PET studies. *Clinical and Translational Imaging*, *1*(4), 217–233. https://doi.org/10.1007/s40336-013-0026-y

Moughamian, A. J., Osborn, G. E., Lazarus, J. E., Maday, S., & Holzbaur, E. L. F. (2013). Ordered Recruitment of Dynactin to the Microtubule Plus-End is Required for Efficient Initiation of Retrograde Axonal Transport. *Journal of Neuroscience*, *33*(32), 13190–13203. https://doi.org/10.1523/JNEUROSCI.0935-13.2013

Mowla, S. J., Farhadi, H. F., Pareek, S., Atwal, J. K., Morris, S. J., Seidah, N. G., & Murphy, R. A. (2001). Biosynthesis and Post-translational Processing of the Precursor to Brain-derived Neurotrophic Factor. *Journal of Biological Chemistry*, *276*(16), 12660–12666. https://doi.org/10.1074/jbc.M008104200

Mowla, S. J., Pareek, S., Farhadi, H. F., Petrecca, K., Fawcett, J. P., Seidah, N. G., Morris, S. J., Sossin, W. S., & Murphy, R. A. (1999). Differential Sorting of Nerve Growth Factor and Brain-Derived Neurotrophic Factor in Hippocampal Neurons. *The Journal of Neuroscience*, *19*(6), 2069–2080. https://doi.org/10.1523/JNEUROSCI.19-06-02069.1999

Mullane, K., & Williams, M. (2018). Alzheimer's disease (AD) therapeutics – 1: Repeated clinical failures continue to question the amyloid hypothesis of AD and the current understanding of AD causality. *Biochemical Pharmacology*, *158*, 359–375. https://doi.org/10.1016/j.bcp.2018.09.026

Nagappan, G., Zaitsev, E., Senatorov, V. V., Yang, J., Hempstead, B. L., & Lu, B. (2009). Control of extracellular cleavage of ProBDNF by high frequency neuronal activity. *Proceedings of the National Academy of Sciences*, *106*(4), 1267–1272. https://doi.org/10.1073/pnas.0807322106

Navarro, A., López-Cepero, J. M., Bández, M. J., Sánchez-Pino, M.-J., Gómez, C., Cadenas, E., & Boveris, A. (2008). Hippocampal mitochondrial dysfunction in rat aging. *American Journal of Physiology-Regulatory, Integrative and Comparative Physiology*, *294*(2), R501–R509. https://doi.org/10.1152/ajpregu.00492.2007

Niewiadomska, G., Komorowski, S., & Baksalerska-Pazera, M. (2002). Amelioration of cholinergic neurons dysfunction in aged rats depends on the continuous supply of NGF. *Neurobiology of Aging*, *23*(4), 601–613. https://doi.org/10.1016/S0197-4580(01)00345-1

Nissanka, N., & Moraes, C. T. (2018). Mitochondrial DNA damage and reactive oxygen species in neurodegenerative disease. *FEBS Letters*, *592*(5), 728–742. https://doi.org/10.1002/1873-3468.12956

Noble, W., Hanger, D. P., Miller, C. C. J., & Lovestone, S. (2013). The Importance of Tau Phosphorylation for Neurodegenerative Diseases. *Frontiers in Neurology*, *4*. https://doi.org/10.3389/fneur.2013.00083

Palomer, E., Martín-Segura, A., Baliyan, S., Ahmed, T., Balschun, D., Venero, C., Martin, M. G., & Dotti, C. G. (2016). Aging Triggers a Repressive Chromatin State at Bdnf Promoters in Hippocampal Neurons. *Cell Reports*, *16*(11), 2889–2900. https://doi.org/10.1016/j.celrep.2016.08.028

Parikh, V., Howe, W. M., Welchko, R. M., Naughton, S. X., D'Amore, D. E., Han, D. H., Deo, M., Turner, D. L., & Sarter, M. (2013). Diminished trkA receptor signaling reveals cholinergic-attentional vulnerability of aging. *European Journal of Neuroscience*, *37*(2), 278–293. https://doi.org/10.1111/ejn.12090

Perez, S. E., He, B., Muhammad, N., Oh, K.-J., Fahnestock, M., Ikonomovic, M. D., & Mufson, E. J. (2011). Cholinotrophic basal forebrain system alterations in 3xTg-AD transgenic mice. *Neurobiology of Disease*, *41*(2), 338–352. https://doi.org/10.1016/j.nbd.2010.10.002

Petersen, R. C., Smith, G., Kokmen, E., Ivnik, R. J., & Tangalos, E. G. (1992). Memory function in normal aging. *Neurology*, *42*(2), 396–396. https://doi.org/10.1212/WNL.42.2.396

Poon, W. W., Blurton-Jones, M., Tu, C. H., Feinberg, L. M., Chabrier, M. A., Harris, J. W., Jeon, N. L., & Cotman, C. W. (2011). β-Amyloid impairs axonal BDNF retrograde trafficking. *Neurobiology of Aging*, *32*(5), 821–833. https://doi.org/10.1016/j.neurobiolaging.2009.05.012

Porter, N. M., Thibault, O., Thibault, V., Chen, K. C., & Landfield, P. W. (1997). Calcium channel density and hippocampal cell death with age in long-term culture. *The Journal of Neuroscience : The Official Journal of the Society for Neuroscience*, *17*(14), 5629–5639.

Pruunsild, P., Kazantseva, A., Aid, T., Palm, K., & Timmusk, T. (2007). Dissecting the human BDNF locus: Bidirectional transcription, complex splicing, and multiple promoters. *Genomics*, *90*(3), 397–406. https://doi.org/10.1016/j.ygeno.2007.05.004

Quinlan, C. L., Perevoshchikova, I. V., Hey-Mogensen, M., Orr, A. L., & Brand, M. D. (2013). Sites of reactive oxygen species generation by mitochondria oxidizing different substrates. *Redox Biology*, *1*(1), 304–312. https://doi.org/10.1016/j.redox.2013.04.005

Rao, A. N., & Baas, P. W. (2018). Polarity Sorting of Microtubules in the Axon. *Trends in Neurosciences*, *41*(2), 77–88. https://doi.org/10.1016/j.tins.2017.11.002

Rasmussen, J., Jucker, M., & Walker, L. C. (2017). Aβ seeds and prions: How close the fit? *Prion*, *11*(4), 215–225. https://doi.org/10.1080/19336896.2017.1334029

Rauskolb, S., Zagrebelsky, M., Dreznjak, A., Deogracias, R., Matsumoto, T., Wiese, S., Erne, B., Sendtner, M., Schaeren-Wiemers, N., Korte, M., & Barde, Y.-A. (2010). Global Deprivation of Brain-Derived Neurotrophic Factor in the CNS Reveals an Area-Specific Requirement for Dendritic Growth. *Journal of Neuroscience*, *30*(5), 1739–1749. https://doi.org/10.1523/JNEUROSCI.5100-09.2010

Roberts, A. J., Kon, T., Knight, P. J., Sutoh, K., & Burgess, S. A. (2013). Functions and mechanics of dynein motor proteins. *Nature Reviews Molecular Cell Biology*, *14*(11), 713–726. https://doi.org/10.1038/nrm3667

Roland, J. J., Stewart, A. L., Janke, K. L., Gielow, M. R., Kostek, J. A., Savage, L. M., Servatius, R. J., & Pang, K. C. H. (2014). Medial Septum-Diagonal Band of Broca (MSDB) GABAergic Regulation of Hippocampal Acetylcholine Efflux Is Dependent on Cognitive Demands. *Journal of Neuroscience*, *34*(2), 506–514. https://doi.org/10.1523/JNEUROSCI.2352-13.2014

Rong, J. (2006). Regulation of Intracellular Trafficking of Huntingtin-Associated Protein-1 Is Critical for TrkA Protein Levels and Neurite Outgrowth. *Journal of Neuroscience*, *26*(22), 6019–6030. https://doi.org/10.1523/JNEUROSCI.1251-06.2006

Runfeldt, M. J., Sadovsky, A. J., & MacLean, J. N. (2014). Acetylcholine functionally reorganizes neocortical microcircuits. *Journal of Neurophysiology*, *112*(5), 1205–1216. https://doi.org/10.1152/jn.00071.2014

Rylett, R. J., & Williams, L. R. (1994). Role of neurotrophins in cholinergic-neurone function in the adult and aged CNS. *Trends in Neurosciences*, *17*(11), 486–490. https://doi.org/10.1016/0166-2236(94)90138-4

Salehi, A., Delcroix, J.-D., Belichenko, P. V., Zhan, K., Wu, C., Valletta, J. S., Takimoto-Kimura, R., Kleschevnikov, A. M., Sambamurti, K., Chung, P. P., Xia, W., Villar, A., Campbell, W. A., Kulnane, L. S., Nixon, R. A., Lamb, B. T., Epstein, C. J., Stokin, G. B., Goldstein, L. S. B., & Mobley, W. C. (2006). Increased App Expression in a Mouse Model of Down's Syndrome Disrupts NGF Transport and Causes Cholinergic Neuron Degeneration. *Neuron*, *51*(1), 29–42. https://doi.org/10.1016/j.neuron.2006.05.022

Sanchez-Ortiz, E., Yui, D., Song, D., Li, Y., Rubenstein, J. L., Reichardt, L. F., & Parada, L. F. (2012). TrkA Gene Ablation in Basal Forebrain Results in Dysfunction of the Cholinergic Circuitry. *Journal of Neuroscience*, *32*(12), 4065–4079. https://doi.org/10.1523/JNEUROSCI.6314-11.2012

Schmitz, T. W., Nathan Spreng, R., Weiner, M. W. M., Aisen, P., Petersen, R., Jack, C. R., Jagust, W., Trojanowki, J. Q., Toga, A. W., Beckett, L., Green, R. C., Saykin, A. J., Morris, J., Shaw, L. M., Khachaturian, Z., Sorensen, G., Kuller, L., Raichle, M., Paul, S., … Furst, A. J. (2016). Basal forebrain degeneration precedes and predicts the cortical spread of Alzheimer's pathology. *Nature Communications*, *7*(1), 13249. https://doi.org/10.1038/ncomms13249

Schulte-Herbrüggen, O., Eckart, S., Deicke, U., Kühl, A., Otten, U., Danker-Hopfe, H., Abramowski, D., Staufenbiel, M., & Hellweg, R. (2008). Age-dependent time course of cerebral brain-derived neurotrophic factor, nerve growth factor, and neurotrophin-3 in APP23 transgenic mice. *Journal of Neuroscience Research*, *86*(12), 2774–2783. https://doi.org/10.1002/jnr.21704

Scott, S. A., Mufson, E. J., Weingartner, J. A., Skau, K. A., & Crutcher, K. A. (1995). Nerve growth factor in Alzheimer's disease: Increased levels throughout the brain coupled with declines in nucleus basalis. *The Journal of Neuroscience : The Official Journal of the Society for Neuroscience*, *15*(9), 6213–6221.

Scott-Solomon, E., & Kuruvilla, R. (2018). Mechanisms of neurotrophin trafficking via Trk receptors. *Molecular and Cellular Neuroscience*, *91*, 25–33. https://doi.org/10.1016/j.mcn.2018.03.013

Seidah, N. G., Benjannet, S., Pareek, S., Chrétien, M., & Murphy, R. A. (1996). Cellular processing of the neurotrophin precursors of NT3 and BDNF by the mammalian proprotein convertases. *FEBS Letters*, *379*(3), 247–250. https://doi.org/10.1016/0014-5793(95)01520-5

Seidah, N. G., Benjannet, S., Pareek, S., Savaria, D., Hamelin, J., Goulet, B., Laliberte, J., Lazure, C., Chretein, M., & Murphy, R. A. (1996). Cellular processing of the nerve growth factor precursor by the mammalian pro-protein convertases. *Biochemical Journal*, *314*(3), 951–960. https://doi.org/10.1042/bj3140951

Seiler, M., & Schwab, M. E. (1984). Specific retrograde transport of nerve growth factor (NGF) from neocortex to nucleus basalis in the rat. *Brain Research*, *300*(1), 33–39. https://doi.org/10.1016/0006-8993(84)91338-6

Selby, M. J., Edwards, R., Sharp, F., & Rutter, W. J. (1987). Mouse nerve growth factor gene: Structure and expression. *Molecular and Cellular Biology*, *7*(9), 3057–3064. https://doi.org/10.1128/MCB.7.9.3057

Sen, P., Georgalas, C., & Bhattacharyya, A. K. (2006). A systematic review of the role of proton pump inhibitors for symptoms of laryngopharyngeal reflux. *Clinical Otolaryngology*, *31*(1), 20–24. https://doi.org/10.1111/j.1749-4486.2006.01134.x

Senger, D. L., & Campenot, R. B. (1997). Rapid Retrograde Tyrosine Phosphorylation of trkA and Other Proteins in Rat Sympathetic Neurons in Compartmented Cultures. *Journal of Cell Biology*, *138*(2), 411–421. https://doi.org/10.1083/jcb.138.2.411

Sengupta, U., Nilson, A. N., & Kayed, R. (2016). The Role of Amyloid-β Oligomers in Toxicity, Propagation, and Immunotherapy. *EBioMedicine*, *6*, 42–49. https://doi.org/10.1016/j.ebiom.2016.03.035

Shekari, A., Mahadeo, C., Sanwalka, N., and Fahnestock, M. Neurotrophins and Cell Death. *Neurodevelopmental Pediatrics: Genetic and Environmental Influences*, Springer. In press (2022)

Shelton, D. L., & Reichardt, L. F. (1986). Studies on the expression of the beta nerve growth factor (NGF) gene in the central nervous system: Level and regional distribution of NGF mRNA suggest that NGF functions as a trophic factor for several distinct populations of neurons. *Proceedings of the National Academy of Sciences*, *83*(8), 2714–2718. https://doi.org/10.1073/pnas.83.8.2714

Sheng, Z.-H. (2014). Mitochondrial trafficking and anchoring in neurons: New insight and implications. *The Journal of Cell Biology*, *204*(7), 1087–1098. https://doi.org/10.1083/jcb.201312123

Simon, A. R., Rai, U., Fanburg, B. L., & Cochran, B. H. (1998). Activation of the JAK-STAT pathway by reactive oxygen species. *American Journal of Physiology-Cell Physiology*, *275*(6), C1640–C1652. https://doi.org/10.1152/ajpcell.1998.275.6.C1640

Smith, M. A., Richey Harris, P. L., Sayre, L. M., Beckman, J. S., & Perry, G. (1997). Widespread peroxynitrite-mediated damage in Alzheimer's disease. *The Journal*

of Neuroscience: The Official Journal of the Society for Neuroscience, *17*(8), 2653–2657.

Sodero, A. O., Weissmann, C., Ledesma, M. D., & Dotti, C. G. (2011). Cellular stress from excitatory neurotransmission contributes to cholesterol loss in hippocampal neurons aging in vitro. *Neurobiology of Aging*, *32*(6), 1043–1053. https://doi.org/10.1016/j.neurobiolaging.2010.06.001

Stykel, M. G., Humphries, K., Kirby, M. P., Czaniecki, C., Wang, T., Ryan, T., Bamm, V., & Ryan, S. D. (2018). Nitration of microtubules blocks axonal mitochondrial transport in a human pluripotent stem cell model of Parkinson's disease. *The FASEB Journal*, *32*(10), 5350–5364. https://doi.org/10.1096/fj.201700759RR

Subbarao, K. V., Richardson, J. S., & Ang, L. C. (1990). Autopsy Samples of Alzheimer's Cortex Show Increased Peroxidation In Vitro. *Journal of Neurochemistry*, *55*(1), 342–345. https://doi.org/10.1111/j.1471-4159.1990.tb08858.x

Sun, Chen, B.-Y., Xia, Y., Wang, J.-J., & Chen, L.-W. (2013). Functional switch from pro-neurotrophins to mature neurotrophins. *Current Protein & Peptide Science*, *14*(7), 617–625. https://doi.org/10.2174/1389203711209070658

Sun, Li, Y., Li, T., Ma, H., Guo, Y., Jiang, X., Hou, M., Huang, S., & Chen, Z. (2017). JIP1 and JIP3 cooperate to mediate TrkB anterograde axonal transport by activating kinesin-1. *Cellular and Molecular Life Sciences*, *74*(21), 4027–4044. https://doi.org/10.1007/s00018-017-2568-z

Sun, Y., Lim, Y., Li, F., Liu, S., Lu, J.-J., Haberberger, R., Zhong, J.-H., & Zhou, X.-F. (2012). ProBDNF Collapses Neurite Outgrowth of Primary Neurons by Activating RhoA. *PLoS ONE*, *7*(4), e35883. https://doi.org/10.1371/journal.pone.0035883

Tanaka, Y., Niwa, S., Dong, M., Farkhondeh, A., Wang, L., Zhou, R., & Hirokawa, N. (2016). The Molecular Motor KIF1A Transports the TrkA Neurotrophin Receptor and Is Essential for Sensory Neuron Survival and Function. *Neuron*, *90*(6), 1215–1229. https://doi.org/10.1016/j.neuron.2016.05.002

Tapia-Arancibia, L., Aliaga, E., Silhol, M., & Arancibia, S. (2008). New insights into brain BDNF function in normal aging and Alzheimer disease. *Brain Research Reviews*, *59*(1), 201–220. https://doi.org/10.1016/j.brainresrev.2008.07.007

Taylor, A. M., Blurton-Jones, M., Rhee, S. W., Cribbs, D. H., Cotman, C. W., & Jeon, N. L. (2005). A microfluidic culture platform for CNS axonal injury, regeneration and transport. *Nature Methods*, *2*(8), 599–605. https://doi.org/10.1038/nmeth777

Thal, D. R., Attems, J., & Ewers, M. (2014). Spreading of Amyloid, Tau, and Microvascular Pathology in Alzheimer's Disease: Findings from Neuropathological and Neuroimaging Studies. *Journal of Alzheimer's Disease*, *42*(s4), S421–S429. https://doi.org/10.3233/JAD-141461

Timmusk, T., Palm, K., Metsis, M., Reintam, T., Paalme, V., Saarma, M., & Persson, H. (1993). Multiple promoters direct tissue-specific expression of the rat BDNF gene. *Neuron*, *10*(3), 475–489. https://doi.org/10.1016/0896-6273(93)90335-O

Tönnies, E., & Trushina, E. (2017). Oxidative Stress, Synaptic Dysfunction, and Alzheimer's Disease. *Journal of Alzheimer's Disease*, *57*(4), 1105–1121. https://doi.org/10.3233/JAD-161088

Torreilles, F., Salman-Tabcheh, S., Guérin, M.-C., & Torreilles, J. (1999). Neurodegenerative disorders: The role of peroxynitrite. *Brain Research Reviews*, *30*(2), 153–163. https://doi.org/10.1016/S0165-0173(99)00014-4

Tramutola, A., Lanzillotta, C., Perluigi, M., & Butterfield, D. A. (2017). Oxidative stress, protein modification and Alzheimer disease. *Brain Research Bulletin*, *133*, 88–96. https://doi.org/10.1016/j.brainresbull.2016.06.005

Tsui-Pierchala, B. A., & Ginty, D. D. (1999). Characterization of an NGF–P-TrkA Retrograde-Signaling Complex and Age-Dependent Regulation of TrkA Phosphorylation in Sympathetic Neurons. *The Journal of Neuroscience*, *19*(19), 8207–8218. https://doi.org/10.1523/JNEUROSCI.19-19-08207.1999

Uday Bhanu, M., Mandraju, R. K., Bhaskar, C., & Kondapi, A. K. (2010). Cultured cerebellar granule neurons as an in vitro aging model: Topoisomerase IIβ as an additional biomarker in DNA repair and aging. *Toxicology in Vitro*, *24*(7), 1935–1945. https://doi.org/10.1016/j.tiv.2010.08.003

Vaegter, C. B., Jansen, P., Fjorback, A. W., Glerup, S., Skeldal, S., Kjolby, M., Richner, M., Erdmann, B., Nyengaard, J. R., Tessarollo, L., Lewin, G. R., Willnow, T. E., Chao, M. V., & Nykjaer, A. (2011). Sortilin associates with Trk receptors to enhance anterograde transport and neurotrophin signaling. *Nature Neuroscience*, *14*(1), 54–61. https://doi.org/10.1038/nn.2689

van Spronsen, M., Mikhaylova, M., Lipka, J., Schlager, M. A., van den Heuvel, D. J., Kuijpers, M., Wulf, P. S., Keijzer, N., Demmers, J., Kapitein, L. C., Jaarsma, D., Gerritsen, H. C., Akhmanova, A., & Hoogenraad, C. C. (2013). TRAK/Milton Motor-Adaptor Proteins Steer Mitochondrial Trafficking to Axons and Dendrites. *Neuron*, *77*(3), 485–502. https://doi.org/10.1016/j.neuron.2012.11.027

Venditti, P., Di Stefano, L., & Di Meo, S. (2013). Mitochondrial metabolism of reactive oxygen species. *Mitochondrion*, *13*(2), 71–82. https://doi.org/10.1016/j.mito.2013.01.008

Villarin, J. M., McCurdy, E. P., Martínez, J. C., & Hengst, U. (2016). Local synthesis of dynein cofactors matches retrograde transport to acutely changing demands. *Nature Communications*, *7*(1), 13865. https://doi.org/10.1038/ncomms13865

Volosin, M., Song, W., Almeida, R. D., Kaplan, D. R., Hempstead, B. L., & Friedman, W. J. (2006). Interaction of Survival and Death Signaling in Basal Forebrain Neurons: Roles of Neurotrophins and Proneurotrophins. *Journal of Neuroscience*, *26*(29), 7756–7766. https://doi.org/10.1523/JNEUROSCI.1560-06.2006

Wallenstein, G. V., & Vago, D. R. (2001). Intrahippocampal Scopolamine Impairs Both Acquisition and Consolidation of Contextual Fear Conditioning. *Neurobiology of Learning and Memory*, *75*(3), 245–252. https://doi.org/10.1006/nlme.2001.4005

Wayne, D. B., & Heaton, M. B. (1988). Retrograde transport of NGF by early chick embryo spinal cord motoneurons. *Developmental Biology*, *127*(1), 220–223. https://doi.org/10.1016/0012-1606(88)90203-5

Weiss, P., & Hiscoe, H. B. (1948). Experiments on the mechanism of nerve growth. *Journal of Experimental Zoology*. https://doi.org/10.1002/jez.1401070302

Whitehouse, P., Price, D., Struble, R., Clark, A., Coyle, J., & Delon, M. (1982). Alzheimer's disease and senile dementia: Loss of neurons in the basal forebrain. *Science*, *215*(4537), 1237–1239. https://doi.org/10.1126/science.7058341

Williams, B. J., Bimonte-Nelson, H. A., & Granholm-Bentley, A.-C. (2006). ERK-mediated NGF signaling in the rat septo-hippocampal pathway diminishes with age. *Psychopharmacology*, *188*(4), 605–618. https://doi.org/10.1007/s00213-006-0477-1

Williams, Granholm, A.-C., & Sambamurti, K. (2007). Age-dependent loss of NGF signaling in the rat basal forebrain is due to disrupted MAPK activation. *Neuroscience Letters*, *413*(2), 110–114. https://doi.org/10.1016/j.neulet.2006.11.040

Woolf, N. J. (1991). Cholinergic systems in mammalian brain and spinal cord. *Progress in Neurobiology*, *37*(6), 475–524. https://doi.org/10.1016/0301-0082(91)90006-m

Wu, C., Cui, B., He, L., Chen, L., & Mobley, W. C. (2009). The coming of age of axonal neurotrophin signaling endosomes. *Journal of Proteomics*, *72*(1), 46–55. https://doi.org/10.1016/j.jprot.2008.10.007

Wu, Williams, J., & Nathans, J. (2014). Complete morphologies of basal forebrain cholinergic neurons in the mouse. *ELife*, *3*. https://doi.org/10.7554/eLife.02444

Xia, X., Jiang, Q., McDermott, J., & Han, J.-D. J. (2018). Aging and Alzheimer's disease: Comparison and associations from molecular to system level. *Aging Cell*, *17*(5), e12802. https://doi.org/10.1111/acel.12802

Xue, X., Jaulin, F., Espenel, C., & Kreitzer, G. (2010). PH-domain-dependent selective transport of p75 by kinesin-3 family motors in non-polarized MDCK cells. *Journal of Cell Science*, *123*(10), 1732–1741. https://doi.org/10.1242/jcs.056366

Yang, G.-Z., Yang, M., Lim, Y., Lu, J.-J., Wang, T.-H., Qi, J.-G., Zhong, J.-H., & Zhou, X.-F. (2012). Huntingtin associated protein 1 regulates trafficking of the amyloid precursor protein and modulates amyloid beta levels in neurons. *Journal of Neurochemistry*, *122*(5), 1010–1022. https://doi.org/10.1111/j.1471-4159.2012.07845.x

Yankner, B. A., Lu, T., & Loerch, P. (2008). The Aging Brain. *Annual Review of Pathology: Mechanisms of Disease*, *3*(1), 41–66. https://doi.org/10.1146/annurev.pathmechdis.2.010506.092044

Ypsilanti, A. R., Girão da Cruz, M. T., Burgess, A., & Aubert, I. (2008). The length of hippocampal cholinergic fibers is reduced in the aging brain. *Neurobiology of Aging*, *29*(11), 1666–1679. https://doi.org/10.1016/j.neurobiolaging.2007.04.001

Zhou, W., Zhang, J., Wang, G., Ling, L., & Yan, C. (2016). Permeability and distribution of nerve growth factor in the brain of neonatal rats by periphery venous injection in hypoxic-ischemic state. *SpringerPlus*, *5*(1), 1893. https://doi.org/10.1186/s40064-016-3594-2

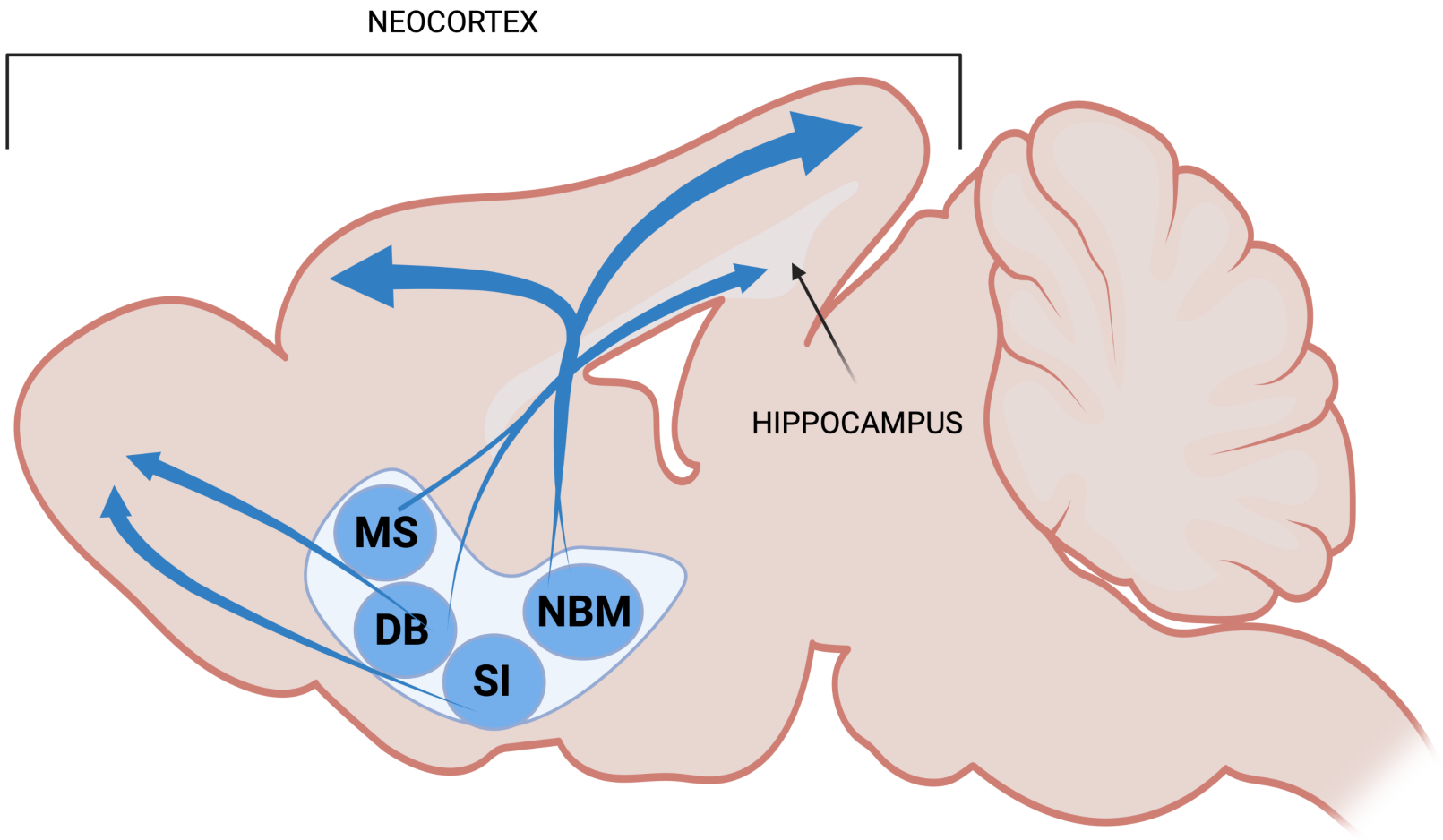

Figure 1. Schematic illustrating the murine basal forebrain cholinergic system. MS = Medial Septal Nucleus, DB = Diagonal Band of Broca, SI = Substantia Inominatia, NBM= Nucleus Basalis of Mynert

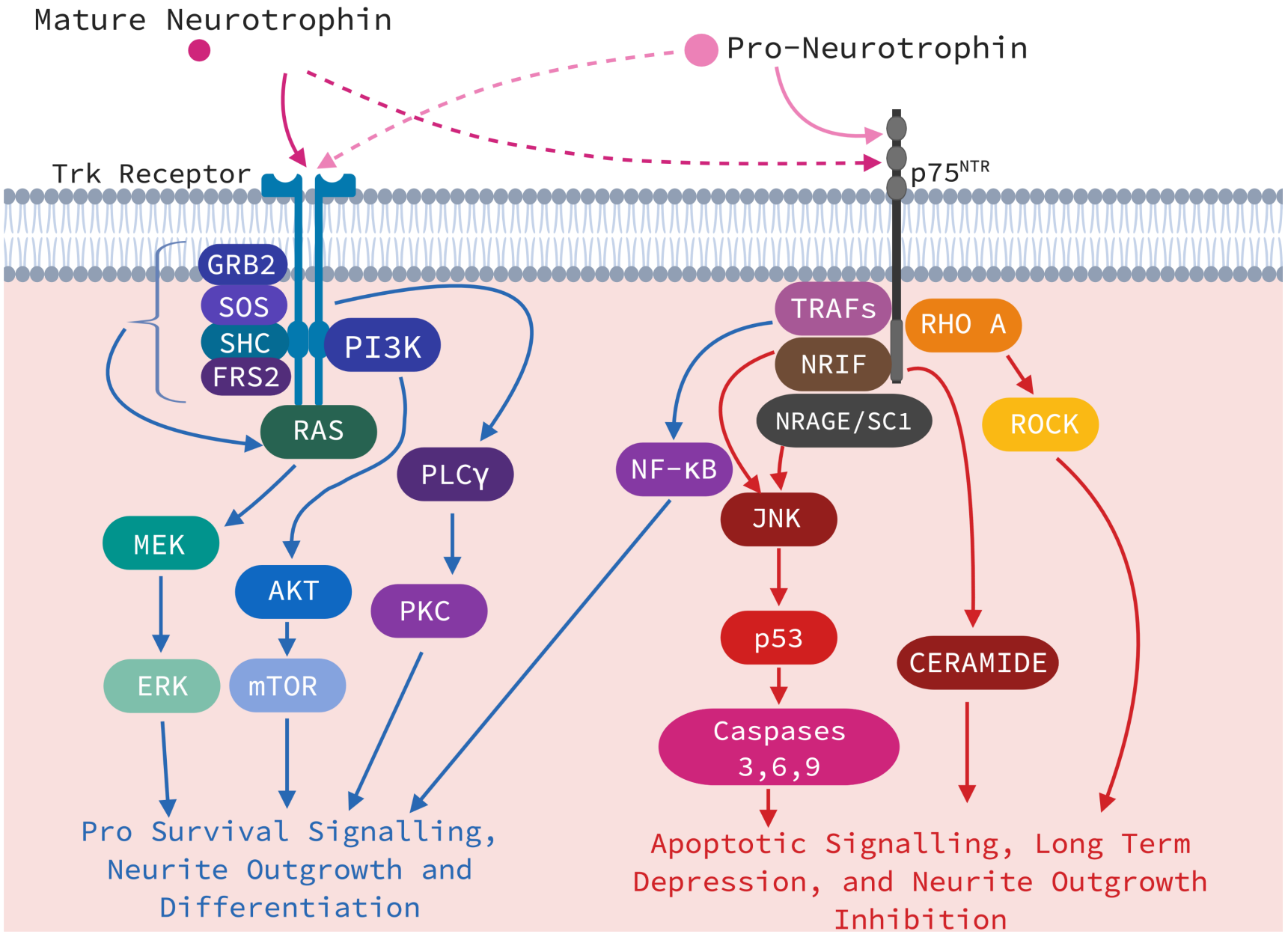

Figure 2. A schematic of the signaling pathways activated by Trk and p75^{NTR} receptors.

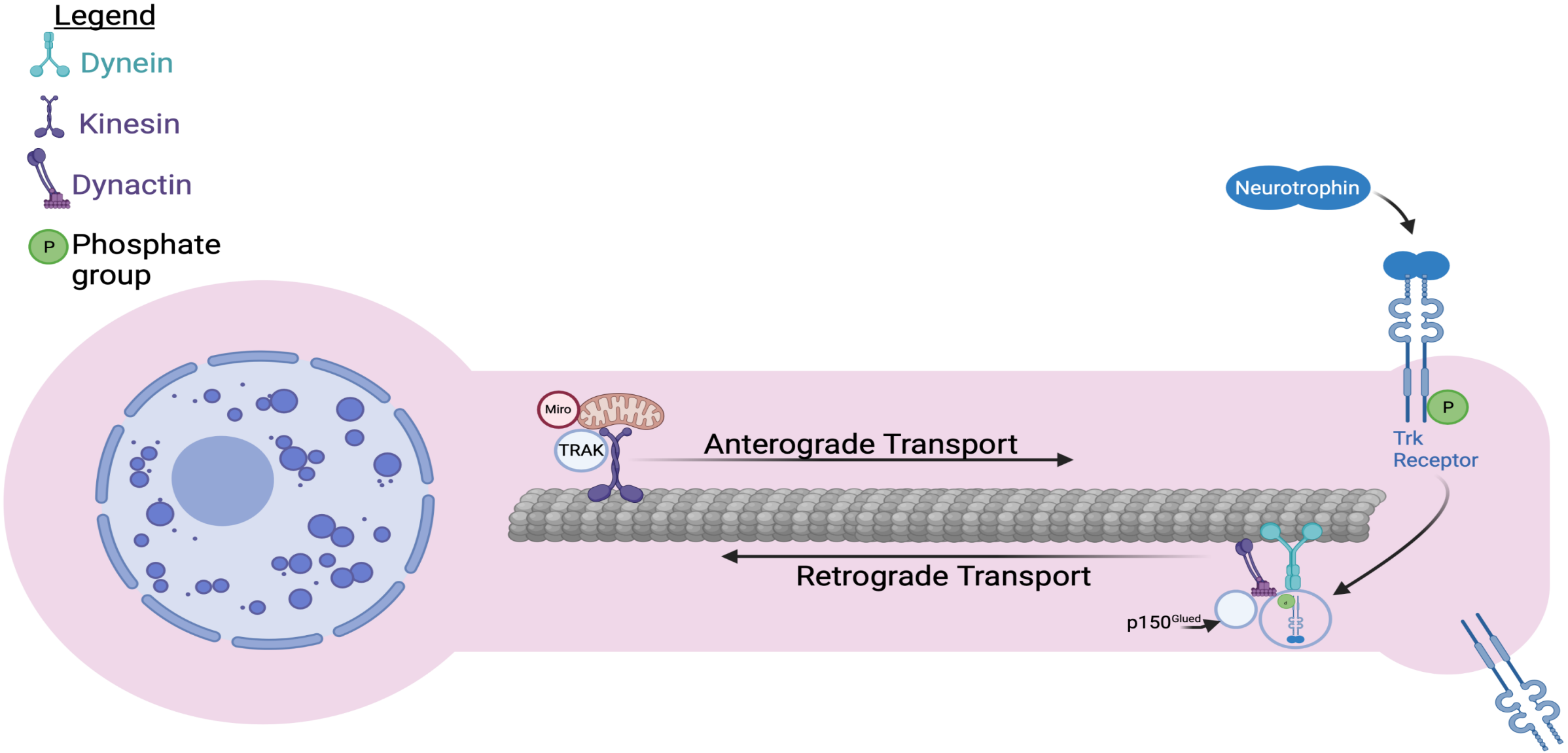

Figure 3. Graphical illustration of anterograde and retrograde axonal trafficking carried out by kinesin and dynein, respectively. Kinesin and dynein both require adapter proteins to facilitate axonal trafficking. The adapter protein trafficking kinesin protein (TRAK) binds to Miro on the outer mitochondrial membrane to facilitate the anterograde trafficking of mitochondria to the axon. The adapters $p150^{Glued}$ and dynactin facilitate the movement of neurotrophins to the soma.

Preface

The initial stages of my thesis were devoted to establishing protocols for the assay for retrograde neurotrophin transport in basal forebrain cholinergic neurons cultured in microfluidic chambers. The following manuscript is the culmination of this initial work. I established all the protocols outlined in this chapter and prepared the manuscript.

2. Retrograde Axonal Transport of Neurotrophins in Basal Forebrain Cholinergic Neurons

Shekari, A., & Fahnestock, M. (2021). Retrograde Axonal Transport of Neurotrophins in Basal Forebrain Cholinergic neurons. *Methods in Molecular Biology*. 1-34 (Accepted)

Authors:

Arman Shekari, shekara@mcmaster.ca

Department of Psychiatry and Behavioural Neurosciences, McMaster University, Hamilton, Ontario, Canada

Margaret Fahnestock, fahnest@mcmaster.ca

Department of Psychiatry and Behavioural Neurosciences, McMaster University. Hamilton, Ontario, Canada

i. Chapter Title: Retrograde Axonal Transport of Neurotrophins in Basal Forebrain Cholinergic Neurons

Running Head: Axonal Transport in Basal Forebrain Neurons

ii. Abstract: Axonal transport is key for the survival and function of all neurons. This process is especially important in basal forebrain cholinergic neurons due to their extremely long and diffuse axonal projections. These neurons are critical for learning and memory and degenerate rapidly in age-related neurodegenerative disorders like Alzheimer's and Parkinson's disease. The vulnerability of these neurons to age-related neurodegeneration may be partially attributed to their reliance on retrograde axonal transport for neurotrophic support. Unfortunately, little is known about the molecular biology underlying the retrograde transport dynamics of these neurons due to the difficulty associated with their maintenance *in vitro*. Here, we outline a protocol for culturing primary rodent basal forebrain cholinergic neurons in microfluidic chambers, devices designed specifically for the study of axonal transport *in vitro*. We outline protocols for labeling neurotrophins and tracking neurotrophin transport in these neurons. Our protocols can also be used to study axonal transport in other types of primary neurons such as cortical and hippocampal neurons.

iii. Key Words: Neurotrophins, Cholinergic, Microfluidic chambers, Aging, BDNF, NGF, proNGF, Axonal transport, Basal forebrain, Retrograde

1. Introduction

Intracellular trafficking is critical for the survival and proper function of all neurons due to their extreme structural and biochemical polarity. Neurons orchestrate the bidirectional transport of a wide variety of cellular cargo, from proteins and RNA to entire organelles, along their lengthy axonal projections in a tightly regulated manner via a process termed axonal transport [1]. Axonal transport occurs along microtubules, cytoskeletal elements composed of polarized tubulin polymers that span the entirety of the axon [2]. These polymers are organized in parallel radial arrays, forming unipolar filaments with plus ends proximal to the axon tip and minus ends proximal to the cell body [2, 3]. The transport of cargo towards the axon tip is referred to as anterograde or "plus-end directed" while transport towards the cell body is referred to as retrograde or "minus-end directed".

Anterograde and retrograde transport occur via the procession of two classes of ATP-dependent molecular motors along microtubules: kinesin and dynein. Kinesin family motor proteins are responsible for carrying out anterograde transport, while the cytoplasmic dynein motor protein is responsible for carrying out retrograde transport [2, 4]. Both kinesin family and dynein motors are large and complex proteins consisting of multiple polypeptide chains classified as either heavy, light, or intermediate chains, depending on their molecular weight [5]. The association of these chains via their N-terminal tail domains creates binding domains for cargo adapter proteins [2]. A wide variety of adapter proteins exist and facilitate critical functions of both kinesin family and dynein motors, including the binding of cargo to the motors themselves and the binding of motors to microtubule tracks [2, 6–9].

While the motor proteins underlying retrograde and anterograde transport share some similarities, they, like the transport processes they govern, are distinct from one another. This chapter will focus largely on retrograde axonal transport, specifically within the basal forebrain, a brain area where deficits in retrograde transport have been heavily implicated in the development of age-related neurodegenerative disorders [10, 11].

The basal forebrain is located at the ventral rostrocaudal extent of the brain and consists of multiple structures including the diagonal band of Broca, nucleus basalis of Meynert, and the medial septal nucleus [12, 13]. Most neurons within these structures produce the neurotransmitter acetylcholine, making the basal forebrain the major cholinergic output of the central nervous system (CNS). Basal forebrain projections are extremely lengthy and diffuse, projecting upwards and terminating widely throughout the hippocampus and neocortex [12, 13]. These projections are critical for learning, memory, and attention, making the basal forebrain a vital cognitive center [13].

The degeneration of ascending basal forebrain cholinergic projections occurs both in normal aging and with increased severity in age-related neurodegenerative disorders like Alzheimer's and Parkinson's disease [14–16]. Loss of cholinergic innervation correlates strongly with cognitive decline and is considered a hallmark of Alzheimer's disease (AD) [13, 15, 17, 18]. Basal forebrain cholinergic neurons (BFCNs) demonstrate a striking selective vulnerability in AD, as they are amongst the first neurons in the brain to degenerate in the disorder [15, 18–22]. This vulnerability results in up to 95% of BFCNs degenerating by the end stages of AD [23, 24].

One factor that may explain the selective vulnerability of BFCNs to age-related neurodegenerative disorders is their inability to produce a family of growth factors termed neurotrophins. Neurotrophins are a family of extracellular signaling proteins that are critical for

neuronal development, survival and plasticity [25]. BFCNs are dependent upon the neurotrophins nerve growth factor (NGF) and brain derived neurotrophic factor (BDNF) for their survival and function [26–32]. NGF and BDNF, like all neurotrophins, are initially synthesized as proproteins that can be processed to their mature forms [33]. However, pro-neurotrophins are capable of facilitating intracellular signaling independently of their mature counterparts [34–37]. Additionally, while pro and mature BDNF and proNGF are detectable in the mammalian CNS, mature NGF is not, further highlighting the importance of studying proneurotrophins in the context of CNS neurons like BFCNs [38–40].

BFCNs are completely reliant on their synaptic targets in the hippocampus and cortex for their supply of BDNF and proNGF [41–43]. Upon release, these neurotrophins bind to either tropomyosin-related kinase (Trk) or $p75^{NTR}$ receptors at BFCN axon terminals and are retrogradely transported to BFCN cell bodies [10, 11, 25, 41, 44, 45]. In AD and in animal models of AD, NGF-immunoreactive material accumulates in BFCN target areas and is decreased in the basal forebrain itself, suggesting impaired retrograde neurotrophin axonal transport [46, 47]. Additionally, both BDNF and proNGF retrograde transport are reduced in aged BFCNs, further implicating dysfunctional retrograde transport in the selective vulnerability of these neurons to age-related neurodegeneration [10]. Unfortunately, the mechanisms underlying these observed transport deficits are currently unknown. In fact, very little is known about the mechanisms governing retrograde neurotrophin transport in this highly vulnerable neuron population.

The mechanistic study of retrograde neurotrophin transport is complicated by the diffuse and highly arborized projections primary neurons develop *in vitro*. Organizing and separating neuronal cell bodies and axon terminals facilitates the accurate assessment and quantification of

axonal transport *in vitro*. Recently, microfluidic chambers have been developed to achieve this organization and to advance the direction-specific assay of axonal transport in CNS neurons [48, 49]. These chambers contain microgrooves that are connected to a main channel that houses neuronal cell bodies. Axons grow through these microgrooves and emerge into another channel that maintains fluidic isolation from the channel that houses the cell bodies, permitting the independent manipulation of neuronal cell bodies and axons. This fluidic isolation allows neurotrophins to be administered exclusively to the axon terminals of neurons. The microgrooves also linearize axons and enable anterograde and retrograde transport to be accurately quantified. While BFCNs seem like ideal candidates for study using microfluidic chambers due to their unique reliance on retrograde transport, they are difficult to maintain *in vitro*.

Here we describe a protocol for the culture and maintenance of embryonic rodent BFCNs in microfluidic culture, as well as a protocol for the tracking of retrograde transport of biotinylated neurotrophins conjugated to streptavidin-labelled quantum dot fluorophores. We provide a protocol for the purification of biotinylated proNGF from the medium of human embryonic kidney (HEK) cells transfected with a plasmid coding for Avi-tagged, cleavage-resistant proNGF [10,52]. We also provide a protocol for the immunocytochemical analysis of these neurons to validate cholinergic phenotype. These protocols may be used in conjunction with other primary neuron types such as cortical neurons, however with some minor modifications that are mentioned below.

2. Materials

2.1 Preparation of Microfluidic Chambers

1. XC450 Microfluidic devices (Xona Microfluidics, Research Triangle Park, NC, USA)

2. Precoat ethanol solution (Xona Microfluidics, included with XC450 devices)
3. Humidity-controlled ChipTrays™ (Recommended only, *see* **Note 1**) (Xona Microfluidics)
4. 1X phosphate buffered saline (PBS): 137 mM NaCl, 2.7 mM KCl, 10 mM Na_2HPO_4, and 1.8 mM KH_2PO_4 in 1 L of distilled water. Adjust solution to pH 7.4.
5. 0.01% sterile-filtered Poly-L-Lysine (PLL) solution

2.2 Dissection and Processing of Basal Forebrain Tissue

1. Dissection tools suitable for embryonic murine dissection (fine tip Dumont forceps and scissors, tweezers, petri dishes)
2. Dissection microscope
3. Clinical centrifuge capable of reaching 250xg
4. Hemocytometer
5. 100X Penicillin-Streptomycin (P/S) (10,000 units/mL of penicillin and 10,000 µg/mL of streptomycin)
6. 1X Hank's Balanced Salt Solution (HBSS): Dilute 10X HBSS stock solution using sterile double-distilled water, add 1% P/S and pH to 7.4 before sterile filtering.
7. Fine fire-polished glass Pasteur Pipettes: Expose the tip of a glass Pasteur pipette to the flame of a Bunsen burner for a few seconds while rotating the base of the pipette. Repeat until the tip has become smooth and the opening has shrunk to about 1mm in diameter (*see* **Note 2**). Autoclave and keep sterile before use.
8. DNase I solution (1mg/mL)
9. 10X Trypsin-EDTA solution

10. BFCN Plating Medium: Neurobasal medium, 1% P/S, 2% B27 serum-free supplement, 1% GlutaMAX, 10% fetal bovine serum (FBS), 50ng/mL recombinant murine BDNF (Peprotech, Rocky Hill. NJ, USA), 50ng/mL recombinant human β-NGF (Peprotech).

2.3 Plating and Maintenance of BFCNs in Microfluidic Chambers

1. BFCN Plating Medium: Neurobasal medium, 1% P/S, 2% B27 serum-free supplement. 1% GlutaMAX, 10% fetal bovine serum (FBS), 50ng/mL recombinant murine BDNF, 50ng/mL recombinant human β-NGF.
2. BFCN Maintenance Medium: Neurobasal medium, 1% P/S, 2% B27 serum-free supplement, 1% GlutaMAX, 50ng/mL recombinant murine BDNF, 50ng/mL recombinant human β-NGF (*see* **Note 3**).

2.4 Immunocytochemical Staining of BFCNs in Microfluidic Chambers

1. Widefield or confocal microscope capable of fluorescence microscopy
2. 4% paraformaldehyde (PFA) sterile solution: Dilute 1g of PFA powder per 15mL of sterile water. Water should be heated to 60°C before addition of PFA. Add 1N NaOH until powder has fully dissolved, then add 10mL of 3X PBS for every 15mL of water. Adjust the pH of the solution to 7.2 and sterile filter before use.
3. 10% Triton-X100 Solution
4. PBS-A: 0.01% Triton-X100 diluted in 1X PBS
5. PBS-B: Dissolve 300mg bovine serum albumin in ~8mL of 1X PBS and add 500uL of FBS. Bring the solution to a final volume of 10mL, and sterile filter before use.
6. Primary antibodies: Any primary antibody compatible with immunocytochemistry can be used. To confirm cholinergic phenotype, vesicular acetylcholine transporter (VAChT,

Santa Cruz Biotechnology, Dallas, TX, USA) antibodies can be used. TrkA antibodies (Alomone Labs, Jerusalem BioPark, Israel) can also be used to confirm cholinergic phenotype, as all BFCNs express TrkA [50, 51].

7. Secondary antibodies: Any secondary antibodies compatible with immunocytochemistry can be used. Our lab uses AlexaFluor antibodies.
8. DAPI nuclear counterstain
9. Silicone immersion oil (Ibidi, Fitchburg, WI, USA) (*see* **Note 4**)

2.5 Purification of Biotinylated proNGF

1. HEK293-FT cells (ATCC, Manassas, VA, USA)
2. Centrifuge capable of reaching speeds of 300xg
3. 10kDa centrifugal concentrators
4. Cold room or large refrigerator
5. HEK Plating Medium: Dulbecco's Modified Eagle Medium (DMEM), 10% FBS, 1% GlutaMAX, 1% P/S, 1% sodium pyruvate, 1% Non-essential amino acids.
6. HEK Transfection Medium: Dulbecco's Modified Eagle Medium (DMEM) (ThermoFisher Scientific), 1% GlutaMAX, 1% P/S, 1% sodium pyruvate, 1% Non-essential amino acids, 1mg/mL d-biotin
7. Turbofect™ transfection reagent (ThermoFisher Scientific)
8. Nickel Nitrotriacetic acid (Ni-NTA) resin
9. Reusable nickel purification columns
10. proNGF-R-1G-Avi-His and Bir-A biotin ligase pcDNA-3.1 plasmids [10, 52] (Bir-A biotin ligase plasmid also available from Addgene, Watertown, MA, USA)

11. Ni-NTA wash buffer: 1X PBS, 20mM imidazole, 1mM phenylmethylsulfonyl fluoride (PMSF). Adjust to a final pH of 8.0
12. Ni-NTA elution buffer (50mL): 1X PBS, 300mM imidazole, phosSTOP and ULTRA tablets (Roche, Basel, Switzerland). Adjusted to a final pH of 8.0

2.6 Tracking and Analysis of Neurotrophin Axonal Transport

1. Widefield or confocal microscope equipped with an on-stage incubator capable of maintaining 37°C, 5% CO_2 and capable of fluorescence microscopy
2. Quantum dot (Qdot) 625-streptavidin conjugate (ThermoFisher Scientific) (*see* **Note 5**)
3. Qdot625 or TexasRed fluorescence filter cube set (*see* **Note 6**)
4. DAPI and Cy5 fluorescence filter cube set
5. Biotinylated neurotrophins (Alomone or via Ni-NTA chromatography)
6. TubulinTracker™ Deep Red (ThermoFisher Scientific), optional (*see* **Note 7**)
7. Axonal Imaging Medium: Neurobasal medium minus phenol red, 1X P/S, 1X B27 serum-free supplement, 1X GlutaMAX
8. Somal Imaging Medium: Neurobasal medium minus phenol red, 1% P/S, 2% B27 serum-free supplement, 1% GlutaMAX, 50ng/mL recombinant BDNF, 50ng/mL recombinant β-NGF.
9. NucBlue™ LiveReadyProbes™ Hoechst nuclear counterstain (ThermoFisher Scientific)
10. ImageJ 1.53c equipped with the "ImageScience" plugin set (included with ImageJ) and the KymoToolBox plugin (available from: https://github.com/fabricecordelieres/IJ-Plugin_KymoToolBox)

3. Methods

3.1 Preparation of Microfluidic Chambers (to be done 24 hours before dissection)

XC450 devices must be sterilized using the included precoat solution before use. The devices must also be coated with an adhesion substrate, in this case poly-L-lysine (PLL), to improve the adherence of primary neurons to the channels of the device. Working with microfluidic chambers requires a great deal of patience and care. The fluidic isolation and neuronal organization these devices provide is only possible if the devices are handled optimally, which we outline below (Figures 1-2).

1. Within a biosafety cabinet, add 100µL of precoat solution to the top left well of each chamber (Figure 1) and let stand for 1 minute (*see* **Note 8**)
2. Add 100µL of precoat solution to the bottom left well of each chamber and let stand for 5 minutes
3. Add 100µL of precoat solution to the top right well of each chamber and let stand for 1 minute
4. Add 100µL of precoat solution to the bottom right well of each chamber and let stand for 5 minutes
5. Aspirate the precoat solution from every well, making sure to leave ~20uL of residual solution within each well, and immediately add 150µL of PBS to the top left well of each chamber. Let stand for 1 minute (*see* **Note 9, 10**)
6. Repeat steps 2-5 with 150µL of PBS (Figure 1)
7. Add 150µL of PBS to both top wells of the device. Immediately repeat for both bottom wells (Figure 2)

8. Aspirate the PBS solution from all wells and then repeat steps 1-4 using 120µL of 0.01 % PLL solution (warmed to 37°C) (Figure 1).
9. Place chambers in a 37°C, 5% CO_2 incubator for 24 hours
10. Inspect all chambers to ensure no bubbles have formed within the main channels (*see* **Note 11**)
11. Aspirate the PLL from all wells and repeat steps 1-4 with 150µL of PBS
12. Aspirate the PBS from all wells and add 150µL of plating medium that has been warmed to 37°C to both top wells of the device (Figure 2). Immediately repeat for both bottom wells
13. Store chambers in a 37°C, 5% CO_2 incubator until plating

3.2 Dissection and Processing of Embryonic Basal Forebrain Tissue (Figure 3)

The basal forebrain is relatively small compared to commonly dissected neural structures like the cortex and hippocampus. Thankfully, its structure is very distinct and can be easily distinguished from neighboring brain areas. The small working volumes afforded by microfluidic culture allow many chambers to be prepared using a minimal amount of tissue.

The following protocol can also be used for preparing cortical and hippocampal neuronal cultures. These neurons are far more robust in culture and can be plated at higher densities than basal forebrain (within the 10^5 cells/mL range). The plating medium for cortical and hippocampal neurons does not need to contain any neurotrophins.

1. Sacrifice a pregnant rat or mouse at embryonic day (E)18 using CO_2 euthanasia or cervical dislocation and remove all embryos (*see* **Note 12**). Place embryos on ice.

2. Remove embryos from the embryonic sac using fine Dumont forceps, and separate the head from the body using a small pair of scissors. Place the head in a petri dish containing a small amount of cold HBSS solution and remove the brain from the skull using fine Dumont forceps.
3. Place the brain in a separate petri dish containing a small amount of HBSS. Under a dissection microscope, remove the meninges from the brain using fine Dumont forceps
4. Remove the olfactory bulbs using a small pair of scissors. Place two medial cuts at the front of each cortical lobe. Fan out each lobe to expose the basal forebrain (*see* **Note 13**). Remove the basal forebrain from the brain using a pair of small scissors. Aspirate the tissue into a tube filled with a small amount of cold HBSS, and place on ice.
5. Repeat steps 2-4 for each embryo (*see* **Note 14**)
6. In a biosafety cabinet, aspirate as much HBSS solution as possible from the collection tube without disturbing the tissue. Add 1mL of fresh, cold HBSS to the tube. Repeat 5 times to wash.
7. Aspirate as much HBSS solution from the collection tube as possible without disturbing the tissue. Add 450 µL of fresh, cold HBSS to the tube. Immediately add 50uL of 10X trypsin to the tub and incubate in a 37°C water bath for 20 minutes, gently agitating the tube every 5 minutes.
8. Add 50uL of 10X DNase I to the collection tube. Triturate the tissue using a fire-polished glass Pasteur pipette until the solution becomes cloudy and no visible chunks of tissue remain. Add 1mL of plating medium warmed to 37°C to quench the trypsin.

9. Centrifuge the solution at 250xg for 4 minutes and remove the supernatant. Resuspend the cell pellet using warm plating medium to a final density of $1x10^6$ cells/mL using a hemocytometer. Repeatedly triturate this cell mixture to ensure homogeneity.

3.3 Plating and Maintenance of BFCNs in Microfluidic Chambers

BFCNs are difficult to maintain in culture and require consistent media changes using neurotrophin-rich medium. These neurons must be plated at high densities (in the range of 10^6 cells/mL) to be viable in microfluidic culture. BFCNs produce axonal projections *in vitro* that cross the microgrooves in a matter of days if properly maintained (Figure 4).

Cortical and hippocampal neurons can also be maintained using this protocol. However, like the plating medium, the maintenance medium used for these neurons does not need to contain any neurotrophins.

1. In a biosafety cabinet, aspirate the plating medium from all wells (*see* **Note 9**).
2. Inject 10µL of the previously prepared cell solution into the top left well of the chamber by placing the tip of the pipette directly adjacent to the opening of the main channel to ensure the cell solution flows from the well into the main channel (*see* **Note 15**). Repeat for the bottom left well and place the chambers in a 37°C 5% CO_2 incubator for 5 minutes to allow neuronal adherence to the substratum.
3. Add 150µL of plating medium to both top wells. Immediately repeat for both bottom wells. Incubate the chambers at 37°C, 5% CO_2 for 24 hours.
4. Replace the plating medium with maintenance medium after 24 hours (Figure 2). Repeat every 48-72 hours (*see* **Notes 9,10**). Axonal projections usually take 5-7 days to cross the

microgrooves (Figure 3). Basal forebrain neurons maintain transport for 2 weeks [10] (*see* **Note 16**).

3.4 Immunocytochemical Staining of BFCNs in Microfluidic Chambers

Immunostaining neurons cultured in microfluidic chambers requires many incubations and washes. This is mainly due to the restrictive opening joining the wells of the device to the main channels. High quality images comparable to those obtained using cells cultured in standard well plates on glass coverslips can be obtained from microfluidic chambers using this protocol (Figure 5).

1. In a biosafety cabinet, perform a PBS wash by replacing the maintenance medium in all wells with 150µL of PBS. Immediately replace the PBS with a 4% PFA solution (*see* **Notes 9,10**). Incubate at room temperature for 30 minutes in a light-proof box. The chambers must be protected from light during all subsequent incubations.
2. Perform a PBS wash with 150µL of PBS and then immediately add 150µL of PBS-A to all wells (*see* **Notes 9,10**). Incubate at room temperature for 30 minutes.
3. Replace the PBS-A solution with 150µL of PBS-B per well (*see* **Notes 9,10**). Incubate at room temperature for 30 minutes. During this time, prepare the primary antibody solution using PBS-B as the diluent.
4. Replace the PBS-B solution with 150µL of the primary antibody solution per well (*see* **Notes 9,10**). Incubate at 4°C overnight.
5. Perform 3 washes using 150µL of PBS-B per well (*see* **Notes 9,10**). Incubate at room temperature for 10 minutes in between each wash. During the last wash, prepare the secondary antibody solution using PSB-B as the diluent.

6. Replace the PBS-B solution with 150µL of the secondary antibody solution per well (*see* **Notes 9,10**). Incubate at room temperature for 2 hours. During this time, prepare a DAPI nuclear counterstain using PBS as the diluent.
7. Aspirate the secondary antibody solution from all wells and add 150µL of the DAPI counterstain solution to the top left well, followed by 150µL of PBS to the top right well. Repeat this for the bottom two wells and incubate at room temperature for 10 minutes.
8. Perform two 150µL PBS washes. Incubate at room temperature and wait 5 minutes between each wash. Perform two additional 150µL PBS washes in immediate succession (*see* **Notes 9,10**).
9. Image the cells using either wide field or confocal fluorescence microscopy (*see* **Note 17**)

3.5 Purification of Biotinylated proNGF

Our lab uses a slightly modified version of the protocol outlined in Sung et al. (2011) to obtain monobiotinylated proNGF from transfected HEK cell medium [52]. HEK cells are grown in a biotin-containing transfection medium and are co-transfected with the biotin-ligase coding construct BirA and our custom proNGF construct. Biotinylation of proNGF occurs due to the inclusion of a biotin-accepting AviTag™ region within our construct. This process can be skipped when studying BDNF, proBDNF, and NGF, as biotinylated versions of these neurotrophins are available commercially (Alomone). Due to the lack of mature NGF in the CNS, we recommend the use of proNGF over mature NGF when studying transport in CNS neurons [10,38].

1. Plate HEK293 cells at an initial density of $1.5x10^6$ cells/mL to ~50% confluence in 30mL of growth medium in a 30cm petri dish.

2. In a biosafety cabinet, replace the growth medium with transfection medium and incubate cells for 72 hours at 37°C, 5% CO_2
3. Dilute 20µg of proNGF-R-1G-Avi-His and Bir-A biotin ligase pcDNA-3.1 plasmids into 1mL of DMEM. Add 60µL of Turbofect™ to this solution, mix via inversion, and incubate at room temperature for 15 minutes
4. Add the transfection solution dropwise and incubate cells for 72 hours in a 37°C 5% CO_2 incubator (*see* **Note 18**).
5. Harvest the medium from the cells and adjust to 50mL (per 30mm dish) using Ni-NTA wash buffer. Let stand on ice for 5 minutes.
6. Centrifuge the harvested medium at 300xg for 20 minutes at 4°C. Collect the supernatant and adjust to 300mL (per 30cm dish) using Ni-NTA wash buffer.
7. Add 300µL (per 30cm dish) of Ni-NTA resin (dissolved in wash buffer) to the harvested medium and incubate at 4°C with gentle stirring overnight.
8. In a cold room or large refrigerator, load the solution into a reusable nickel chromatography column. Let stand for 5 minutes to allow the Ni-NTA resin to settle. Purify using 2 column volumes of wash buffer (discard) followed by 1/10 column volumes of elution buffer.
9. Load eluate onto a 10kD centrifugal concentrator and centrifuge at 300xg for 20 minutes at 4°C, discarding the flow through. Aliquot the reserved solution and store at -80°C.

3.6 Tracking and Analysis of Neurotrophin Axonal Transport

The brightness of quantum dots allows visualization of single particle neurotrophin transport without the need for expensive confocal microscopy. However, confocal microscopy is recommended for maximum visual fidelity. Biotinylated BDNF and proNGF are both easily

conjugated to streptavidin-conjugated quantum dots. However, the conditions required to promote the transport of BDNF and proNGF are different and are discussed below.

3.6.1 Conjugation of Quantum Dots and Administration of Labeled BDNF to Axon Terminals

1. 24 hours prior to the transport assay, view the neurons under a widefield microscope using bright-field light to confirm that the axonal compartment is populated with axonal projections. If axons are present, replace the axonal medium with neurotrophin-free axonal imaging medium. Incubate the neurons for 24 hours at 37°C, 5% CO_2. BFCN axons usually populate the axonal compartment by days *in vitro* (DIV) 5-7.
2. In a biosafety cabinet, add 1µL of Qdot625 streptavidin conjugate stock solution to 20µL of 300nM biotinylated BDNF solution. Mix via brief centrifugation, and incubate on ice, protected from light, for 1 hour (*see* **Note 19**).
3. Dilute the QD-BDNF solution to 1nM using axonal imaging medium.
4. (Optional) Dilute TubulinTracker™ Deep Red 1:1000 into both the somal and axonal imaging medium.
5. Administer 80µL of the dilute QD-BDNF solution to the top right well, wait 30 seconds, and repeat with the bottom right well (*see* **Note 20**). Incubate for 1 hour at 37°C, 5% CO_2. During this time, equilibrate the microscope stage to 37°C, 5% CO_2 (*see* **Note 21**).
6. Wash the axonal side 3 times with 120µL of axonal imaging medium before imaging

3.6.2 Conjugation of Quantum Dots and Administration of Labeled proNGF to Axon Terminals

1. Observe neurons under a widefield microscope using bright-field light to confirm that the axonal compartment is populated with axonal projections. Return the chambers to the incubator.

2. In a biosafety cabinet, add 1µL of QD625 streptavidin conjugate stock solution to 20µL of 400pM biotinylated proNGF solution. Mix via brief centrifugation, and incubate on ice, protected from light, for 1 hour (*see* **Note 19**)
3. Dilute the QD-proNGF solution to a final concentration of 50pM using axonal imaging medium.
4. (Optional) Dilute TubulinTracker™ Deep Red 1:1000 into both the somal and axonal imaging medium.
5. Aspirate the medium from all wells and replace the medium in the top left well with 150µL of somal imaging medium. Immediately replace the medium in the top left well with 80µL of the dilute QD-proNGF solution. Repeat for the bottom two wells (*see* **Note 22**).
6. Incubate for at least 15 minutes at 37°C 5% CO_2. During this time, equilibrate the microscope stage to 37°C, 5% CO_2 (*see* **Note 22**).

3.6.3 Image Acquisition

1. Stage neurons in either a widefield or confocal microscope equipped with an on-stage incubator, 60-100X oil immersion objective (N.A 1.40), and requisite fluorescent filter cubes (*see* **Notes 5,6**).
2. Focus on the neurons using bright-field light. Translate the stage towards the middle of the device so that the microgrooves are visible.
3. Switch to either the Qdot625 or TexasRed channels and search for labelled neurotrophins traversing the microgrooves (*see* **Note 23**). Quantum dots exhibit a blinking behavior and are very sensitive to focus changes, making them difficult to locate at first.

4. Once the labelled neurotrophins have been located, create a time-lapse by acquiring images at a single location at fixed intervals. Our lab uses intervals of 2-5 seconds for time-lapses lasting 2-5 minutes. If TubulinTracker™ is being used, acquire a single image of the axon projections at the desired site using the Cy5 channel before beginning the time-lapse (*see* **Note 24**)
5. Repeat step 4 on as many QD-positive microgrooves as possible. A minimum of 5 microgrooves containing at least 20 QD particles in total is recommended for statistical analysis. When using a 60X objective, microgrooves can be divided into approximately 3 non-overlapping sections: retrograde (proximal to the axonal channel), middle, and anterograde (proximal to the somal channel). Ensure time-lapses are taken at all locations (*see* **Note 25**). Distal projections within the axonal compartment can also be imaged for the purposes of determining axonal uptake (*see* **Note 26**).

3.6.4 Image Analysis

1. Import time-lapse images into ImageJ by selecting "File > Import > Image Sequence…" and selecting the first image within the sequence, ensuring that all the images from the time-lapse are within a single folder and are in chronological order based on file name.
2. Open the "Properties" window by pressing "Control + Shift + P" and ensure that the "Pixel width" unit is in μM and not inches. If inches are selected by default, simply type "um" in its place. Set the "Frame interval" to the time interval between each of the images within the time-lapse.
3. Select "MTrackJ" under the "Plugins" tab of the ImageJ toolbar. The efficiency of retrograde transport can be determined in multiple ways using this plugin, the simplest of which compares how many particles are present in the section of the microgrooves

closest to the cell body compartment between conditions. To do this, select “Tracking” on the MTrackJ pop-up menu and uncheck the “move to next time index after adding point” option. Individual particles can then be indexed by simply pressing “add” on the MTrackJ menu and clicking on the dots. This can be done using the “Multi point tool” (without MTrackJ, present on the ImageJ toolbar by default) if there are a small number of dots present.

4. Retrograde transport can also be assessed by quantifying the speed and pause duration of individual neurotrophin particles using MTrackJ. To do this, select “Tracking” on the MTrackJ pop-up menu and check the “move to next time index after adding point” option. Select “Add” on the MTrackJ popup menu and continually click on the particle to trace its path (*see* **Note 27**). Repeat this process with all visible particles in the time-lapse and select “Measure” on the MTrackJ popup menu. Particle speed can be calculated by taking the average value of the “v (μM/s)” column per particle. Pause duration can be calculated by multiplying the number of instances where the speed of a particle is 0 μM/s by the frame duration of the time-lapse. Approximately 60-100 particles per group are recommended for statistical analysis.
5. Finally, retrograde transport can also be assessed by generating kymographs from the time-lapse images to trace the overall path of the particles. To do this, first repeat step 2 and then draw a single, straight line across a single microgroove using the “Single segmented line tool” found on the ImageJ toolbar. Open the KymoToolBox plugin by navigating to “Plugins > KymoToolBox> Draw Kymo” from the ImageJ menu bar and set the width value to 100. Particle speed can also be calculated from kymographs by calculating the slope of the path traced by the particles. However, we recommend

determining particle speed using single particle analysis via MTrackJ. The clarity of the kymograph can be improved by pressing "Control + Shift + C" and adjusting the brightness and contrast sliders. If images were saved as greyscale, we recommend inverting the lookup table (LUT) for better clarity by pressing the "LUT" button on the ImageJ toolbar and selecting "Invert LUT".

4. Notes

1. Each of the 4 wells of the microfluidic chamber holds only ~150uL of media. Because of this small volume, significant evaporation occurs during handling. We recommend that chambers be handled in humidity-controlled containers (Proprietary ChipTrays™ from Xona Microfluidics, or any suitable holder with a small water reservoir) and in an incubator that is seldom opened, if possible, to avoid any confounding effects linked to excess evaporation.
2. Ensure that the opening of the pipette is not bent or sealed during the fire polishing process. An opening of <1mm will result in reduced cell yield due to excessive shearing force during trituration.
3. We do not recommend using maintenance medium older than 1 week to ensure the health of BFCNs in culture. Preparing multiple aliquots of medium components for the quick and convenient preparation of small volumes of maintenance medium is recommended.
4. XC450 devices are made of an optically neutral plastic that is not compatible with most mineral-based immersion oils.
5. While quantum-dot streptavidin conjugates are available in a variety of wavelengths, we do not recommend the use of conjugates in the yellow-green spectrum due to their relatively weak fluorescence compared to conjugates in the orange-red spectrum. We

recommend the 625 variant, as its emission spectrum aligns very well with the commonly-used Texas Red filter set.

6. Quantum dots exhibit a very large stokes shift in their excitation-emission properties. Qdot filter cube sets account for this shift and are recommended for optimal imaging. However, the brightness of quantum dots allows non-proprietary filter cube sets to be used, albeit with higher background noise due to the increased light intensities required to excite quantum dots using non-optimal wavelengths.
7. The fluorescent labelling of tubulin using TubulinTracker™ in live cells is helpful, but not required, for imaging axonal projections within microgrooves (standard brightfield microscopy can also be used to image axonal projections, but with less clarity). While our lab has not observed significant differences in neurotrophin uptake and transport between labelled and unlabeled conditions, we recommend running pilot experiments using both labelled and unlabeled neurons to ensure that the labelling does not interfere with axonal transport in your specific experimental paradigm.
8. It is **critical** to adhere to the listed standing times during microfluidic chamber preparation. These standing times allow liquid to fully penetrate throughout all compartments of the device, reducing the risk of air bubble formation within the main channels. Refer to Figure 6 for an example of an improperly prepared chamber containing an air bubble.
9. It is **critical** to never completely aspirate liquid from the wells of the devices. A residual volume of approximately 20µL remaining within each well is recommended to avoid forming air bubbles and drying out the cells in the main channel.

10. Solutions should be aspirated from the top 2 wells of all devices first, followed by the bottom 2 (Figure 2). This creates a transient volume difference across the top and bottom of the device, ensuring adequate liquid flow within the main channel.
11. Air bubbles within the main channel must be removed before plating cells. This can be done by placing the tip of a micropipette against the opening of the main channel and gently depressing and releasing the plunger.
12. Our protocol is compatible with both rat and mouse embryonic tissue. Please be sure to follow all institutional guidelines regarding proper animal care and safety during the euthanasia and dissection process.
13. A helpful video of this procedure is included in Schnitzler et al. 2008 [53]
14. The tissue from 3 Sprague Dawley rat embryos is usually sufficient to prepare 8 microfluidic chambers.
15. The devices are symmetrical, and any side can be used to house the cell bodies.
16. The axonal transport of BDNF and proNGF is reduced in BFCNs after 18 days *in vitro* [10].
17. XC450 devices are designed to fit into most standard slide holders.
18. HEK293 cells should be plated in petri dishes as opposed to flasks to facilitate the dropwise addition of the transfection solution.
19. The neurotrophin concentration can be increased or decreased depending on the experimental paradigm. However, the ratio of neurotrophin to quantum dots should remain constant.

20. Maintaining an 80μL volume difference between the somal and axonal sides of the chambers creates a small anterograde liquid flux, ensuring that any retrograde transport is due to axonal uptake and not incidental retrograde liquid flux.
21. BDNF uptake is significantly more rapid in BFCNs compared to cortical neurons [10]. If cortical neurons are being used, incubate the QD-BDNF solution for 4 hours before imaging.
22. proNGF uptake is significantly more efficient compared to BDNF uptake in BFCNs and can be visualized using concentrations within the picomolar range [10]. The uptake also occurs much more rapidly, with QD-proNGF particles appearing in axons within 15 minutes [10]. Unlike BDNF, proNGF uptake is significantly inhibited upon axonal neurotrophin starvation [10].
23. Excessive exposure of neurons to light from the QD625 filter cube set is damaging due to its use of high-energy 445nm light to maximally excite the quantum dots. We recommend minimizing both the light intensity and duration neurons are exposed to this light to avoid damaging cells.
24. We recommend staggering the incubation of individual chambers with labelled neurotrophins by between 30 minutes to 1 hour to account for the time it takes to image a single chamber.
25. Ensure that time-lapses at each of the 3 sections of the microgrooves are taken at identical time intervals after neurotrophin addition to avoid the passage of time as a confound when comparing chambers.
26. Time-lapses are not necessary when imaging axonal projections for the purposes of assessing neurotrophin uptake. Uptake can simply be quantified by counting labelled

particles present within a predefined length of distal axon (our lab uses 100μM). Length can be measured using the "Straight segmented line tool" in ImageJ.

27. Neurotrophin particles can exhibit bidirectional movement during transport within the span of a single time lapse. It is recommended to analyze the retrograde and anterograde components of a given particle's transport separately. This can be done by selecting "Add" in the MTrackJ popup window following the completion of the retrograde movement of a particle and treating the anterograde component of its movement as a separate particle.

5. Figure Captions

Figure 1: Microfluidic device schematic depicting the well order to be followed during device preparation.

Figure 2: Microfluidic device schematic depicting the well order to be followed during media changes and washes. This well order is also used once during device preparation for the second PBS incubation.

Figure 3: Graphical depiction of the dissection and processing procedure outlined in section 3.2.

Figure 4: Basal forebrain cholinergic neurons (BFCNs) stained for tubulin (cyan) and DAPI (red) at day *in vitro* (DIV) 5. The left panel depicts BFCN cell bodies extending their axons into the microgrooves. The right panel depicts BFCN axons extending across the entire length of the 450μM microgroove barrier and beginning to enter the axonal main channel.

Figure 5: Basal forebrain cholinergic neurons (BFCNs) cultured in microfluidic chambers stained for tubulin (cyan) and DAPI (red) at day *in vitro* (DIV) 7 following the immunocytochemical staining protocol outlined in section 3.4.

Figure 6: A microfluidic device with an air bubble (marked with a red oval) present within one of the 2 main channels.

6. Acknowledgements

We thank Dr. Chengbiao Wu (Department of Neurosciences, University of California at San Diego, La Jolla, CA, USA) for providing us with an NGF-Avi-His plasmid and for his assistance in the development of our monobiotinylated neurotrophin purification protocols. Supported by grant #PJT-159493 from the Canadian Institutes of Health Research to MF.

7. References

1. Terenzio M, Schiavo G, Fainzilber M (2017) Compartmentalized Signaling in Neurons: From Cell Biology to Neuroscience. Neuron 96:667–679. https://doi.org/10.1016/j.neuron.2017.10.015

2. Maday S, Twelvetrees AE, Moughamian AJ, Holzbaur ELF (2014) Axonal Transport: Cargo-Specific Mechanisms of Motility and Regulation. Neuron 84:292–309. https://doi.org/10.1016/j.neuron.2014.10.019

3. Rao AN, Baas PW (2018) Polarity Sorting of Microtubules in the Axon. Trends Neurosci 41:77–88. https://doi.org/10.1016/j.tins.2017.11.002

4. Roberts AJ, Kon T, Knight PJ, et al (2013) Functions and mechanics of dynein motor proteins. Nat Rev Mol Cell Biol 14:713–726. https://doi.org/10.1038/nrm3667

5. Hirokawa N (1998) Kinesin and Dynein Superfamily Proteins and the Mechanism of Organelle Transport. Science (80-) 279:519–526. https://doi.org/10.1126/science.279.5350.519

6. van Spronsen M, Mikhaylova M, Lipka J, et al (2013) TRAK/Milton Motor-Adaptor Proteins Steer Mitochondrial Trafficking to Axons and Dendrites. Neuron 77:485–502. https://doi.org/10.1016/j.neuron.2012.11.027

7. Lin MY, Sheng ZH (2015) Regulation of mitochondrial transport in neurons. Exp Cell Res 334:35–44

8. Debattisti V, Gerencser AA, Saotome M, et al (2017) ROS Control Mitochondrial Motility through p38 and the Motor Adaptor Miro/Trak. Cell Rep 21:1667–1680. https://doi.org/10.1016/j.celrep.2017.10.060

9. Moughamian AJ, Osborn GE, Lazarus JE, et al (2013) Ordered Recruitment of Dynactin to the Microtubule Plus-End is Required for Efficient Initiation of Retrograde Axonal Transport. J Neurosci 33:13190–13203. https://doi.org/10.1523/JNEUROSCI.0935-13.2013

10. Shekari A, Fahnestock M (2019) Retrograde axonal transport of BDNF and proNGF diminishes with age in basal forebrain cholinergic neurons. Neurobiol Aging 84:131–140. https://doi.org/10.1016/j.neurobiolaging.2019.07.018

11. Fahnestock M, Shekari A (2019) ProNGF and Neurodegeneration in Alzheimer's Disease. Front Neurosci 13:129. https://doi.org/10.3389/fnins.2019.00129

12. Woolf NJ (1991) Cholinergic systems in mammalian brain and spinal cord. Prog Neurobiol 37:475–524. https://doi.org/10.1016/0301-0082(91)90006-m

13. Ballinger EC, Ananth M, Talmage DA, Role LW (2016) Basal Forebrain Cholinergic Circuits and Signaling in Cognition and Cognitive Decline. Neuron 91:1199–1218.

https://doi.org/10.1016/j.neuron.2016.09.006

14. Köppen JR, Stuebing SL, Sieg ML, et al (2016) Cholinergic deafferentation of the hippocampus causes non-temporally graded retrograde amnesia in an odor discrimination task. Behav Brain Res 299:97–104. https://doi.org/10.1016/j.bbr.2015.11.021

15. Ypsilanti AR, Girão da Cruz MT, Burgess A, Aubert I (2008) The length of hippocampal cholinergic fibers is reduced in the aging brain. Neurobiol Aging 29:1666–1679. https://doi.org/10.1016/j.neurobiolaging.2007.04.001

16. Whitehouse PJ, Hedreen JC, White CL, Price DL (1983) Basal forebrain neurons in the dementia of Parkinson disease. Ann Neurol 13:243–248. https://doi.org/10.1002/ana.410130304

17. H. Ferreira-Vieira T, M. Guimaraes I, R. Silva F, M. Ribeiro F (2016) Alzheimer's disease: Targeting the Cholinergic System. Curr Neuropharmacol 14:101–115. https://doi.org/10.2174/1570159X13666150716165726

18. Whitehouse P, Price D, Struble R, et al (1982) Alzheimer's disease and senile dementia: loss of neurons in the basal forebrain. Science (80-) 215:1237–1239. https://doi.org/10.1126/science.7058341

19. Ginsberg SD, Mufson EJ, Alldred MJ, et al (2011) Upregulation of select rab GTPases in cholinergic basal forebrain neurons in mild cognitive impairment and Alzheimer's disease. J Chem Neuroanat 42:102–110. https://doi.org/10.1016/j.jchemneu.2011.05.012

20. Schmitz TW, Nathan Spreng R (2016) Basal forebrain degeneration precedes and predicts the cortical spread of Alzheimer's pathology. Nat Commun 7:13249.

https://doi.org/10.1038/ncomms13249

21. Whitehouse PJ (1998) The cholinergic deficit in Alzheimer's disease. J Clin Psychiatry 59 Suppl 1:19–22

22. Hyman B, Van Hoesen G, Damasio A, Barnes C (1984) Alzheimer's disease: cell-specific pathology isolates the hippocampal formation. Science (80-) 225:1168–1170. https://doi.org/10.1126/science.6474172

23. Baker-Nigh A, Vahedi S, Davis EG, et al (2015) Neuronal amyloid-β accumulation within cholinergic basal forebrain in ageing and Alzheimer's disease. Brain 138:1722–1737. https://doi.org/10.1093/brain/awv024

24. Schmitz TW, Nathan Spreng R, Weiner MWM, et al (2016) Basal forebrain degeneration precedes and predicts the cortical spread of Alzheimer's pathology. Nat Commun 7:13249. https://doi.org/10.1038/ncomms13249

25. Bothwell M (2014) NGF, BDNF, NT3, and NT4. In: Lewin G, Carter B (eds) Neurotrophic Factors. Handbook of Experimental Pharmacology, vol 220. Springer, Berlin, Heidelberg, pp 3–15

26. Alderson RF, Alterman AL, Barde YA, Lindsay RM (1990) Brain-derived neurotrophic factor increases survival and differentiated functions of rat septal cholinergic neurons in culture. Neuron 5:297–306. https://doi.org/0896-6273(90)90166-D [pii]

27. Sanchez-Ortiz E, Yui D, Song D, et al (2012) TrkA Gene Ablation in Basal Forebrain Results in Dysfunction of the Cholinergic Circuitry. J Neurosci 32:4065–4079. https://doi.org/10.1523/JNEUROSCI.6314-11.2012

28. Latina V, Caioli S, Zona C, et al (2017) Impaired NGF/TrkA Signaling Causes Early AD-Linked Presynaptic Dysfunction in Cholinergic Primary Neurons. Front Cell Neurosci 11:68. https://doi.org/10.3389/fncel.2017.00068

29. Hartikka J, Hefti F (1988) Development of septal cholinergic neurons in culture: plating density and glial cells modulate effects of NGF on survival, fiber growth, and expression of transmitter-specific enzymes. J Neurosci 8:2967–85

30. Hatanaka H, Tsukui H, Nihonmatsu I (1988) Developmental change in the nerve growth factor action from induction of choline acetyltransferase to promotion of cell survival in cultured basal forebrain cholinergic neurons from postnatal rats. Dev Brain Res 39:85–95. https://doi.org/10.1016/0165-3806(88)90069-7

31. Rylett RJ, Williams LR (1994) Role of neurotrophins in cholinergic-neurone function in the adult and aged CNS. Trends Neurosci 17:486–490. https://doi.org/10.1016/0166-2236(94)90138-4

32. Hefti F (1986) Nerve growth factor promotes survival of septal cholinergic neurons after fimbrial transections. J Neurosci 6:2155–2162. https://doi.org/10.1523/JNEUROSCI.06-08-02155.1986

33. Sun, Chen B-Y, Xia Y, et al (2013) Functional switch from pro-neurotrophins to mature neurotrophins. Curr Protein Pept Sci 14:617–25. https://doi.org/10.2174/1389203711209070658

34. Clewes O, Fahey MS, Tyler SJ, et al (2008) Human ProNGF: Biological effects and binding profiles at TrkA, P75NTRand sortilin. J Neurochem 107:1124–1135. https://doi.org/10.1111/j.1471-4159.2008.05698.x

35. Fahnestock, Yu G, Michalski B, et al (2004) The nerve growth factor precursor proNGF exhibits neurotrophic activity but is less active than mature nerve growth factor. J Neurochem 89:581–592. https://doi.org/10.1111/j.1471-4159.2004.02360.x

36. Ioannou M, Fahnestock M (2017) ProNGF, but Not NGF, Switches from Neurotrophic to Apoptotic Activity in Response to Reductions in TrkA Receptor Levels. Int J Mol Sci 18:599. https://doi.org/10.3390/ijms18030599

37. Koshimizu H, Kiyosue K, Hara T, et al (2009) Multiple functions of precursor BDNF to CNS neurons: negative regulation of neurite growth, spine formation and cell survival. Mol Brain 2:27. https://doi.org/10.1186/1756-6606-2-27

38. Fahnestock, Michalski B, Xu B, Coughlin M (2001) The precursor pro-nerve growth factor is the predominant form of nerve growth factor in brain and is increased in Alzheimer's disease. Mol Cell Neurosci 18:210–220. https://doi.org/10.1006/mcne.2001.1016

39. Garcia KLP, Yu G, Nicolini C, et al (2012) Altered balance of proteolytic isoforms of pro-brain-derived neurotrophic factor in autism. J Neuropathol Exp Neurol. https://doi.org/10.1097/NEN.0b013e31824b27e4

40. Michalski B, Fahnestock M (2003) Pro-brain-derived neurotrophic factor is decreased in parietal cortex in Alzheimer's disease. Mol Brain Res 111:148–154. https://doi.org/10.1016/S0169-328X(03)00003-2

41. Seiler M, Schwab ME (1984) Specific retrograde transport of nerve growth factor (NGF) from neocortex to nucleus basalis in the rat. Brain Res 300:33–39. https://doi.org/10.1016/0006-8993(84)91338-6

42. Lu B, Nagappan G, Lu Y (2014) BDNF and synaptic plasticity, cognitive function, and dysfunction. In: Lewin G, Carter B (eds) Neurotrophic Factors. Handbook of Experimental Pharmacology, vol 220. Springer, Berlin, Heidelberg, pp 223-250

43. Lauterborn JC, Bizon JL, Tran TMD, Gall CM (1995) NGF mRNA is expressed by GABAergic but not cholinergic neurons in rat basal forebrain. J Comp Neurol 360:454–462. https://doi.org/10.1002/cne.903600307

44. Ha DH, Robertson RT, Roshanaei M, Weiss JH (1999) Enhanced survival and morphological features of basal forebrain cholinergic neurons in vitro: Role of neurotrophins and other potential cortically derived cholinergic trophic factors. J Comp Neurol 406:156–170. https://doi.org/10.1002/(SICI)1096-9861(19990405)406:2<156::AID-CNE2>3.0.CO;2-K

45. DiStefano PS, Friedman B, Radziejewski C, et al (1992) The neurotrophins BDNF, NT-3, and NGF display distinct patterns of retrograde axonal transport in peripheral and central neurons. Neuron 8:983–993. https://doi.org/10.1016/0896-6273(92)90213-W

46. Scott SA, Mufson EJ, Weingartner JA, et al (1995) Nerve growth factor in Alzheimer's disease: increased levels throughout the brain coupled with declines in nucleus basalis. J Neurosci 15:6213–6221. https://doi.org/10.1523/JNEUROSCI.15-09-06213.1995

47. Salehi A, Delcroix J-D, Belichenko P V., et al (2006) Increased App Expression in a Mouse Model of Down's Syndrome Disrupts NGF Transport and Causes Cholinergic Neuron Degeneration. Neuron 51:29–42. https://doi.org/10.1016/j.neuron.2006.05.022

48. Taylor AM, Blurton-Jones M, Rhee SW, et al (2005) A microfluidic culture platform for CNS axonal injury, regeneration and transport. Nat Methods 2:599–605.

https://doi.org/10.1038/nmeth777

49. Taylor AM, Rhee SW, Jeon NL (2006) Microfluidic Chambers for Cell Migration and Neuroscience Research. In: In: Minteer SD (eds) Microfluidic Techniques. Methods In Molecular Biology™, vol 321. Humana Press, New Jersey, pp 167–178

50. Holtzman D, Kilbridge J, Li Y, et al (1995) TrkA expression in the CNS: evidence for the existence of several novel NGF-responsive CNS neurons. J Neurosci 15:1567–1576. https://doi.org/10.1523/JNEUROSCI.15-02-01567.1995

51. Holtzman DM, Li Y, Parada LF, et al (1992) p140trk mRNA marks NGF-responsive forebrain neurons: Evidence that trk gene expression is induced by NGF. Neuron 9:465–478. https://doi.org/10.1016/0896-6273(92)90184-F

52. Sung K, Maloney MT, Yang J, Wu C (2011) A novel method for producing mono-biotinylated, biologically active neurotrophic factors: An essential reagent for single molecule study of axonal transport. J Neurosci Methods 200:121–128. https://doi.org/10.1016/j.jneumeth.2011.06.020

53. Schnitzler AC, Lopez-Coviella I, Blusztajn JK (2008) Purification and culture of nerve growth factor receptor (p75)-expressing basal forebrain cholinergic neurons. Nat Protoc 3:34–40. https://doi.org/10.1038/nprot.2007.477

Figure 1: Microfluidic device schematic depicting the well order to be followed during device preparation

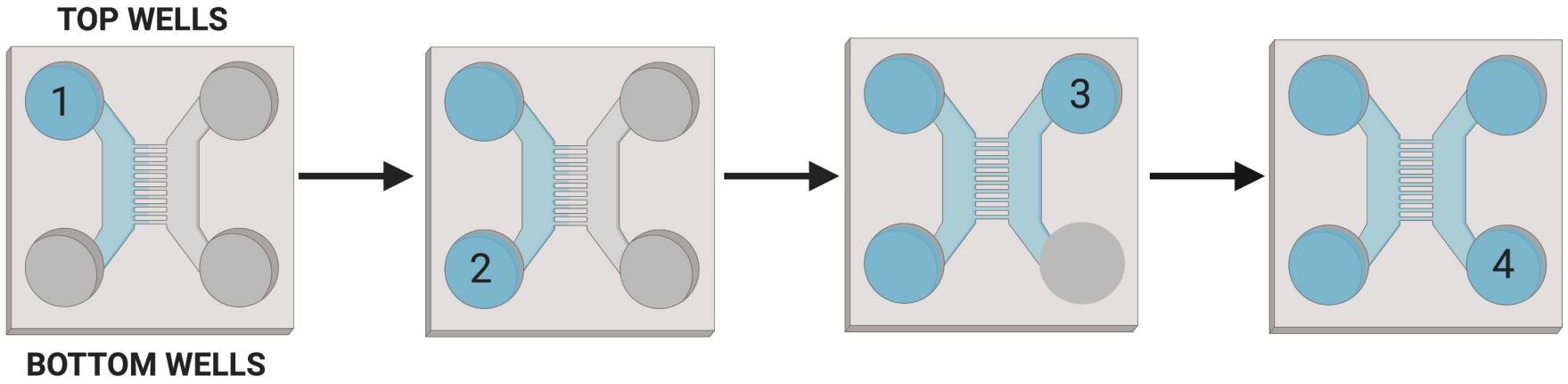

Figure 2: Microfluidic device schematic depicting the well order to be followed during media changes and washes

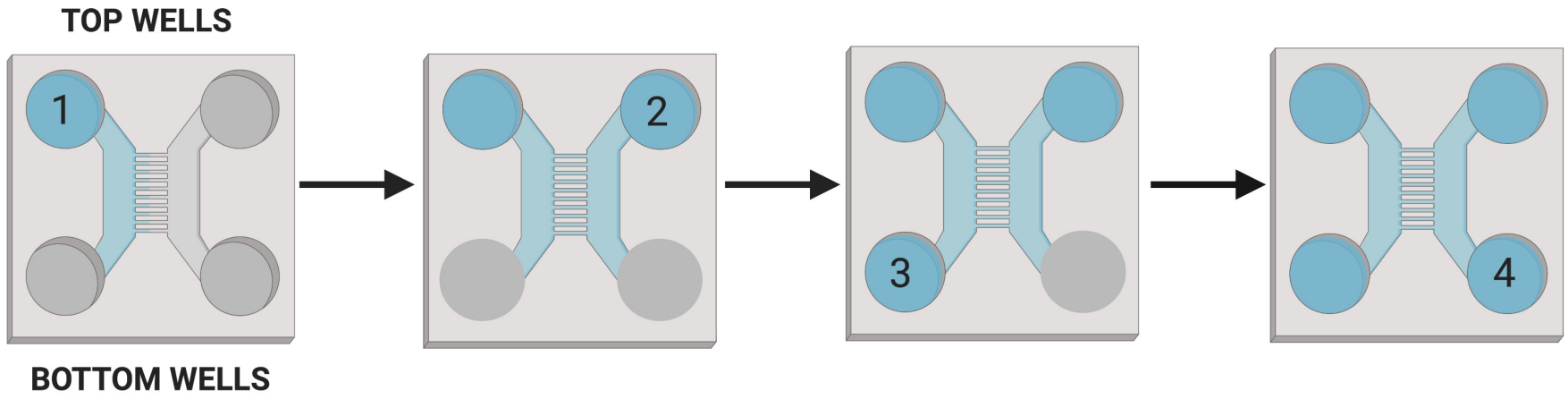

Figure 3: Graphical depiction of the dissection and processing procedure outlined in section 3.2

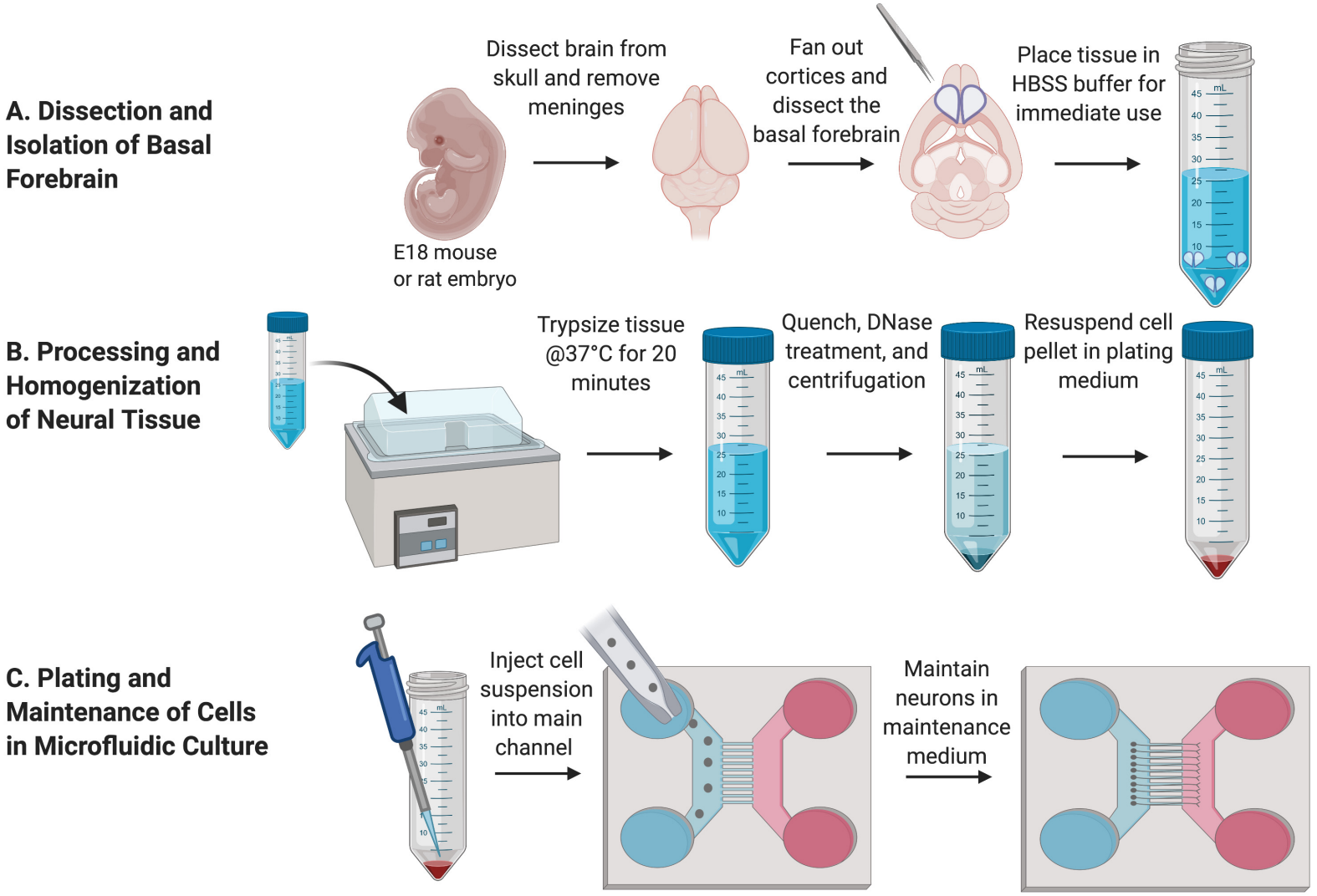

Figure 4: Basal Forebrain Cholinergic Neuron Axonal Extension Across Linear Microgrooves

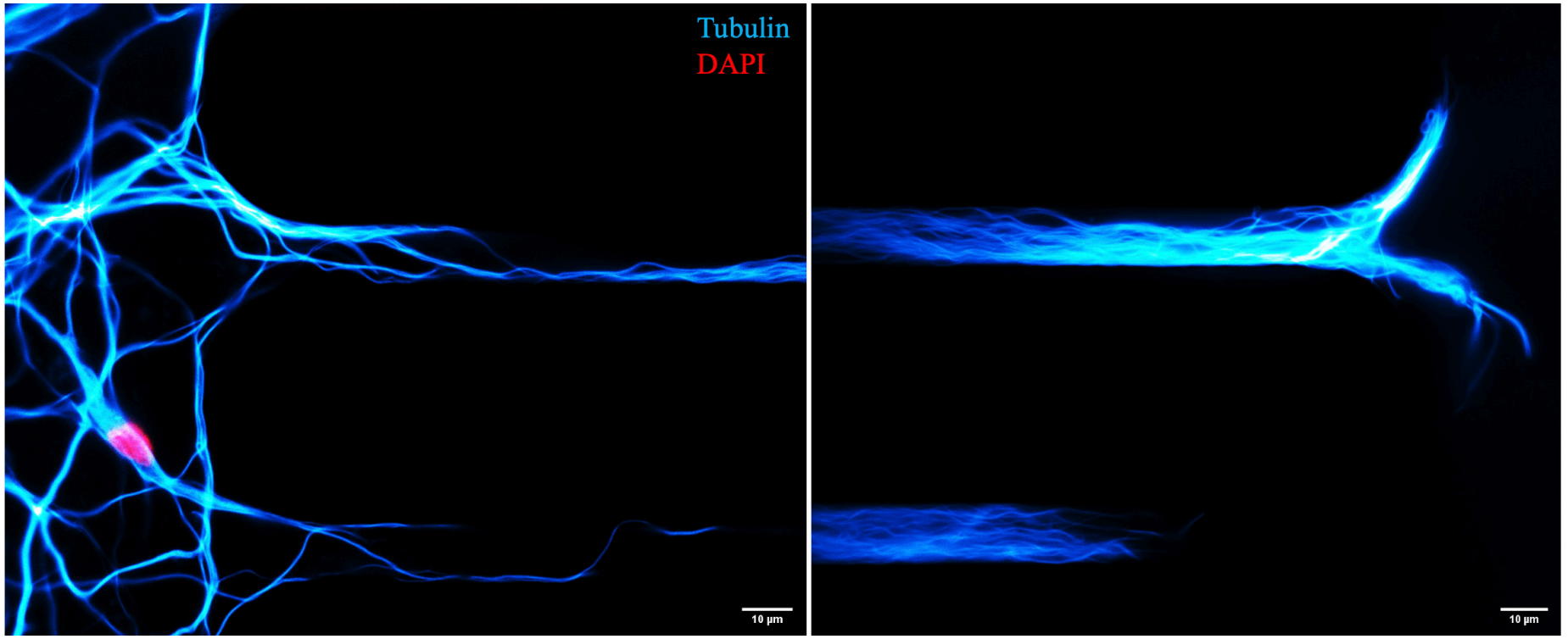

Figure 4. Basal forebrain cholinergic neurons (BFCNs) stained for tubulin (cyan) and DAPI (red) at day *in vitro* (DIV) 5. The left panel depicts BFCN cell bodies extending their axons into the microgrooves. The right panel depicts BFCN axons extending across the entire length of the 450µM microgroove barrier and beginning to enter the axonal main channel

Figure 5: Immunocytochemical Staining of Basal Forebrain Cholinergic Neurons Cultured in Microfluidic Chambers

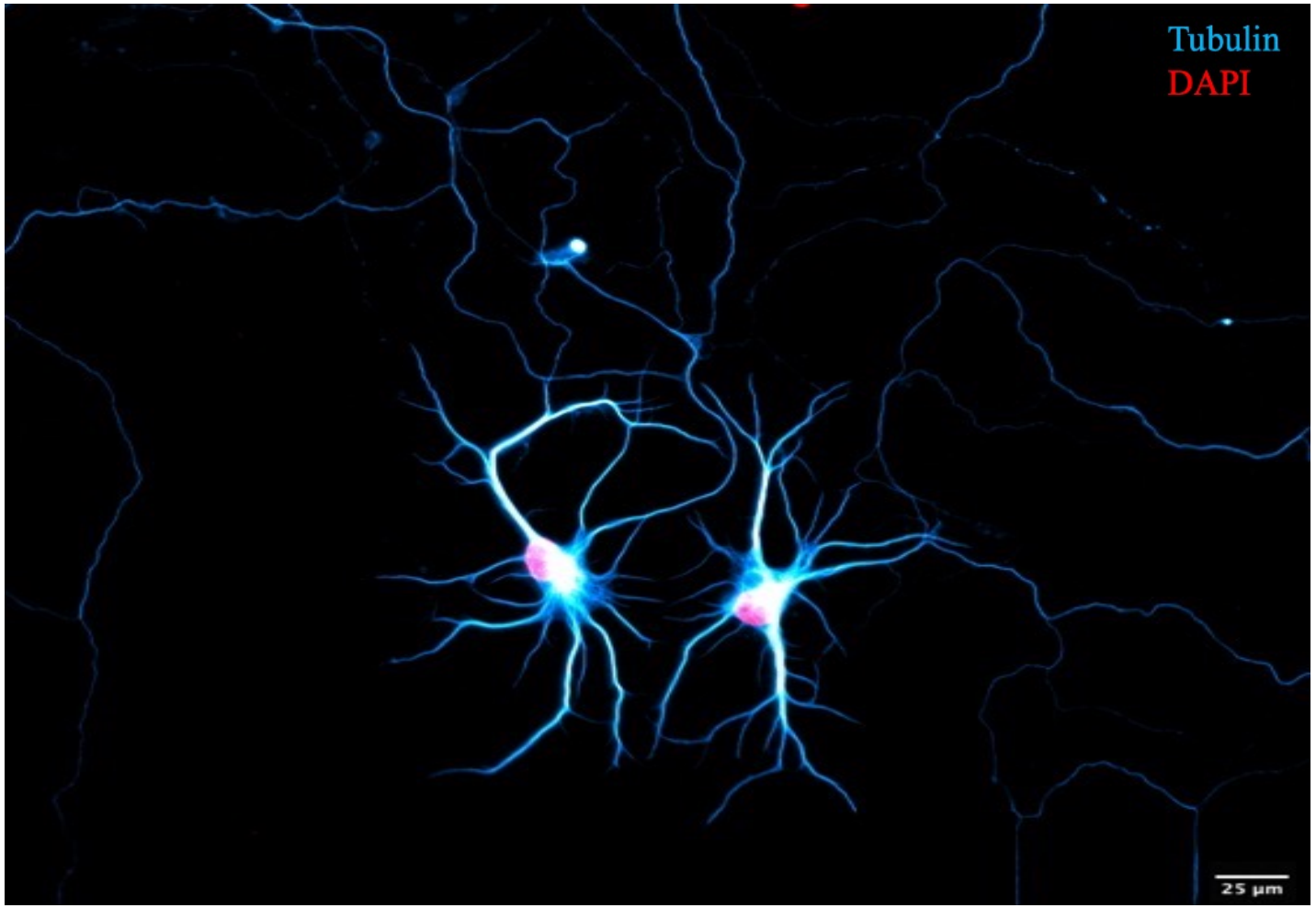

Figure 5. Basal forebrain cholinergic neurons (BFCNs) cultured in microfluidic chambers stained for tubulin (cyan) and DAPI (red) at day *in vitro* (DIV) 7 following the immunocytochemical staining protocol outlined in section 3.4.

Figure 6: A Microfluidic Device With an Air Bubble Present Within One of the 2 Main Channels

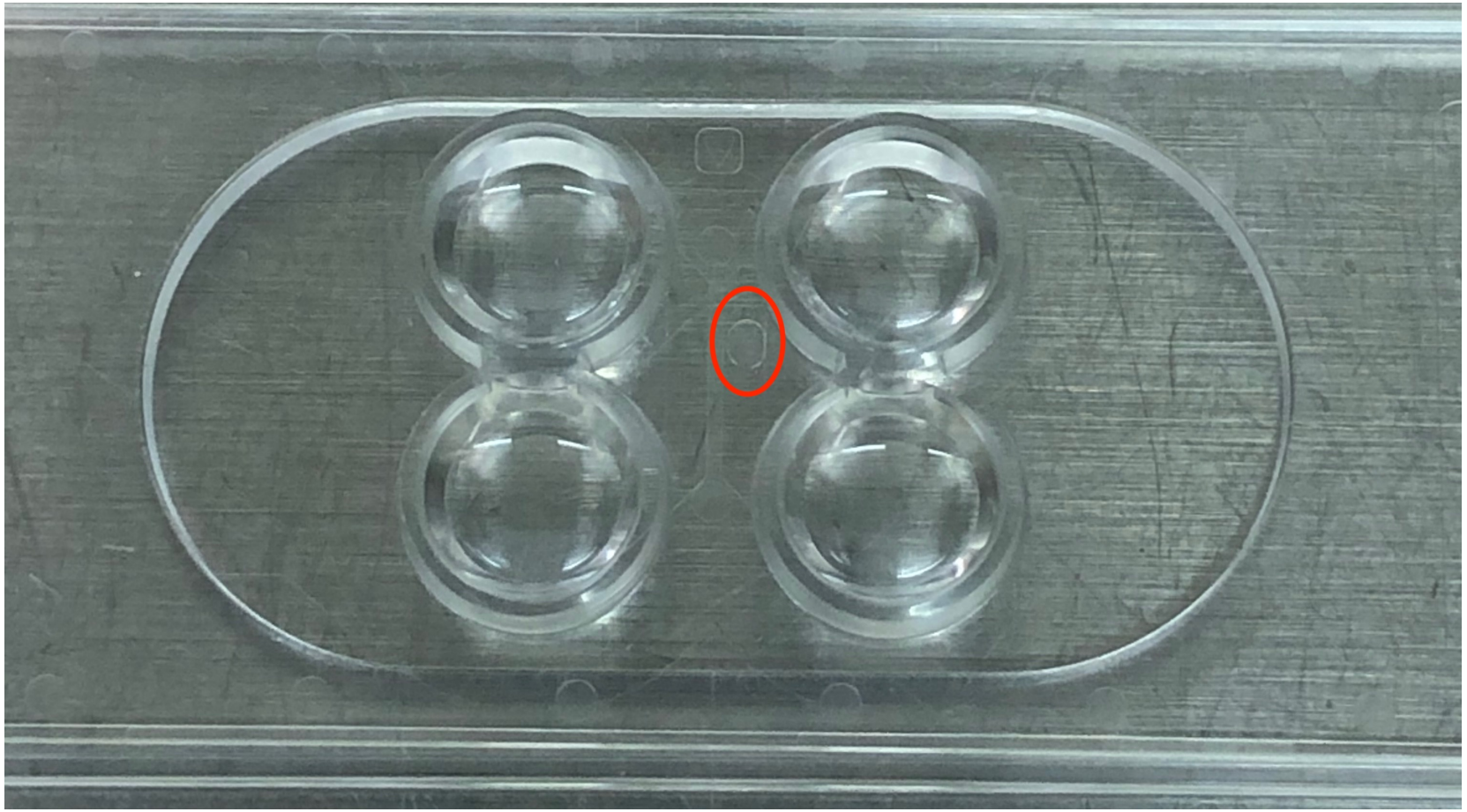

Preface

In this manuscript, the methodological insight gained from the previous chapter was used to determine the effect of age, the single greatest risk factor for developing AD, on neurotrophin transport in basal forebrain cholinergic neurons. I designed the experiments, collected and analyzed all of the data in this chapter, and prepared the manuscript.

3. Retrograde Axonal Transport of BDNF and proNGF Diminishes with Age in Basal Forebrain Cholinergic Neurons

Shekari, A., & Fahnestock, M. (2019). Retrograde axonal transport of BDNF and proNGF diminishes with age in basal forebrain cholinergic neurons. *Neurobiology of Aging*, *84*, 131–140.

Neurobiology of Aging 84 (2019) 131–140

Contents lists available at ScienceDirect

Neurobiology of Aging

journal homepage: www.elsevier.com/locate/neuaging

Retrograde axonal transport of BDNF and proNGF diminishes with age in basal forebrain cholinergic neurons

Arman Shekari, Margaret Fahnestock*

Department of Psychiatry and Behavioural Neurosciences, McMaster University, Hamilton, Ontario, Canada

ARTICLE INFO

Article history:
Received 25 March 2019
Received in revised form 22 July 2019
Accepted 31 July 2019
Available online 10 August 2019

Keywords:
Axonal transport
Neurotrophins
Neurodegeneration
Basal forebrain
Alzheimer's disease
Trk receptors

ABSTRACT

Basal forebrain cholinergic neurons (BFCNs) are critical for learning and memory and degenerate early in Alzheimer's disease (AD). BFCNs depend for their survival and function on nerve growth factor (NGF) and brain-derived neurotrophic factor (BDNF), which are retrogradely transported from BFCN targets. Age is the greatest risk factor for developing AD, yet the influence of age on BFCN axonal transport is poorly understood. To model aging, embryonic rat basal forebrain or cortical neurons were cultured in microfluidic chambers. Senescence-associated beta-galactosidase staining indicated an aging phenotype only in BFCNs cultured for 18+ days in vitro. BDNF axonal transport impairments were observed exclusivley in aged BFCNs. BFCNs displayed robust proNGF transport, which also diminished with in vitro age. The expression of NGF receptor tropomyosin-related kinase-A and BDNF receptor tropomyosin-related kinase-B also decreased significantly with in vitro age in BFCNs only. These results suggest a unique vulnerability of BFCNs to age-induced transport deficits. These deficits, coupled with the reliance of BFCNs on neurotrophin transport, may explain their vulnerability to age-related neurodegenerative disorders like AD.

1. Introduction

The basal forebrain is the primary source of cholinergic innervation in the central nervous system (CNS) and plays a critical role in learning, memory, attention, and regulation of cortical blood flow (Ballinger et al., 2016; Baxter and Chiba, 1999; Linville and Arnerić, 1991). Diffuse projections from basal forebrain cholinergic neurons (BFCNs) terminate mainly in the hippocampus and throughout the cortex (Ballinger et al., 2016). These projections, especially those of the septohippocampal tract, have been shown to degenerate with age (Grothe et al., 2012; Ypsilanti et al., 2008). Degeneration of the basal forebrain has been repeatedly observed in age-related neurodegenerative disorders like Alzheimer's disease (AD), with multiple studies demonstrating that basal forebrain dysfunction is predictive of the disorder (Baker-Nigh et al., 2015; Ballinger et al., 2016; Schmitz et al., 2016; Teipel et al., 2014). Furthermore, synaptic loss in BFCNs correlates strongly with dementia severity in AD and is implicated in aging and age-associated memory deficits (Ballinger et al., 2016; Ferreira-Vieira et al., 2016; Whitehouse et al., 1982; Ypsilanti et al., 2008).

Age-related degeneration of BFCNs may occur because of their unique reliance on target-derived trophic support. BFCNs do not make their own neurotrophins. They rely on their cortical and hippocampal targets to produce brain-derived neurotrophic factor (BDNF) and nerve growth factor (NGF) that are transported back to BFCN cell bodies via retrograde axonal transport (DiStefano et al., 1992; Götz et al., 2001; Seiler and Schwab, 1984; Sobreviela et al., 1996). Neurotrophins like BDNF and NGF are critical for a wide variety of cellular processes including apoptotic suppression, differentiation, activity-dependent plasticity, and maintenance of synaptic connectivity (Bothwell, 2014). As a result, retrograde axonal transport of neurotrophins by BFCNs is crucial for their proper function and survival. NGF receptor alterations have been observed before phenotypic alteration of BFCNs in AD, suggesting that a lack of neurotrophic support is causative with respect to basal forebrain degeneration (Mufson et al., 2000, 2003). In postmortem AD BFCN, tropomyosin-related kinase A (TrkA) receptor is lost whereas the pan-neurotrophin receptor ($p75^{NTR}$) and tropomyosin-related kinase B (TrkB) receptors are stable (Counts et al., 2004; Ginsberg et al., 2006; Mufson et al., 2000). Increased NGF-like immunoreactivity has been found in both the AD cortex and hippocampus, with decreased levels in the basal forebrain, suggesting a deficit in retrograde axonal NGF transport (Scott et al., 1995). Impaired NGF transport in BFCNs has also been demonstrated in the amyloid

* Corresponding author at: Department of Psychiatry and Behavioural Neurosciences, McMaster University, 1280 Main Street West, Hamilton, Ontario L8S 4K1, Canada. Tel.: +1 905 525 9140 ×- 23344; fax: +1 905 522 8804.
E-mail address: fahnest@mcmaster.ca (M. Fahnestock).

0197-4580/$ – see front matter © 2019 Elsevier Inc. All rights reserved.
https://doi.org/10.1016/j.neurobiolaging.2019.07.018

precursor protein overexpressing Ts65Dn Down syndrome mouse model (Cooper et al., 2001; Salehi et al., 2006). These results implicate dysfunctional BFCN retrograde axonal transport in AD pathogenesis.

Aside from AD, age itself has been shown to negatively impact the basal forebrain. BFCN nuclear size and overall BFCN numbers are decreased in aged rats (Altavista et al., 1990). TrkA receptor levels, the receptor for NGF, and levels of downstream NGF signaling proteins are decreased in aged rat BFCNs (Parikh et al., 2013; Williams et al., 2006, 2007). The length of cholinergic fibers projecting to the hippocampus from the basal forebrain is reduced with age (Ypsilanti et al., 2008). Moreover, general retrograde axonal transport is diminished in aged rat BFCNs (Bearer et al., 2018; Cooper et al., 1994; De Lacalle et al., 1996). These deficits have behavioral consequences, as both aged rats and Lim Homebox-7 (LHX7) knockout mice that fail to develop forebrain cholinergic neurons show learning and memory impairments (Fragkouli et al., 2005; Gustilo et al., 1999).

Although aging has been demonstrated to impact general axonal transport in the basal forebrain, the impact of aging on neurotrophin-specific transport is poorly understood. Although both proBDNF and BDNF are found in the CNS (Michalski and Fahnestock, 2003), the form of NGF found in both human and rodent brain is proNGF (Fahnestock et al., 2001). ProNGF binds to TrkA and activates mitogen-activated protein kinase and Akt pathways to signal survival and neurite outgrowth (Clewes et al., 2008; Fahnestock and Shekari, 2019; Fahnestock et al., 2004; Ioannou and Fahnestock, 2017; Masoudi et al., 2009). ProNGF is retrogradely transported by peripheral dorsal root ganglion neurons (DRGs) and colocalizes with TrkA and $p75^{NTR}$ in DRG axons (De Nadai et al., 2016). However, proNGF axonal transport in the CNS has not been reported in the literature. BDNF retrograde transport has been demonstrated in both cortical and hippocampal neurons, but not in BFCNs (Poon et al., 2011; Zhao et al., 2014). As a result, we sought to explore the impact of age on proNGF and BDNF axonal transport in BFCNs.

To study transport in BFCNs, we adopted a microfluidic platform to separate neuronal cell bodies from axons. To model aging, cells were assayed after either 7–10 days in vitro (DIV), just enough time to allow axons to cross the 450 μM microgroove barrier, or 18–20 DIV. Aging in vitro is not a perfect analog of in vivo aging, but it is commonly used in both primary neuron and stem cell cultures to examine age-sensitive phenomena (Campos et al., 2014; Martin et al., 2008; Palomer et al., 2016; Sodero et al., 2011; Uday Bhanu et al., 2010). To confirm an aging phenotype in our neurons, BFCNs were stained with senescence-associated beta-galactosidase (SaβG), a well-validated marker of aging in humans, primates, and rodents both in vivo and in vitro (Dimri et al., 1995; Kurz et al., 2000; Mishima et al., 1999; Uday Bhanu et al., 2010).

2. Methods

All reagents were purchased from ThermoFisher Scientific (Burlington, Ontario, Canada) unless otherwise stated.

2.1. Neuron culture in microfluidic chambers

One day before dissection, microfluidic chambers (Xona Microfluidics, Temecula, CA, USA) were prepared according to the manufacturer's instruction. Briefly, 95% ethanol was added to each well of the chamber, followed by 2 phosphate-buffered saline (PBS) washes. One hundred microliters of poly-L-lysine (Sigma-Aldrich, Burlington, Ontario, Canada) was added to each of the wells, and the chambers were left to incubate overnight in an incubator at 37 °C and 5% CO_2. The chambers were then washed once with PBS, and 150 μL of cell culture medium was added to each of the wells. The cell culture medium consisted of Neurobasal, 1% Penicillin-Streptomycin, 1X B27 supplement, 1X GlutaMAX supplement, 1% fetal bovine serum, 50 ng/mL BDNF (Peprotech, Rocky Hill, NJ), and 50 ng/mL NGF (generous gift from Dr Michael Coughlin, McMaster University, Hamilton, Canada). The chambers were left to incubate at 37 °C and 5% CO_2 during the dissection.

Whole basal forebrain and cortex were dissected from embryonic day 18 rat embryos and immediately placed on ice in a solution of Hank's balanced salt solution with 1% Penicillin-Streptomycin. The tissue from 5 embryos was pooled for each round of dissection; therefore, sex was not determined. The neural tissue was washed with fresh Hank's balanced salt solution 5 times and then trypsinized in a water bath at 37 °C for 20 minutes. DNase I (Sigma-Aldrich) was added to a final concentration of 1×, and the tissue was triturated using a sterile, small-bore, fire-polished, glass pipette. Then 1 mL of cell culture medium was added, and the suspension was centrifuged at 250*g* for 4 minutes. The cell pellet was resuspended in 300 μL of cell culture medium, and the volume was adjusted to a final concentration of 1.0×10^6 cells/mL. After this, 140 μL of medium was removed from each of the 4 wells of the chambers, and 10 μL of cell suspension was added to the 2 left wells. The chambers were incubated for 10 minutes to allow cell adherence, which was confirmed under a microscope (Zeiss AxioVert A1). Then 150 μL of cell culture medium was added to all wells, and the cells were incubated overnight at 37 °C and 5% CO_2. The next day, all the medium was removed and replaced with a serum-free variant of the medium described previously. Cells were maintained in this medium for the duration of the experiments, with medium changes occurring every 48–72 hours.

2.2. Immunostaining and confirmation of BFCN phenotype

Neurons were stained for TrkA, TrkB, $p75^{NTR}$, and vesicular acetylcholine transporter (VAChT). Immunostaining was carried out in the microfluidic devices themselves. Cells were fixed in freshly prepared 4% paraformaldehyde for 30 minutes at room temperature (RT). Cells were washed 2 times with PBS, permeabilized with 0.2% Triton-X100 in PBS for 30 minutes at RT and blocked with 3% bovine serum albumin in PBS for 30 minutes at RT. Primary antibodies anti-TrkA (Santa Cruz Biotechnology, Santa Cruz, CA) or anti-VAChT (Santa Cruz Biotechnology) were added at a 1:500 dilution, anti-TrkB (Cell Signaling Technologies, Danvers, MA, USA) at a 1:500 dilution, and anti-$p75^{NTR}$ (Cell Signaling Technologies) at a 1:1600 dilution and were left to incubate overnight at 4 °C. Cells were washed with blocking solution 3 times on the following day. Alexa Fluor 488 secondary antibody was then added at a 1:1000 dilution and was left to incubate for 2 hours at RT. Neurons were visualized via fluorescence microscopy using a yellow fluorescent protein filter cube set (488 nm excitation, 525 nm emission). All immunostaining was carried out in microfluidic chambers between DIV10 and DIV18. TrkA and VAChT staining was robust at DIV10 (Supplementary Fig. 1A and B). Cortical neurons, as expected, did not express either and were used as a negative control (Supplementary Fig. 1C).

2.3. Histologic staining

Neurons were stained for SaβG at DIV7–10 and at DIV18–20. Cells were stained within the chambers themselves, with 150 μL of fixative added to all wells, followed by 150 μL of staining solution prepared according to the manufacturer's instruction (Cell Signaling). Cells were imaged using a Zeiss AxioVert A1 microscope.

2.4. Preparation of labeled neurotrophins

2.4.1. BDNF

Biotinylated BDNF was purchased from Alomone Labs (Tel Aviv, Israel). BDNF-biotin was incubated with Quantum Dot 625 Streptavidin conjugate at a 1:1 molar ratio on ice for 1 hour in the dark, and then diluted to 1 nM using serum-free cell culture medium without BDNF and NGF.

2.4.2. proNGF

We use a cleavage-resistant proNGF mutant containing a cytosine-to-guanine point mutation at position 633, resulting in an arginine-to-glycine substitution at the −1 position (ProNGF[R-1G]; Fahnestock et al., 2004). This cleavage-resistant proNGF binds to TrkA and $p75^{NTR}$, is internalized, and activates mitogen-activated protein kinase and Akt pathways (Fahnestock et al., 2004; Ioannou and Fahnestock, 2017; Masoudi et al., 2009). This sequence was engineered to include both a biotin-accepting Avi and a nickel-binding histidine tag, as described in Sung et al. (2011). Briefly, a vector containing proNGF-Avi (a generous gift from Dr Chengbiao Wu, UCSD) was digested using *Eco*R1 and *Bam*H1, and the excised proNGF-Avi fragment was ligated into a pcDNA 3.1 myc.his(+) vector. The R-1G mutation was then introduced using site-directed mutagenesis as described in Fahnestock et al. (2004) using the QuikChange II site-directed mutagenesis kit from Agilent Technologies (Santa Clara, CA, USA).

One microgram of the tagged proNGF[R-1G] plasmid, along with 20 μg of a plasmid encoding biotin ligase (a generous gift from Dr Chengbiao Wu, USCD), was cotransfected into HEK293FT cells using Lipofectamine 3000. Cells were grown to 70% confluency in medium containing Dulbecco's minimal essential medium, 1% fetal bovine serum, 1% Penicillin-Streptomycin, 200 mM GlutaMAX supplement, 50 μM D-biotin (Sigma-Aldrich), and 100 mM sodium pyruvate (Sigma-Aldrich). Medium was collected 72 hours post-transfection. ProNGF-biotin was purified from the medium via nickel affinity chromatography. Protein concentration was determined via an in-house NGF enzyme-liked immunosorbent assay (Fahnestock et al., 2004). Biotinylated proNGF was shown to be intact by Western blotting (Supplementary Fig. 2) and was labeled with Quantum Dot 625 as described previously for BDNF.

2.5. Tracking neurotrophin transport

2.5.1. BDNF

Neuronal cell bodies and axons were starved of neurotrophin by incubating overnight in medium containing only Neurobasal, 1% Penicillin-Streptomycin, 1X B27 supplement, and 1X GlutaMAX supplement. The next day, cells were washed 3 times with this neurotrophin-free medium to remove any residual neurotrophins. To the axonal side of the chambers was added 160 μL of 1 nM quantum dot-labeled BDNF (QD-BDNF) and was incubated for 1 hour (BFCNs) or 4 hours (cortical neurons) to account for differences in BDNF uptake efficiency between the cell types. The chambers were then transferred to an EVOS2 FL Microscope (ThermoFisher Scientific) with an environmental chamber set to 37 °C and 5% CO_2. QDs were visualized using a TexasRed filter, exciting at 585 nm and detecting emission at 624 nm. Kymographs were generated by compiling 120 images (from the TexasRed filter only) taken every 2 seconds into a vertical Z-stack using ImageJ. Particle speeds and pause duration were calculated using the mTrackJ ImageJ plug-in to track the distance traveled by labeled particles between images. Experiments were repeated 3 times.

2.5.2. proNGF

BFCN cell bodies were starved of neurotrophins as described previously, and 160 μL of 50 pM quantum dot-labeled proNGF (QD-proNGF) was added to the axons immediately and incubated for 1 hour. The same microscope described previously was used to capture the proNGF data. Mean fluorescence intensity was determined by measuring the mean gray value of pixels within proNGF-positive cell bodies with ImageJ. Experiments were repeated 3 times.

2.6. Statistical analysis

Sample sizes were similar to those reported in other related publications (Mufson et al., 2000; Poon et al., 2011; Zhao et al., 2014). Unpaired, 2-tailed Student's *t* tests were performed when comparing 2 groups, with a confidence interval of 95%. One-way analysis of variance (ANOVA) with post hoc Tukey tests was performed when more than 2 groups were compared, with a p value of 0.05 being considered significant. All error bars represent the standard error of the mean. Statistical methods are further elaborated on in the text and in all figure legends.

3. Results

3.1. BDNF transport is impaired in aged BFCNs but not cortical neurons

To determine the effect of aging in vitro on retrograde neurotrophin transport in BFCNs, axonal transport assays using QD-BDNF were carried out and kymographs were generated using neurons kept in culture for differing lengths of time. DIV8 BFCNs (Fig. 1A–C) and DIV22 cortical neurons (Fig. 1G–I) showed robust BDNF transport as indicated by sloped diagonal lines in the kymographs, whereas QD-BDNF taken up by DIV21 BFCNs were largely stationary as shown by the vertical lines (Fig. 1D–F). Quantification of QD-BDNF particle movement (Fig. 2A and B) demonstrated that the speed of QD-BDNF particles decreased significantly in DIV18–20 BFCNs compared with DIV7–10 BFCNs (N =60 QD-BDNF particles per group, $p = 0.003$, 1-way ANOVA and post hoc Tukey test). However, QD-BDNF particle speed did not differ between DIV7–10 BFCNs and DIV18 cortical neurons (N = 60 QD-BDNF particles per group $p = 0.9$, 1-way ANOVA and post hoc Tukey test). QD-BDNF particles also paused for significantly longer in DIV18–20 BFCNs compared with DIV7–10 BFCNs (N = 60 QD-BDNF particles per group, $p < 0.001$, 1-way ANOVA and post hoc Tukey test). QD-BDNF particles in DIV18–20 cortical neurons did not differ significantly in pause duration from DIV7–10 BFCNs (N = 60 QD-BDNF particles per group, $p = 0.928$, 1-way ANOVA and post hoc Tukey test). BDNF transport did not decrease significantly with further in vitro aging, as DIV21–24 BFCNs were not significantly different from DIV18–20 BFCNs in terms of BDNF speed and pause duration (data not shown).

3.2. proNGF uptake is robust in young BFCNs and is reduced with age in vitro

Next, we aimed to characterize proNGF transport in BFCNs and to assess the role of in vitro aging on the process. To determine if similar axonal transport deficits could be seen with proNGF, experiments were repeated using the same time points with cleavage-resistant proNGF as opposed to BDNF. Of note, cortical neurons could not be used as a comparison group because of their lack of TrkA expression.

The conditions required for proNGF uptake differed from BDNF: neurotrophic starvation of axon terminals and cell bodies, as carried out for BDNF, resulted in no proNGF being taken up by BFCNs; proNGF transport occurred only after cell bodies alone instead of axon terminals and cell bodies were starved of neurotrophins

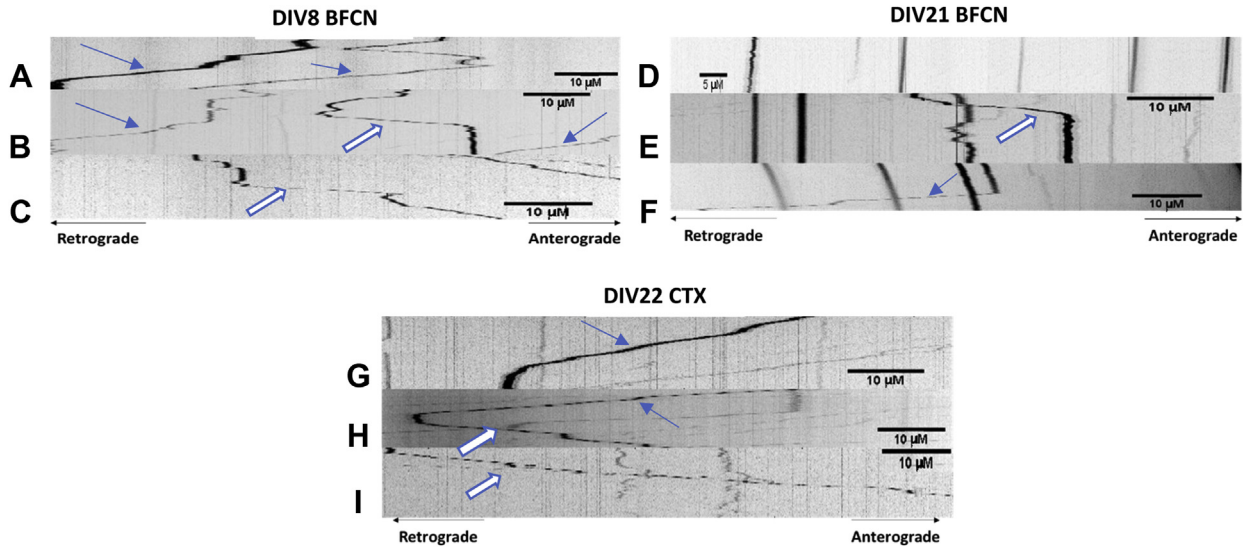

Fig. 1. BDNF transport in BFCNs and CTXs aged in culture. Kymographs of quantum dot–labeled BDNF (QD-BDNF) particles within the microgrooves of BFCNs (A–F) and CTXs (G–I) in microfluidic chambers. Sloped lines represent movement in the anterograde or retrograde direction as indicated by open or closed arrows, respectively. Vertical line segments indicate instances of no movement or pausing. Neurons were cultured for at least 7 DIV to allow axons to fully traverse the microgrooves. Images were taken 1 hour after 1 nM QD-BDNF was added to the axon terminal side only. Aged (DIV21) BFCNs clearly show stationary QD-BDNF (D–F). Abbreviations: BDNF, brain-derived neurotrophic factor; BFCN, basal forebrain cholinergic neuron; CTX, cortical neuron; DIV, days in vitro.

(Fig. 3A and B). We also determined that proNGF uptake by DIV7–10 BFCNs was extremely rapid. ProNGF uptake occurred within 15 minutes of its administration, and it accumulated in cell bodies after just 1 hour (Figs. 3A and 4A). ProNGF uptake in DIV7–10 BFCNs was also extremely robust, as just 50 pM proNGF was enough to yield a QD-proNGF signal along the entire length of the BFCN axons (Figs. 3A and 4C). For comparison, BDNF uptake was undetectable at 50 pM (data not shown), and transport required at least 1 nM BDNF and starvation of both axons and cell bodies (Fig. 3C and D).

Next, we assessed the effect of in vitro aging on proNGF uptake. Experiments were completed at DIV7–10 and DIV18–20, with the only difference being the starvation conditions required for proNGF uptake as described previously; cell bodies were starved of neurotrophins and QD-proNGF was added immediately to the axonal compartment. ProNGF accumulation in DIV18–20 BFCN cell bodies was significantly diminished compared with DIV7–10 BFCNs (Figs. 4A, B and 5, N = 100 cell bodies, $p < 0.001$, Student's t test).

3.3. Aged BFCNs stain positive for SaβG

To determine if neurons cultured for extended periods of time displayed signs of aging, we carried out histologic staining for SaβG. BFCNs cultured for 10 DIV did not stain for SaβG (Fig. 6A). Only BFCNs cultured for 18 days or more stained positive for SaβG (Fig. 6B and C). Staining became more pronounced as the neurons were kept longer in culture, with DIV21–24 BFCNs demonstrating robust SaβG staining (Fig. 6C). Cortical neurons did not stain positive for SaβG even at DIV24 (Fig. 6D and E).

3.4. TrkB immunoreactivity is decreased in BFCNs but not cortical neurons aged in vitro

To determine if a reduction in the BDNF receptor TrkB was facilitating the impaired BDNF transport in aged BFCNs, immunostaining for TrkB was carried out at both time points. DIV18 BFCNs displayed significantly reduced TrkB immunoreactivity compared

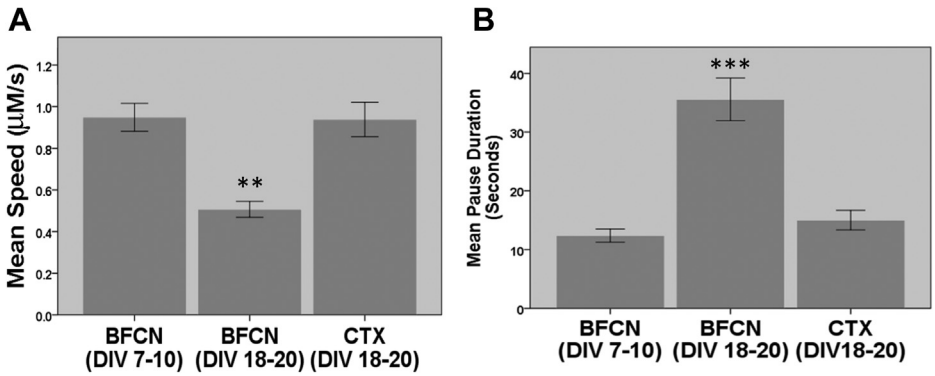

Fig. 2. BDNF transport speed and pause duration in basal forebrain BFCNs and CTXs aged in culture. Quantification of speed (A) and pause duration (B) of quantum dot-labeled BDNF (QD-BDNF) in basal forebrain cholinergic neurons (BFCNs) and CTXs. Data were collected 1 hour after 1 nM QD-BDNF was added to the axon terminal side of the microfluidic chambers for BFCNs, and 4 hours for CTXs. Neurons cultured for either 7–10 days in vitro (DIV) or 18–20 DIV. The mTrackJ plug-in for ImageJ was used to determine the distanced traveled by QD-BDNF particles between time-lapse images. Each bar shows N = 60 QD-BDNF particles from 3 different chambers and 3 rounds of dissection (5 embryos each). Data are represented as the mean ± SE. $^{**}p < 0.01$, $^{***}p < 0.001$, 1-way ANOVA and post hoc Tukey test. Abbreviations: ANOVA, analysis of variance; BDNF, brain-derived neurotrophic factor; BFCN, basal forebrain cholinergic neuron; CTX, cortical neuron; DIV, days in vitro; SE, standard error.

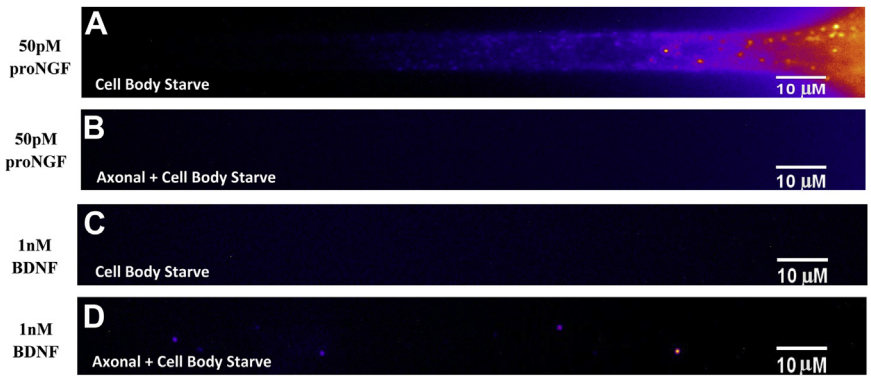

Fig. 3. Representative uptake of neurotrophins in BFCNs. proNGF uptake (C) by BFCNs is more robust than BDNF uptake (A and B). proNGF uptake conditions differ from BDNF (A–D). All images were taken at the first instance of fluorescence in the microgrooves after quantum dot (QD)-labeled neurotrophin administration to axon terminals only. For QD-BDNF, images were taken 1 hour after neurotrophin addition following starvation of axons and cell bodies overnight. For QD-proNGF, images were taken 15 minutes after starvation of cell bodies only followed by immediate QD-proNGF addition. Individual microgrooves visualized. Abbreviation: BDNF, brain-derived neurotrophic factor; BFCN, basal forebrain cholinergic neuron; NGF, nerve growth factor.

with DIV10 (Fig. 7A, B, and E, N = 60 cell bodies, $p < 0.001$, 1-way ANOVA and post hoc Tukey test). TrkB immunoreactivity in cortical neurons did not change significantly with in vitro age (Fig. 7C–E, N = 60 cell bodies, $p = 0.8$, 1-way ANOVA and post hoc Tukey test). TrkB immunoreactivity in DIV10 BFCNs was significantly higher compared with cortical neurons at both DIV10 and DIV18 (Fig. 7A, C–E) N = 60 cell bodies, $p < 0.001$, 1-way ANOVA and post hoc Tukey test).

3.5. TrkA, but not $p75^{NTR}$, immunoreactivity is decreased in BFCNs aged in vitro

To determine if a reduction in proNGF receptors TrkA and $p75^{NTR}$ was mediating the reduced proNGF uptake in DIV18–20 BFCNs, immunostaining for TrkA and $p75^{NTR}$ was carried out at both time points. TrkA immunoreactivity was significantly reduced in BFCNs at DIV18 compared with DIV10 (Fig. 8, N = 60 cell bodies, $p < 0.001$, Student's t test), whereas $p75^{NTR}$ immunoreactivity did not change significantly between the 2 time points (Fig. 9, $N = 60$ cell bodies, $p = 0.09$, Student's t test).

4. Discussion

Here, we characterized neurotrophin axonal transport and neurotrophin receptor expression in BFCNs. We demonstrated that both BDNF transport and proNGF transport diminish with in vitro aging in BFCNs and that BDNF transport deficits are unique to BFCNs. For BDNF, significant increases in pause duration and decreases in axonal transport speed were seen in DIV18–20 BFCNs but not in younger BFCNs or in DIV18–20 cortical neurons. Cortical neurons whose axons were clearly degenerated (e.g., whose axons were no longer smooth and continuous) ceased to take up BDNF only at DIV28. For proNGF, levels of uptake were significantly diminished in DIV20 BFCNs compared with DIV8 BFCNs. BFCNs cultured for 18 days or more, but not cortical neurons, stained positive for SaβG and were the only neurons that displayed

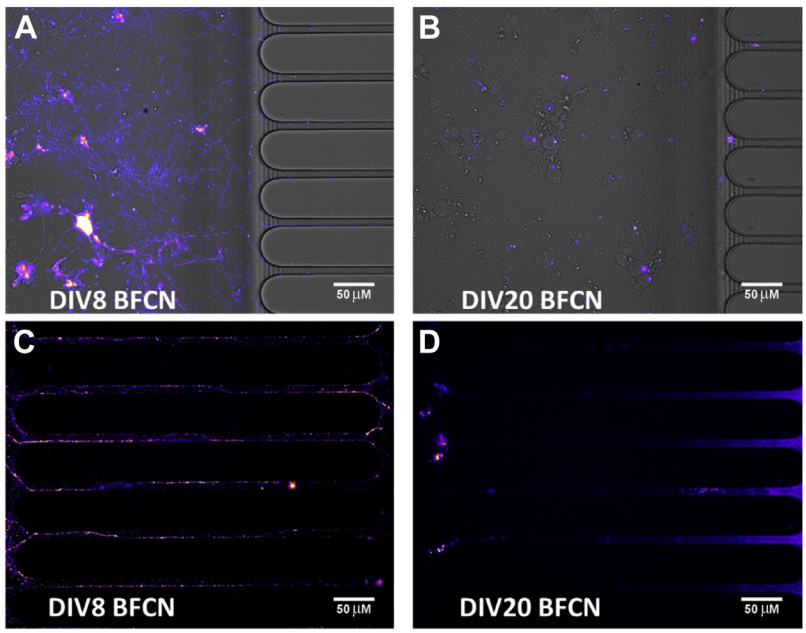

Fig. 4. Uptake and transport of quantum dot-labeled proNGF (QD-proNGF) in BFCNs. Data were collected 1 hour after 50 pM QD-proNGF[R-1G] was added to the axon terminal side of the microfluidic chambers. (A and B) Cell bodies; (C and D) microgrooves (axons). Abbreviations: DIV, days in vitro; NGF, nerve growth factor.

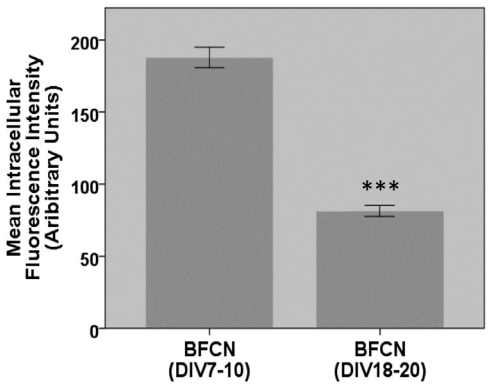

Fig. 5. Quantification of quantum dot-labeled proNGF (QD-proNGF) uptake by BFCNs. BFCN cell bodies demonstrated more proNGF[R-1G] at DIV8 compared with DIV20. N = 100 cell bodies per group, from 3 different chambers and 2 rounds of dissection (5 embryos each). Data are represented as the mean ± SE. ***$p < 0.001$ by Student's t test. Abbreviations: DIV, days in vitro; NGF, nerve growth factor; SE, standard error.

neurotrophic transport deficits. BFCNs aged in vitro displayed significantly reduced TrkA and TrkB immunoreactivity. $p75^{NTR}$ immunoreactivity did not change significantly in BFCNs aged in vitro. These findings strongly suggest that BFCNs are particularly susceptible to senescence and age-induced neurotrophin transport deficits and to TrkA and TrkB receptor downregulation.

BFCNs were much more efficient in their uptake of BDNF compared with their cortical counterparts. We found that cortical neurons required a 4-hour incubation with QD-BDNF in order for transport within the microgrooves to be observed, in line with previously reported findings in hippocampal neurons (Poon et al., 2011; Zhao et al., 2014). BFCNs, on the other hand, required only 1 hour of incubation time. This is most likely because of the greater TrkB expression observed in BFCNs compared with cortical neurons. BDNF uptake was slower in DIV18 BFCNs (data not shown) compared with DIV10, further implicating TrkB levels in BDNF uptake latency. Once taken up, transport speed (1 μM/s) and mean pause duration (12.4 seconds) of BDNF by DIV10 BFCNs were similar to both cortical and hippocampal neurons (Poon et al., 2011; Zhao et al., 2014). Reduced TrkB receptor levels do not account for the decreased motility of BDNF particles in DIV18 BFCNs because DIV18 cortical neurons displayed significantly less TrkB immunoreactivity compared with DIV10 BFCNs, but their BDNF transport dynamics did not differ. Although differences in TrkB expression may explain the variance in BDNF uptake efficiency between cell types, the mechanism of decreased BDNF motility along axons with increased in vitro age remains unknown.

The efficiency of BFCN neurotrophin transport was even more evident with proNGF than with BDNF, with proNGF uptake beginning within 10 minutes of neurotrophin addition to BFCN axon terminals. This time course was even faster than in DRGs, a class of neurons in which proNGF transport is well characterized. In DRGs, proNGF transport occurs after 35 minutes (De Nadai et al., 2016; Villarin et al., 2016). Taken together, these results suggest that both CNS and peripheral nervous system neurons are capable of rapid proNGF uptake and subsequent retrograde axonal transport. The functional implications of this rapid uptake are currently unknown.

The conditions required for uptake differed between BDNF and proNGF. For BDNF, both axons and cell bodies were deprived of neurotrophin for at least 1 hour before uptake was observed. For proNGF, depriving both the axons and cell bodies of neurotrophin completely inhibited uptake. This finding suggests that TrkA trafficking in BFCNs is similar to DRGs, where NGF-bound TrkA promotes the recruitment of additional TrkA receptors to axon terminals in a positive feedback loop (Yamashita et al., 2017). Cutting off neurotrophin supply to the axons abolishes this positive feedback loop, reducing TrkA trafficking to the terminals. This finding also suggests that TrkA and TrkB trafficking are governed by distinct mechanisms in BFCNs, because axonal neurotrophin starvation abolishes TrkA-mediated (proNGF) transport but not TrkB-mediated (BDNF) transport (Zhao et al., 2014).

The uptake of proNGF was diminished in BFCNs aged in vitro. This diminished uptake coincided with a significant decrease in TrkA receptor immunoreactivity. $p75^{NTR}$ immunoreactivity did not decrease with in vitro age. These findings suggest that the reduction in TrkA receptor levels is responsible for the reduced uptake of proNGF by BFCNs aged in vitro. $p75^{NTR}$ has a higher binding affinity for proNGF compared with TrkA (Clewes et al., 2008; Nykjaer et al.,

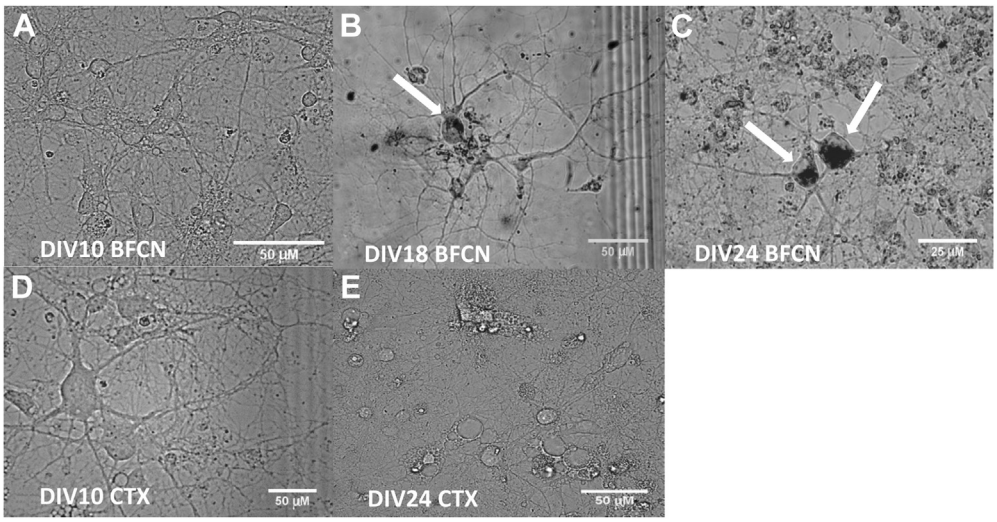

Fig. 6. Senescence-associated beta-galactosidase stain of BFCN and (CTX) aged in culture. DIV10 BFCNs and CTXs do not stain for senescence-associated beta-galactosidase (A and D). BFCNs begin to stain positive at DIV18, with more pronounced staining occurring at DIV24 (B and C). DIV24 CTXs do not stain positive for senescence-associated beta-galactosidase (E). Arrows indicate labeled cell bodies. Abbreviations: BFCN, basal forebrain cholinergic neuron; CTX, cortical neuron; DIV, days in vitro.

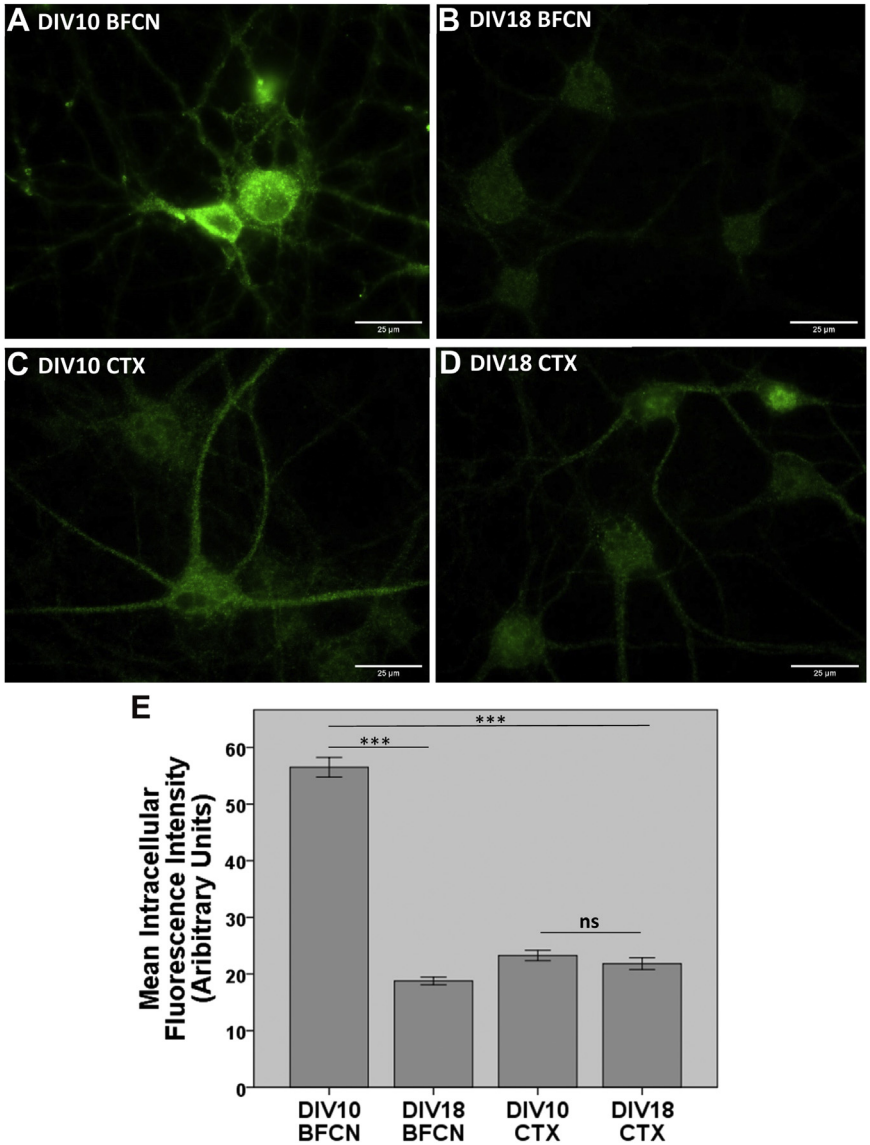

Fig. 7. Decreased TrkB immunoreactivity in BFCNs but not CTXs aged in vitro. BFCN cell bodies demonstrated significantly less TrkB immunoreactivity at DIV18 (B) compared with DIV10 (A). TrkB immunoreactivity did not change significantly in CTXs between DIV10 (C) and DIV18 (D). TrkB immunoreactivity was significantly greater in BFCNs at DIV10 (A) compared with CTXs at all time points (C,D). Quantification in (E). Each bar shows N = 60 cell bodies from 3 different chambers and 3 rounds of dissection (5 embryos each). Data are represented as the mean ± SE. $^{***}p < 0.001$, "ns" = not significant ($p = 0.8$) 1-way ANOVA and post hoc Tukey test. Abbreviations: ANOVA, analysis of variance; BFCN, basal forebrain cholinergic neuron; CTX, cortical neuron; DIV, days in vitro; SE, standard error; TrkB tropomyosin-related kinase B.

2004). However, its maintenance in DIV18 BFCNs did not result in maintenance of proNGF transport at this time point, suggesting that the balance between TrkA and $p75^{NTR}$ levels is important for the retrograde transport of proNGF and that loss of TrkA contributes to reduced proNGF transport in aged BFCNs.

Although the uptake of proNGF was diminished in aged BFCNs, the robust level of uptake observed in young BFCNs was surprising. To observe a QD-proNGF signal along the entire length of the microgrooves 50 pM of proNGF was enough. This rapid and robust uptake of proNGF made generating kymographs with individual trackable particles difficult. With BDNF, even concentrations of over 1 nM resulted in few particles populating the microgrooves. These results strongly suggest that proNGF uptake is more efficient than BDNF uptake in BFCNs.

One of the key limitations of this work is the in vitro model of aging. Cultured CNS neurons are viable for 3–4 weeks in culture before they degenerate. With the lifespan of healthy rats being around 2 years, the degeneration seen in vitro occurs at an accelerated rate compared with in vivo. However, many of the hallmarks associated with neuronal aging in vivo are recapitulated in vitro. Hippocampal neurons kept in culture for 3 weeks display reactive oxygen species accumulation, lipofuscin granules, loss of cholesterol from cell membranes, and activation of both the phosphorylated c-Jun N-terminal kinase and p53/p21 pathways, all of which are also seen in neurons taken from aged animals (Brewer et al., 2007; Calvo et al., 2015; Porter et al., 1997; Sodero et al., 2011). Furthermore, it has recently been demonstrated that general axonal transport through the septohippocampal tract is reduced in vivo with normal aging in mice and is exacerbated by AD pathology (Bearer et al., 2018). Our BFCNs, but not cortical neurons, stained positive for SaβG at DIV18, a well-validated marker of aging both in vivo and in vitro. By DIV28, axons were clearly degenerating in both groups. TrkA downregulation in the absence of $p75^{NTR}$ downregulation has been repeatedly observed in both aging and

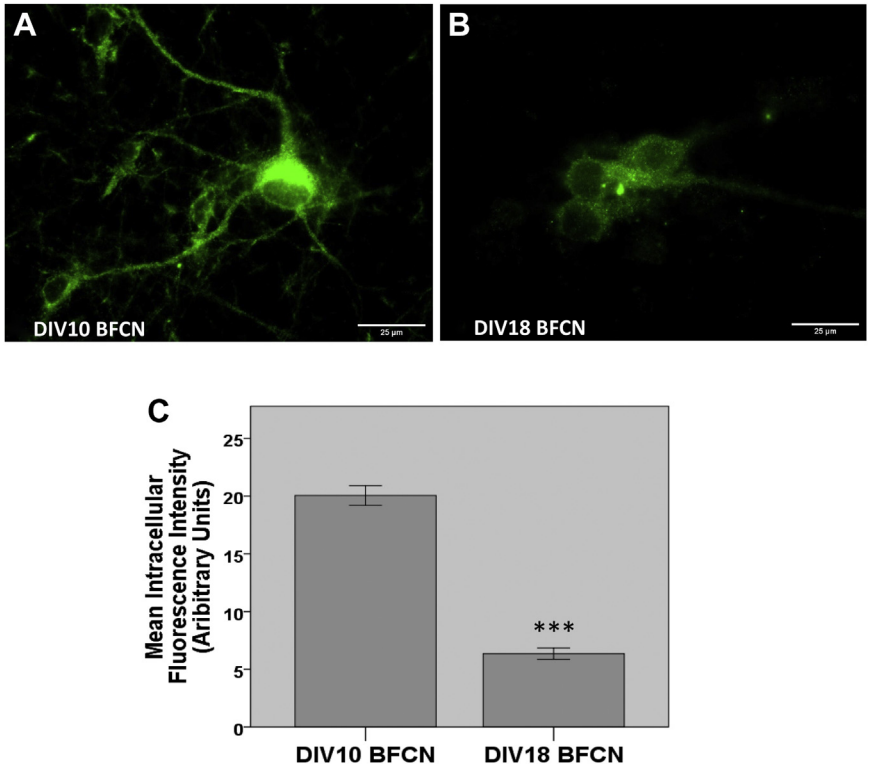

Fig. 8. Decreased TrkA immunoreactivity in BFCNs aged in vitro. BFCN cell bodies demonstrated significantly less TrkA immunoreactivity at DIV18 (B) compared with DIV10 (A). Quantification in (C). N = 60 cell bodies per group, from 3 different chambers and 3 rounds of dissection (5 embryos each). Data are represented as the mean ± SE. ***$p < 0.001$ by Student's *t* test. Abbreviations: BFCN, basal forebrain cholinergic neuron; DIV, days in vitro; SE, standard error; TrkA, tropomyosin-related kinase A.

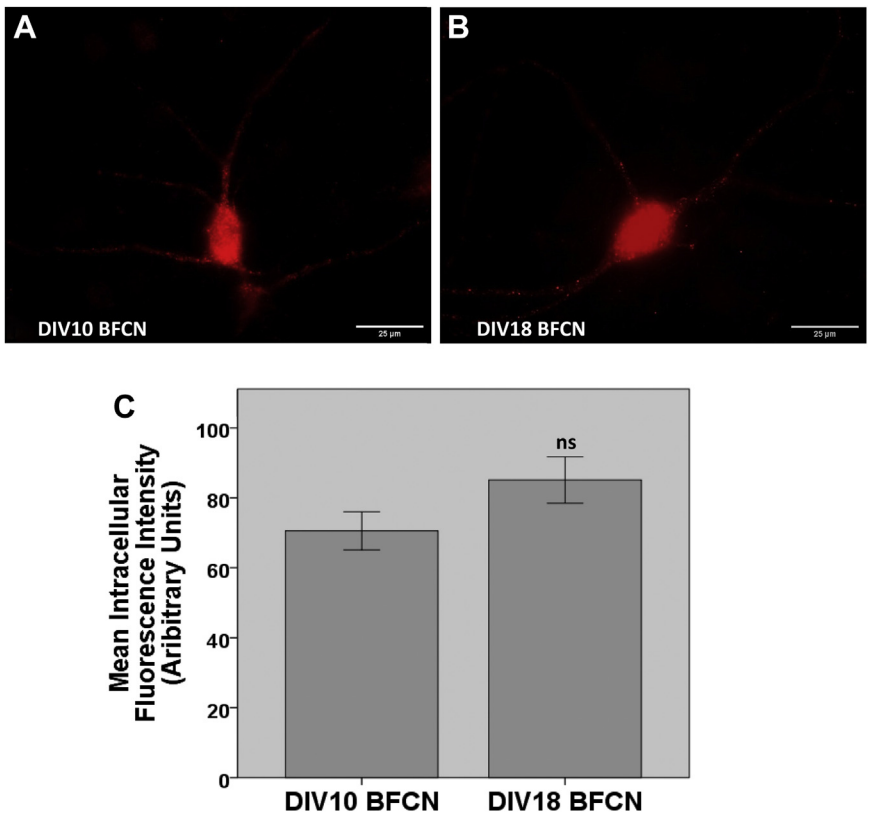

Fig. 9. $p75^{NTR}$ immunoreactivity in BFCNs does not change during aging in vitro. $p75^{NTR}$ immunoreactivity did not change significantly between DIV10 (A) and DIV18 (B) in BFCNs. Quantification in (C). N = 60 cell bodies per group, from 3 different chambers and 3 rounds of dissection (5 embryos each). Data are represented as the mean ± SE. $p = 0.09$ by Student's *t* test. ns = not significant ($p = 0.8$). Abbreviations: BFCN, basal forebrain cholinergic neuron; DIV, days in vitro; $p75^{NTR}$, pan-neurotrophin receptor; SE, standard error.

AD-affected basal forebrain neurons in humans and rodents (Fahnestock and Shekari, 2019; Gibbs, 1998; Ginsberg et al., 2006; Mufson et al., 2000; Niewiadomska et al., 2002). Thus, although the molecular mechanisms underlying neuronal degeneration in vivo are accelerated in vitro, they are not dissimilar. Studying in vitro aging provides an effective way to gain insight into the mechanisms underlying aging in paradigms where in vivo work is difficult.

In conclusion, our data suggest that BFCNs display unique, age-dependent deficits in TrkA and TrkB receptor expression and the retrograde axonal transport of BDNF and proNGF. These deficits support previous findings that demonstrate the susceptibility of the basal forebrain to age-related degeneration and may explain the extreme susceptibility of the basal forebrain to AD. The basal forebrain projects to almost all areas of the cortex and the hippocampus. It plays canonical and crucial roles in learning, memory, and attention and is also involved in other important functions including regulation of blood flow to the cortex. Understanding how and why these neurons degenerate both with age and in AD is critical for our understanding of aging, neurodegenerative diseases, and the nervous system as a whole.

Disclosure

The authors have no actual or potential conflicts of interest.

Acknowledgements

The authors are grateful to Drs Wayne Poon and Carl Cotman (UC Irvine) and Dr Chengbiao Wu (UCSD) for help with microfluidic chambers and transport assays.

This work was supported by grants to M.F. from the Alzheimer Society of Canada and the Canadian Institutes of Health Research (MOP-102723, PJT-159493), and by an Ontario Graduate Scholarship to A.S.

The data contained in this manuscript being submitted have not been previously published, have not been submitted elsewhere and will not be submitted elsewhere while under consideration at Neurobiology of Aging.

All authors have reviewed the contents of the manuscript, approved its contents, and validated the accuracy of the data.

Appendix A. Supplementary data

Supplementary data to this article can be found online at https://doi.org/10.1016/j.neurobiolaging.2019.07.018.

References

Altavista, M.C., Rossi, P., Bentivoglio, A.R., Crociani, P., Albanese, A., 1990. Aging is associated with a diffuse impairment of forebrain cholinergic neurons. Brain Res. 508, 51–59.

Baker-Nigh, A., Vahedi, S., Davis, E.G., Weintraub, S., Bigio, E.H., Klein, W.L., Geula, C., 2015. Neuronal amyloid-β accumulation within cholinergic basal forebrain in ageing and Alzheimer's disease. Brain 138, 1722–1737.

Ballinger, E.C., Ananth, M., Talmage, D.A., Role, L.W., 2016. Basal forebrain cholinergic circuits and signaling in cognition and cognitive decline. Neuron 91, 1199–1218.

Baxter, M.G., Chiba, A.A., 1999. Cognitive functions of the basal forebrain. Curr. Opin. Neurobiol. 9, 178–183.

Bearer, E.L., Manifold-Wheeler, B.C., Medina, C.S., Gonzales, A.G., Chaves, F.L., Jacobs, R.E., 2018. Alterations of functional circuitry in aging brain and the impact of mutated APP expression. Neurobiol. Aging 70, 276–290.

Bothwell, M., 2014. NGF, BDNF, NT3, and NT4. Handb. Exp. Pharmacol. 220, 3–15.

Brewer, L.D., Thibault, O., Staton, J., Thibault, V., Rogers, J.T., Garcia-Ramos, G., Kraner, S., Landfield, P.W., Porter, N.M., 2007. Increased vulnerability of hippocampal neurons with age in culture: temporal association with increases in NMDA receptor current, NR2A subunit expression and recruitment of L-type calcium channels. Brain Res. 1151, 20–31.

Calvo, M., Sanz-Blasco, S., Caballero, E., Villalobos, C., Núñez, L., 2015. Susceptibility to excitotoxicity in aged hippocampal cultures and neuroprotection by non-steroidal anti-inflammatory drugs: role of mitochondrial calcium. J. Neurochem. 132, 403–417.

Campos, P.B., Paulsen, B.S., Rehen, S.K., 2014. Accelerating neuronal aging in in vitro model brain disorders: a focus on reactive oxygen species. Front. Aging Neurosci. 6, 292.

Clewes, O., Fahey, M.S., Tyler, S.J., Watson, J.J., Seok, H., Catania, C., Cho, K., Dawbarn, D., Allen, S.J., 2008. Human ProNGF: biological effects and binding profiles at TrkA, P75NTR and sortilin. J. Neurochem. 107, 1124–1135.

Cooper, J.D., Lindholm, D., Sofroniew, M.V., 1994. Reduced transport of [125I]nerve growth factor by cholinergic neurons and down-regulated trka expression in the medial septum of aged rats. Neuroscience 62, 625–629.

Cooper, J.D., Salehi, A., Delcroix, J.-D., Howe, C.L., Belichenko, P.V., Chua-Couzens, J., Kilbridge, J.F., Carlson, E.J., Epstein, C.J., Mobley, W.C., 2001. Failed retrograde transport of NGF in a mouse model of Down's syndrome: reversal of cholinergic neurodegenerative phenotypes following NGF infusion. Proc. Natl. Acad. Sci. U. S. A. 98, 10439–10444.

Counts, S.E., Nadeem, M., Wuu, J., Ginsberg, S.D., Saragovi, H.U., Mufson, E.J., 2004. Reduction of cortical TrkA but not p75 NTR protein in early-stage Alzheimer's disease. Ann. Neurol. 56, 520–531.

De Lacalle, S., Cooper, J.D., Svendsen, C.N., Dunnett, S.B., Sofroniew, M.V., 1996. Reduced retrograde labelling with fluorescent tracer accompanies neuronal atrophy of basal forebrain cholinergic neurons in aged rats. Neuroscience 75, 19–27.

De Nadai, T., Marchetti, L., Di Rienzo, C., Calvello, M., Signore, G., Di Matteo, P., Gobbo, F., Turturro, S., Meucci, S., Viegi, A., Beltram, F., Luin, S., Cattaneo, A., 2016. Precursor and mature NGF live tracking: one versus many at a time in the axons. Sci. Rep. 6, 20272.

Dimri, G.P., Lee, X., Basile, G., Acosta, M., Scott, G., Roskelley, C., Medrano, E.E., Linskens, M., Rubelj, I., Pereira-Smith, O., 1995. A biomarker that identifies senescent human cells in culture and in aging skin in vivo. Proc. Natl. Acad. Sci. U. S. A. 92, 9363–9367.

DiStefano, P.S., Friedman, B., Radziejewski, C., Alexander, C., Boland, P., Schick, C.M., Lindsay, R.M., Wiegand, S.J., 1992. The neurotrophins BDNF, NT-3, and NGF display distinct patterns of retrograde axonal transport in peripheral and central neurons. Neuron 8, 983–993.

Fahnestock, M., Shekari, A., 2019. ProNGF and neurodegeneration in Alzheimer's disease. Front. Neurosci. 13, 129.

Fahnestock, M., Michalski, B., Xu, B., Coughlin, M.D., 2001. The precursor pro-nerve growth factor is the predominant form of nerve growth factor in brain and is increased in Alzheimer's disease. Mol. Cell. Neurosci. 18, 210–220.

Fahnestock, M., Yu, G., Michalski, B., Mathew, S., Colquhoun, A., Ross, G.M., Coughlin, M.D., 2004. The nerve growth factor precursor proNGF exhibits neurotrophic activity but is less active than mature nerve growth factor. J. Neurochem. 89, 581–592.

Ferreira-Vieira, H., Guimaraes, T.M., Silva, I.R., Ribeiro, F.M., 2016. Alzheimer's disease: targeting the cholinergic system. Curr. Neuropharmacol. 14, 101–115.

Fragkouli, A., Hearn, C., Errington, M., Cooke, S., Grigoriou, M., Bliss, T., Stylianopoulou, F., Pachnis, V., 2005. Loss of forebrain cholinergic neurons and impairment in spatial learning and memory in LHX7-deficient mice. Eur. J. Neurosci. 21, 2923–2938.

Gibbs, R.B., 1998. Impairment of basal forebrain cholinergic neurons associated with aging and long-term loss of ovarian function. Exp. Neurol. 151, 289–302.

Ginsberg, S.D., Che, S., Wuu, J., Counts, S.E., Mufson, E.J., 2006. Down regulation of trk but not p75NTR gene expression in single cholinergic basal forebrain neurons mark the progression of Alzheimer's disease. J. Neurochem. 97, 475–487.

Götz, J., Chen, F., van Dorpe, J., Nitsch, R.M., 2001. Formation of neurofibrillary tangles in P301l tau transgenic mice induced by Abeta 42 fibrils. Science 293, 1491–1495.

Grothe, M., Heinsen, H., Teipel, S.J., 2012. Atrophy of the cholinergic basal forebrain over the adult age range and in early stages of Alzheimer's disease. Biol. Psychiatry 71, 805–813.

Gustilo, M.C., Markowska, A.L., Breckler, S.J., Fleischman, C.A., Price, D.L., Koliatsos, V.E., 1999. Evidence that nerve growth factor influences recent memory through structural changes in septohippocampal cholinergic neurons. J. Comp. Neurol. 405, 491–507.

Ioannou, M.S., Fahnestock, M., 2017. ProNGF, but not NGF, switches from neurotrophic to apoptotic activity in response to reductions in TrKA receptor levels. Int. J. Mol. Sci. 18, E599.

Kurz, D.J., Decary, S., Hong, Y., Erusalimsky, J.D., 2000. Senescence-associated (beta)-galactosidase reflects an increase in lysosomal mass during replicative ageing of human endothelial cells. J. Cell Sci. 113, 3613–3622.

Linville, D.G., Arnerić, S.P., 1991. Cortical cerebral blood flow governed by the basal forebrain: age-related impairments. Neurobiol. Aging 12, 503–510.

Martin, M.G., Perga, S., Trovo, L., Rasola, A., Holm, P., Rantamaki, T., Harkany, T., Castren, E., Chiara, F., Dotti, C.G., 2008. Cholesterol loss enhances TrkB signaling in hippocampal neurons aging in vitro. Mol. Biol. Cell. 19, 2101–2112.

Masoudi, R., Ioannou, M.S., Coughlin, M.D., Pagadala, P., Neet, K.E., Clewes, O., Allen, S.J., Dawbarn, D., Fahnestock, M., 2009. Biological activity of nerve growth factor precursor is dependent upon relative levels of its receptors. J. Biol. Chem. 284, 18424–18433.

Michalski, B., Fahnestock, M., 2003. Pro-brain-derived neurotrophic factor is decreased in parietal cortex in Alzheimer's disease. Brain Res Mol Brain Res 111, 148–154.

Mishima, K., Handa, J.T., Aotaki-Keen, A., Lutty, G.A., Morse, L.S., Hjelmeland, L.M., 1999. Senescence-associated β-galactosidase histochemistry for the primate eye. Invest. Ophthalmol. Vis. Sci. 40, 1590–1593.

Mufson, E.J., Ma, S.Y., Cochran, E.J., Bennett, D.A., Beckett, L.A., Jaffar, S., Saragovi, H.U., Kordower, J.H., 2000. Loss of nucleus basalis neurons containing trkA immunoreactivity in individuals with mild cognitive impairment and early Alzheimer's diseases. J. Comp. Neurol. 427, 19–30.

Mufson, E.J., Ginsberg, S.D., Ikonomovic, M.D., DeKosky, S.T., 2003. Human cholinergic basal forebrain: chemoanatomy and neurologic dysfunction. J. Chem. Neuroanat. 26, 233–242.

Niewiadomska, G., Komorowski, S., Baksalerska-Pazera, M., 2002. Amelioration of cholinergic neurons dysfunction in aged rats depends on the continuous supply of NGF. Neurobiol. Aging 23, 601–613.

Nykjaer, A., Lee, R., Teng, K.K., Jansen, P., Madsen, P., Nielsen, M.S., Jacobsen, C., Kliemannel, M., Schwarz, E., Willnow, T.E., Hempstead, B.L., Petersen, C.M., 2004. Sortilin is essential for proNGF-induced neuronal cell death. Nature 427, 843–848.

Palomer, E., Martín-Segura, A., Baliyan, S., Ahmed, T., Balschun, D., Venero, C., Martin, M.G., Dotti, C.G., 2016. Aging triggers a repressive chromatin state at BDNF promoters in hippocampal neurons. Cell Rep. 16, 2889–2900.

Parikh, V., Howe, W.M., Welchko, R.M., Naughton, S.X., D'Amore, D.E., Han, D.H., Deo, M., Turner, D.L., Sarter, M., 2013. Diminished trkA receptor signaling reveals cholinergic-attentional vulnerability of aging. Eur. J. Neurosci. 37, 278–293.

Poon, W.W., Blurton-Jones, M., Tu, C.H., Feinberg, L.M., Chabrier, M.A., Harris, J.W., Jeon, N.L., Cotman, C.W., 2011. β-Amyloid impairs axonal BDNF retrograde trafficking. Neurobiol. Aging 32, 821–833.

Porter, N.M., Thibault, O., Thibault, V., Chen, K.C., Landfield, P.W., 1997. Calcium channel density and hippocampal cell death with age in long-term culture. J. Neurosci. 17, 5629–5639.

Salehi, A., Delcroix, J.D., Belichenko, P.V., Zhan, K., Wu, C., Valletta, J.S., Takimoto-Kimura, R., Kleschevnikov, A.M., Sambamurti, K., Chung, P.P., Xia, W., Villar, A., Campbell, W.A., Kulnane, L.S., Nixon, R.A., Lamb, B.T., Epstein, C.J., Stokin, G.B., Goldstein, L.S.B., Mobley, W.C., 2006. Increased app expression in a mouse model of down's syndrome disrupts NGF transport and causes cholinergic neuron degeneration. Neuron 51, 29–42.

Schmitz, T.W., Nathan Spreng, R., Weiner, M.W., Aisen, P., Petersen, R., Jack, C.R., Jagust, W., Trojanowki, J.Q., Toga, A.W., Beckett, L., Green, R.C., Saykin, A.J., Morris, J., Shaw, L.M., Khachaturian, Z., Sorensen, G., Kuller, L., Raichle, M., Paul, S., Davies, P., Fillit, H., Hefti, F., Holtzman, D., Mesulam, M.M., Potter, W., Snyder, P., Schwartz, A., Montine, T., Thomas, R.G., Donohue, M., Walter, S., Gessert, D., Sather, T., Jiminez, G., Harvey, D., Bernstein, M., Fox, N., Thompson, P., Schuff, N., Borowski, B., Gunter, J., Senjem, M., Vemuri, P., Jones, D., Kantarci, K., Ward, C., Koeppe, R.A., Foster, N., Reiman, E.M., Chen, K., Mathis, C., Landau, S., Cairns, N.J., Householder, E., Taylor-Reinwald, L., Lee, V., Korecka, M., Figurski, M., Crawford, K., Neu, S., Foroud, T.M., Potkin, S., Shen, L., Faber, K., Kim, S., Nho, K., Thal, L., Buckholtz, N., Albert, M., Frank, R., Hsiao, J., Kaye, J., Quinn, J., Lind, B., Carter, R., Dolen, S., Schneider, L.S., Pawluczyk, S., Beccera, M., Teodoro, L., Spann, B.M., Brewer, J., Vanderswag, H., Fleisher, A., Heidebrink, J.L., Lord, J.L., Mason, S.S., Albers, C.S., Knopman, D., Johnson, K., Doody, R.S., Villanueva-Meyer, J., Chowdhury, M., Rountree, S., Dang, M., Stern, Y., Honig, L.S., Bell, K.L., Ances, B., Carroll, M., Leon, S., Mintun, M.A., Schneider, S., Oliver, A., Marson, D., Griffith, R., Clark, D., Geldmacher, D., Brockington, J., Roberson, E., Grossman, H., Mitsis, E., de Toledo-Morrell, L., Shah, R.C., Duara, R., Varon, D., Greig, M.T., Roberts, P., Albert, M., Onyike, C., D'Agostino, D., Kielb, S., Galvin, J.E., Cerbone, B., Michel, C.A., Rusinek, H., de Leon, M.J., Glodzik, L., De Santi, S., Doraiswamy, P.M., Petrella, J.R., Wong, T.Z., Arnold, S.E., Karlawish, J.H., Wolk, D., Smith, C.D., Jicha, G., Hardy, P., Sinha, P., Oates, E., Conrad, G., Lopez, O.L., Oakley, M., Simpson, D.M., Porsteinsson, A.P., Goldstein, B.S., Martin, K., Makino, K.M., Ismail, M.S., Brand, C., Mulnard, R.A., Thai, G., Mc-Adams-Ortiz, C., Womack, K., Mathews, D., Quiceno, M., Diaz-Arrastia, R., King, R., Weiner, M., Martin-Cook, K., DeVous, M., Levey, A.I., Lah, J.J., Cellar, J.S., Burns, J.M., Anderson, H.S., Swerdlow, R.H., Apostolova, L., Tingus, K., Woo, E., Silverman, D.H.S., Lu, P.H., Bartzokis, G., Graff-Radford, N.R., Parfitt, F., Kendall, T., Johnson, H., Farlow, M.R., Hake, A., Matthews, B.R., Herring, S., Hunt, C., van Dyck, C.H., Carson, R.E., MacAvoy, M.G., Chertkow, H., Bergman, H., Hosein, C., Black, S., Stefanovic, B., Caldwell, C., Robin Hsiung, G.-Y., Feldman, H., Mudge, B., Assaly, M., Kertesz, A., Rogers, J., Bernick, C., Munic, D., Kerwin, D., Mesulam, M.-M., Lipowski, K., Wu, C.-K., Johnson, N., Sadowsky, C., Martinez, W., Villena, T., Turner, R.S., Johnson, K., Reynolds, B., Sperling, R.A., Johnson, K.A., Marshall, G., Frey, M., Lane, B., Rosen, A., Tinklenberg, J., Sabbagh, M.N., Belden, C.M., Jacobson, S.A., Sirrel, S.A., Kowall, N., Killiany, R., Budson, A.E., Norbash, A., Johnson, P.L., Allard, J., Lerner, A., Ogrocki, P., Hudson, L., Fletcher, E., Carmichael, O., Olichney, J., DeCarli, C., Kittur, S., Borrie, M., Lee, T.-Y., Bartha, R., Johnson, S., Asthana, S., Carlsson, C.M., Potkin, S.G., Preda, A., Nguyen, D., Tariot, P., Reeder, S., Bates, V., Capote, H., Rainka, M., Scharre, D.W., Kataki, M., Adeli, A., Zimmerman, E.A., Celmins, D., Brown, A.D., Pearlson, G.D., Blank, K., Anderson, K., Santulli, R.B., Kitzmiller, T.J., Schwartz, E.S., Sink, K.M., Williamson, J.D., Garg, P., Watkins, F., Ott, B.R., Querfurth, H., Tremont, G., Salloway, S., Malloy, P., Correia, S., Rosen, H.J., Miller, B.L., Mintzer, J., Spicer, K., Bachman, D., Finger, E., Pasternak, S., Rachinsky, I., Drost, D., Pomara, N., Hernando, R., Sarrael, A., Schultz, S.K., Boles Ponto, L.L., Shim, H., Smith, K.E., Relkin, N., Chaing, G., Raudin, L., Smith, A., Fargher, K., Raj, B.A., Neylan, T., Grafman, J., Davis, M., Morrison, R., Hayes, J., Finley, S., Friedl, K., Fleischman, D., Arfanakis, K., James, O., Massoglia, D., Fruehling, J.J., Harding, S., Peskind, E.R., Petrie, E.C., Li, G., Yesavage, J.A., Taylor, J.L., Furst, A.J., 2016. Basal forebrain degeneration precedes and predicts the cortical spread of Alzheimer's pathology. Nat. Commun. 7, 13249.

Scott, S.A., Mufson, E.J., Weingartner, J.A., Skau, K.A., Crutcher, K.A., 1995. Nerve growth factor in Alzheimer's disease: increased levels throughout the brain coupled with declines in nucleus basalis. J. Neurosci. 15, 6213–6221.

Seiler, M., Schwab, M.E., 1984. Specific retrograde transport of nerve growth factor (NGF) from neocortex to nucleus basalis in the rat. Brain Res. 300, 33–39.

Sobreviela, T., Pagcatipunan, M., Kroin, J.S., Mufson, E.J., 1996. Retrograde transport of brain-derived neurotrophic factor (BDNF) following infusion in neo- and limbic cortex in rat: relationship to BDNF mRNA expressing neurons. J. Comp. Neurol. 375, 417–444.

Sodero, A.O., Weissmann, C., Ledesma, M.D., Dotti, C.G., 2011. Cellular stress from excitatory neurotransmission contributes to cholesterol loss in hippocampal neurons aging in vitro. Neurobiol. Aging 32, 1043–1053.

Sung, K., Maloney, M.T., Yang, J., Wu, C., 2011. A novel method for producing mono-biotinylated, biologically active neurotrophic factors: an essential reagent for single molecule study of axonal transport. J. Neurosci. Methods 200, 121–128.

Teipel, S., Heinsen, H., Amaro, E., Grinberg, L.T., Krause, B., Grothe, M., 2014. Cholinergic basal forebrain atrophy predicts amyloid burden in Alzheimer's disease. Neurobiol. Aging 35, 482–491.

Uday Bhanu, M., Mandraju, R.K., Bhaskar, C., Kondapi, A.K., 2010. Cultured cerebellar granule neurons as an in vitro aging model: topoisomerase IIβ as an additional biomarker in DNA repair and aging. Toxicol. In Vitro 24, 1935–1945.

Villarin, J.M., McCurdy, E.P., Martínez, J.C., Hengst, U., 2016. Local synthesis of dynein cofactors matches retrograde transport to acutely changing demands. Nat. Commun. 7, 13865.

Whitehouse, P.J., Price, D.L., Struble, R.G., Clark, A.W., Coyle, J.T., DeLong, M.R., 1982. Alzheimer's disease and senile dementia: loss of neurons in the basal forebrain. Science 215, 1237–1239.

Williams, B.J., Bimonte-Nelson, H.A., Granholm-Bentley, A.C., 2006. ERK-mediated NGF signaling in the rat septo-hippocampal pathway diminishes with age. Psychopharmacology (Berl) 188, 605–618.

Williams, B., Granholm, A.C., Sambamurti, K., 2007. Age-dependent loss of NGF signaling in the rat basal forebrain is due to disrupted MAPK activation. Neurosci. Lett. 413, 110–114.

Yamashita, N., Joshi, R., Zhang, S., Zhang, Z.Y., Kuruvilla, R., 2017. Phospho-regulation of soma-to-axon transcytosis of neurotrophin receptors. Dev. Cell 42, 626–639.e5.

Ypsilanti, A.R., Girão da Cruz, M.T., Burgess, A., Aubert, I., 2008. The length of hippocampal cholinergic fibers is reduced in the aging brain. Neurobiol. Aging 29, 1666–1679.

Zhao, X., Zhou, Y., Weissmiller, A.M., Pearn, M.L., Mobley, W.C., Wu, C., 2014. Real-time imaging of axonal transport of quantum dot-labeled BDNF in primary neurons. J. Vis. Exp. e51899.

Preface

The experiments outlined in this chapter aim to determine if Rab proteins, key regulators of intracellular trafficking, mediate the retrograde transport impairments observed in the previous chapter. This chapter also outlines experiments done in 3xTg-AD mice, an Alzheimer's Disease model, to determine if the retrograde transport impairments observed in the previous chapter are exacerbated Alzheimer's-specific pathology. I designed the experiments, collected and analyzed all of the data in this chapter, and prepared the report.

4. Contributions of Rab Proteins and Familial Alzheimer's Disease Mutations to Retrograde Neurotrophin Transport in Basal Forebrain Cholinergic Neurons – Beyond *In Vitro* Aging

4.1 Introduction – Rab Proteins

Ras-associated binding (Rab) proteins make up the largest branch of the Ras superfamily of small GTPases and are master regulators of intracellular trafficking (Bucci et al., 2014; Xu et al., 2018). Rab proteins orchestrate a wide variety of functions critical to membrane trafficking, specifically the delivery of cargo to and from membrane-bound intracellular compartments, (Homma et al., 2021). The expression of specific Rab proteins on membrane-bound cargoes plays a critical role in determining the directionality and specificity of the trafficking pathways that govern cargo transport (Bucci et al., 2014; Mignogna & D'Adamo, 2018). In other words, Rab protein expression contributes to establishing the "identity" of membrane-bound cargoes and ensures that they are transported to the correct intracellular destination.

Like other GTPases, Rab proteins cycle between an active GTP-bound and inactive GDP-bound state. The nucleotide cycling of Rab proteins is tightly controlled by guanine exchange factors (GEFs) and GTPase-activating proteins (GAPs) (Homma et al., 2021). Rab activation is mediated by GEFs which promote the exchange of GDP for GTP, while inactivation is mediated by GAPs which catalyze the hydrolysis of GTP to GDP (Barr & Lambright, 2010). Unique GAPs and GEFs exist for specific Rab proteins, making nucleotide exchange a highly specific and controlled process (Barr & Lambright, 2010). Interestingly, Rab inactivation is not solely contingent on GAP activity — all Rab proteins possess the intrinsic ability to hydrolyze GTP to GDP, and GAPs operate to enhance this intrinsic ability (Zhen & Stenmark, 2015). Inactive, GDP-bound Rab proteins are bound by GDP dissociation inhibitor (GDI) proteins, which trigger their dissociation from membranes and solubilize inactive Rab proteins in the cytosol (Goody et al., 2005).

Nucleotide cycling results in conformational changes at two highly conserved regions across all Rab proteins termed switch I and switch II (Eathiraj et al., 2005). Contact of both switch regions with γ phosphate of GTP results in conformational changes that facilitate the binding of Rab effector proteins to these regions (M.-T. G. Lee et al., 2009). Rab effectors are a diverse family of proteins that facilitate many functions related to membrane trafficking including, but not limited to, membrane fusion, tethering cargoes to molecular motors, and post translational modification (Gillingham et al., 2014). While specificity does exist between specific Rab proteins and their effectors, different Rab proteins are able to bind to overlapping sites on common effectors (Zhen & Stenmark, 2015). In essence, Rab proteins work as a complex family of binary switches, each with their own unique activating, inactivating, and binding factors that work together to facilitate the highly complex task of membrane trafficking.

Membrane trafficking is critical to retrograde neurotrophin transport, as the neurotrophin-receptor complex must be internalized from the outer axonal membrane and transported along the axon to the soma. Rab proteins are also critical for the delivery of somal-derived receptors to the axonal membrane (Stenmark, 2009). While very little is known about the role Rab proteins play in the retrograde transport of proNGF in the CNS, this process has been extensively studied in the context of NGF-TrkA trafficking in the PNS. The retrograde trafficking of the NGF-TrkA signaling endosome is largely reliant

on the activities of two specific Rab proteins, Rab5 and Rab7. Rab5 associates with early endosomes and is critical for early endosomal fusion and formation (Mignogna & D'Adamo, 2018). The downstream activities of Rab5 are extremely complex and involve the recruitment of over 50 effector proteins (Christoforidis et al., 1999). Components of this complex regulate phosphoinositide metabolism which in turn regulates early endosome formation through the recruitment of additional Rab effector proteins (Wandinger-Ness & Zerial, 2014). The Rab5 effector VPS34 catalyzes the phosphorylation of phosphatidylinositol to phosphatidylinositol-3-phosphate (PI3P), which cooperates directly with Rab5 to recruit additional effector proteins critical to the endocytosis of the TrkA-NGF complex such as early endosome antigen 1 (EEA1), among others (Barford et al., 2018; Simonsen et al., 1998; Wandinger-Ness & Zerial, 2014).

Phosphoinositide metabolism is also important for the function of Rab7, a critical regulator of retrograde transport (Vieira et al., 2003). Like Rab5, Rab7 recruits many effector proteins to mediate its function. Notable amongst these is the Rab-interacting lysosomal protein (RILP), which interacts directly with the dynactin subunit $p150^{glued}$ to recruit the dynein retrograde motor (Cantalupo et al., 2001). Rab7 also mediates endosome maturation and lysosomal fusion (Cantalupo et al., 2001; Stenmark, 2009; Vanlandingham & Ceresa, 2009). Experiments utilizing the expression of dominant-negative forms of Rab7 have demonstrated that Rab7 is required for retrograde axonal transport (Deinhardt et al., 2006). Peripheral neurons injected with dominant-negative Rab7 retain the ability to internalize cargo and form endosomes, presumably due to the presence of a functioning Rab5, but these endosomes exhibited only shortrange bidirectional movement with no retrograde progression. While both Rab5 and Rab7 are known to be critical for the retrograde transport of the NGF-TrkA complex, the Rab identity of this complex is currently controversial with evidence existing for the complex existing as both a Rab5-positive early endosome and Rab7-positive late endosome (Harrington & Ginty, 2013; J. Liu et al., 2007; Saxena et al., 2005)

The heterogeneity observed with respect to the Rab identity NGF-TrkA signaling endosome may be explained by the effector proteins recruited by both Rab5 and Rab7. Some of the effector proteins recruited by these Rabs possess intrinsic GEF activity. For example, the Rabaptin-5-Rabex complex, a Rab5 effector, acts as a Rab5 GEF, causing its sustained activation (H. Horiuchi et al., 1997). Sustained activation of Rab5 results in the recruitment of the Sand1/Mon1-Ccz1 complex, another Rab5 effector that displaces the Rabaptin-5-Rabex complex and also acts as a Rab7 GEF (Nordmann et al., 2010; Poteryaev et al., 2007). Rab5 activation also triggers the recruitment the hexameric tethering (HOPS) complex, another Rab7 GEF (Peralta et al., 2010; Plemel et al., 2011; Rink et al., 2005). The recruitment of Rab7 GEFs by Rab5 is referred to as Rab conversion, where the activation of one Rab protein directly results in the downstream activation of another (Mottola, 2014; Rink et al., 2005). Rab conversion allows for the Rab identity of cargoes to shift over time, possibly explaining the heterogeneous Rab expression of the NGF-TrkA signaling endosome.

The dysregulation of Rab5-mediated endocytic pathways is a hallmark of AD (Xu et al., 2018). Interestingly, the levels of Rab5, but not Rab7, are significantly increased in the basal forebrain of human AD brains compared to healthy controls (Ginsberg et al.,

2010, 2011). This increase is thought to underlie the abnormal enlargement of Rab5-positive endosomes in the AD brain (Nixon, 2017). The mechanism behind the selective increase of Rab5 in the basal forebrain of AD patients is currently unknown. A failure of Rab5 to Rab7 conversion may underlie these changes. This failure may also account for the retrograde neurotrophin transport deficits observed in the basal forebrain, as Rab7 is a key mediator of retrograde trafficking. The contributions of Rab conversion to the retrograde neurotrophin transport impairments observed within the basal forebrain in AD have not been explored. This chapter aims to determine if Rab5 to Rab7 conversion mediates the *in vitro* aging-induced retrograde neurotrophin transport impairments observed in the previous chapter. Work from this chapter will also shed light on the Rab identity of the proNGF retrograde signalling complex.

The rest of this chapter will be focused on the contribution of classic AD pathological hallmarks, Aβ and tau, to neurotrophin transport deficits in the basal forebrain. This work was done in recognition that aging, while being the greatest risk factor for developing AD, does not fully encompass the pathological changes that occur in the AD brain. The following is an introduction to the triple transgenic mouse, the most commonly used AD animal model, that develops both amyloid and tau pathology in an age-dependent manner.

4.2 Introduction –Triple Transgenic (3xTg-AD) Mice

The following introduction is taken (with minor changes) from Shekari & Fahnestock. (2021). Cholinergic Degeneration in Alzheimer's Disease Mouse Models. Handbook of Clinical Neurology (in press).

Classical pathologic hallmarks of Alzheimer's Disease (AD) include deposits throughout the neocortex of aggregated amyloid-β (Aβ) known as plaques and aggregated tau protein known as neurofibrillary tangles (Bierer et al., 1995). While most cases of AD are sporadic, familial forms of AD are also recognized that are more rapid in their progression and earlier in onset. The creation of animal models for the study of AD has largely been focused on the genetic mutations that underlie familial AD.

Familial AD is an autosomal dominant disorder caused by mutations in genes involved in the amyloid processing pathway (Bateman et al., 2011). Mutations in or increased copy numbers of the *APP* gene are known to cause familial AD (Ballard et al., 2016; Bateman et al., 2011). APP is a type 1 transmembrane protein that is cleaved sequentially by β-secretase and γ-secretase, respectively, to produce Aβ peptides of varying size, among other cleavage products (Thinakaran & Koo, 2008). Mutations in genes coding for Presenilin 1 and 2 (*PSEN1, PSEN2*) – proteins that are essential components of the γ-secretase complex – also cause familial AD (Bateman et al., 2011).

Aside from extracellular Aβ plaque deposition, the intracellular accumulation of the tau protein, referred to as tau tangles, is also observed in AD. Tau is a microtubule-stabilizing protein that becomes hyperphosphorylated in AD, detaches from microtubules, and forms intracellular aggregates. (Goedert & Spillantini, 2011). Mutations in the tau protein are not associated with familial AD, but instead cause other age-related neurodegenerative disorders termed "tauopathies" (Goedert & Spillantini, 2011). In AD, Aβ oligomers may contribute to tau hyperphosphorylation and subsequent aggregation as

a downstream consequence in the absence of tau mutations (Ballinger et al., 2016; Hardy, 2002; Selkoe & Hardy, 2016).

Research exploring the pathogenesis of AD has largely been focused on the Aβ peptide. While Aβ plaques were initially considered primary toxic agents, Aβ oligomers, the precursors to plaques, are now viewed as the precipitating insult in AD (Mroczko et al., 2018). Soluble Aβ oligomers are thought to trigger downstream signaling cascades that lead to hallmarks of the disorder including cholinergic system dysfunction, synaptic loss and eventually gross neurodegeneration (Ballinger et al., 2016; Hardy, 2002; Selkoe & Hardy, 2016). This viewpoint is termed the "amyloid cascade hypothesis" and represents a longstanding hypothesis in AD research. The initial focus on Aβ coupled with the discovery of familial forms of AD caused by mutations in amyloid processing genes heavily influenced the creation of animal models of AD.

Initial mouse models of AD were based on causal mutations found in patients with familial AD. Early models focused exclusively on mutations within the *APP* gene. Later models focused on combining known familial *APP* and *PSEN1* mutations to further compromise APP processing. Subsequent models introduced a mutation within the *MAPT* gene, coding for tau, to replicate tau pathology in addition to plaques. However, it is important to keep in mind that tau mutations, unlike amyloid, are not associated with familial AD and instead are involved in the development of tauopathies (Goedert & Spillantini, 2011).

The triple transgenic (3xTg-AD) mouse is one of the most widely used AD models This model combines the expression of mutations in the genes coding for APP, tau, and presenilin-1 known to be associated with genetic forms of the disorder (Oddo et al., 2003). Specifically, expression of humanized K670N/M671L *APP* and M146V *PSEN1* transgenes, point mutations associated with familial AD, are combined with expression of the human tau P301L *MAPT* transgene in these mice. The P301L point mutation is associated with the familial neurodegenerative tauopathy FTDP-17 and causes increased tau aggregation (Barghorn et al., 2000; Hutton et al., 1998). Plaques and tangles develop in an age-associated manner throughout the neocortex of these animals, although recent sex differences in this pathology have been reported (Kapadia et al., 2018; Marchese et al., 2014; Oddo et al., 2003).

Initial characterization of 3xTg-AD mice demonstrated the presence of Aβ plaques at 6 months of age and tau tangles at 12 months of age, with synaptic dysfunction occurring before plaque and tangle deposition (Oddo et al., 2003). However, more recent reports indicate that plaque and tangle pathology are minimal to absent in male mice at 12 months of age while female mice still exhibit plaque pathology at 12 months and tau hyperphosphorylation at 6 months of age (Marchese et al., 2014).

Cholinergic degeneration, a hallmark of AD, is also present in these mice. However, like plaque and tangle pathology, sex differences are also observed with respect to cholinergic degeneration. The presence of dystrophic cholinergic projections within the hippocampus and cortex increases with age compared to wildtype controls in female 3xTg-AD mice only (Perez et al., 2011). Levels of TrkA in the cortex and hippocampus are significantly lower in female 3xTg-AD mice between 3 and 15 months of age compared to age-matched 3xTg-AD males (Perez et al., 2011). However, both male and

female 3xTg-AD mice display significant age-related reductions in TrkA levels between 15 and 18 months, mirroring the TrkA reduction seen in AD (E. Mufson et al., 2007; Perez et al., 2011). Significant age-related increases in proNGF are seen in basal forebrain target areas of both males and females and may reflect a failure of neurotrophin retrograde transport by basal forebrain neurons in 3xTg-AD mice (Perez et al., 2011). In contrast, BDNF mRNA levels are significantly decreased within the cortex of both male and female 3xTg-AD mice compared to age-matched wildtype controls, mirroring the situation in human AD (Kapadia et al., 2018). Aβ and tau may act synergistically to reduce BDNF levels, as their overexpression has been shown to transcriptionally downregulate BDNF (Belrose et al., 2014; Rosa et al., 2016; Rosa & Fahnestock, 2015). The number of cholinergic acetyltransferase (ChAT)-positive neurons in the basal forebrain decreases between 3 and 18 months in both sexes, demonstrating an age-related loss of cholinergic neurons in 3xTg-AD mice (Girão da Cruz et al., 2012; Perez et al., 2011).

While these mice were initially reported to exhibit age-associated learning and memory deficits, more recent studies have demonstrated the presence of cognitive dysfunction including anxiety and impaired olfaction as early as 2 months of age (Marchese et al., 2014). Furthermore, increased amyloid and tau expression concomitant with impaired calcium homeostasis and mitochondrial dysfunction have been observed in embryonic neural tissue derived from 3xTg-AD mice, suggesting that the pathologies associated with this model begin very early on (Cavendish et al., 2019; Vale et al., 2010). While these findings may not be reflective of events that occur in the human disorder, they suggest that the biology of amyloid and tau can be studied *in vitro* using embryonic culture systems derived from 3xTg-AD neural tissue.

This chapter assesses retrograde neurotrophin transport impairments in basal forebrain cholinergic neurons derived from 3xTg-AD animals. This chapter also explores the contribution of oxidative stress to these transport impairments. ROS accumulation precedes Aβ deposition in the AD brain (Arimon et al., 2015; Praticò et al., 2001; X. Zhang et al., 2018). Furthermore, Aβ aggregation is induced by ROS accumulation, suggesting that ROS accumulation precedes amyloid pathology (Siegel et al., 2007). This chapter focuses on nitrative stress, a subset of ROS involving reactive nitrogenous compounds like nitric oxide, as nitration has been shown been shown to impact Aβ processing and secretion specifically (Guix et al., 2012).

4.3 Methods

All dissections, cell culture, and axonal transport assays were completed as described in Chapter 2.

3xTg-AD Mice Breeding and Genotyping

The initial breeding pairs of homozygous 3xTg-AD mice possessing $PS1_{M146V}$, $A\beta PP_{swe}$, and tau_{P301L} transgenes (Oddo et al. 2003) were purchased at 6 weeks of age from the Jackson Laboratory (Bar Harbor, ME). All mice were group-housed (for breeding pairs, 2-3 mice/cage, otherwise 4-5 mice/cage) and kept under standard

laboratory conditions and 12-hour reverse light cycle: light phase (7 P.M.-7 A.M). Mice were genotyped regularly over the course of breeding to ensure the maintenance of transgene expression. Genotyping was done following protocols provided by the Jackson Laboratory. Briefly, crude DNA extraction of 2-3 mm mouse tail was done using the REDExtract-N-Amp™ Tissue PCR Kit (Sigma). The expression of the mutant tau^{P301L} transgene was assayed using the following primers via polymerase chain reaction (PCR): (5'-3') fwd: TGA ACC AGG ATG GCT GAG, rev: TTG TCA TCG CTT CCA GTC C. Amplifications were performed in a total volume of 15µl containing 7.5µl of REDExtract-N-Amp PCR mix (Sigma). The PCR protocol consisted of an initial 10 cycles (30 seconds each, 1°C dropped every 2 cycles for an annealing temperature beginning at 65°C and ending at 60°C), followed by 28 cycles of 30s at 94°C, 1 minute at 60°C, and 1 minute at 72°C. The final extension cycle was 10 min at 72°C.

Immunostaining

Immunostaining was carried out in the microfluidic devices themselves. Cells were fixed in freshly prepared 4% paraformaldehyde for 30 minutes at room temperature (RT). Cells were washed twice with PBS, permeabilized with 0.1% Triton-X100 in PBS for 30 minutes at RT and blocked with 3% bovine serum albumin in PBS for 30 minutes at RT. Rabbit anti-Rab5 (ProteinTech, Rosemont, United States), or mouse anti-Rab7 (Cell Signaling Technologies) primary antibodies were added at a 1:500 dilution and left to incubate overnight at 4°C. Cells were washed with blocking solution 3 times on the following day. Alexa Fluor 488 Goat Anti-Mouse (for Rab7) or Alexa Fluor 647 Goat Anti-Rabbit (for Rab5) secondary antibody was then added at a 1:1000 dilution and was left to incubate for 2 hours at RT. Neurons were visualized via fluorescence microscopy using either a YFP (488nm excitation, 525nm emission) or Cy5 (649nm excitation, 666nm emission) filter. Mean grey value of pixels within fluorescent cell bodies was measured using ImageJ.

Rab-proNGF Immunostaining

proNGF (either wild type, or $p75^{NTR}$ binding proNGF-9/13 mutant) isoforms were conjugated to quantum dots and added to the axonal compartment of the chambers as described above. After 15 minutes, the medium was removed from all 4 wells of the chambers and was replaced with PBS. Cells were then fixed and stained as described above. Neurons were visualized via fluorescence microscopy using an EVOS2FL microscope (ThermoFisher Scientific) equipped with YFP (488nm excitation, 525nm emission), Cy5 (649nm excitation, 666nm emission) and Texas Red (585nm excitation, 624nm emission) filters. Experiments were completed twice from 2 different litters.

Neurite Length Analysis

Neurons were imaged between days 7-10 *in vitro* (DIV7-10) using an EVOS2 FL Microscope. Bright-field images of the axonal compartment were taken and analyzed using the Fiji software suite in NIH ImageJ. Specifically, the ICA-2 lookup table was used to better visualize neurites. High contrast images were analyzed for neurite length

using the built-in segmentation feature in ImageJ. Experiments were completed twice from 2 different litters of each genotype.

Nitrative Stress Manipulation

BFCNs were treated with 1mM N(G)-Nitro-L-arginine methyl ester (L-NAME), a nitric oxide synthase inhibitor, for 24 hours prior to analysis.

4.4 Results

proNGF Fails to Colocalize with Rab7 in Aged BFCNs

Rab5 and Rab7 expression of young (DIV10) and aged (DIV18) BFCNs upon proNGF treatment were compared to determine if failed Rab conversion was responsible for the proNGF transport impairments associated with *in vitro* aging. Axonal administration of 50pM proNGF-QD in young BFCNs resulted in the almost exclusive colocalization of proNGF-QD particles with Rab7 (Fig. 1A). Wild type proNGF-QD particles were observed within the microgrooves at this timepoint, indicating retrograde transport. Axonal administration of 50pM proNGF-QD in aged BFCNs resulted in exclusive colocalization of proNGF-QD particles with Rab5 (Fig. 1B). proNGF particles were not retrogradely transported and stalled at the distal end of the microgrooves (Fig 1B).

proNGF-p75^{NTR} Fails to Colocalize with Rab7 in BFCNs

To determine if Rab5 to Rab7 conversion mediates retrograde proNGF transport in BFCNs via TrkA or p75^{NTR}, BFCNs were co-stained with antibodies against Rab5 and Rab7 following either 50pM proNGF-QD or proNGF-9/13 -QD treatment. Axonal administration of wild type proNGF resulted in the almost exclusive colocalization of proNGF-QD particles with Rab7 while administration of proNGF-p75^{NTR} resulted in exclusive colocalization of proNGF-9/13-QD particles with Rab5 (Fig. 2A-B). proNGF-p75^{NTR} particles were not retrogradely transported and were observed solely within distal axon projections (Fig. 2B).

Axonal Outgrowth and Neurotrophin Transport are Impaired in BFCNs from 3xTg-AD Mice

To determine if classical AD pathological hallmarks like amyloid-β and tau exacerbate age-induced BDNF and proNGF transport deficits in BFCNs, transport assays were repeated on neurons derived from 3x-TG mice. BDNF and proNGF uptake could not be measured in DIV7-10 3xTg-AD BFCNs, as there was a significant decrease in axon length compared to wild-type neurons, resulting very few axons crossing the 450μM microgroove barrier at this timepoint (Fig. 3A-B, D N= 5, $p< 0.01$, Student's t-test). A majority of 3xTg-AD axons crossed the microgroove barrier by DIV14 (Fig. 3C). However, neurotrophin transport at this timepoint was severely impaired in DIV14 3xTg-AD BFCNs; no moving BDNF particles were detected and BDNF aggregates were

observed within axons (Fig. 4A-B). proNGF was not detected in BFCN axons at DIV15 (Fig. 5A)

proNGF, but not BDNF, Transport Deficits are Partially Rescued in 3xTg-AD BFCNs After 24-hour L-NAME Treatment

Next, L-NAME was used to determine if inhibiting nitric oxide synthesis could ameliorate axonal transport deficits in 3xTg-AD neurons. Following 24 hours of 1mM L-NAME exposure, proNGF transport deficits were partially rescued in DIV16 BFCNs. proNGF-QD particles were absent in vehicle-treated neurons (Fig. 5A) and were present within the microgrooves in L-NAME treated neurons (Fig. 5B). proNGF-QD particles stalled within the microgrooves and did not accumulate in cell bodies, demonstrating only a partial rescue (Fig. 5B). BDNF transport deficits were not rescued under these conditions. No BDNF-QD signal was present in the microgrooves in either vehicle-treated or L-NAME treated neurons (Fig. 5C, D).

4.5 Discussion

Rab Conversion May be Required for proNGF Retrograde Transport and is Impaired with *in vitro* Aging

These results suggest that Rab5 to Rab7 conversion mediates the retrograde transport of proNGF, and that this process is contingent on the presence and/or binding of TrkA. Wild type proNGF-QD particles colocalized with Rab7 and were observed within the microgrooves, while proNGF-9/13-QD particles colocalized with Rab5 and were observed within the distal axons. Additionally, wild type proNGF colocalized solely with Rab5 in aged neurons and was not able to be retrogradely transported. The localization of proNGF-9/13 with Rab5 provides further evidence that proNGF-p75^{NTR} is internalized by BFCNs, as Rab5 has been shown to play a critical role in receptor endocytosis (Barbieri et al., 1996; Harrington & Ginty, 2013; Jovic et al., 2010; Vanlandingham & Ceresa, 2009).

These preliminary results are in agreement with existing literature observing significantly increased levels of Rab5 in the basal forebrain of AD patients (X.-Q. Chen & Mobley, 2019; Ginsberg et al., 2011; Xu et al., 2018). If the conversion of Rab5 to Rab7 is dependent on the presence and/or activation of TrkA, the overexpression of Rab5 seen in AD may be attributable to the loss of TrkA seen in AD. However, the involvement of Rab proteins in the trafficking of proNGF is unknown. Additionally, the involvement of Rab proteins in NGF tracking in the periphery is controversial, with evidence existing for both the maintenance of Rab5 and the conversion of Rab5 to Rab7 during trafficking (Harrington & Ginty, 2013).

Interestingly, NGF binding to TrkA has been shown to recruit RabGAP5, a Rab5 effector that possesses GAP activity, to a subset of internalized TrkA-NGF endosomes (J. Liu et al., 2007). Recruitment of RabGAP5 is thought to prevent the sustained activation of Rab5 and subsequent conversion of Rab5 to Rab7. It is hypothesized that this inhibition delays the retrograde trafficking of some NGF endosomes to retain them within

axons (Marlin & Li, 2015). Under this model, the co-existence of both Rab5-positive and Rab7-positive NGF endosomes would be expected, explaining the heterogeneity observed with respect to the reported Rab identity of the NGF signaling endosome.

Heterogeneity is also observed with respect to the transport of proNGF particles by BFCNs. The maintenance of proNGF-QD particles at the distal ends of axon projections has commonly been observed, both in these experiments and many others (data not shown). While most particles successfully transit retrogradely across the linear microgrooves, some particles remain within axons and exhibit a vibratory bidirectional movement pattern. This movement pattern is similar to what has been observed in endosomes from DRG neurons lacking functional Rab7 (Deinhardt et al., 2006). These "axon-docked" particles may represent a subset of proNGF signaling endosomes that have failed Rab5-Rab7 conversion.

The maintenance of a subpopulation of proNGF-QD particles in BFCN axons may serve to provide the axon with local neurotrophic survival signaling. An underappreciated function of the signaling endosome is its ability to *continuously* signal over the course of retrograde transport (Marlin & Li, 2015). This continuous signaling allows for the propagation of TrkA-mediated survival signaling along the entire length of the neuron. In other words, the delivery of the signaling complex to the soma is not always the sole purpose of retrograde axonal transport. The consequences of local axonal NGF-TrkA signaling are still being elucidated. However, the axonal translation of myoinositol monophosphatase-1, a key regulator of phosphatidylinositol metabolism, and lamin B2 and Bcl-w, key neuronal support proteins, have recently been shown to be dependent on NGF-TrkA signaling within the axon (Andreassi et al., 2010; Cosker et al., 2016). Local neurotrophic signaling within the axon may be especially paramount to BFCN survival and function due to their exceptionally long and diffuse axonal projections. The unique morphology of these neurons may suggest the existence of unique regulatory pathways that serve to maintain large pools of ligand-bound receptors within their axon projections. Understanding how BFCNs regulate the axonal transport vs. maintenance of retrogradely transported cargo is critical to our understanding of these neurons. These findings suggest that Rab conversion may mediate this unique regulation. Exploring this concept in the context of TrkA-dependent Rab5-Rab7 conversion is a promising and exciting avenue to pursue given these results.

3xTg-AD BFCNs Show Impaired Axonal Outgrowth and Neurotrophic Transport Deficits

A significant impairment in axonal outgrowth was observed in embryonic BFCNs derived from 3xTg-AD mice. Neurite length beyond the 450μM microgroove barrier was significantly decreased in 3xTg-AD neurons compared to wild type. BDNF transport was significantly impaired in 3xTg-AD BFCNs; large BDNF-QD inclusions were present within axonal projections with no moving particles detected. proNGF transport was also impaired in these neurons.

Taken together, these observations suggest that the pathological changes associated with the mutations present in this model occur extremely early and have potential developmental consequences. Embryonic cortical neurons from 3xTg-AD mice

have been shown to display increased amyloid-β and hyperphosphorylated tau immunoreactivity compared to wild-type neurons as early as DIV6 (Vale et al., 2010). 3xTg-AD mice harbor the P301L point mutation in the gene coding for tau (Johnson, 2004). This mutation is associated with increased tau phosphorylation, a post-translational change that reduces the microtubule binding affinity of tau (Johnson, 2004). Hyperphosphorylated tau and the microtubule instability that accompanies this post-translational modification likely contribute to the impaired axonal outgrowth observed in 3xTg-AD BFCNs, as tau polymerization is critical for axonal outgrowth during development (Biswas & Kalil, 2018).

Cognitive deficits in 3xTg-AD mice are observed as early as 4 months after birth and progressively increase with age (Belfiore et al., 2019; Billings et al., 2005). Early axonal outgrowth impairments and retrograde neurotrophin transport deficits in the basal forebrain due to microtubule instability may contribute to the early and progressive cognitive decline seen in 3xTg-AD mice. Interestingly, improving microtubule stability using pharmacological microtubule stabilizing agents has been shown to improve cognitive function in AD mouse models (Barten et al., 2012). Determining if microtubule stabilization ameliorates the observed neurotrophin transport deficits in 3xTg-AD BFCNs is an exciting future aspect of this research that is further discussed in chapter 6.

While both BDNF and proNGF transport were observed to be impaired in 3xTg-AD BFCNs, the nature of the impairment differed between each neurotrophin. BDNF was found to accumulate in large inclusions within axons while proNGF was completely absent. These results suggest that BDNF is still being taken up by 3xTg-AD BFCNs while proNGF is not. The differential mechanistic underpinnings of proNGF and BDNF transport in these neurons is discussed in the next section in the context of oxidative stress reduction.

L-NAME Treatment Partially Rescues proNGF, but not BDNF, Axonal Transport in 3xTg-AD BFCNs

Reduction of nitric oxide synthase activity via L-NAME treatment partially rescued proNGF axonal transport deficits in 3xTg-AD BFCNs. However, BDNF transport was not rescued by the same treatment. The sole rescue of proNGF transport may be explained by the positive feedback loop that governs TrkA trafficking. The retrograde delivery of axonal TrkA triggers the anterograde trafficking of somal TrkA, forming a feedforward loop that is regulated by PTP1B (Yamashita et al., 2017). L-NAME treatment has been shown to increase anterograde axonal transport specifically (Stykel et al., 2018). Based on these reports, L-NAME treatment likely triggered an increase in anterograde TrkA trafficking in BFCNs. Fuelling the TrkA positive feedback loop by increasing the anterograde delivery of somal TrkA to the axon terminal likely contributed to the partial rescue of proNGF transport by L-NAME. The lack of BDNF transport rescue under the same conditions suggests that TrkA and TrkB are trafficked via distinct mechanisms in BFCNs. This is further supported by the findings of the previous chapter that observed proNGF, but not BDNF, uptake was impaired by axonal neurotrophin starvation (Shekari & Fahnestock, 2019).

Although proNGF transport was partially rescued in 3xTg-AD BFCNs following L-NAME treatment, the particles were not transported far enough to accumulate in the

cell body. Instability in the microtubule network due to the impaired ability of tau-P301L to stabilize microtubules may explain why proNGF could not be transported down the full length of the axon (Dayanandan et al., 1999; Hutton et al., 1998). Microtubule instability may be further exacerbated in 3xTg-AD neurons, as amyloid-β has been shown to trigger tau hyperphosphorylation, a post translational modification that triggers its detachment from microtubules (Oddo et al., 2003; Oliveira et al., 2015; Zheng et al., 2002). The presence of both amyloid and tau mutations in these mice may explain why pathological changes associated with these mutations were present even in embryonic-derived neurons. Existing reports of increased amyloid and tau levels in embryonic cortical neurons further support this notion (Vale et al., 2010).

Taken together, these data suggest that the pathological AD-linked mutations present in 3xTg-AD mice have developmental consequences pertaining to axonal outgrowth and neurotrophin transport in BFCNs. These deficits were partially ameliorated following oxidative stress reduction via L-NAME treatment. While ROS accumulation precedes amyloid pathology in AD, the amyloid-β peptide has been shown to further exacerbate oxidative stress in neurons (Ahmad et al., 2017; Cheignon et al., 2018; Davalli et al., 2016; Leutner et al., 2005; Tönnies & Trushina, 2017). ROS accumulation and subsequent neurodegeneration may be accelerated in 3xTg-AD neurons that harbor mutations in amyloid and amyloid-processing genes due to this feed-forward loop. These data also suggest that ROS reduction specifically rescues proNGF uptake. Reports demonstrating anterograde trafficking improvements following L-NAME treatment suggest that this rescue is due to the increased anterograde delivery of TrkA to the axon terminal. The impact of ROS on proNGF transport and TrkA trafficking is further explored in the next chapter.

References

Ahmad, W., Ijaz, B., Shabbiri, K., Ahmed, F., & Rehman, S. (2017). Oxidative toxicity in diabetes and Alzheimer's disease: Mechanisms behind ROS/ RNS generation. *Journal of Biomedical Science*, *24*(1), 76. https://doi.org/10.1186/s12929-017-0379-z

Andreassi, C., Zimmermann, C., Mitter, R., Fusco, S., De Vita, S., Devita, S., Saiardi, A., & Riccio, A. (2010). An NGF-responsive element targets myo-inositol monophosphatase-1 mRNA to sympathetic neuron axons. *Nature Neuroscience*, *13*(3), 291–301. https://doi.org/10.1038/nn.2486

Arimon, M., Takeda, S., Post, K. L., Svirsky, S., Hyman, B. T., & Berezovska, O. (2015). Oxidative stress and lipid peroxidation are upstream of amyloid pathology. *Neurobiology of Disease*, *84*, 109–119. https://doi.org/10.1016/j.nbd.2015.06.013

Ballard, C., Mobley, W., Hardy, J., Williams, G., & Corbett, A. (2016). Dementia in Down's syndrome. *The Lancet Neurology*, *15*(6), 622–636. https://doi.org/10.1016/S1474-4422(16)00063-6

Ballinger, E. C., Ananth, M., Talmage, D. A., & Role, L. W. (2016). Basal Forebrain Cholinergic Circuits and Signaling in Cognition and Cognitive Decline. *Neuron*, *91*(6), 1199–1218. https://doi.org/10.1016/j.neuron.2016.09.006

Barbieri, M. A., Roberts, R. L., Mukhopadhyay, A., & Stahl, P. D. (1996). Rab5 regulates the dynamics of early endosome fusion. *Biocell*, *20*(3), 331–338.

Barford, K., Keeler, A., McMahon, L., McDaniel, K., Yap, C. C., Deppmann, C. D., & Winckler, B. (2018). Transcytosis of TrkA leads to diversification of dendritic signaling endosomes. *Scientific Reports*, *8*(1), 4715. https://doi.org/10.1038/s41598-018-23036-8

Barghorn, S., Zheng-Fischhofer, Q., Ackmann, M., Biernat, J., Von Bergen, M., Mandelkow, E. M., & Mandelkow, E. (2000). Structure, microtubule interactions, and paired helical filament aggregation by tau mutants of frontotemporal dementias. *Biochemistry*. https://doi.org/10.1021/bi000850r

Barr, F., & Lambright, D. G. (2010). Rab GEFs and GAPs. *Current Opinion in Cell Biology*, *22*(4), 461–470. https://doi.org/10.1016/j.ceb.2010.04.007

Barten, D. M., Fanara, P., Andorfer, C., Hoque, N., Wong, P. Y. A., Husted, K. H., Cadelina, G. W., Decarr, L. B., Yang, L., Liu, V., Fessler, C., Protassio, J., Riff, T., Turner, H., Janus, C. G., Sankaranarayanan, S., Polson, C., Meredith, J. E., Gray, G., … Albright, C. F. (2012). Hyperdynamic microtubules, cognitive deficits, and pathology are improved in tau transgenic mice with low doses of the microtubule-stabilizing agent BMS-241027. *The Journal of Neuroscience: The Official Journal of the Society for Neuroscience*, *32*(21), 7137–7145. https://doi.org/10.1523/JNEUROSCI.0188-12.2012

Bateman, R. J., Aisen, P. S., De Strooper, B., Fox, N. C., Lemere, C. A., Ringman, J. M., Salloway, S., Sperling, R. A., Windisch, M., & Xiong, C. (2011). Autosomal-dominant Alzheimer's disease: A review and proposal for the prevention of Alzheimer's disease. In *Alzheimer's Research and Therapy*. https://doi.org/10.1186/alzrt59

Belfiore, R., Rodin, A., Ferreira, E., Velazquez, R., Branca, C., Caccamo, A., & Oddo, S. (2019). Temporal and regional progression of Alzheimer's disease-like pathology

in 3xTg-AD mice. *Aging Cell*, *18*(1), e12873. https://doi.org/10.1111/acel.12873

Belrose, J. C., Masoudi, R., Michalski, B., & Fahnestock, M. (2014). Increased pro-nerve growth factor and decreased brain-derived neurotrophic factor in non-Alzheimer's disease tauopathies. *Neurobiology of Aging*, *35*(4), 926–933. https://doi.org/10.1016/j.neurobiolaging.2013.08.029

Bierer, L. M., Haroutunian, V., Gabriel, S., Knott, P. J., Carlin, L. S., Purohit, D. P., Perl, D. P., Schmeidler, J., Kanof, P., & Davis, K. L. (1995). Neurochemical correlates of dementia severity in Alzheimer's disease: Relative importance of the cholinergic deficits. *Journal of Neurochemistry*, *64*(2), 749–760. https://doi.org/10.1046/j.1471-4159.1995.64020749.x

Billings, L. M., Oddo, S., Green, K. N., McGaugh, J. L., & LaFerla, F. M. (2005). Intraneuronal Aβ causes the onset of early Alzheimer's disease-related cognitive deficits in transgenic mice. *Neuron*, *45*(5), 675–688. https://doi.org/10.1016/j.neuron.2005.01.040

Biswas, S., & Kalil, K. (2018). The Microtubule-Associated Protein Tau Mediates the Organization of Microtubules and Their Dynamic Exploration of Actin-Rich Lamellipodia and Filopodia of Cortical Growth Cones. *The Journal of Neuroscience*, *38*(2), 291–307. https://doi.org/10.1523/JNEUROSCI.2281-17.2017

Bucci, C., Alifano, P., & Cogli, L. (2014). The Role of Rab Proteins in Neuronal Cells and in the Trafficking of Neurotrophin Receptors. *Membranes*, *4*(4), 642–677. https://doi.org/10.3390/membranes4040642

Cantalupo, G., Alifano, P., Roberti, V., Bruni, C. B., & Bucci, C. (2001). Rab-interacting lysosomal protein (RILP): The Rab7 effector required for transport to lysosomes. *The EMBO Journal*, *20*(4), 683–693. https://doi.org/10.1093/emboj/20.4.683

Cavendish, J. Z., Sarkar, S. N., Colantonio, M. A., Quintana, D. D., Ahmed, N., White, B. A., Engler-Chiurazzi, E. B., & Simpkins, J. W. (2019). Mitochondrial Movement and Number Deficits in Embryonic Cortical Neurons from 3xTg-AD Mice. *Journal of Alzheimer's Disease*, *70*(1), 139–151. https://doi.org/10.3233/JAD-190143

Cheignon, C., Tomas, M., Bonnefont-Rousselot, D., Faller, P., Hureau, C., & Collin, F. (2018). Oxidative stress and the amyloid beta peptide in Alzheimer's disease. *Redox Biology*, *14*, 450–464. https://doi.org/10.1016/j.redox.2017.10.014

Chen, X.-Q., & Mobley, W. C. (2019). Exploring the Pathogenesis of Alzheimer Disease in Basal Forebrain Cholinergic Neurons: Converging Insights From Alternative Hypotheses. *Frontiers in Neuroscience*, *13*. https://doi.org/10.3389/fnins.2019.00446

Christoforidis, S., McBride, H. M., Burgoyne, R. D., & Zerial, M. (1999). The Rab5 effector EEA1 is a core component of endosome docking. *Nature*, *397*(6720), 621–625. https://doi.org/10.1038/17618

Cosker, K. E., Fenstermacher, S. J., Pazyra-Murphy, M. F., Elliott, H. L., & Segal, R. A. (2016). The RNA-binding protein SFPQ orchestrates an RNA regulon to promote

axon viability. *Nature Neuroscience*, *19*(5), 690–696. https://doi.org/10.1038/nn.4280

Davalli, P., Mitic, T., Caporali, A., Lauriola, A., & D'Arca, D. (2016). ROS, Cell Senescence, and Novel Molecular Mechanisms in Aging and Age-Related Diseases. *Oxidative Medicine and Cellular Longevity*, *2016*, 1–18. https://doi.org/10.1155/2016/3565127

Dayanandan, R., Van Slegtenhorst, M., Mack, T. G., Ko, L., Yen, S. H., Leroy, K., Brion, J. P., Anderton, B. H., Hutton, M., & Lovestone, S. (1999). Mutations in tau reduce its microtubule binding properties in intact cells and affect its phosphorylation. *FEBS Letters*, *446*(2–3), 228–232. https://doi.org/10.1016/s0014-5793(99)00222-7

Deinhardt, K., Salinas, S., Verastegui, C., Watson, R., Worth, D., Hanrahan, S., Bucci, C., & Schiavo, G. (2006). Rab5 and Rab7 Control Endocytic Sorting along the Axonal Retrograde Transport Pathway. *Neuron*, *52*(2), 293–305. https://doi.org/10.1016/j.neuron.2006.08.018

Eathiraj, S., Pan, X., Ritacco, C., & Lambright, D. G. (2005). Structural basis of family-wide Rab GTPase recognition by rabenosyn-5. *Nature*, *436*(7049), 415–419. https://doi.org/10.1038/nature03798

Gillingham, A. K., Sinka, R., Torres, I. L., Lilley, K. S., & Munro, S. (2014). Toward a Comprehensive Map of the Effectors of Rab GTPases. *Developmental Cell*, *31*(3), 358–373. https://doi.org/10.1016/j.devcel.2014.10.007

Ginsberg, S. D., Mufson, E. J., Alldred, M. J., Counts, S. E., Wuu, J., Nixon, R. A., & Che, S. (2011). Upregulation of select rab GTPases in cholinergic basal forebrain neurons in mild cognitive impairment and Alzheimer 's disease. *Journal of Chemical Neuroanatomy*, *42*(2), 102–110. https://doi.org/10.1016/j.jchemneu.2011.05.012

Ginsberg, S. D., Mufson, E. J., Counts, S. E., Wuu, J., Alldred, M. J., Nixon, R. A., & Che, S. (2010). Regional selectivity of rab5 and rab7 protein upregulation in mild cognitive impairment and Alzheimer 's disease. *Journal of Alzheimer 's Disease: JAD*, *22*(2), 631–639. https://doi.org/10.3233/JAD-2010-101080

Girão da Cruz, M. T., Jordão, J., DaSilva, K. A., Ayala-Grosso, C. A., Ypsilanti, A., Weng, Y.-Q., LaFerla, F. M., McLaurin, J., & Aubert, I. (2012). Early Increases in Soluble Amyloid-β Levels Coincide with Cholinergic Degeneration in 3xTg-AD Mice. *Journal of Alzheimer 's Disease*, *32*(2), 267–272.

Goedert, M., & Spillantini, M. G. (2011). Pathogenesis of the Tauopathies. *Journal of Molecular Neuroscience*, *45*(3), 425–431. https://doi.org/10.1007/s12031-011-9593-4

Goody, R. S., Rak, A., & Alexandrov, K. (2005). The structural and mechanistic basis for recycling of Rab proteins between membrane compartments. *Cellular and Molecular Life Sciences CMLS*, *62*(15), 1657–1670. https://doi.org/10.1007/s00018-005-4486-8

Guix, F. X., Wahle, T., Vennekens, K., Snellinx, A., Chávez-Gutiérrez, L., Ill-Raga, G., Ramos-Fernandez, E., Guardia-Laguarta, C., Lleó, A., Arimon, M., Berezovska,

O., Muñoz, F. J., Dotti, C. G., & De Strooper, B. (2012). Modification of γ-secretase by nitrosative stress links neuronal ageing to sporadic Alzheimer's disease. *EMBO Molecular Medicine*, *4*(7), 660–673. https://doi.org/10.1002/emmm.201200243

Hardy, J. (2002). The Amyloid Hypothesis of Alzheimer's Disease: Progress and Problems on the Road to Therapeutics. *Science*, *297*(5580), 353–356. https://doi.org/10.1126/science.1072994

Harrington, A. W., & Ginty, D. D. (2013). Long-distance retrograde neurotrophic factor signalling in neurons. *Nature Reviews Neuroscience*, *14*(3), 177–187. https://doi.org/10.1038/nrn3253

Homma, Y., Hiragi, S., & Fukuda, M. (2021). Rab family of small GTPases: An updated view on their regulation and functions. *The FEBS Journal*, *288*(1), 36–55. https://doi.org/10.1111/febs.15453

Horiuchi, H., Lippé, R., McBride, H. M., Rubino, M., Woodman, P., Stenmark, H., Rybin, V., Wilm, M., Ashman, K., Mann, M., & Zerial, M. (1997). A Novel Rab5 GDP/GTP Exchange Factor Complexed to Rabaptin-5 Links Nucleotide Exchange to Effector Recruitment and Function. *Cell*, *90*(6), 1149–1159. https://doi.org/10.1016/S0092-8674(00)80380-3

Hutton, M., Lendon, C. L., Rizzu, P., Baker, M., Froelich, S., Houlden, H., Pickering-Brown, S., Chakraverty, S., Isaacs, A., Grover, A., Hackett, J., Adamson, J., Lincoln, S., Dickson, D., Davies, P., Petersen, R. C., Stevens, M., de Graaff, E., Wauters, E., … Heutink, P. (1998). Association of missense and 5′-splice-site mutations in tau with the inherited dementia FTDP-17. *Nature*, *393*(6686), 702–705. https://doi.org/10.1038/31508

Johnson, G. V. W. (2004). Tau phosphorylation in neuronal cell function and dysfunction. *Journal of Cell Science*, *117*(24), 5721–5729. https://doi.org/10.1242/jcs.01558

Jovic, M., Sharma, M., Rahajeng, J., & Caplan, S. (2010). The early endosome: A busy sorting station for proteins at the crossroads. *Histology and Histopathology*, *25*(1), 99–112. https://doi.org/10.14670/HH-25.99

Kapadia, M., Mian, M. F., Michalski, B., Azam, A. B., Ma, D., Salwierz, P., Christopher, A., Rosa, E., Zovkic, I. B., Forsythe, P., Fahnestock, M., & Sakic, B. (2018). Sex-Dependent Differences in Spontaneous Autoimmunity in Adult 3xTg-AD Mice. *Journal of Alzheimer's Disease*, *63*(3), 1191–1205. https://doi.org/10.3233/JAD-170779

Lee, M.-T. G., Mishra, A., & Lambright, D. G. (2009). Structural Mechanisms for Regulation of Membrane Traffic by Rab GTPases. *Traffic*, *10*(10), 1377–1389. https://doi.org/10.1111/j.1600-0854.2009.00942.x

Leutner, S., Schindowski, K., Frölich, L., Maurer, K., Kratzsch, T., Eckert, A., & Müller, W. E. (2005). Enhanced ROS-Generation in Lymphocytes from Alzheimer's Patients. *Pharmacopsychiatry*, *38*(6), 312–315. https://doi.org/10.1055/s-2005-916186

Liu, J., Lamb, D., Chou, M. M., Liu, Y.-J., & Li, G. (2007). Nerve Growth Factor-mediated Neurite Outgrowth via Regulation of Rab5. *Molecular Biology of the Cell*, *18*(4), 1375–1384. https://doi.org/10.1091/mbc.e06-08-0725

Marchese, M., Cowan, D., Head, E., Ma, D., Karimi, K., Ashthorpe, V., Kapadia, M., Zhao, H., Davis, P., & Sakic, B. (2014). Autoimmune Manifestations in the 3xTg-AD Model of Alzheimer's Disease. *Journal of Alzheimer's Disease*, *39*(1), 191–210. https://doi.org/10.3233/JAD-131490

Marlin, M. C., & Li, G. (2015). Biogenesis and Function of the NGF/TrkA Signaling Endosome. In *International Review of Cell and Molecular Biology* (pp. 239–257). https://doi.org/10.1016/bs.ircmb.2014.10.002

Mignogna, M. L., & D'Adamo, P. (2018). Critical importance of RAB proteins for synaptic function. *Small GTPases*, *9*(1–2), 145–157. https://doi.org/10.1080/21541248.2016.1277001

Mottola, G. (2014). The complexity of Rab5 to Rab7 transition guarantees specificity of pathogen subversion mechanisms. *Frontiers in Cellular and Infection Microbiology*, *4*. https://doi.org/10.3389/fcimb.2014.00180

Mroczko, B., Groblewska, M., Litman-Zawadzka, A., Kornhuber, J., & Lewczuk, P. (2018). Amyloid β oligomers (AβOs) in Alzheimer's disease. *Journal of Neural Transmission*, *125*(2), 177–191. https://doi.org/10.1007/s00702-017-1820-x

Mufson, E., Counts, S., Fahnestock, M., & Ginsberg, S. (2007). Cholinotrophic Molecular Substrates of Mild Cognitive Impairment in the Elderly. *Current Alzheimer Research*. https://doi.org/10.2174/156720507781788855

Nixon, R. A. (2017). Amyloid precursor protein and endosomal–lysosomal dysfunction in Alzheimer's disease: Inseparable partners in a multifactorial disease. *The FASEB Journal*, *31*(7), 2729–2743. https://doi.org/10.1096/fj.201700359

Nordmann, M., Cabrera, M., Perz, A., Bröcker, C., Ostrowicz, C., Engelbrecht-Vandré, S., & Ungermann, C. (2010). The Mon1-Ccz1 Complex Is the GEF of the Late Endosomal Rab7 Homolog Ypt7. *Current Biology*, *20*(18), 1654–1659. https://doi.org/10.1016/j.cub.2010.08.002

Oddo, S., Caccamo, A., Shepherd, J. D., Murphy, M. P., Golde, T. E., Kayed, R., Metherate, R., Mattson, M. P., Akbari, Y., & LaFerla, F. M. (2003). Triple-Transgenic Model of Alzheimer's Disease with Plaques and Tangles. *Neuron*, *39*(3), 409–421. https://doi.org/10.1016/S0896-6273(03)00434-3

Oliveira, J. M., Henriques, A. G., Martins, F., Rebelo, S., & da Cruz e Silva, O. A. B. (2015). Amyloid-β Modulates Both AβPP and Tau Phosphorylation. *Journal of Alzheimer's Disease*, *45*(2), 495–507. https://doi.org/10.3233/JAD-142664

Peralta, E. R., Martin, B. C., & Edinger, A. L. (2010). Differential Effects of TBC1D15 and Mammalian Vps39 on Rab7 Activation State, Lysosomal Morphology, and Growth Factor Dependence*. *Journal of Biological Chemistry*, *285*(22), 16814–16821. https://doi.org/10.1074/jbc.M110.111633

Perez, S. E., He, B., Muhammad, N., Oh, K.-J., Fahnestock, M., Ikonomovic, M. D., & Mufson, E. J. (2011). Cholinotrophic basal forebrain system alterations in 3xTg-AD transgenic mice. *Neurobiology of Disease*, *41*(2), 338–352. https://doi.org/10.1016/j.nbd.2010.10.002

Plemel, R. L., Lobingier, B. T., Brett, C. L., Angers, C. G., Nickerson, D. P., Paulsel, A., Sprague, D., & Merz, A. J. (2011). Subunit organization and Rab interactions of Vps-C protein complexes that control endolysosomal membrane traffic.

Molecular Biology of the Cell, *22*(8), 1353–1363. https://doi.org/10.1091/mbc.e10-03-0260

Poteryaev, D., Fares, H., Bowerman, B., & Spang, A. (2007). Caenorhabditis elegans SAND-1 is essential for RAB-7 function in endosomal traffic. *The EMBO Journal*, *26*(2), 301–312. https://doi.org/10.1038/sj.emboj.7601498

Praticò, D., Uryu, K., Leight, S., Trojanoswki, J. Q., & Lee, V. M. (2001). Increased lipid peroxidation precedes amyloid plaque formation in an animal model of Alzheimer amyloidosis. *The Journal of Neuroscience : The Official Journal of the Society for Neuroscience*, *21*(12), 4183–4187.

Rink, J., Ghigo, E., Kalaidzidis, Y., & Zerial, M. (2005). Rab Conversion as a Mechanism of Progression from Early to Late Endosomes. *Cell*, *122*(5), 735–749. https://doi.org/10.1016/j.cell.2005.06.043

Rosa, E., & Fahnestock, M. (2015). CREB expression mediates amyloid β-induced basal BDNF downregulation. *Neurobiology of Aging*. https://doi.org/10.1016/j.neurobiolaging.2015.04.014

Rosa, E., Mahendram, S., Ke, Y. D., Ittner, L. M., Ginsberg, S. D., & Fahnestock, M. (2016). Tau downregulates BDNF expression in animal and cellular models of Alzheimer's disease. *Neurobiology of Aging*, *48*, 135–142. https://doi.org/10.1016/j.neurobiolaging.2016.08.020

Saxena, S., Bucci, C., Weis, J., & Kruttgen, A. (2005). The Small GTPase Rab7 Controls the Endosomal Trafficking and Neuritogenic Signaling of the Nerve Growth Factor Receptor TrkA. *The Journal of Neuroscience*, *25*(47), 10930–10940. https://doi.org/10.1523/JNEUROSCI.2029-05.2005

Selkoe, D. J., & Hardy, J. (2016). The amyloid hypothesis of Alzheimer's disease at 25 years. *EMBO Molecular Medicine*. https://doi.org/10.15252/emmm.201606210

Shekari, A., & Fahnestock, M. (2019). Retrograde axonal transport of BDNF and proNGF diminishes with age in basal forebrain cholinergic neurons. *Neurobiology of Aging*, *84*, 131–140. https://doi.org/10.1016/j.neurobiolaging.2019.07.018

Siegel, S. J., Bieschke, J., Powers, E. T., & Kelly, J. W. (2007). The Oxidative Stress Metabolite 4-Hydroxynonenal Promotes Alzheimer Protofibril Formation †. *Biochemistry*, *46*(6), 1503–1510. https://doi.org/10.1021/bi061853s

Simonsen, A., Lippé, R., Christoforidis, S., Gaullier, J. M., Brech, A., Callaghan, J., Toh, B. H., Murphy, C., Zerial, M., & Stenmark, H. (1998). EEA1 links PI(3)K function to Rab5 regulation of endosome fusion. *Nature*, *394*(6692), 494–498. https://doi.org/10.1038/28879

Stenmark, H. (2009). Rab GTPases as coordinators of vesicle traffic. *Nature Reviews. Molecular Cell Biology*, *10*(8), 513–525. https://doi.org/10.1038/nrm2728

Stykel, M. G., Humphries, K., Kirby, M. P., Czaniecki, C., Wang, T., Ryan, T., Bamm, V., & Ryan, S. D. (2018). Nitration of microtubules blocks axonal mitochondrial transport in a human pluripotent stem cell model of Parkinson's disease. *The FASEB Journal*, *32*(10), 5350–5364. https://doi.org/10.1096/fj.201700759RR

Thinakaran, G., & Koo, E. H. (2008). Amyloid precursor protein trafficking, processing, and function. In *Journal of Biological Chemistry*. https://doi.org/10.1074/jbc.R800019200

Tönnies, E., & Trushina, E. (2017). Oxidative Stress, Synaptic Dysfunction, and Alzheimer's Disease. *Journal of Alzheimer's Disease*, *57*(4), 1105–1121. https://doi.org/10.3233/JAD-161088

Vale, C., Alonso, E., Rubiolo, J. A., Vieytes, M. R., LaFerla, F. M., Giménez-Llort, L., & Botana, L. M. (2010). Profile for Amyloid-β and Tau Expression in Primary Cortical Cultures from 3xTg-AD Mice. *Cellular and Molecular Neurobiology*, *30*(4), 577–590. https://doi.org/10.1007/s10571-009-9482-3

Vanlandingham, P. A., & Ceresa, B. P. (2009). Rab7 Regulates Late Endocytic Trafficking Downstream of Multivesicular Body Biogenesis and Cargo Sequestration. *Journal of Biological Chemistry*, *284*(18), 12110–12124. https://doi.org/10.1074/jbc.M809277200

Vieira, O. V., Bucci, C., Harrison, R. E., Trimble, W. S., Lanzetti, L., Gruenberg, J., Schreiber, A. D., Stahl, P. D., & Grinstein, S. (2003). Modulation of Rab5 and Rab7 recruitment to phagosomes by phosphatidylinositol 3-kinase. *Molecular and Cellular Biology*, *23*(7), 2501–2514. https://doi.org/10.1128/mcb.23.7.2501-2514.2003

Wandinger-Ness, A., & Zerial, M. (2014). Rab Proteins and the Compartmentalization of the Endosomal System. *Cold Spring Harbor Perspectives in Biology*, *6*(11). https://doi.org/10.1101/cshperspect.a022616

Xu, W., Fang, F., Ding, J., & Wu, C. (2018). Dysregulation of Rab5-mediated endocytic pathways in Alzheimer's disease. *Traffic*, *19*(4), 253–262. https://doi.org/10.1111/tra.12547

Yamashita, N., Joshi, R., Zhang, S., Zhang, Z.-Y., & Kuruvilla, R. (2017). Phospho-Regulation of Soma-to-Axon Transcytosis of Neurotrophin Receptors. *Developmental Cell*, *42*(6), 626-639.e5. https://doi.org/10.1016/j.devcel.2017.08.009

Zhang, X., Fu, Z., Meng, L., He, M., & Zhang, Z. (2018). The Early Events That Initiate β-Amyloid Aggregation in Alzheimer's Disease. *Frontiers in Aging Neuroscience*, *10*(November), 1–13. https://doi.org/10.3389/fnagi.2018.00359

Zhen, Y., & Stenmark, H. (2015). Cellular functions of Rab GTPases at a glance. *Journal of Cell Science*, jcs.166074. https://doi.org/10.1242/jcs.166074

Zheng, W.-H., Bastianetto, S., Mennicken, F., Ma, W., & Kar, S. (2002). Amyloid β peptide induces tau phosphorylation and loss of cholinergic neurons in rat primary septal cultures. *Neuroscience*, *115*(1), 201–211. https://doi.org/10.1016/S0306-4522(02)00404-9

Figure 1: proNGF Fails to Colocalize with Rab7 in Aged Basal Forebrain Cholinergic Neurons (BFCNs)

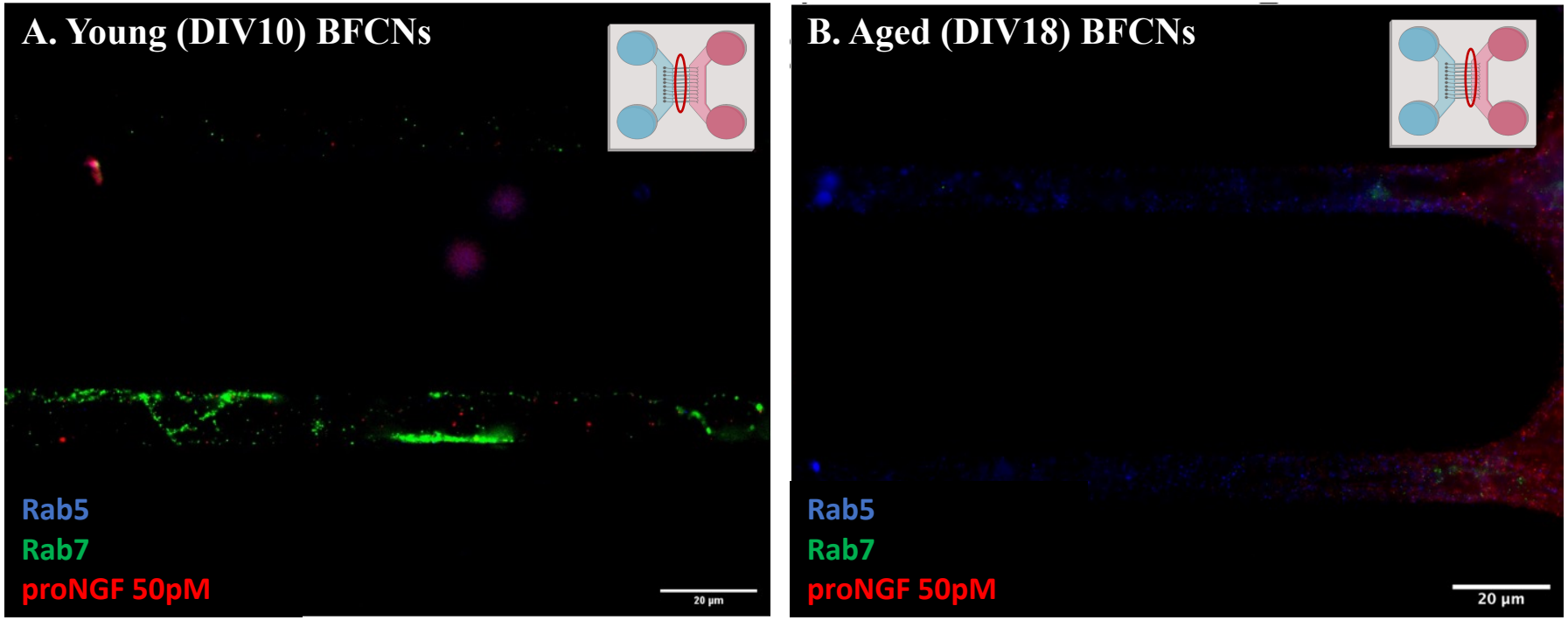

Fig 20. proNGF Fails to Colocalize with Rab7 in aged Basal Forebrain Cholinergic Neurons (BFCNs). Axonal administration of 50pM wild type proNGF-QD in young (DIV10) BFCNs resulted in the almost exclusive colocalization of proNGF-QD particles (red) with Rab7 (green). At DIV10, wild type proNGF particles were observed within the microgrooves, indicating retrograde transport. Axonal administration 50pM proNGF in aged (DIV18) BFCNs resulted in exclusive colocalization of proNGF-QD particles with Rab5 (blue). proNGF-QD particles were not retrogradely transported and stalled at the distal end of the microgrooves. Schematic indicating where each image was taken. Representative results, Representative images from 30 microgrooves, 2 chambers per group (2 liters, 5 embryos each). Red oval indicating where the images were taken

Figure 2: proNGF-p75^{NTR} Fails to Colocalize with Rab7 in DIV10 Basal Forebrain Cholinergic Neurons (BFCNs)

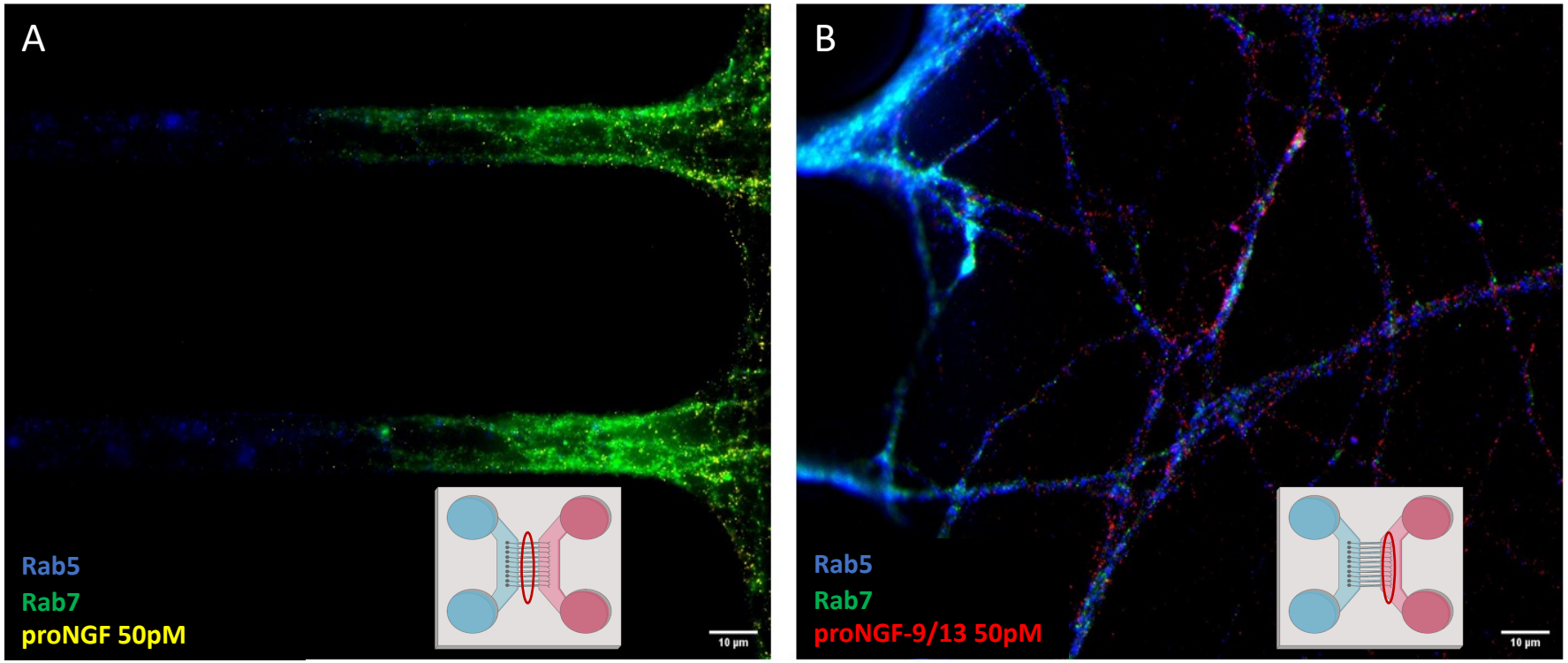

proNGF-9/13 Fails to Colocalize with Rab7 in Basal Forebrain Cholinergic Neurons (BFCNs). Axonal administration of wild type proNGF (yellow) resulted in the almost exclusive colocalization of proNGF-QD particles with Rab7 (green) while administration of proNGF-9/13 (red) resulted in exclusive colocalization of proNGF-9/13-QD particles with Rab5 (blue). Representative results, Representative images from 30 microgrooves, 2 chambers per group (2 liters, 5 embryos each). Red oval indicating where the images were taken.

Figure 3: Axonal Outgrowth in 3xTg-AD and Wild-type (WT) Basal Forebrain Cholinergic Neurons (BFCNs)

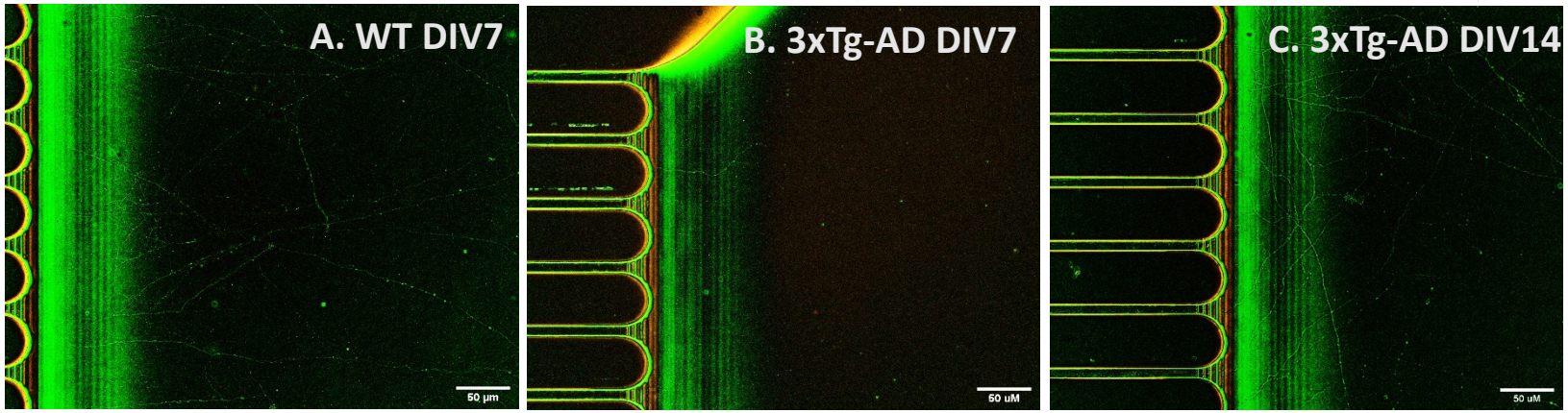

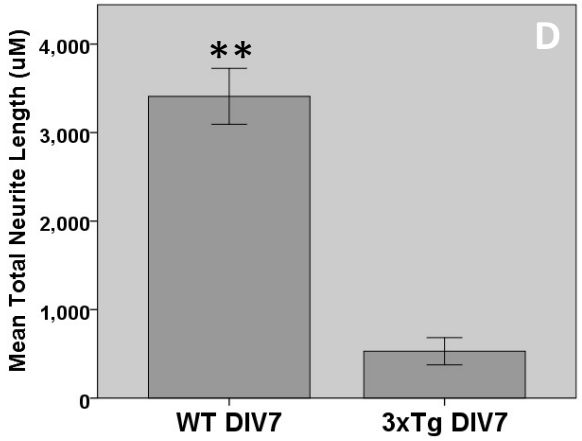

Axonal Outgrowth in 3xTg-AD and Wild-type (WT) Basal Forebrain Cholinergic Neurons (BFCNs) 3xTg-AD BFCNs were observed to have significantly shorter axonal projections compared to WT BFCNs by day *in vitro* (DIV)7. 3xTg-AD axonal projections had lengthened by DIV14. However, WT axonal projections were extremely arborized by DIV14, making meaningful comparisons between both groups difficult (data not shown). *N*= 5 chambers per group, from 2 liters (5 embryos each). Data represented as mean ±SE. $^{**}p<0.01$ by Student's *t*-test.

Figure 4: BDNF Axonal Transport in DIV14 3xTg-AD Basal Forebrain Cholinergic Neurons (BFCNs)

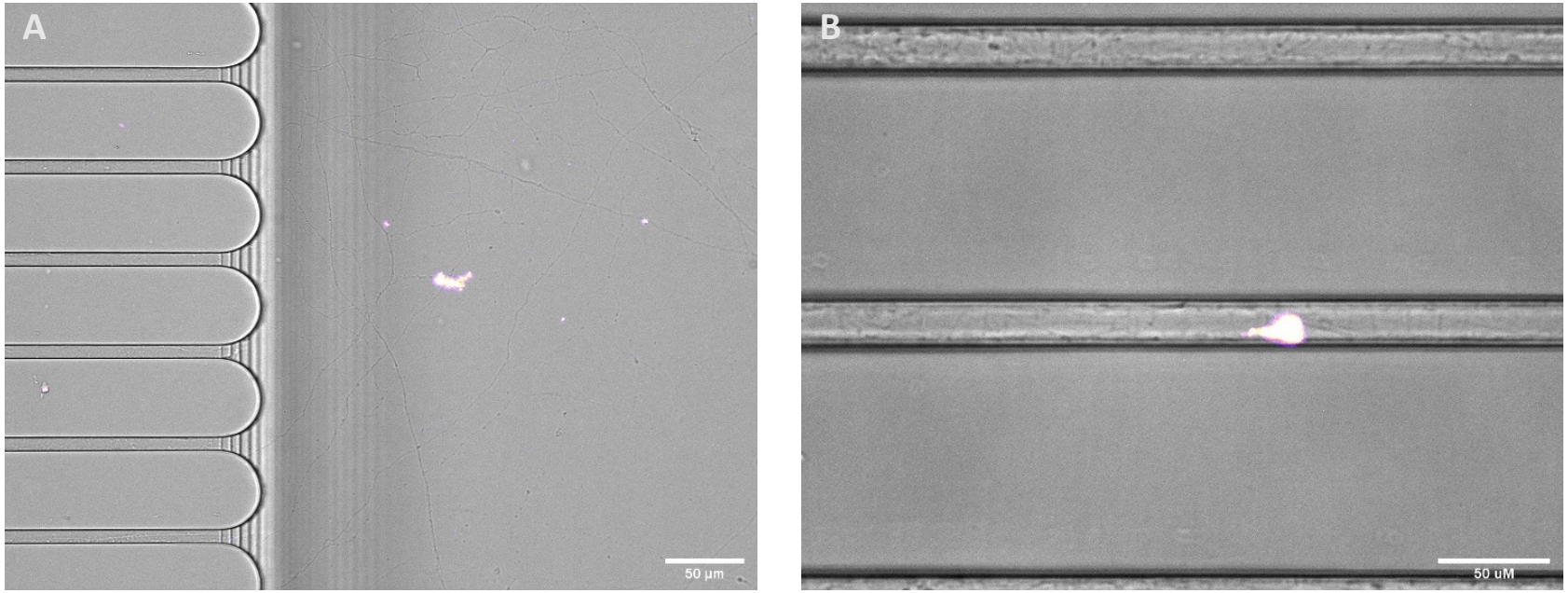

BDNF Axonal Transport in DIV14 3xTg-AD Basal Forebrain Cholinergic Neurons (BFCNs). Quantum-dot labelled BDNF (QD-BDNF) was observed to aggregate within axonal projections of BFCNs from 3xTg-AD mice. No individual moving particles of BDNF were detected. Aggregates were present both at axon terminals (A) and within microgrooves (B).

Figure 5: proNGF Transport Deficits are Partially Rescued in 3xTg-AD BFCNs After 24-hour L-NAME Treatment

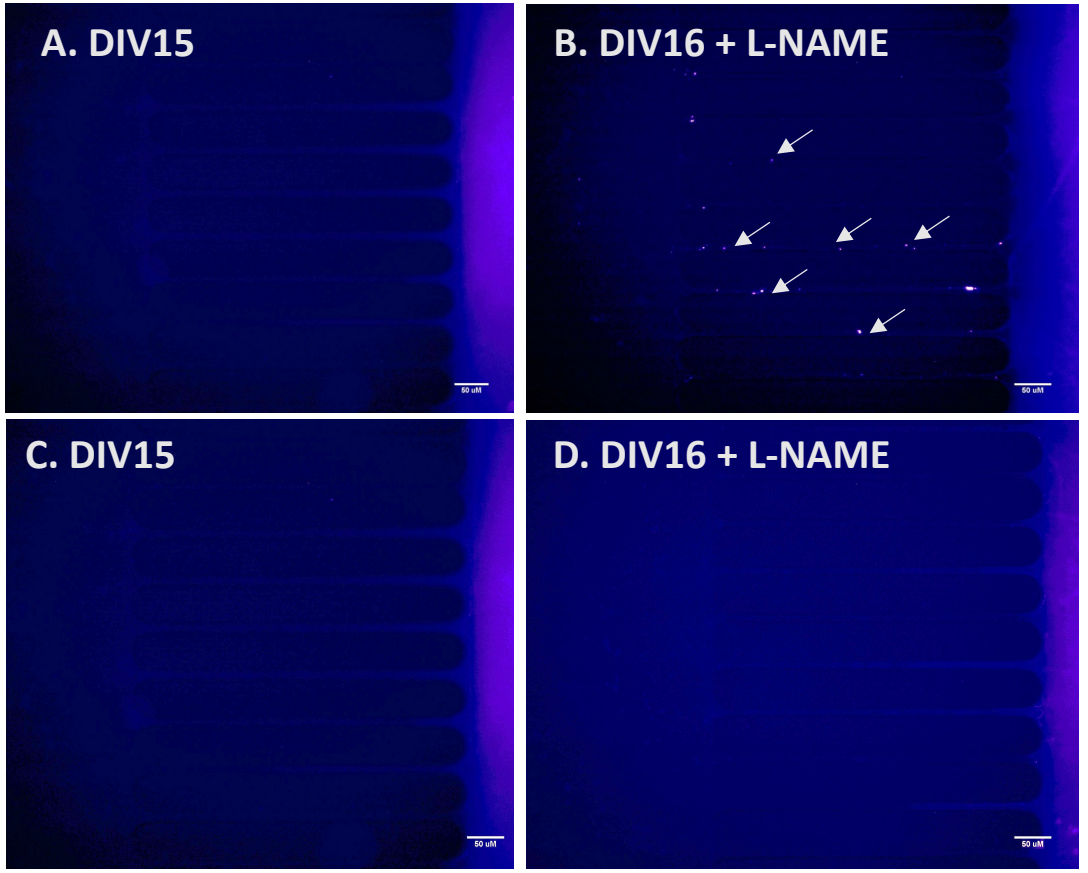

proNGF, but not BDNF, Transport Deficits are Partially Rescued in 3xTg-AD BFCNs After 24-hour L-NAME Treatment . Quantum-dot labelled proNGF (QD-proNGF, indicated by white arrows) was only detected in BFCN microgrooves following L-NAME treatment (A, B). proNGF-QD failed to accumulate in BFCN cell bodies located to the left of the microgrooves. QD-BDNF was not detected cell bodies or axons in either condition (C, D).

Preface

This manuscript builds on the experiments outlined in the last chapter that demonstrated that proNGF transport can be partially rescued by reducing oxidative stress. The goal of this work was to determine the mechanistic contribution of oxidative stress to proNGF transport impairments in BFCNs. I designed the experiments, collected and analyzed all of the data in this chapter, and prepared the manuscript.

5. Oxidative Stress Reduces proNGF Transport in Basal Forebrain Cholinergic Neurons

Shekari, A., Wu, C., & Fahnestock, M. (2021). Oxidative stress Reduces proNGF transport in basal forebrain cholinergic neurons.

Title

Oxidative Stress Triggers Basal Forebrain Cholinergic Neuron Degeneration by Reducing TrkA Levels and Impairing proNGF Axonal Transport

Authors

Arman Shekari[a], Chengbiao Wu[b], *Margaret Fahnestock[a*]

Affiliations

[a] Department of Psychiatry and Behavioral Neurosciences, McMaster University, Hamilton, Ontario, L8S 4K1, Canada

[b] Department of Neurosciences, University of California at San Diego, La Jolla, San Diego, California, 92093-0624

Corresponding Author

Margaret Fahnestock, Ph.D.

Department of Psychiatry & Behavioural Neurosciences

McMaster University

1280 Main Street West

Hamilton, ON L8S 4K1, Canada

Tel. 1-905-525-9140, ext. 23344

Fax 1-905-522-8804

E-mail: fahnest@mcmaster.ca

Keywords

neurotrophin, retrograde transport, TrkA, $p75^{NTR}$, ROS, antioxidant, PTP1B, aging, Alzheimer's disease

Classification: Biological Sciences

Abstract

Basal forebrain cholinergic neuron (BFCN) degeneration is a hallmark of aging and Alzheimer's disease (AD) (1). BFCNs depend on retrograde axonal transport of neurotrophins like pro nerve growth factor (proNGF) for survival (2, 3). This transport is reduced in aging and AD (4–6). We sought to determine whether mechanisms related to oxidative stress, a hypothesized contributor to aging and AD, account for this loss (7). We demonstrate that proNGF retrograde transport depends upon tropomyosin-related kinase A (TrkA) but not on the pan-neurotrophin receptor ($p75^{NTR}$). We observe significantly reduced TrkA, but not $p75^{NTR}$, immunoreactivity and impaired proNGF transport in antioxidant deprived BFCNs. Antagonism of protein tyrosine phosphatase-1B (PTP1B), an oxidation-sensitive enzyme involved in TrkA trafficking, triggers similar TrkA receptor loss and transport impairment. Treatment of BFCNs with PTP1B-reducing antioxidants rescues TrkA levels, proNGF transport and axonal degeneration. These results suggest impaired proNGF transport via oxidative PTP1B-mediated TrkA loss contributes to BFCN degeneration in aging and AD.

Significance Statement

The basal forebrain is a particularly vulnerable brain area in Alzheimer's disease (AD). Degeneration of basal forebrain cholinergic neurons (BFCNs) is implicated in memory loss in aging and AD. Mechanisms explaining this degeneration are lacking. BFCNs rely for survival and function on transporting neurotrophins, a class of signaling proteins, from the ends of their axons to their cell bodies. We demonstrate that oxidative stress, a hypothesized contributor to aging and AD, causes BFCN degeneration by impairing neurotrophin axonal transport. We establish that this transport impairment is due to oxidative inactivation of protein tyrosine phosphatase 1B which decreases the neurotrophin receptor TrkA. This mechanism explains the early degeneration of BFCNs, providing new therapeutic targets for memory loss in aging and AD.

Introduction

The basal forebrain exists at the ventral rostrocaudal extent of the brain and serves as the primary source of cholinergic innervation in the central nervous system (CNS) (1, 8). Basal forebrain cholinergic neurons (BFCNs) have extremely long and diffuse axonal projections that terminate widely throughout the hippocampus and neocortex (1, 9). These projections are critical for learning, memory, and attention, as they modulate hippocampal and cortical circuit dynamics that underlie these cognitive functions (1, 10). The degeneration of BFCN projections is a hallmark of aging and Alzheimer's disease (1, 11).

Alzheimer's disease (AD) is an age-related neurodegenerative disorder characterized symptomatically by progressive learning and memory deficits (12, 13). Up to 95% of BFCNs degenerate by the end-stages of AD, demonstrating a severe vulnerability of these neurons in the disorder (14, 15). Degeneration of BFCNs in AD leads to reductions in acetylcholine levels in upstream brain regions like the hippocampus and cortex (1, 16, 17). These cholinergic deficits correlate strongly with the cognitive decline seen in AD (11, 14, 18). Recent research has suggested that basal forebrain degeneration predicts and precedes the degeneration of upstream cortical brain areas, challenging the long-held belief that AD pathology is cortical in its origin (15). These findings highlight the importance of understanding how and why BFCNs are vulnerable to neurodegeneration.

A factor that may contribute to the vulnerability of BFCNs is their lack of neurotrophin synthesis. Neurotrophins are a family of extracellular signaling molecules that are critical for neuronal survival. Neurotrophins like nerve growth factor (NGF) and brain derived neurotrophic factor (BDNF) mediate a wide variety of cellular processes including apoptotic suppression, differentiation, activity-dependent plasticity, and maintenance of synaptic connectivity (19). Neurotrophins are initially translated as precursor "pro" proteins that can be later processed to their mature forms (20). However, unlike proBDNF and BDNF, proNGF is not processed to NGF in the mammalian CNS – the only detectable form of NGF in the brain is proNGF (5).

Neurotrophins exert their biological activity by binding to tropomyosin related kinases (Trks), with proNGF and NGF binding to TrkA (21, 22). All neurotrophins and proneurotrophins also bind to the pan-neurotrophin $p75^{NTR}$ receptor (19). Proneurotrophins bind to $p75^{NTR}$ with a higher affinity compared to Trk receptors, while mature neurotrophins bind Trk receptors with a higher affinity. (19, 23, 24). TrkA activation promotes neuronal survival and differentiation (25). This survival signaling is enhanced when TrkA is co-expressed with $p75^{NTR}$ (26). However, when $p75^{NTR}$ is solely expressed on neuronal surfaces, apoptosis occurs following neurotrophin binding (27–29). The activity of proNGF is contingent on the receptor complement of its target cell; lack of TrkA expression renders proNGF apoptotic, while expression of TrkA alone or in the presence of $p75^{NTR}$ renders proNGF neurotrophic (22, 27, 30). The maintenance of TrkA/$p75^{NTR}$ balance is critical for BFCNs due to their TrkA expression (31, 32) and the presence of proNGF, which is highly sensitive to relative levels of these receptors (Ioannou and Fahnestock, 2017; Masoudi et al., 2009).

Due to their lack of neurotrophin synthesis, BFCNs rely on their hippocampal and cortical targets for retrograde neurotrophin transport for the survival of their synaptic circuits (2, 3, 33). In AD, proNGF accumulates in BFCN target tissue(s) and is reduced in the basal forebrain itself, indicating that retrograde axonal transport is impaired (4–6). This transport loss occurs concurrent with reduced TrkA, but not $p75^{NTR}$, in the AD basal forebrain (34–37). Reduced proNGF transport and reduced TrkA, but not $p75^{NTR}$, are also observed in cultured BFCNs aged *in vitro* (38). However, mechanisms explaining these deficits remain unclear.

One factor that may contribute to these deficits is oxidative stress. Increased reactive oxygen species (ROS) load is a longstanding hypothesized contributor to aging and AD pathogenesis (7, 39–42). Almost all cellular macromolecules are found in their oxidized form in post-mortem AD brain tissue (43–45). Mitochondria, the predominant source of ROS in neurons, are themselves especially sensitive to oxidative stress (46). Mitochondrial respiratory efficiency is reduced under conditions of high oxidative load, increasing mitochondrial ROS output (46–48). Loss of mitochondrial efficiency along with increased ROS generation are commonly observed in both the aging and AD brain (47, 49–51)

While ROS accumulation has long been known to be a contributing factor to aging and AD pathogenesis, a causal link between oxidative stress and basal forebrain degeneration remains absent from the literature. However, recent findings may shed light on this link. TrkA levels are partially regulated by protein tyrosine phosphatase 1B (PTP1B), an endoplasmic reticulum-resident enzyme that dephosphorylates somal TrkA to regulate its trafficking to the axon terminal (52). Failure of PTP1B to dephosphorylate TrkA results in its lysosomal degradation (52). Phosphatases like PTP1B are regulated by the transient oxidation of their cysteine residues (53, 54). ROS accumulation has been shown to reduce the phosphatase activity of PTP1B by oxidation of a cysteine residue within its active site (55). We hypothesized that increased ROS load inactivates PTP1B, which contributes to the TrkA loss, reduced proNGF retrograde transport and axonal degeneration seen in aged BFCNs.

Methods

All reagents were purchased from ThermoFisher Scientific (Burlington, ON, Canada) unless otherwise stated.

proNGF Constructs

Because proNGF can be cleaved into its mature form *in vitro*, a cleavage-resistant form of proNGF was used in all experiments. Recombinant, cleavage resistant, (R-1G) proNGF (57) was engineered to include both a biotin-accepting AVI region and a nickel-binding histidine tag (72) and was subcloned into a pcDNA 3.1 expression vector as described in Shekari & Fahnestock, 2019. Plasmids coding for biotin-accepting plasmids coding for NGF mutants that bind exclusively to TrkA (KKE substitution mutant) and $p75^{NTR}$ (9-13 deletion mutation) underwent site-directed mutagenesis using the QuikChange II Site-Directed Mutagenesis Kit (Agilent, Santa Clara, California) to introduce the R-1G cleavage-resistance mutation.

Purification and Labeling of proNGF

HEK293 cells were grown to 70% confluency in medium containing DMEM, 1% FBS, 1% Penicillin-Streptomycin, 200mM GlutaMAX supplement, 50μM D-biotin (Sigma Aldrich), 100mM non-essential amino acids, and 100mM sodium pyruvate (Sigma Aldrich) (72). Cells were changed to a serum-free variant of this medium 24 hours before transfection. For each proNGF plasmid, 15-21μg of plasmid, along with 15-21μg of a plasmid encoding biotin ligase, were co-transfected into HEK293 cells using TurboFect. Medium was collected 72 hours post-transfection. ProNGF-biotin was purified from the medium via nickel affinity chromatography (38). Protein concentration was determined via an in-house NGF ELISA (57). proNGF-biotin was incubated with Quantum Dot 625 Streptavidin conjugate at a 1:1 molar ratio on ice for one hour in the dark and then diluted to 1nM using serum-free cell culture medium consisting of Neurobasal, 1% Penicillin-Streptomycin, 1X B27 supplement, 1X GlutaMAX supplement. TubulinTracker DeepRed was diluted to a final concentration of 1X in this solution.

Basal Forebrain Neuron Isolation

Whole basal forebrains were dissected from embryonic day 18 rat (Sprague-Dawley) or mouse. C57BL/6J wild-type or $p75^{NTR\ -/-}$ (a generous gift from Dr. Michael Kawaja, Queen's University, Kingston, Ontario Canada) were used only in experiments outlined in Figure 1F-H. Basal forebrains were immediately placed on ice in a solution of Hank's Balanced Salt Solution (HBSS) with 1% Penicillin-Streptomycin (73). The tissue from 5 embryos was pooled for each experiment. The neural tissue was washed with fresh HBSS five times and then trypsinized in a 37°C water bath for 20 minutes. DNase I (Sigma Aldrich, Oakville, Ontario) was added to a final concentration of 1X, and the tissue was triturated using a sterile, small-bore, fire-polished, glass pipette. 1mL of cell culture medium consisting of Neurobasal, 1% Penicillin-Streptomycin, 1X B27 supplement, 1X GlutaMAX supplement, 1% Fetal Bovine Serum, 50ng/mL BDNF (Peprotech, Rocky Hill, New Jersey), and 50 ng/mL NGF (generous gift from Dr. Michael Coughlin, McMaster University, Hamilton, Canada) was then added, and the suspension was centrifuged at 250xg for 4 minutes. The cell pellet was resuspended in 200μL of cell culture medium, and the volume was adjusted to a final concentration of 1.0×10^6 cells/mL.

Microfluidic Culture

BFCNs were cultured in microfluidic chambers (Xona Microfluidics, Research Triangle Park, NC, USA) to fluidically isolate cell bodies from axons and to linearize axonal projections. Microfluidic chambers were prepared as described in Shekari & Fahnestock, 2019, 2021. 140μL of medium was removed from each of the four wells of the chambers, and 10μL of cell suspension was added to the two cell body wells. A total of 6 chambers were prepared from each dissection (5 embryos). The chambers were incubated for 10 minutes to allow cell adherence, which was confirmed under a widefield microscope (Zeiss AxioVert A1). 150μL of cell culture medium was then added to all wells, and the cells were incubated overnight at 37°C and 5% CO_2. The next day, all the medium was removed and replaced with maintenance medium consisting of Neurobasal, 1% Penicillin-Streptomycin, 1X B27 supplement, 1X GlutaMAX supplement, 50ng/mL BDNF, and 50 ng/mL NGF. Cells were maintained in this medium for the

duration of the experiments, with medium changes occurring every 48-72 hours. All experiments were completed between days 8-14 *in vitro*. Cholinergic phenotype was confirmed by immunostaining for TrkA (see next section) (74).

Immunocytochemistry

Immunostaining was carried out in the microfluidic devices. Cells were fixed in freshly prepared 4% paraformaldehyde for 30 minutes in the dark at room temperature (RT). Cells were washed twice with PBS, permeabilized with 0.1% Triton-X100 in PBS for 30 minutes at RT and blocked with 3% bovine serum albumin in PBS for 30 minutes at RT. Anti-TrkA (Alomone, Tel Aviv, Israel), anti-$p75^{NTR}$ (Cell Signaling Technologies), or anti-PTP1B (ProteinTech, Rosemont, United States), primary antibodies were added at a 1:500 dilution and incubated overnight in the dark at 4°C. Cells were washed with blocking solution 3 times on the following day. Alexa Fluor 488 (for TrkA, $p75^{NTR}$) or Alexa Fluor 647 (PTP1B) secondary antibody was then added at a 1:1000 dilution and was incubated for 2 hours in the dark at RT. A nuclear counterstain (NucBlue Fixed Cell DAPI) was then added to the chambers to a final concentration of 1X and was incubated in the dark for 10 minutes at RT. Neurons were visualized via fluorescence microscopy using a DAPI (35nm excitation, 461nm emission), YFP (488nm excitation, 525nm emission) or Cy5 (649nm excitation, 666nm emission) filter cube. All images were taken using an EVOS2FL epifluorescent microscope (ThermoFisher Scientific, Burlington, Canada). Mean grey value of pixels within fluorescent cell bodies was measured using ImageJ (imagej.nih.gov). 82% of the DAPI-positive cells demonstrated TrkA immunoreactivity (data not shown).

Axonal Transport Assays

150µL of fresh maintenance medium was added to each cell body well of the chambers immediately before the addition of 80µL of 50pM quantum dot-labelled proNGF (proNGF-QD) to each axonal well. proNGF-QD was incubated for either 30 minutes or 1 hour for assessment of uptake or axonal transport, respectively. The axonal wells were washed 3 times with neurotrophin-free maintenance medium before imaging.

Axonal transport was quantified by counting the number of QD625-fluorescent particles present at the ends of the linear microgrooves proximal to the cell bodies 1 hour after axonal proNGF-QD administration. Images taken using the QD625 filter were set to threshold using the "Triangle" threshold scheme to assign pixels corresponding to QD-625 fluorescent particles a mean grey value of 255. A rectangular region of interest (ROI) of 150µM was then manually drawn around each microgroove to establish a particle counting area.

Axonal uptake was quantified by counting the number of QD625-fluorescent particles present within the distal axons 30 minutes after proNGF-KKE-QD administration to axon terminals. Images taken using the QD625 filter were set to threshold as described above. Images taken using the Cy5 filter were set to threshold using the default threshold scheme to assign pixels corresponding to axons a mean grey value of 255. Axons were then traced, and custom-shaped ROIs were created based on these shapes. These ROIs were then superimposed onto QD625 images to establish a particle counting area.

ROS Manipulation and Staining

To induce oxidative stress, BFCN cell bodies were cultured in antioxidant-poor medium for 24 hours prior to analysis. Antioxidant-poor medium was identical in composition to maintenance (control) medium apart from the substitution of the standard B27 supplement for a B27 supplement lacking the antioxidants vitamin E, vitamin E acetate, superoxide dismutase, catalase, and glutathione. After 24 hours, CellROX Deep Red, a reagent that only fluoresces in its oxidized state, and MitoSOX Orange, a reagent that fluoresces upon reacting with mitochondrially-generated superoxide ions, were both added to the antioxidant-poor medium at a final concentration of 1X. Neurons were counterstained with DAPI prior to imaging as described above. Neurons were visualized via fluorescence microscopy using a TexasRed (585nm excitation, 624nm emission), Cy5 and DAPI filter set.

To reduce (reactivate) oxidized PTP1B, BFCNs were treated with 800nM of recombinant active thioredoxin-1 (Trx-1) (Abcam, Cambridge, United Kingdom) and 800nM recombinant active thioredoxin reductase (TrxR) antioxidants (MyBioSource, San Diego, United States). Recombinant proteins were diluted to their final concentrations in antioxidant poor medium. This solution was added exclusively to the cell body wells of the chambers 24 hours prior to analysis.

PTP1B Inhibition and Knockdown

To inhibit PTP1B activity, BFCNs were treated with TCS401 (Tocris, Bristol, United Kingdom), a selective pharmacological inhibitor of PTP1B. TCS401 was diluted in maintenance medium and was added exclusively to the cell body wells of the chambers 72 hours prior to analysis.

To knock down PTP1B, BFCNs were incubated with either siRNA against PTP1B (5'–GUAUUGGCCACAGAAAGAAA – 3') or a GFP-tagged non-targeting siRNA control (5'–UGGUUUACAUGUCGACUUA – 3') (Horizon Discovery, Waterbeach, United Kingdom). siRNA was diluted to a final concentration of 1nM in maintenance medium. This solution was added exclusively to the cell body wells of the chambers 72 hours prior to analysis. Transfected neurons were fixed and stained as previously described using an antibody against PTP1B. siRNA transfection efficiency was 23% and was calculated by dividing the number of GFP-positive cell bodies by total DAPI-positive cell bodies.

Statistical Analysis

Unpaired, 2-tailed Student's *t* tests were performed when comparing 2 groups, with a confidence interval of 95%. One-way analysis of variance (ANOVA) with *post hoc* Tukey tests was performed when more than 2 groups were compared, with a p value of 0.05 being considered significant. All error bars represent the standard error of the mean.

Results

proNGF Retrograde Transport depends upon TrkA but not $p75^{NTR}$ in BFCNs

The receptor dependency of proNGF transport was established by observing the retrograde transport of mutant proNGF isoforms designed to bind only to either TrkA or $p75^{NTR}$. The two mutant isoforms used were the TrkA-binding proNGF-KKE isoform and the $p75^{NTR}$-

binding proNGF-9/13 isoform (56). Both isoforms, along with the wild-type proNGF isoform, contained an R-1G cleavage resistance mutation to prevent cleavage to mature NGF (57).

BFCNs were co-incubated at the distal axons with 50pM of proNGF-KKE-QD and proNGF-9/13-QD in separate compartments using a triple channel device containing 2 sets of fluidically isolated microgrooves (shown in Fig 1E) to visualize both mutant proteins concurrently. Both mutant isoforms were able to be internalized (Fig. 1 A, B). proNGF-KKE-QD was observed within microgrooves proximal to cell bodies after 1 hour (Fig. 1C), indicating retrograde transport, while proNGF-9/13-QD was not (Fig. 1D), indicating impaired retrograde transport.

To further explore the receptor dependency of proNGF retrograde transport, proNGF axonal transport assays were carried out using BFCNs isolated from $p75^{NTR-/-}$ mice. 50pM proNGF-QD was added to the axonal compartment of the chambers for 1 hour, enough time for proNGF particles to transit across the microgrooves. The number of proNGF-QD particles present at the distal ends of the microgrooves did not differ significantly between BFCNs isolated from wild-type mice and $p75^{NTR-/-}$ mice, demonstrating that proNGF transport can occur in the absence of $p75^{NTR}$ (Fig. 1F-H. *N*= 60 microgrooves from 3 chambers per group, p= 0.46, Student's *t*-test).

Antioxidant Deprivation Significantly Increases Reactive Oxygen Species and Decreases TrkA, but not $p75^{NTR}$, Immunoreactivity

BFCN cell bodies were cultured in antioxidant poor medium for 24 hours to determine if this treatment triggered somal ROS accumulation. BFCNs demonstrated significantly increased CellROX fluorescence, indicative of ROS accumulation, after being cultured in antioxidant poor medium for 24 hours (A-C). (Fig 2 A-C *N*= 40 images (120 cell bodies) from 2 chambers per group. ***p*= 0.007, Student's t-test).

BFCNs were then stained for TrkA and $p75^{NTR}$ following somal antioxidant deprivation to determine if oxidative stress affects proNGF receptor levels. BFCN cell bodies cultured in antioxidant-poor medium for 24 hours demonstrated significantly less TrkA immunoreactivity compared to neurons cultured in maintenance medium. (Fig. 2D-F. *N*= 30 images comprising an average of 200 cell bodies per group, p= 0.005, Student's t-test). BFCN cell bodies cultured in antioxidant-poor medium for 24 hours did not demonstrate significantly different $p75^{NTR}$ immunoreactivity compared to neurons cultured in maintenance medium. (Fig. 2G-I. *N*= 30 images comprising an average of 200 cell bodies per group, p= 0.49, Student's t-test).

Somal Antioxidant Deprivation Decreases proNGF Uptake via TrkA at Axon Terminals and Decreases proNGF Retrograde Transport

The axonal uptake of proNGF-KKE was assessed following somal antioxidant deprivation to determine if somal oxidative stress impacts TrkA activity at the axon terminal. Antioxidant depleted or control cells were incubated with 50pM proNGF-KKE-QD for 30 minutes to allow ample time for proNGF-KKE uptake before imaging at the axonal compartment. BFCN axon terminals demonstrated significantly reduced proNGF-KKE uptake

following 24-hour somal antioxidant deprivation compared to neurons cultured in maintenance medium (Fig. 3A-C. *N*= 60 axons from 3 chambers per group, p<0.001, Student's *t*-test).

To determine if antioxidant deprivation at the soma impacts the axonal transport of proNGF, the retrograde axonal transport of proNGF-QD was observed following 24 hours of somal antioxidant deprivation. Significantly fewer proNGF-QD particles were detected at the ends of the microgrooves proximal to the cell body in BFCNs cultured in antioxidant poor medium compared to control medium, demonstrating impaired retrograde transport (Fig. 3D-F. *N*= 60 microgrooves from 3 chambers per group, p<0.001, Student *t*-test.).

Inhibition of PTP1B Significantly Decreases TrkA, but not $p75^{NTR}$, Immunoreactivity and Decreases proNGF Retrograde Transport

To determine the effect of PTP1B activity on TrkA and $p75^{NTR}$ levels, BFCNs were treated with the selective PTP1B antagonist TCS401 for 72 hours prior to immunostaining. BFCN cell bodies demonstrated significantly less TrkA immunoreactivity after being treated with 200nM TCS401 compared to vehicle treated BFCNs (Fig. 4A-C. *N*= 30 images comprising an average of 200 cell bodies per group, p< 0.001, Student's *t*-test). Following treatment with 200nM TCS401, $p75^{NTR}$ immunoreactivity in BFCN cell bodies did not differ significantly from vehicle treated BFCNs (Fig. 4D-F. *N*= 30 images comprising an average of 200 cell bodies per group, p= 0.54, Student's *t*-test).

Next, the axonal uptake of proNGF-KKE was assessed in BFCNs following the somal administration of TCS401 to determine if inhibition of PTP1B at the cell body impacts the levels of TrkA at the axon terminal. Cells were incubated with 50pM proNGF-KKE-QD for 30 minutes to allow ample time for proNGF-KKE uptake before imaging at the axonal compartment. BFCN axon terminals demonstrated reduced axonal proNGF-KKE uptake after somal treatment with 200nM TCS401 compared to vehicle-treated BFCNs (Fig. 5A-C. *N*= 60 axons per group, p<0.001, Student's *t*-test).

To determine if somal PTP1B antagonism impacts the retrograde axonal transport of proNGF, proNGF-QD transport was observed following the somal administration of TCS401. Significantly fewer proNGF-QD particles were detected at the ends of the microgrooves proximal to the cell body in BFCNs treated with TCS401 compared to vehicle-treated BFCNs, demonstrating impaired retrograde transport (Fig. 5D-F. *N*= 60 microgrooves from 3 chambers per group, p<0.001, Student's *t*-test.)

To rule out the involvement of off-target effects from the use of TSC401, BFCN cell bodies were incubated with siRNA against PTP1B for 72 hours prior to immunostaining. Transfection of BFCNs with 1nM siRNA against PTP1B significantly reduced PTP1B immunoreactivity compared to transfection with a control non-targeting siRNA (Fig. 6A-C. *N*= 20 images comprising an average of 133 cell bodies per group, p<0.001, Student's *t*-test). BFCN cell bodies transfected with siRNA against PTP1B demonstrated significantly less TrkA immunoreactivity compared to neurons transfected with a control non-targeting siRNA (Fig. 6D-F. *N*= 30 images comprising an average of 200 cell bodies per group, p= 0.007, Student's *t*-test). BFCN cell bodies transfected with siRNA against PTP1B did not demonstrate significantly

different $p75^{NTR}$ immunoreactivity compared to compared to neurons transfected with a control non-targeting siRNA. (Fig. 6G-I. *N*= 30 images comprising an average of 200 cell bodies per group, p= 0.94, Student's *t*-test).

Somal Administration of Thioredoxin-1 and Thioredoxin Reductase Rescues Oxidative Stress Induced TrkA Loss and Normalizes proNGF Retrograde Transport

To determine if the reactivation (oxidative reduction) of oxidized PTP1B could rescue ROS-induced TrkA loss, BFCN cell bodies were cultured in antioxidant poor medium supplemented with PTP1B-reducing antioxidants thioredoxin-1 (Trx1) and thioredoxin-reductase (TrxR). BFCN cell bodies demonstrated significantly less TrkA immunoreactivity after being cultured in antioxidant poor medium than in control medium for 24 hours (Fig. 7A, B, D. *N*= 30 images comprising an average of 200 cell bodies per group, p<0.001, 1-way ANOVA and *post hoc* Tukey test). However, TrkA immunoreactivity did not differ significantly between neurons cultured in antioxidant poor medium supplemented with 800nM Trx1 and 800nM TrxR and neurons cultured in control medium, demonstrating a rescue effect (Fig. 7 A, C, D. *N*= 30 images comprising an average of 200 cell bodies per group, p= 0.36 1-way ANOVA and *post hoc* Tukey test). BFCN axon terminals also demonstrated significantly reduced proNGF-KKE-QD uptake after somal antioxidant deprivation compared to neurons cultured in maintenance medium (Fig 7E, F, H. *N*= 60 axons from 3 chambers per group, p<0.001, 1-way ANOVA and *post hoc* Tukey test). However, proNGF-KKE-QD uptake did not differ significantly between neurons cultured in antioxidant poor medium supplemented with 800nM Trx1 and 800nM TrxR and neurons cultured in control medium, demonstrating a rescue effect (Fig. 7E, G, H. *N*= 60 axons from 3 chambers per group, p= 0.95, 1-way ANOVA and *post hoc* Tukey test).

Next, the axonal transport of proNGF-QD was observed in BFCNs cultured in antioxidant-poor medium supplemented with Trx1 and TrxR to determine if the rescue of axonal TrkA levels affected proNGF retrograde transport. Significantly fewer proNGF-QD particles were detected at the ends of the microgrooves proximal to the cell body in BFCNs cultured in antioxidant poor medium compared to control medium (Fig. 7I, J, L. *N*= 60 microgrooves from 3 chambers per group p<0.001, 1-way ANOVA and *post hoc* Tukey test). However, the number of proNGF-QD particles at the ends of the microgrooves proximal to the cell body did not differ significantly between neurons cultured in control medium and neurons cultured in antioxidant-poor medium supplemented with 800nM Trx1 and 800nM TrxR, demonstrating a rescue effect (Fig. 7I, K, L. *N*= 60 microgrooves from 3 chambers per group p= 0.66 1-way ANOVA and *post hoc* Tukey test).

proNGF-Induced Axonal Degeneration is Mediated by the Loss of TrkA

Axonal proNGF administration resulted in the morphological degeneration of BFCN axonal projections subjected to 24 hours of somal antioxidant deprivation (Figure 8A). This degeneration was absent in neurons cultured in control medium (Figure 8D) and in neurons cultured in antioxidant-poor medium supplemented with 800nM Trx1 and 800nM TrxR (Figure 8B). Axonal degeneration was also absent following administration of 50pM proNGF-KKE to

neurons cultured in antioxidant-poor medium (Figure 8C) but was observed following the administration of proNGF-9/13 (Figure 8F).

Discussion

TrkA, but not $p75^{NTR}$, is Required for proNGF Retrograde Transport in BFCNs

Here we demonstrate the receptor dependency of proNGF retrograde transport by observing that its transport is contingent solely upon TrkA. Both the TrkA-binding proNGF-KKE and $p75^{NTR}$-binding proNGF-9/13 mutants were internalized by BFCNs. The time-course of internalization did not differ between either of the mutants and wild-type proNGF; all isoforms were visualized within axonal projections 30 minutes after addition. However, only proNGF-KKE was retrogradely transported to BFCN cell bodies. proNGF transport was also unimpaired in BFCNs derived from $p75^{NTR\ -/-}$ mice, demonstrating that retrograde transport of proNGF can occur in the absence of $p75^{NTR}$.

The mechanism behind the lack of retrograde transport demonstrated by proNGF-9/13 cannot be conclusively determined based on these experiments due to the degenerative effect proNGF-9/13 has on BFCN axon terminals. Lack of proNGF-9/13 transport may simply be due to the significant axonal degeneration that occurs following its administration as activation of $p75^{NTR}$-mediated pathways is known to cause acute growth cone collapse by modulating the activity of RhoA, an actin-modifying GTPase (58). Alternatively, it is also possible that proNGF is unable to be retrogradely transported solely via $p75^{NTR}$, leading to its sequestration within BFCN axon terminals in the absence of TrkA binding. Interestingly, proNGF accumulation at BFCN terminals has been observed in AD alongside TrkA loss, suggesting that proNGF bound predominantly to $p75^{NTR}$ *in vivo* is not retrogradely transported and becomes sequestered within axon terminals (1, 6, 9, 22).

The binding of proNGF to TrkA has been well documented (22, 23, 27, 30, 57). However, the prevailing view of proNGF is that of an apoptotic molecule whose activity is reliant solely on $p75^{NTR}$ (59–62). Our data add to the growing body of evidence opposing this zeitgeist by demonstrating that the retrograde transport of proNGF depends upon TrkA and can occur independently of $p75^{NTR}$. This novel observation of TrkA-contingent proNGF transport agrees with the well-documented receptor contingency of proNGF activity – the neurotrophic activity of proNGF is dependent upon the presence of TrkA (22, 27, 30, 57). This concept is explored below in the context of ROS-mediated TrkA loss.

ROS Accumulation and PTP1B Antagonism Reduce TrkA Levels and proNGF Retrograde Transport

BFCN degeneration concomitant with TrkA loss and proNGF transport impairments are longstanding hallmarks of AD (1, 4, 36). Our results provide a mechanism demonstrating that oxidative stress contributes to these deficits. Oxidative stress inactivates PTP1B, an enzyme essential for TrkA trafficking. We demonstrate here that somal PTP1B antagonism, either by raising ROS levels or reducing PTP1B activity, reduces axonal TrkA levels and proNGF retrograde transport. These results suggest that TrkA trafficking in BFCNs occurs similarly to DRGs, where the dephosphorylation of TrkA receptors at the soma by PTP1B determines

whether they will be anterogradely recycled to the axon terminal or degraded at the soma (52). The rescue of axonal TrkA levels, proNGF retrograde transport and axonal degeneration following the oxidative reduction of PTP1B via antioxidants Trx1 and TrxR show that oxidative stress produces BFCN degeneration by reducing TrkA levels and proNGF retrograde transport.

While oxidative stress is a longstanding hypothesized contributor to AD pathogenesis, specific effects in the basal forebrain have not been explored. Interestingly, factors relating to mitochondrial function, the main source of ROS in neurons, suggest that the basal forebrain may exhibit higher levels of oxidative stress compared to other brain areas (51, 63, 64). Basal forebrain neurons rely on axonal transport, a mitochondria-dependent process, for neurotrophic support (2, 65, 66). Basal forebrain neurons have extremely long and diffuse axonal projections compared to other neurons in the central nervous system (CNS), making the transport of mitochondria along their lengthy neurites of vital importance (9, 67, 68). Mitochondrial mass scales directly with neuronal size, amplifying the vulnerability of these large neurons to mitochondria-mediated oxidative damage (68). This increased ROS burden likely results in pathological ROS accumulation occurring earlier and more severely in BFCNs compared to other neurons. An increased ROS burden may contribute to BFCN selective vulnerability in AD and highlights the importance of understanding the consequences of oxidative damage in these neurons.

proNGF-Mediated Axonal Degeneration Depends Upon TrkA Levels in BFCNs

proNGF is widely viewed as an apoptotic molecule. Here we demonstrate that proNGF-mediated BFCN neurodegeneration only occurs following somal antioxidant deprivation, a condition that reduces TrkA levels. We show that the axonal degeneration observed following proNGF administration under antioxidant depletion conditions is associated with the reduced proNGF retrograde transport observed under these conditions. The rescue of axonal degeneration by somal Trx1 and TrxR treatment further highlights the importance of ROS-mediated anterograde TrkA trafficking in maintaining BFCN axonal integrity. Taken together, our results demonstrate that the axonal degeneration that accompanies proNGF administration following somal antioxidant deprivation is due to the absence of TrkA. This is further supported by the lack of axonal degeneration observed following proNGF-KKE administration under somal antioxidant depletion conditions.

These results build on an existing body of literature suggesting that the activation of $p75^{NTR}$-mediated degenerative pathways contributes to the cholinergic degeneration observed in both aging and AD (22, 27, 30, 57). The loss of basal forebrain TrkA levels observed in AD likely results in apoptotic signaling upon proNGF binding to $p75^{NTR}$ at BFCN terminals, contributing to the synaptic degeneration of BFCN projections in AD. Interestingly, the inhibition of $p75^{NTR}$ signaling via small molecule antagonism of the $p75^{NTR}$ receptor prevents the degeneration of cholinergic circuits in both aging and multiple AD mouse models (69, 70). Antagonism of $p75^{NTR}$ also prevents proNGF-mediated neurodegeneration in hippocampal neurons which do not express TrkA (71). Furthermore, $p75^{NTR}$ knockout prevents proNGF-mediated apoptosis in oligodendrocytes (59). The ability of proNGF to be retrogradely

transported in the complete absence of $p75^{NTR}$ demonstrates that $p75^{NTR}$ antagonism won't affect the neurotrophic transport of proNGF via TrkA. These reports, taken together with the current results, suggest that a two-pronged approach targeting PTP1B oxidative reduction at the soma and $p75^{NTR}$ inhibition at the axon is a promising therapeutic avenue to prevent BFCN degeneration in AD.

Conclusions

Here we present a mechanism contributing to the breakdown of cholinergic circuits in age-related neurodegeneration and AD. The increased ROS load that accompanies aging and AD pathology results in an increase in oxidized, inactive PTP1B. This inactivation causes somal TrkA degradation and a subsequent lack of TrkA at axon terminals of BFCNs. As a result, proNGF released from BFCN targets is not retrogradely transported, cannot activate neurotrophic signals via TrkA and accumulates at BFCN axon terminals. The accumulated proNGF binds predominantly to $p75^{NTR}$, causing degeneration of BFCN projections. Reducing intracellular oxidative stress and inhibiting the activation of $p75^{NTR}$-mediated neurodegenerative pathways serve as promising avenues for the prevention of BFCN degeneration and accompanying cognitive deficits in aging and AD.

Acknowledgements

We thank Dr. Michael Kawaja (Queen's University, Kingston Ontario, Canada) for providing us with $p75^{NTR}$ knockout animals. Supported by grant #PJT-159493 from the Canadian Institutes of Health Research to MF and an Ontario Graduate Scholarship to AS.

Author Contributions

AS and MF prepared the manuscript. AS designed and completed all experiments. CW reviewed the manuscript, graciously donated mutant NGF and BirA plasmids, and provided training.

Declaration of Interests

None

Figure Titles and Legends

Figure 1. proNGF Retrograde Transport Requires TrkA but not $p75^{NTR}$. Rat basal forebrain cholinergic neurons (BFCNs) were cultured in triple channel devices containing 2 sets of fluidically isolated microgrooves as indicated in panel E. BFCNs were co-incubated with 50pM TrkA-binding proNGF-KKE (pink section, panel E) and $p75^{NTR}$-binding proNGF-9/13 (blue section, panel E). Both proteins were found within the distal axons after 30 minutes (A-B), demonstrating internalization. proNGF-KKE (green dots) was observed within microgrooves proximal to cell bodies after 1 hour (C). proNGF-9/13 (red dots) was not observed within microgrooves after 1 hour (D). Representative results from 2 chambers per group. The retrograde axonal transport of proNGF did not differ between BFCNs cultured from wild type *vs.* $p75^{NTR}$ knockout (KO) mice (F-H). Wild type and $p75^{NTR}$ KO neurons were incubated with proNGF-QD (yellow dots) at the axonal compartment only (indicated by the pink section of the schematic in panel F) for 1 hour before imaging. The red oval indicates where the images were taken. Experiments were completed three times. N= 60 microgrooves from 3 chambers per group, mean +/- SE. ns (not significant) p= 0.46, Student's t-test.

Figure 2: **Antioxidant Deprivation Decreases Intracellular TrkA but not $p75^{NTR}$ Immunoreactivity.** Basal forebrain cholinergic neuron (BFCN) cell bodies demonstrated significantly increased CellROX fluorescence, indicative of ROS accumulation, after being cultured in antioxidant poor medium for 24 hours (A-C). CellROX fluorescence colocalized with mitochondrial superoxide indicator MitoSOX following antioxidant deprivation (B). *N*= 40 images (120 cell bodies) from 2 chambers per group. Mean ±SE. ***p*= 0.007, Student's *t*-test). Basal forebrain cholinergic neuron cell bodies cultured in antioxidant-poor medium for 24 hours demonstrated significantly less TrkA immunoreactivity compared to neurons cultured in control medium (D-F). $p75^{NTR}$ immunoreactivity did not change following the same treatment (G-I). Experiments were repeated 3 times. *N*= 30 images (200 cell bodies), from 3 chambers per group. Mean ±SE. ***p*= 0.005, ns (not significant) *p*= 0.49, Student's *t*-test.

Figure 3: Axonal uptake of proNGF via TrkA and Retrograde proNGF Transport are Reduced Following Antioxidant Depletion. Basal forebrain cholinergic neurons (BFCNs) demonstrated significantly reduced proNGF-KKE (proNGF binding to TrkA only) uptake at axon terminals after culturing in antioxidant poor medium for 24 hours compared to control medium (A-C). Significantly fewer wild type proNGF-QD particles were detected at the ends of the microgrooves proximal to the cell body in BFCNs cultured in antioxidant poor medium compared to control medium (D-F). Control and antioxidant depleted neurons were incubated with either proNGF-KKE-QD (green) or proNGF-QD (yellow) at the axonal compartment only (pink section of the schematics) for 30 minutes or 1 hour, respectively, before imaging. The red ovals indicate where the images were taken. Experiments were repeated 3 times. *N*= 30 axons (C) and 60 microgrooves (F) from 3 chambers per group. Mean ±SE. ****p*<0.001, Student's *t*-test.

Figure 4. PTP1B Inhibition Decreases Intracellular TrkA but not $p75^{NTR}$ Immunoreactivity. Basal forebrain cholinergic neuron (BFCN) cell bodies demonstrated significantly less TrkA immunoreactivity after being treated with 200nM selective PTP1B antagonist TCS401 compared to vehicle treated BFCNs (A-C). $p75^{NTR}$ immunoreactivity did not change significantly following the same treatment (D-F). Experiments were repeated 3 times. *N*= 30 images (200 cell bodies), from 3 chambers per group. Mean ±SE. ****p*<0.001, ns (not significant) *p*= 0.54, Student's *t*-test.

Figure 5. Axonal uptake of proNGF via TrkA and Retrograde proNGF Transport are Reduced Following PTP1B Inhibition. Basal forebrain cholinergic neuron (BFCN) axons demonstrated reduced proNGF-KKE uptake after treatment with 200nM selective PTP1B antagonist TCS401 compared to vehicle treated BFCNs (A-C). Significantly fewer proNGF-QD particles were detected at the ends of the microgrooves proximal to the cell body in BFCNs treated somally with TCS401 for 72 hours compared to vehicle-treated neurons (D-F). Vehicle and TCS401 treated neurons were incubated with either proNGF-KKE-QD (green) or proNGF-QD (yellow) at the axonal compartment only (indicated by the pink section of the schematic) for 30 minutes or 1 hour, respectively, before imaging. The red ovals indicate where the images were taken. Experiments were completed three times. *N*= 30 axons (C) and 60 microgrooves (F) from 3 chambers per group. Mean ±SE. ****p*<0.001, Student's *t*-test.

Figure 6. siRNA Knockdown of PTP1B Reduces TrkA but not p75^{NTR} Immunoreactivity. PTP1B immunoreactivity was significantly reduced in basal forebrain cholinergic neurons (BFCNs) transfected with 1nM siRNA against PTP1B compared to neurons transfected with a non-targeting siRNA-GFP (A-C). *N*= 20 images (120 cell bodies), from 2 chambers per group. ***p<0.001, Student's *t*-test. BFCN cell bodies demonstrated significantly less TrkA immunoreactivity after being transfected with 1nM siRNA against PTP1B compared to neurons treated with scrambled control siRNA (D-F). p75^{NTR} immunoreactivity did not change significantly following the same treatment (G-H). *N*= 30 images (200 cell bodies), from 3 chambers per group. Mean ±SE. ***p*= 0.007, ns (not significant) *p*= 0.94, Student's *t*-test.

Figure 7. Administration of Thioredoxin-1 and Thioredoxin Reductase Rescues Oxidative Stress-Induced TrkA Loss and proNGF Retrograde Transport. Basal forebrain cholinergic neuron (BFCN) cell bodies exhibited significantly less TrkA immunoreactivity after being cultured in antioxidant poor medium compared to control medium (A,B,D). TrkA immunoreactivity did not differ significantly between neurons cultured in control medium and neurons cultured in antioxidant poor medium supplemented with 800nM thioredoxin-1 and 800nM Thioredoxin Reductase (A,C,D). BFCN axon terminals demonstrated significantly reduced proNGF-KKE uptake after somal antioxidant deprivation compared to neurons cultured in maintenance medium (E,F,H). However, proNGF-KKE uptake did not differ significantly between neurons cultured in antioxidant poor medium supplemented with 800nM Trx1 and 800nM TrxR and neurons cultured in control medium (E,G,H). Significantly fewer proNGF-QD particles were detected at the ends of the microgrooves proximal to the cell body in BFCNs cultured in antioxidant poor medium compared to control medium (I,J,L). Culturing neurons in antioxidant-poor medium supplemented with 800nM Trx1 and 800nM TrxR rescued the number of proNGF-QD particles at the ends of the microgrooves proximal to the cell body (I,K,L). Neurons were incubated with either proNGF-KKE-QD (green) for 30 minutes or proNGF-QD (yellow) for 1 hour at the axonal compartment only (indicated by the pink section of the schematic), before imaging. The red ovals indicate where the images were taken. Experiments were completed 3 times. *N*= 30 images (D, 200 cell bodies), 60 axons (H), and 60 microgrooves (L) from 3 chambers per group. Mean ±SE. ****p*<0.001, ns (not significant) *p*= 0.36 (D), *p*=0.95 (H), *p*= 0. 66 (L). 1-way ANOVA and *post hoc* Tukey test.

Figure 8. Antioxidant Depletion and proNGF binding to p75^{NTR} Cause Axonal Degeneration. Basal forebrain cholinergic neuron (BFCN) axon terminals from neurons cultured in antioxidant-poor medium at the soma for 24 hours exhibited morphological axon degeneration after the axonal administration of 50pM proNGF (A). This degeneration was absent in axons from neurons cultured in antioxidant poor medium supplemented with 800nM Trx1 and 800nM TrxR (B) and in neurons cultured in control medium (D). This degeneration was also absent in neurons cultured in antioxidant-poor medium following axonal proNGF-KKE administration (C). Axonal administration of 50pM proNGF-9/13 resulted in degeneration of the neuronal projections within the axonal compartment while administration of 50pM wild type proNGF or proNGF-KKE did not (D-F). The projections present in the proNGF-9/13 exposed group appear thinner and more dystrophic (F). All groups were incubated with 50pM proNGF at the axonal compartment only (indicated by the pink section of the schematic, red oval indicating where the images were taken) for 1 hour before imaging. Representative images from 30 images collected from 3 chambers per group.

References

1. E. C. Ballinger, M. Ananth, D. A. Talmage, L. W. Role, Basal Forebrain Cholinergic Circuits and Signaling in Cognition and Cognitive Decline. *Neuron* **91**, 1199–1218 (2016).

2. M. Seiler, M. E. Schwab, Specific retrograde transport of nerve growth factor (NGF) from neocortex to nucleus basalis in the rat. *Brain Research* **300**, 33–39 (1984).

3. L. R. Williams, *et al.*, Continuous infusion of nerve growth factor prevents basal forebrain neuronal death after fimbria fornix transection. *Proc Natl Acad Sci U S A* **83**, 9231–9235 (1986).

4. S. A. Scott, E. J. Mufson, J. A. Weingartner, K. A. Skau, K. A. Crutcher, Nerve growth factor in Alzheimer's disease: increased levels throughout the brain coupled with declines in nucleus basalis. *The Journal of neuroscience : the official journal of the Society for Neuroscience* **15**, 6213–6221 (1995).

5. Fahnestock, B. Michalski, B. Xu, M. Coughlin, The precursor pro-nerve growth factor is the predominant form of nerve growth factor in brain and is increased in Alzheimer's disease. *Molecular and Cellular Neuroscience* **18**, 210–220 (2001).

6. S. Peng, J. Wuu, E. Mufson, M. Fahnestock, Increased proNGF levels in subjects with mild cognitive impairment and mild Alzheimer disease. *Journal of neuropathology and experimental neurology* **63**, 641–9 (2004).

7. E. Tönnies, E. Trushina, Oxidative Stress, Synaptic Dysfunction, and Alzheimer's Disease. *Journal of Alzheimer's Disease* **57**, 1105–1121 (2017).

8. N. J. Woolf, Cholinergic systems in mammalian brain and spinal cord. *Progress in neurobiology* **37**, 475–524 (1991).

9. Wu, J. Williams, J. Nathans, Complete morphologies of basal forebrain cholinergic neurons in the mouse. *eLife* **3** (2014).

10. M. G. Baxter, A. A. Chiba, Cognitive functions of the basal forebrain. *Current Opinion in Neurobiology* **9**, 178–183 (1999).

11. J. R. Köppen, *et al.*, Cholinergic deafferentation of the hippocampus causes non-temporally graded retrograde amnesia in an odor discrimination task. *Behavioural Brain Research* **299**, 97–104 (2016).

12. K. Belarbi, *et al.*, Early Tau pathology involving the septo-hippocampal pathway in a Tau transgenic model: relevance to Alzheimer's disease. *Current Alzheimer research* **6**, 152–157 (2009).

13. M. W. Bondi, E. C. Edmonds, D. P. Salmon, Alzheimer's Disease: Past, Present, and Future. *Journal of the International Neuropsychological Society* **23**, 818–831 (2017).

14. A. Baker-Nigh, *et al.*, Neuronal amyloid-β accumulation within cholinergic basal forebrain in ageing and Alzheimer's disease. *Brain* **138**, 1722–1737 (2015).

15. T. W. Schmitz, *et al.*, Basal forebrain degeneration precedes and predicts the cortical spread of Alzheimer's pathology. *Nature Communications* **7**, 13249 (2016).

16. R. Bartus, R. Dean, B. Beer, A. Lippa, The cholinergic hypothesis of geriatric memory dysfunction. *Science* **217**, 408–414 (1982).

17. Davies, Neurotransmitter-related enzymes in senile dementia of the alzheimer type. *Brain Research* **171**, 319–327 (1979).

18. A. R. Ypsilanti, M. T. Girão da Cruz, A. Burgess, I. Aubert, The length of hippocampal cholinergic fibers is reduced in the aging brain. *Neurobiology of Aging* **29**, 1666–1679 (2008).

19. M. Bothwell, "NGF, BDNF, NT3, and NT4" in *Handbook of Experimental Pharmacology*, (2014), pp. 3–15.

20. Sun, B.-Y. Chen, Y. Xia, J.-J. Wang, L.-W. Chen, Functional switch from pro-neurotrophins to mature neurotrophins. *Current protein & peptide science* **14**, 617–25 (2013).

21. K. Deinhardt, M. V. Chao, "Trk Receptors" in *Handbook of Experimental Pharmacology*, (2014), pp. 103–119.

22. M. Fahnestock, A. Shekari, ProNGF and Neurodegeneration in Alzheimer's Disease. *Frontiers in Neuroscience* **13** (2019).

23. O. Clewes, *et al.*, Human ProNGF: Biological effects and binding profiles at TrkA, P75NTRand sortilin. *Journal of Neurochemistry* **107**, 1124–1135 (2008).

24. B. Fayard, S. Loeffler, J. Weis, E. Vögelin, A. Krüttgen, The secreted brain-derived neurotrophic factor precursor pro-BDNF binds to TrkB and p75NTR but not to TrkA or TrkC. *Journal of Neuroscience Research* **80**, 18–28 (2005).

25. D. R. Kaplan, F. D. Miller, Neurotrophin signal transduction in the nervous system. *Current Opinion in Neurobiology* **10**, 381–391 (2000).

26. W. R. Epa, K. Markovska, G. L. Barrett, The p75 neurotrophin receptor enhances TrkA signalling by binding to Shc and augmenting its phosphorylation. *J Neurochem* **89**, 344–353 (2004).

27. M. Ioannou, M. Fahnestock, ProNGF, but Not NGF, Switches from Neurotrophic to Apoptotic Activity in Response to Reductions in TrkA Receptor Levels. *International Journal of Molecular Sciences* **18**, 599 (2017).

28. A. L. Bhakar, *et al.*, Apoptosis induced by p75NTR overexpression requires Jun kinase-dependent phosphorylation of Bad. *The Journal of neuroscience : the official journal of the Society for Neuroscience* **23**, 11373–81 (2003).

29. M. Volosin, *et al.*, Interaction of Survival and Death Signaling in Basal Forebrain Neurons: Roles of Neurotrophins and Proneurotrophins. *Journal of Neuroscience* **26**, 7756–7766 (2006).

30. R. Masoudi, *et al.*, Biological Activity of Nerve Growth Factor Precursor Is Dependent upon Relative Levels of Its Receptors. *Journal of Biological Chemistry* **284**, 18424–18433 (2009).

31. M. Kojima, T. Ikeuchi, H. Hatanaka, Role of nerve growth factor in the expression oftrkA mRNA in cultured embryonic rat basal forebrain cholinergic neurons. *Journal of Neuroscience Research* **42**, 775–783 (1995).

32. E. Sanchez-Ortiz, *et al.*, TrkA Gene Ablation in Basal Forebrain Results in Dysfunction of the Cholinergic Circuitry. *Journal of Neuroscience* **32**, 4065–4079 (2012).

33. B. Lu, G. Nagappan, Y. Lu, *BDNF and synaptic plasticity, cognitive function, and dysfunction.* (2014).

34. S. E. Counts, *et al.*, Reduction of cortical TrkA but not p75NTR protein in early-stage Alzheimer's disease. *Annals of Neurology* **56**, 520–531 (2004).

35. S. D. Ginsberg, S. Che, J. Wuu, S. E. Counts, E. J. Mufson, Down regulation of trk but not p75 NTR gene expression in single cholinergic basal forebrain neurons mark the progression of Alzheimer's disease. *Journal of Neurochemistry* **97**, 475–487 (2006).

36. E. J. Mufson, *et al.*, Loss of nucleus basalis neurons containing trkA immunoreactivity in individuals with mild cognitive impairment and early Alzheimer's disease. *The Journal of Comparative Neurology* **427**, 19–30 (2000).

37. E. J. Mufson, S. D. Ginsberg, M. D. Ikonomovic, S. T. DeKosky, Human cholinergic basal forebrain: chemoanatomy and neurologic dysfunction. *Journal of Chemical Neuroanatomy* **26**, 233–242 (2003).

38. A. Shekari, M. Fahnestock, Retrograde axonal transport of BDNF and proNGF diminishes with age in basal forebrain cholinergic neurons. *Neurobiology of Aging* **84**, 131–140 (2019).

39. W. Ahmad, B. Ijaz, K. Shabbiri, F. Ahmed, S. Rehman, Oxidative toxicity in diabetes and Alzheimer's disease: mechanisms behind ROS/ RNS generation. *Journal of Biomedical Science* **24**, 76 (2017).

40. S. Leutner, *et al.*, Enhanced ROS-Generation in Lymphocytes from Alzheimer's Patients. *Pharmacopsychiatry* **38**, 312–315 (2005).

41. L. Mosconi, Glucose metabolism in normal aging and Alzheimer's disease: methodological and physiological considerations for PET studies. *Clinical and Translational Imaging* **1**, 217–233 (2013).

42. A. Tramutola, C. Lanzillotta, M. Perluigi, D. A. Butterfield, Oxidative stress, protein modification and Alzheimer disease. *Brain Research Bulletin* **133**, 88–96 (2017).

43. P. Mecocci, U. MacGarvey, M. F. Beal, Oxidative damage to mitochondrial DNA is increased in Alzheimer's disease. *Annals of Neurology* **36**, 747–751 (1994).

44. K. V. Subbarao, J. S. Richardson, L. C. Ang, Autopsy Samples of Alzheimer's Cortex Show Increased Peroxidation In Vitro. *Journal of Neurochemistry* **55**, 342–345 (1990).

45. S. J. Kish, *et al.*, Brain Cytochrome Oxidase in Alzheimer's Disease. *Journal of Neurochemistry* **59**, 776–779 (1992).

46. J. S. Bhatti, G. K. Bhatti, P. H. Reddy, Mitochondrial dysfunction and oxidative stress in metabolic disorders — A step towards mitochondria based therapeutic strategies. *Biochimica et Biophysica Acta (BBA) - Molecular Basis of Disease* **1863**, 1066–1077 (2017).

47. D. G. Nicholls, Mitochondrial membrane potential and aging. *Aging Cell* **3**, 35–40 (2004).

48. A. F. Schinder, E. C. Olson, N. C. Spitzer, M. Montal, Mitochondrial dysfunction is a primary event in glutamate neurotoxicity. *The Journal of neuroscience : the official journal of the Society for Neuroscience* **16**, 6125–33 (1996).

49. M. F. Beal, Mitochondria take center stage in aging and neurodegeneration. *Annals of Neurology* **58**, 495–505 (2005).

50. Q. Cai, P. Tammineni, Alterations in Mitochondrial Quality Control in Alzheimer's Disease. *Frontiers in Cellular Neuroscience* **10** (2016).

51. S. Lores-Arnaiz, *et al.*, Brain cortex mitochondrial bioenergetics in synaptosomes and non-synaptic mitochondria during aging. *Neurochemical Research* **41**, 353–363 (2016).

52. N. Yamashita, R. Joshi, S. Zhang, Z.-Y. Zhang, R. Kuruvilla, Phospho-Regulation of Soma-to-Axon Transcytosis of Neurotrophin Receptors. *Developmental Cell* **42**, 626-639.e5 (2017).

53. L. C. Flores, *et al.*, Thioredoxin, oxidative stress, cancer and aging. *Longevity & Healthspan* **1**, 4 (2012).

54. A. Holmgren, J. Lu, Thioredoxin and thioredoxin reductase: Current research with special reference to human disease. *Biochemical and Biophysical Research Communications* **396**, 120–124 (2010).

55. P.-S. Tsou, *et al.*, Effect of oxidative stress on protein tyrosine phosphatase 1B in scleroderma dermal fibroblasts. *Arthritis & Rheumatism* **64**, 1978–1989 (2012).

56. S. Mahapatra, H. Mehta, S. B. Woo, K. E. Neet, Identification of critical residues within the conserved and specificity patches of nerve growth factor leading to survival or differentiation. *J Biol Chem* **284**, 33600–33613 (2009).

57. Fahnestock, *et al.*, The nerve growth factor precursor proNGF exhibits neurotrophic activity but is less active than mature nerve growth factor. *Journal of Neurochemistry* **89**, 581–592 (2004).

58. S. Gehler, G. Gallo, E. Veien, P. C. Letourneau, p75 Neurotrophin Receptor Signaling Regulates Growth Cone Filopodial Dynamics through Modulating RhoA Activity. *J. Neurosci.* **24**, 4363–4372 (2004).

59. M. S. Beattie, *et al.*, ProNGF Induces p75-Mediated Death of Oligodendrocytes following Spinal Cord Injury. *Neuron* **36**, 375–386 (2002).

60. A. W. Harrington, *et al.*, Secreted proNGF is a pathophysiological death-inducing ligand after adult CNS injury. *PNAS* **101**, 6226–6230 (2004).

61. R. Lee, P. Kermani, K. Teng, B. Hempstead, Regulation of Cell Survival by Secreted Proneurotrophins. *Science* **294**, 1945–1948 (2001).

62. A. Nykjaer, *et al.*, Sortilin is essential for proNGF-induced neuronal cell death. *Nature* **427**, 843–848 (2004).

63. A. Navarro, *et al.*, Hippocampal mitochondrial dysfunction in rat aging. *American Journal of Physiology-Regulatory, Integrative and Comparative Physiology* **294**, R501–R509 (2008).

64. A. S. Driver, P. R. S. Kodavanti, W. R. Mundy, Age-related changes in reactive oxygen species production in rat brain homogenates. *Neurotoxicology and Teratology* **22**, 175–181 (2000).

65. S. J. Allen, J. J. Watson, D. Dawbarn, The neurotrophins and their role in Alzheimer's disease. *Current Neuropharmacology* **9**, 559–573 (2011).

66. T. Sobreviela, M. Pagcatipunan, J. S. Kroin, E. J. Mufson, Retrograde transport of brain-derived neurotrophic factor (BDNF) following infusion in neo-and limbic cortex in rat: Relationship to BDNF mRNA expressing neurons. *The Journal of Comparative Neurology* **375**, 417–444 (1996).

67. H. Chen, D. C. Chan, Mitochondrial dynamics-fusion, fission, movement, and mitophagy-in neurodegenerative diseases. *Human Molecular Genetics* **18**, R169–R176 (2009).

68. T. Misgeld, T. L. Schwarz, Mitostasis in Neurons: Maintaining Mitochondria in an Extended Cellular Architecture. *Neuron* **96**, 651–666 (2017).

69. D. A. Simmons, *et al.*, A Small Molecule p75NTR Ligand, LM11A-31, Reverses Cholinergic Neurite Dystrophy in Alzheimer's Disease Mouse Models with Mid- to Late-Stage Disease Progression. *PLoS ONE* **9**, e102136 (2014).

70. Y. Xie, R. B. Meeker, S. M. Massa, F. M. Longo, Modulation of the p75 neurotrophin receptor suppresses age-related basal forebrain cholinergic neuron degeneration. *Scientific Reports* **9**, 5273 (2019).

71. S. M. Massa, *et al.*, Small, nonpeptide p75NTR ligands induce survival signaling and inhibit proNGF-induced death. *The Journal of neuroscience : the official journal of the Society for Neuroscience* **26**, 5288–300 (2006).

72. K. Sung, M. T. Maloney, J. Yang, C. Wu, A novel method for producing mono-biotinylated, biologically active neurotrophic factors: An essential reagent for single molecule study of axonal transport. *Journal of Neuroscience Methods* **200**, 121–128 (2011).

73. N. K. Dhanoa, K. M. Krol, A. Jahed, K. A. Crutcher, M. D. Kawaja, Null mutations for exon III and exon IV of the p75 neurotrophin receptor gene enhance sympathetic sprouting in response to elevated levels of nerve growth factor in transgenic mice. *Exp Neurol* **198**, 416–426 (2006).

74. D. Holtzman, *et al.*, TrkA expression in the CNS: evidence for the existence of several novel NGF-responsive CNS neurons. *The Journal of Neuroscience* **15**, 1567–1576 (1995).

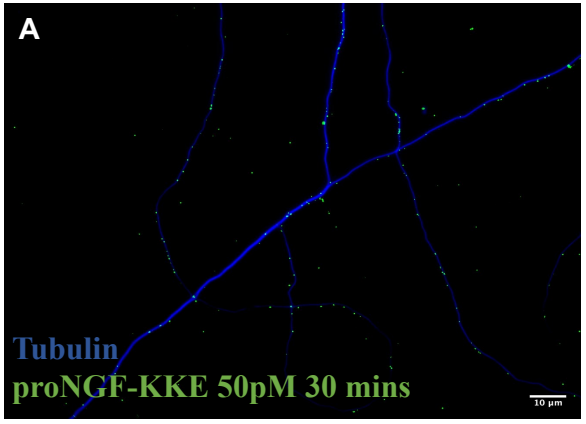
A
Tubulin
proNGF-KKE 50pM 30 mins
10 µm

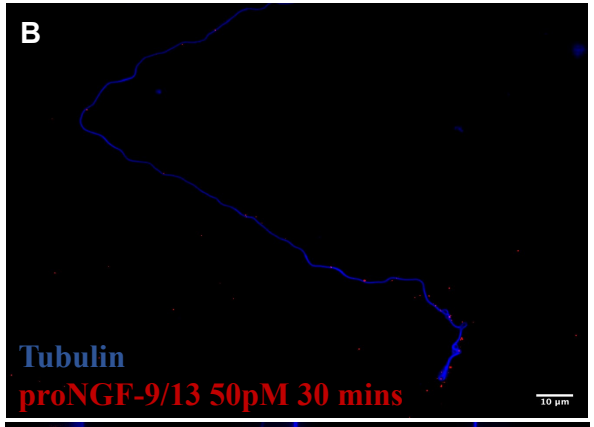
B
Tubulin
proNGF-9/13 50pM 30 mins
10 µm

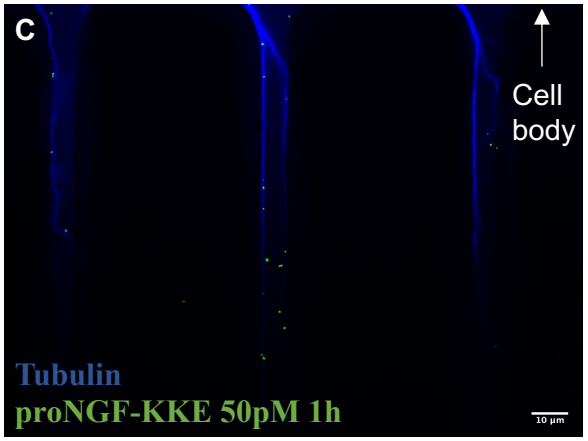
C
Cell body
Tubulin
proNGF-KKE 50pM 1h
10 µm

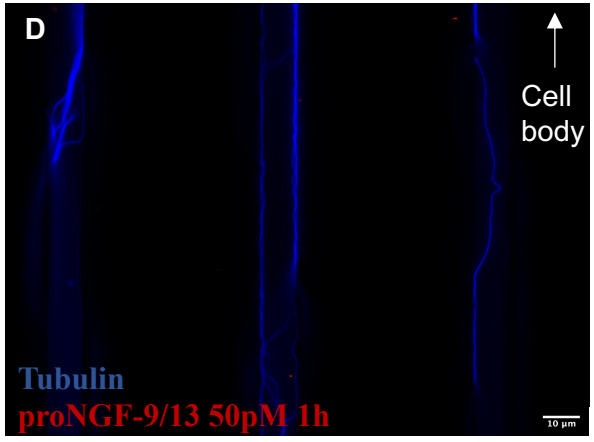
D
Cell body
Tubulin
proNGF-9/13 50pM 1h
10 µm

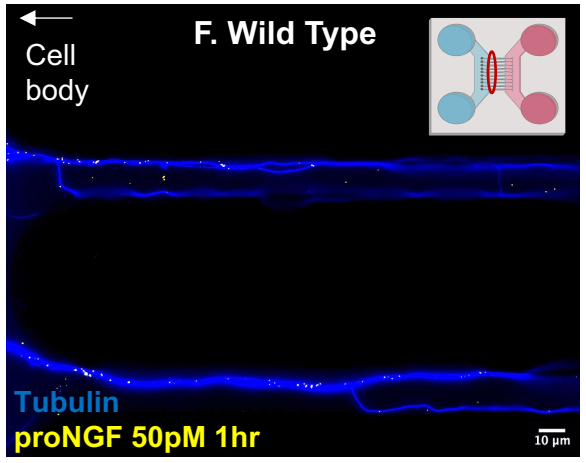
Cell body
F. Wild Type
Tubulin
proNGF 50pM 1hr
10 µm

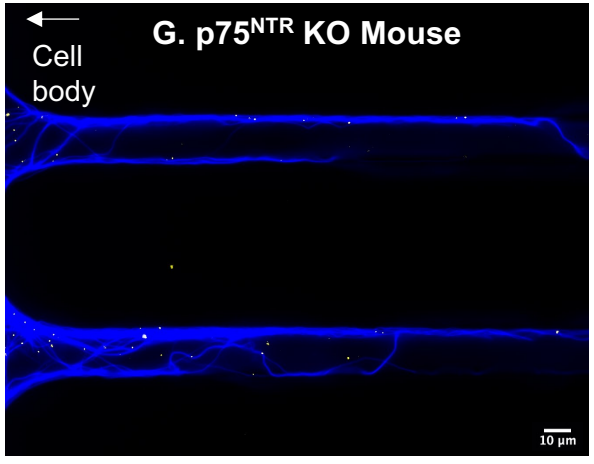
Cell body
G. p75NTR KO Mouse
10 µm

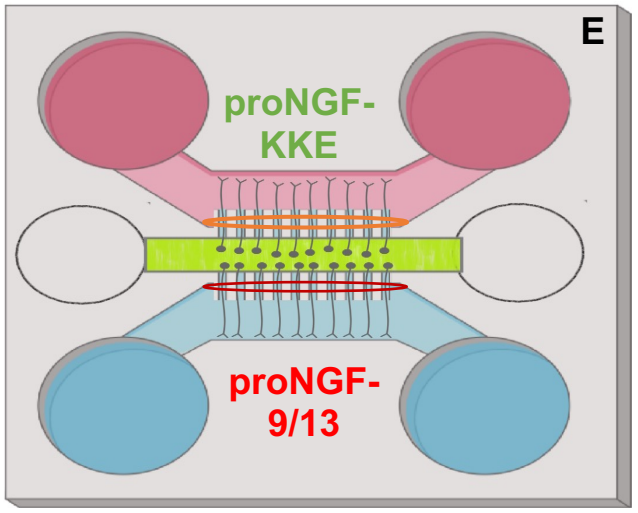
E
proNGF-KKE
proNGF-9/13

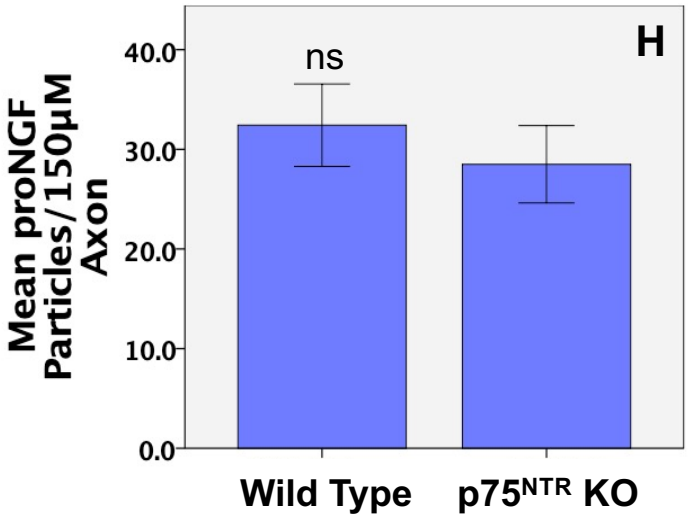
H
Mean proNGF Particles/150µM Axon
40.0
30.0
20.0
10.0
0.0
ns
Wild Type
p75NTR KO

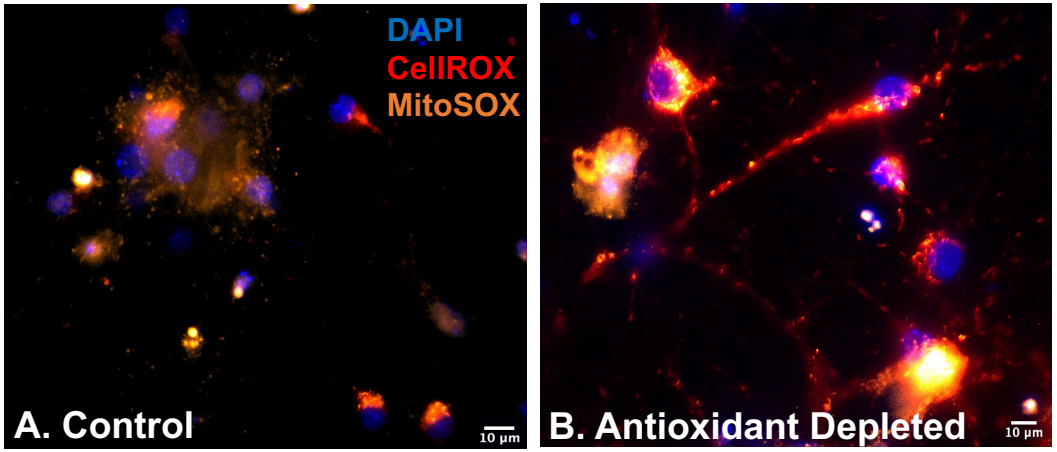
DAPI
CellROX
MitoSOX
A. Control
10 µm
B. Antioxidant Depleted
10 µm

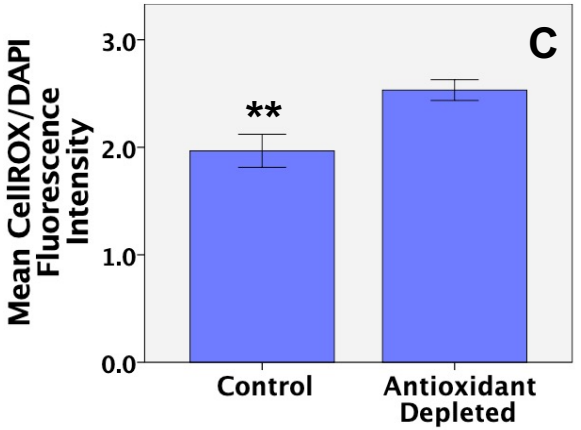
C
Mean CellROX/DAPI Fluorescence Intensity
3.0
2.0
1.0
0.0
**
Control
Antioxidant Depleted

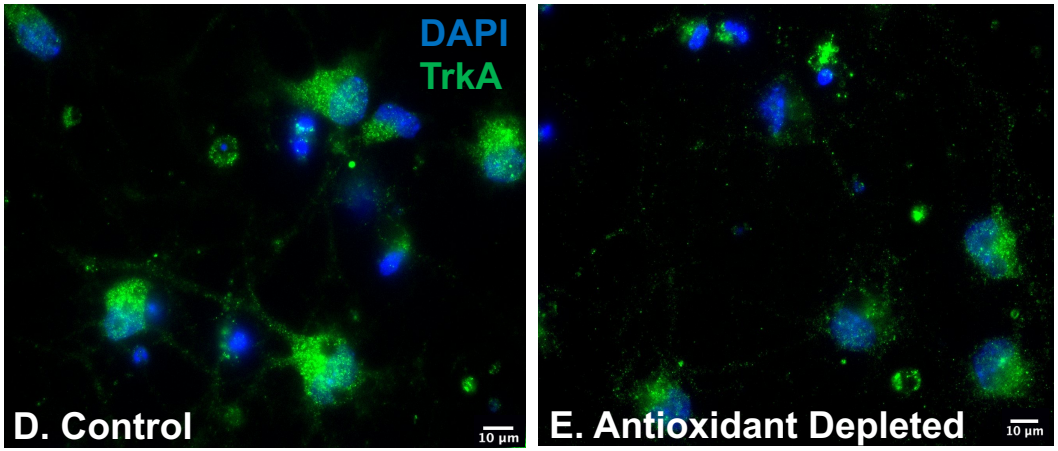
DAPI
TrkA
D. Control
10 µm
E. Antioxidant Depleted
10 µm

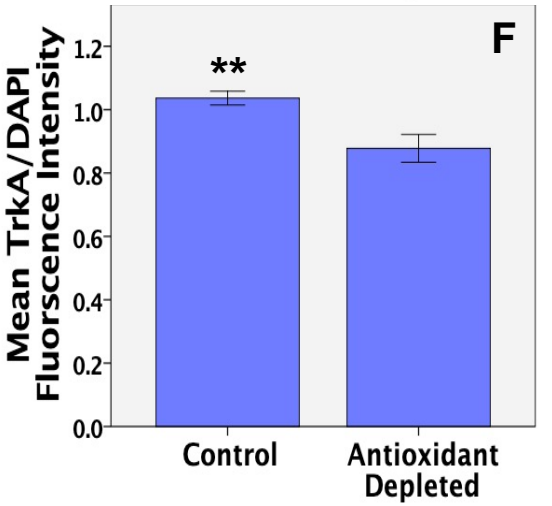
F
Mean TrkA/DAPI Fluorscence Intensity
1.2
1.0
0.8
0.6
0.4
0.2
0.0
**
Control
Antioxidant Depleted

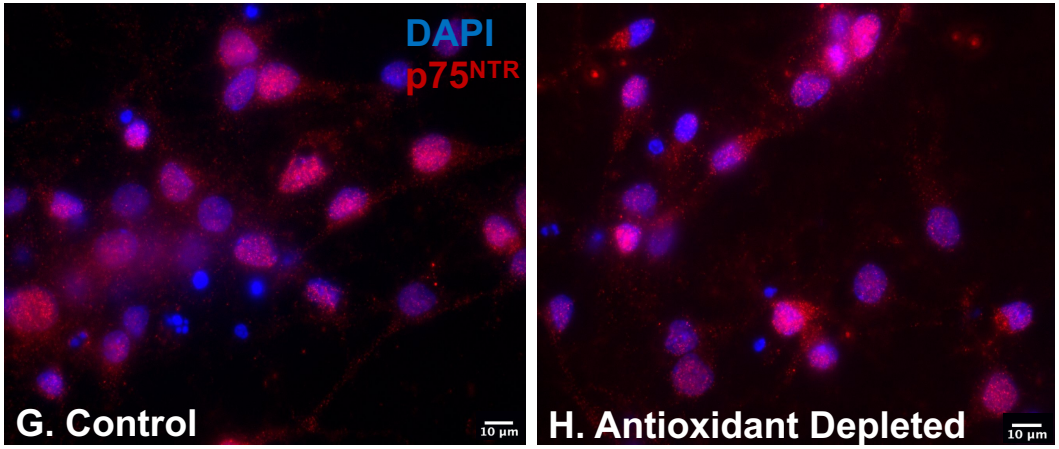
DAPI
p75NTR
G. Control
10 µm
H. Antioxidant Depleted
10 µm

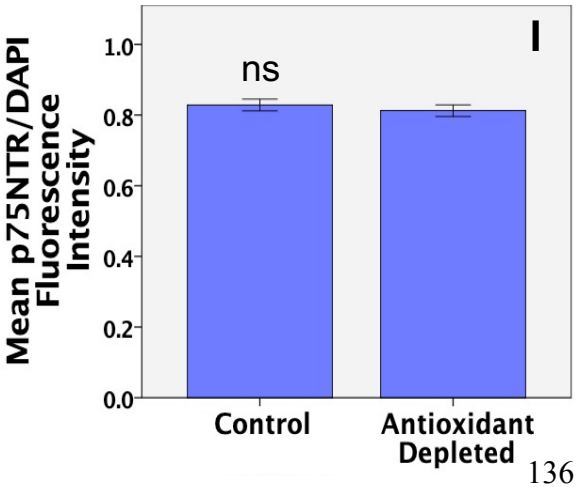
I
Mean p75NTR/DAPI Fluorescence Intensity
1.0
0.8
0.6
0.4
0.2
0.0
ns
Control
Antioxidant Depleted

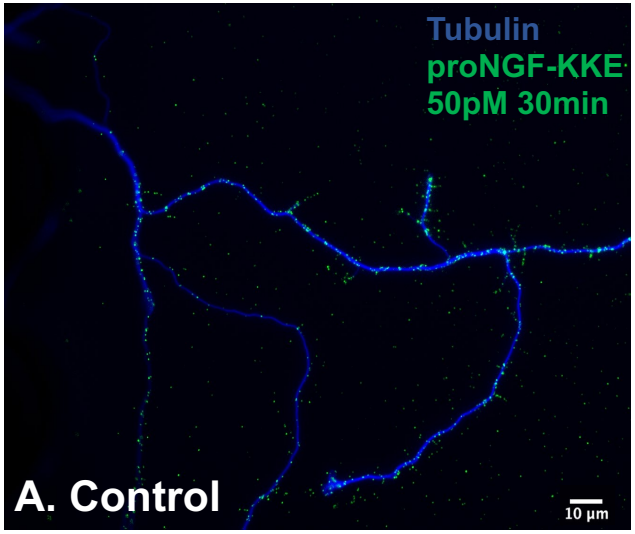
Tubulin
proNGF-KKE
50pM 30min
A. Control
10 µm

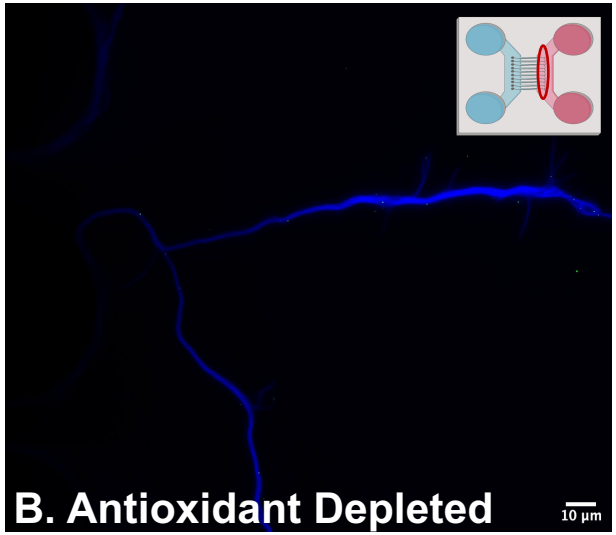
B. Antioxidant Depleted
10 µm

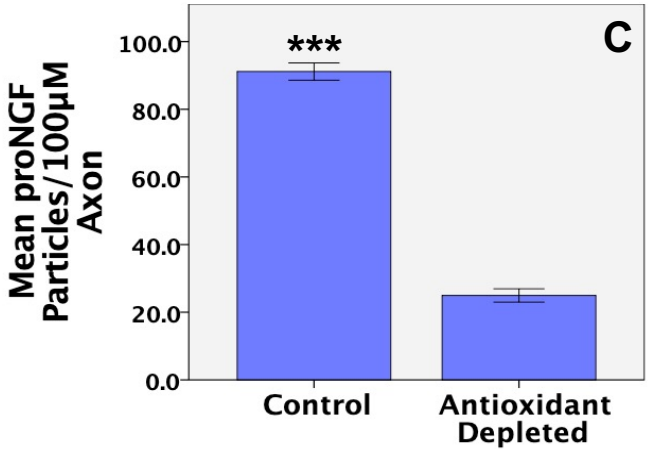
C
Mean proNGF Particles/100µM Axon
100.0
80.0
60.0
40.0
20.0
0.0
***
Control
Antioxidant Depleted

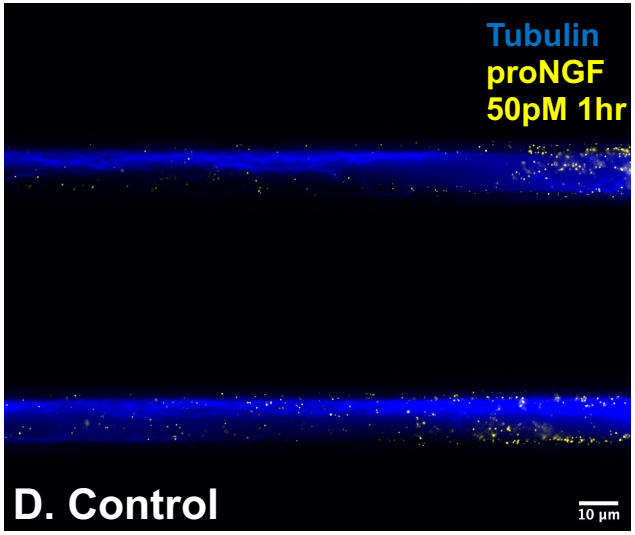
Tubulin
proNGF
50pM 1hr
D. Control
10 µm

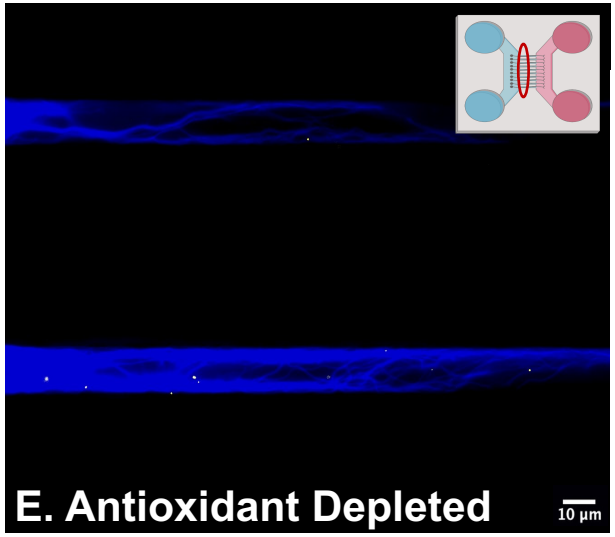
E. Antioxidant Depleted
10 µm

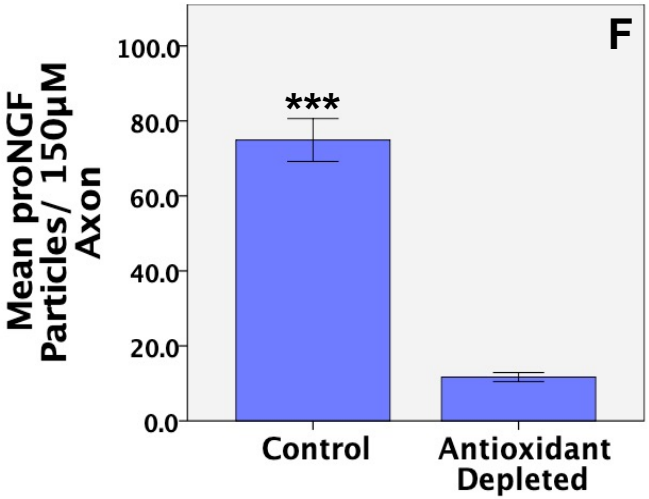
F
Mean proNGF Particles/ 150µM Axon
100.0
80.0
60.0
40.0
20.0
0.0
***
Control
Antioxidant Depleted

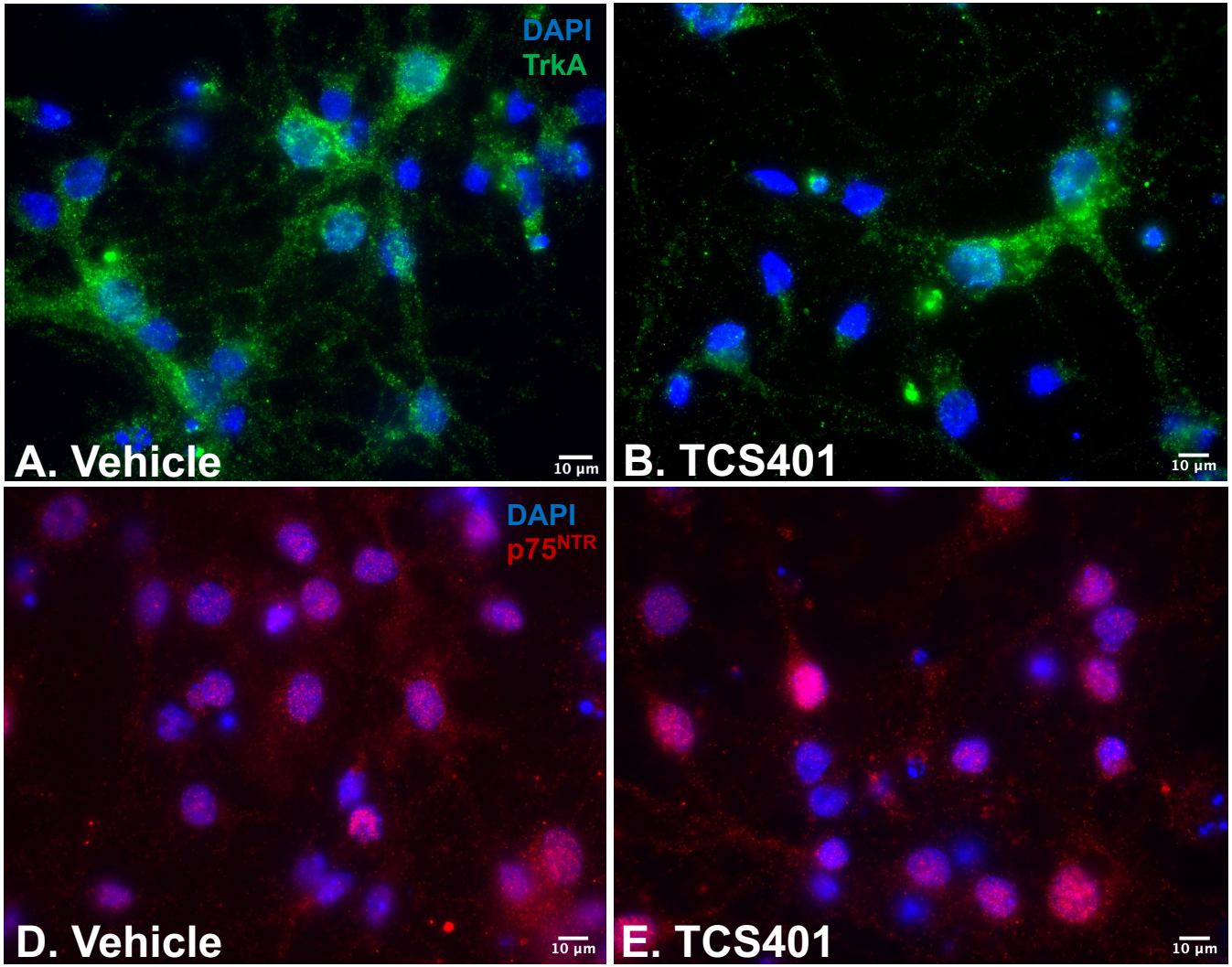
DAPI
TrkA
A. Vehicle
10 µm
B. TCS401
10 µm
DAPI
p75NTR
D. Vehicle
10 µm
E. TCS401
10 µm

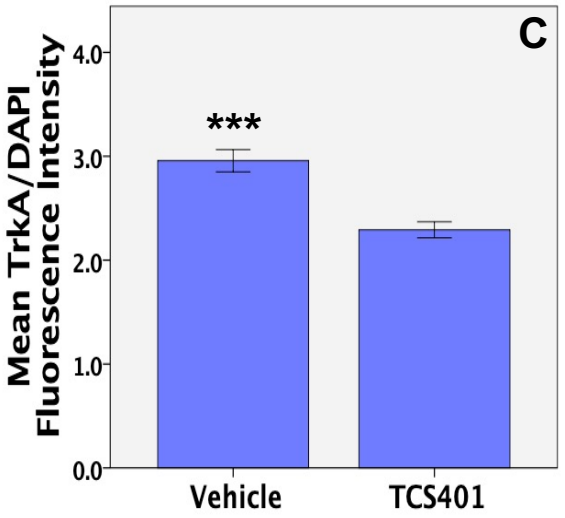
C
Mean TrkA/DAPI Fluorescence Intensity
4.0
3.0
2.0
1.0
0.0
***
Vehicle
TCS401

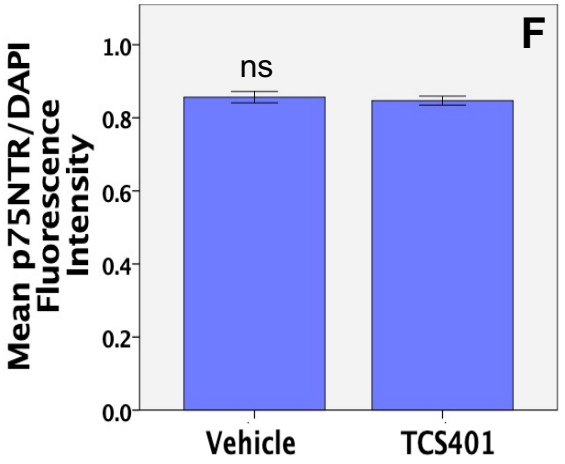
F
Mean p75NTR/DAPI Fluorescence Intensity
1.0
0.8
0.6
0.4
0.2
0.0
ns
Vehicle
TCS401

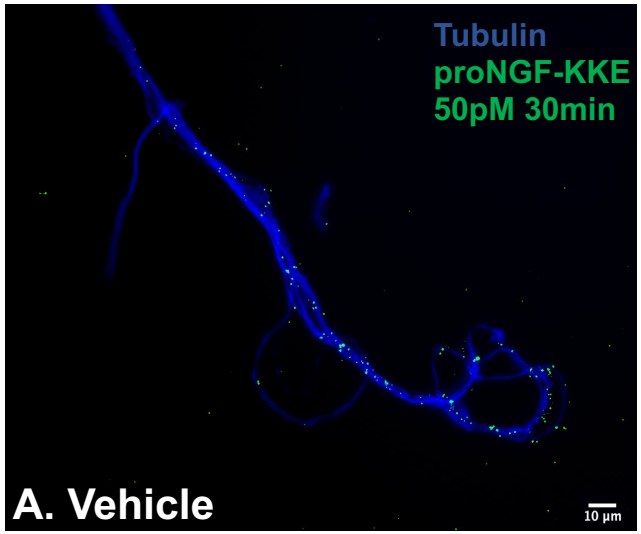
Tubulin
proNGF-KKE
50pM 30min
A. Vehicle
10 µm

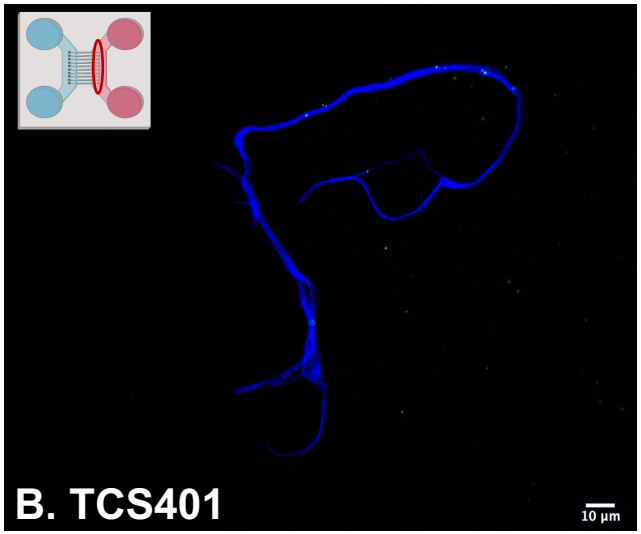
B. TCS401
10 µm

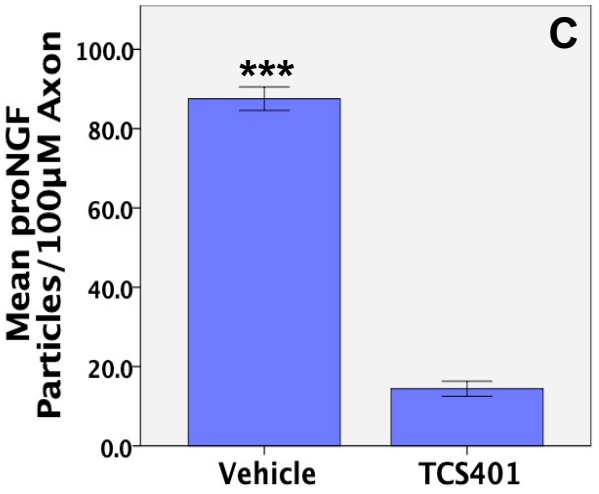
C
Mean proNGF Particles/100µM Axon
100.0
80.0
60.0
40.0
20.0
0.0
***
Vehicle
TCS401

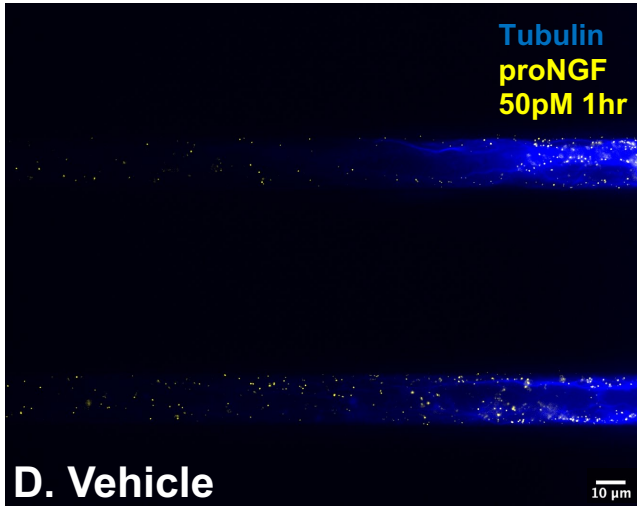
Tubulin
proNGF
50pM 1hr
D. Vehicle
10 µm

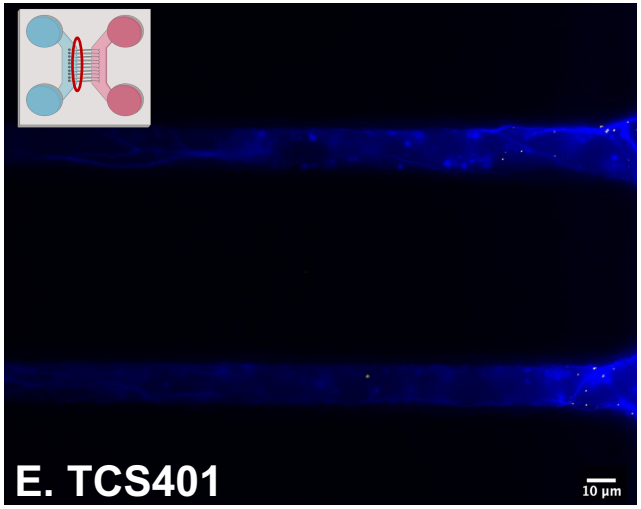
E. TCS401
10 µm

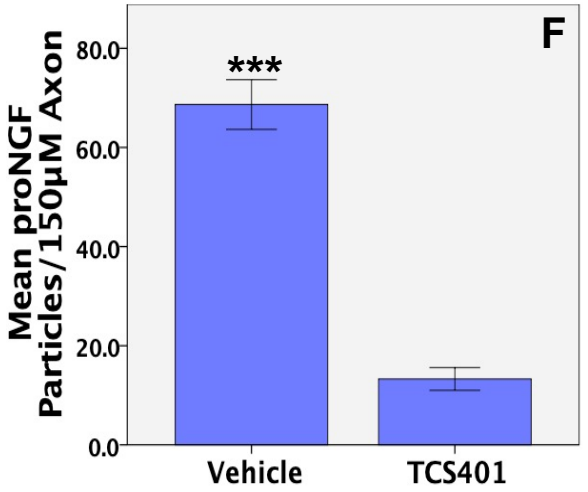
F
Mean proNGF Particles/150µM Axon
80.0
60.0
40.0
20.0
0.0
***
Vehicle
TCS401

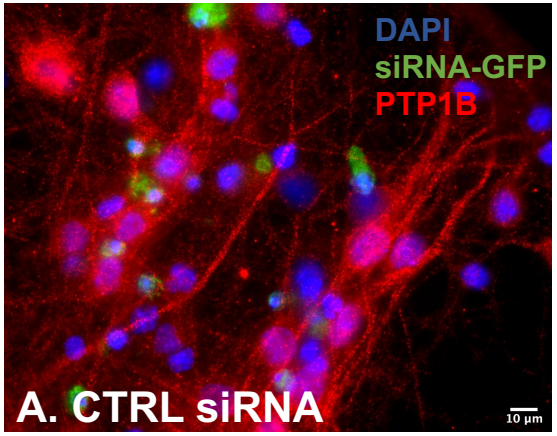
DAPI
siRNA-GFP
PTP1B
A. CTRL siRNA
10 µm

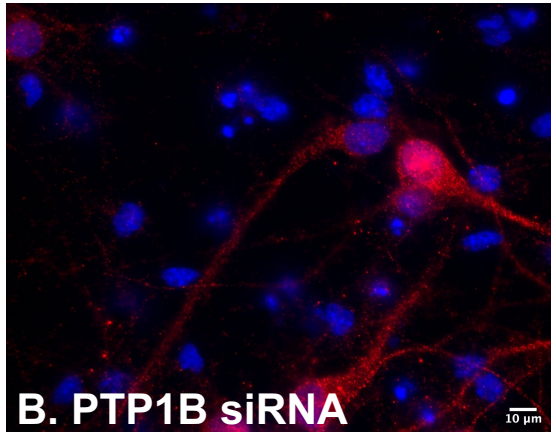
B. PTP1B siRNA
10 µm

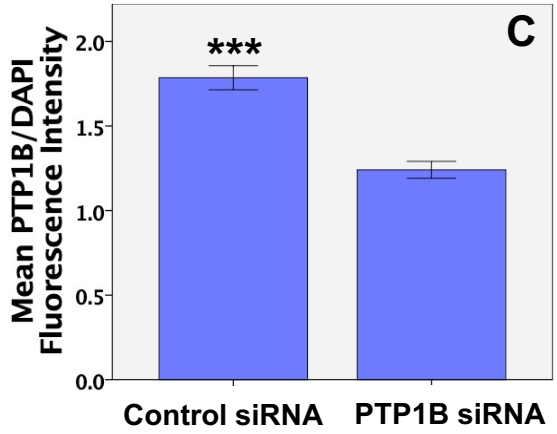
C
***
Mean PTP1B/DAPI Fluorescence Intensity
2.0
1.5
1.0
0.5
0.0
Control siRNA
PTP1B siRNA

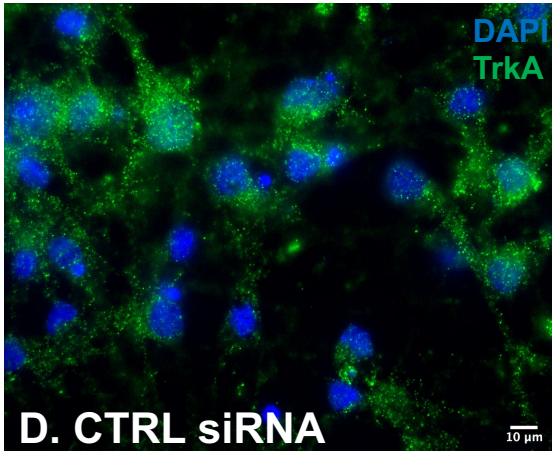
DAPI
TrkA
D. CTRL siRNA
10 µm

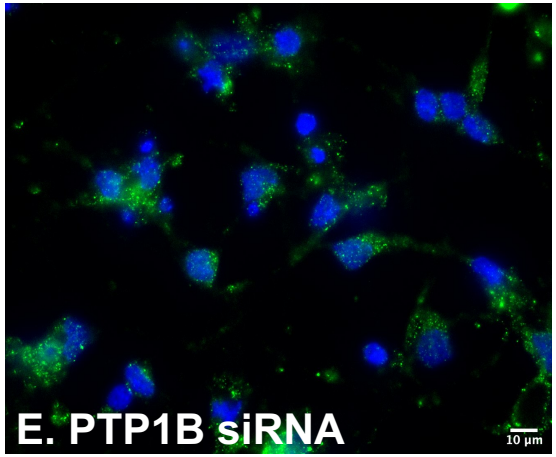
E. PTP1B siRNA
10 µm

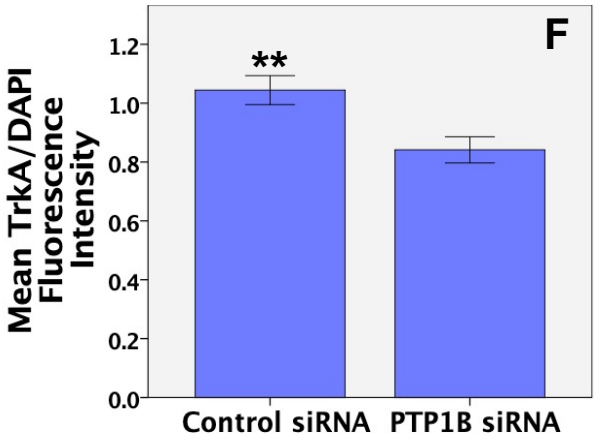
F
**
Mean TrkA/DAPI Fluorescence Intensity
1.2
1.0
0.8
0.6
0.4
0.2
0.0
Control siRNA
PTP1B siRNA

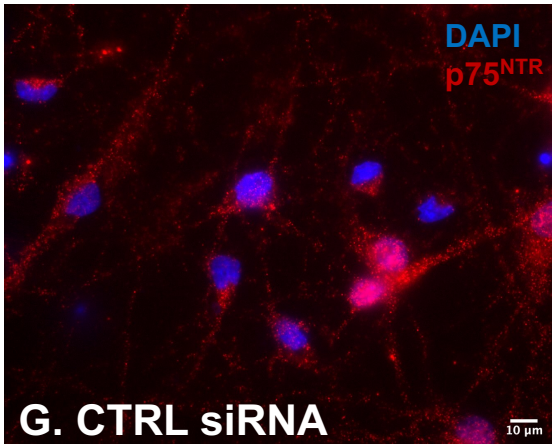
DAPI
p75NTR
G. CTRL siRNA
10 µm

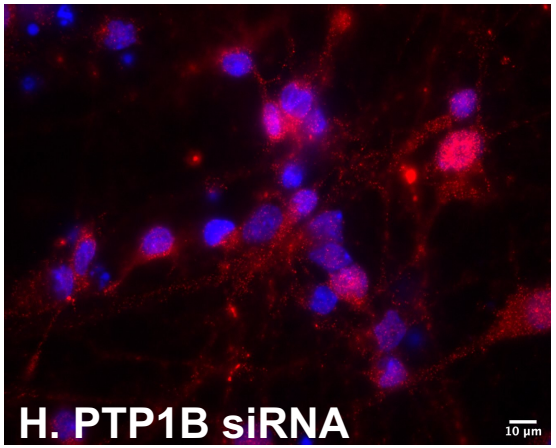
H. PTP1B siRNA
10 µm

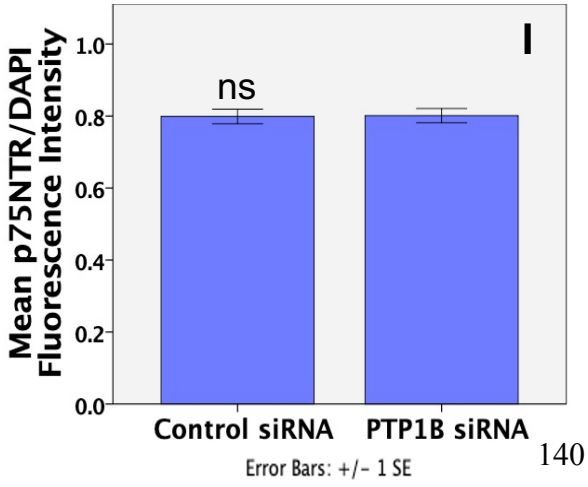
I
ns
Mean p75NTR/DAPI Fluorescence Intensity
1.0
0.8
0.6
0.4
0.2
0.0
Control siRNA
PTP1B siRNA
Error Bars: +/- 1 SE

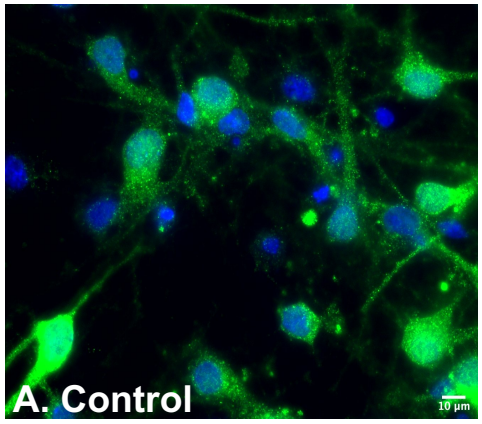
A. Control
10 µm

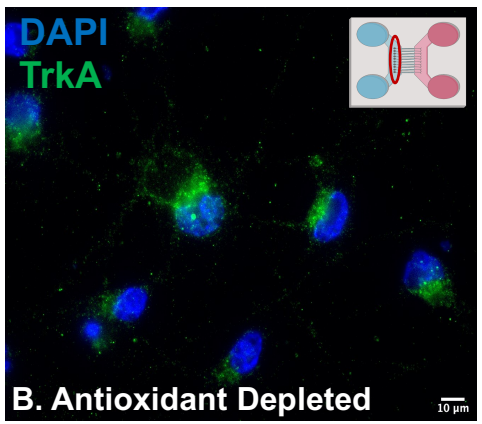
DAPI
TrkA
B. Antioxidant Depleted
10 µm

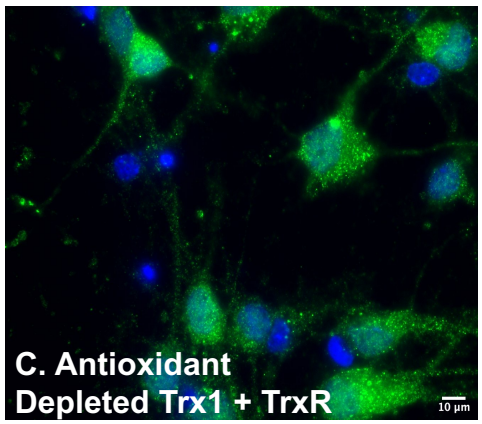
C. Antioxidant
Depleted Trx1 + TrxR
10 µm

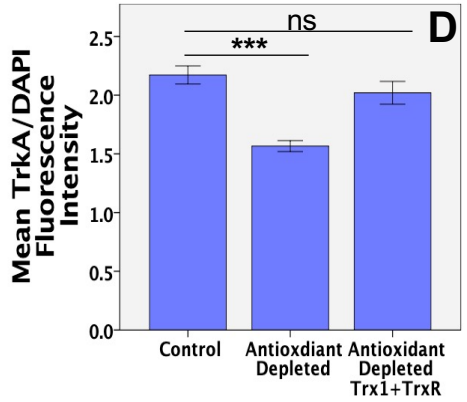
D
ns
***
Mean TrkA/DAPI Fluorescence Intensity
2.5
2.0
1.5
1.0
0.5
0.0
Control
Antioxdiant Depleted
Antioxidant Depleted Trx1+TrxR

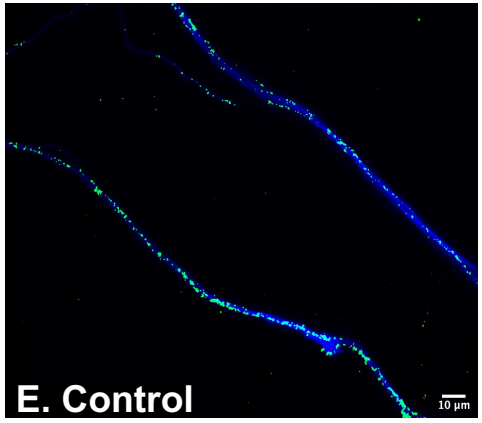
E. Control
10 µm

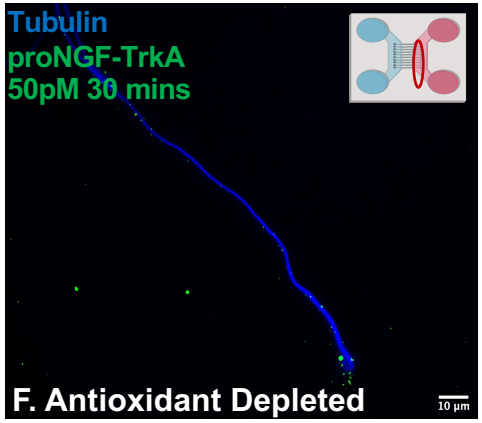
Tubulin
proNGF-TrkA
50pM 30 mins
F. Antioxidant Depleted
10 µm

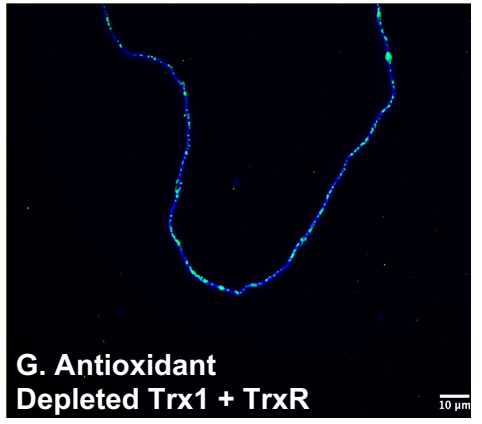
G. Antioxidant
Depleted Trx1 + TrxR
10 µm

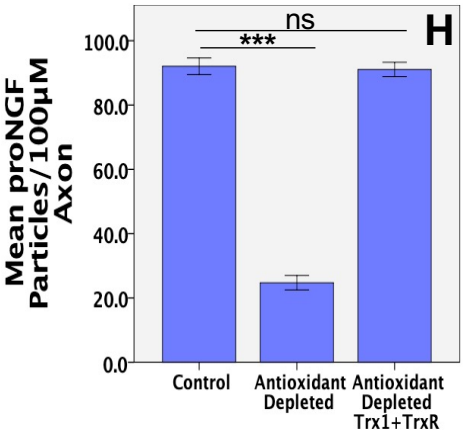
H
ns
***
Mean proNGF Particles/100µM Axon
100.0
80.0
60.0
40.0
20.0
0.0
Control
Antioxidant Depleted
Antioxidant Depleted Trx1+TrxR

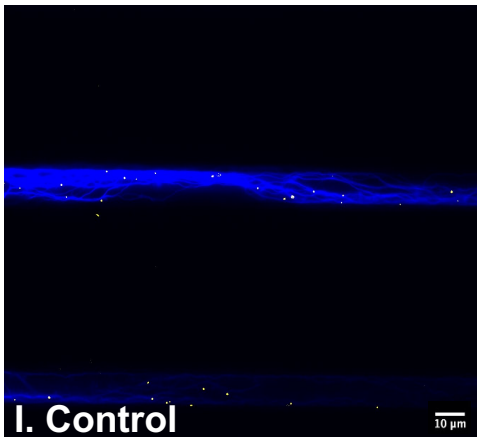
I. Control
10 µm

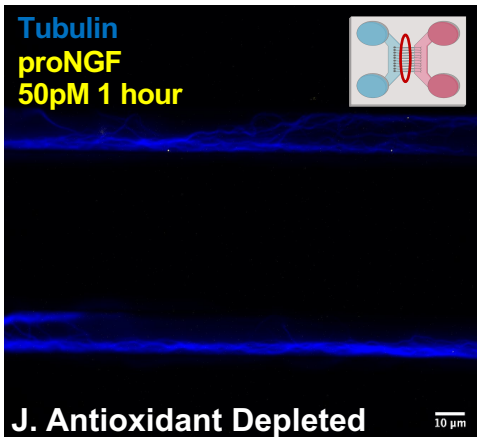
Tubulin
proNGF
50pM 1 hour
J. Antioxidant Depleted
10 µm

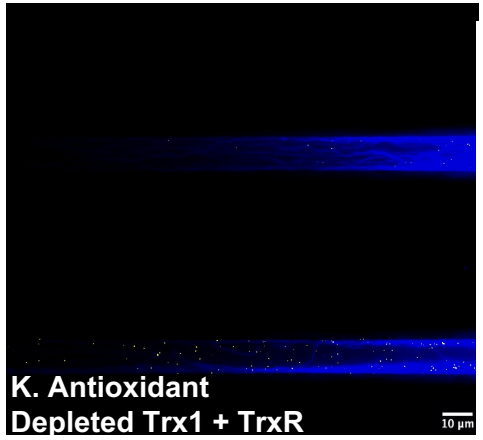
K. Antioxidant
Depleted Trx1 + TrxR
10 µm

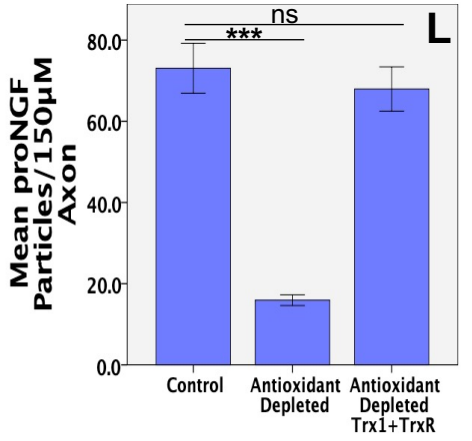
L
ns
***
Mean proNGF Particles/150µM Axon
80.0
60.0
40.0
20.0
0.0
Control
Antioxidant Depleted
Antioxidant Depleted Trx1+TrxR

1 Hour Post proNGF Axonal Administration

Antioxidant Depleted Medium

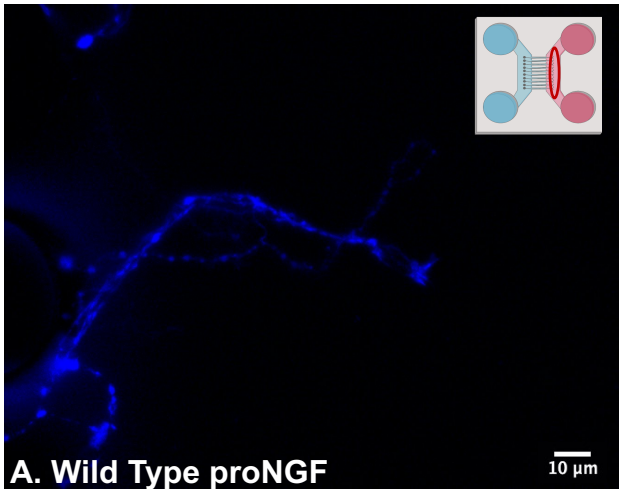

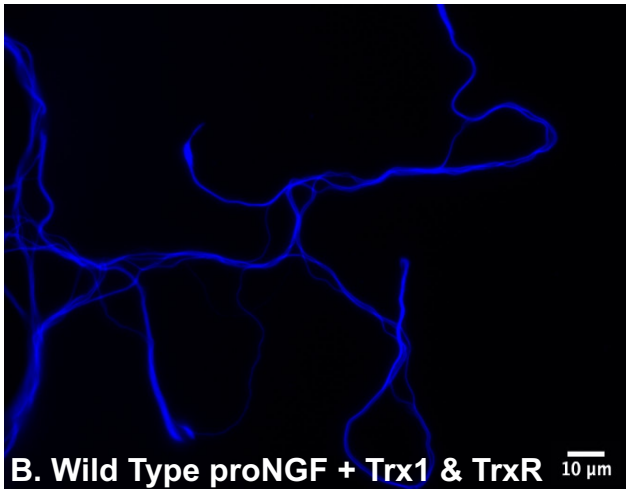

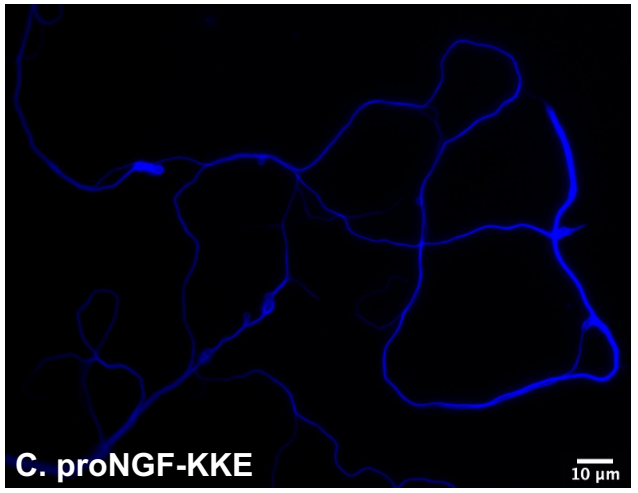

Control Medium

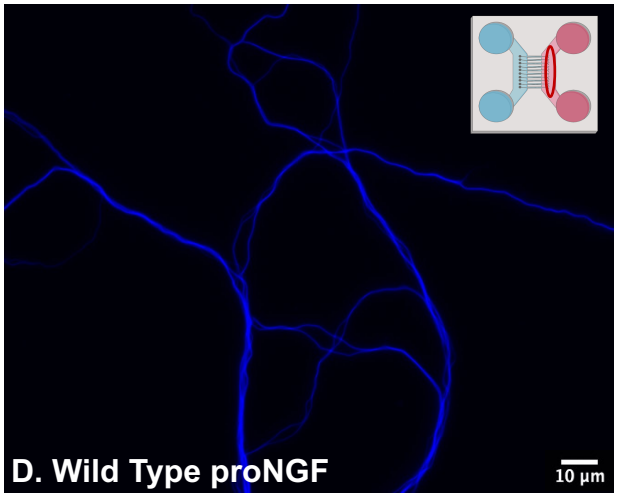

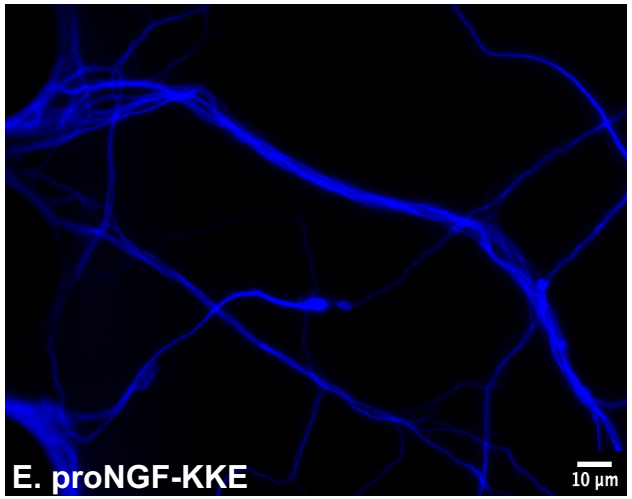

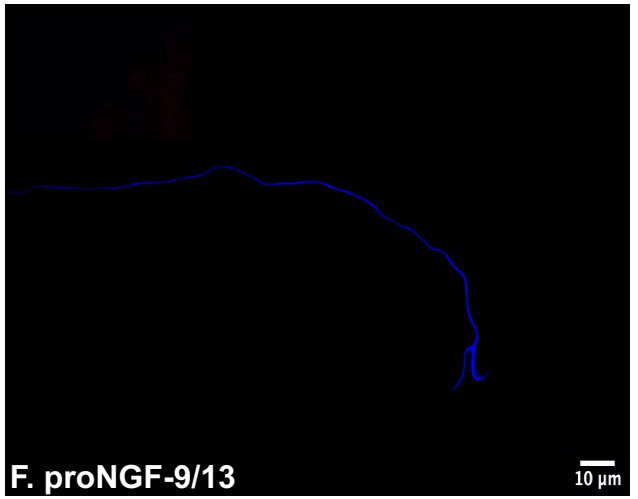

6. Discussion and Future Directions

6.1 Empirical Summary and Implications

This work clearly demonstrates that neurotrophin transport in BFCNs is impaired in an age-dependent manner and that this impairment is mediated by the selective loss of Trk receptors. This work also suggests that mechanisms relating to oxidative stress, an established contributor to age-related neurodegeneration, contribute to these transport deficits (Tramutola et al., 2017). Specifically, this work determined that oxidative stress specifically downregulates TrkA, and that this downregulation is mediated by the inactivation of the phosphatase PTP1B. Key insights and contributions of each chapter of this thesis are outlined below.

Chapters 2 and 3 laid the groundwork for the study of axonal transport in BFCNs using microfluidic culture techniques. The work done in these chapters details the first ever observations of real time axonal transport in BFCNs. We determined the conditions required for proNGF and BDNF transport and demonstrated that the transport of both neurotrophins was reduced following aging *in vitro*. We also validated our use of *in vitro* aging as a model of age-related neurodegeneration by demonstrating the presence of the canonical aging marker, senescence associated ß-galactosidase, in neurons aged *in vitro*. We observed that age-related transport deficits in BFCNs are concomitant with the loss of Trk receptors, but not $p75^{NTR}$. Interestingly, we also observed that age-related deficits in neurotrophin transport are absent in cortical neurons, suggesting a selective vulnerability of BFCNs to age-related neurotrophin transport impairment. These findings led us to surmise that the unique reliance of BFCNs on neurotrophin transport, coupled with the age-related loss of this transport, contribute to the selective vulnerability of these neurons in aging and AD. Overall, this work suggests that elucidating the mechanisms behind the breakdown of axonal transport in BFCNs is critical to preventing their degeneration. The foundational observations within this chapter allowed us to leverage the microfluidic culture system to explore the mechanistic underpinnings of BFCN axonal transport deficits in the following chapters.

Chapter 4 aimed to determine the mechanistic contributions of Rab proteins, master regulators of membrane trafficking, to the neurotrophin transport impairments observed in the previous chapter. The preliminary work described in this chapter was the first ever investigation into the Rab identity of the proNGF signaling complex. These experiments suggest that the retrograde transport of proNGF relies on the conversion of Rab5 to Rab7. Rab5 to Rab7 conversion is dependent on the presence/binding of TrkA, suggesting that TrkA mediates this conversion and subsequently the retrograde transport of proNGF. These results, while preliminary, represent a critical first step in determining the mechanism underlying longstanding observations of Rab5 overexpression in the AD basal forebrain (Nixon, 2017).

This chapter also explored neurotrophin transport in neurons derived from 3xTg-AD mice, a commonly used animal model of AD, to determine the effect of classic AD pathological hallmarks on neurotrophin transport in BFCNs. A striking impairment in

axonal outgrowth was observed in 3xTg-AD neurons, suggesting that the expression of amyloid and tau transgenes has developmental consequences. We also observed both BDNF and proNGF transport impairments in these neurons. These impairments were exacerbated with respect to what was observed in aged wild type neurons in Chapter 3, suggesting that amyloid and tau transgene expression exacerbates neurotrophin transport impairment in BFCNs. These findings are in line with existing reports of increased neurotrophin levels within BFCN target fields of 3xTg-AD mice (Perez et al., 2011). Interestingly, reduction of oxidative stress via nitric oxide synthase inhibition partially rescued proNGF, but not BDNF, transport deficits. Moreover, proNGF, unlike BDNF, was not taken up by 3xTg-AD neurons under baseline conditions. Taken together, these results suggest that oxidative stress impairs proNGF trafficking by impairing the anterograde trafficking of TrkA to the axon terminal. This topic is explored at length in the final chapter, Chapter 5. The observations described in Chapter 4 require additional experiments to validate which are discussed in the Future Directions section.

Chapter 5 represents an extension of the previous chapter by establishing that oxidative stress reduces TrkA and proNGF retrograde transport via the oxidative inactivation of PTP1B. The results in this chapter were the first description of a mechanism contributing to TrkA loss in the AD basal forebrain. We also established that both the transport and function of proNGF are contingent upon TrkA. These results add to an existing body of evidence demonstrating that the activity of proNGF is largely contingent on the presence of TrkA, further refuting the existing zeitgeist surrounding proNGF as that of a purely apoptotic molecule (Fahnestock, Yu, & Coughlin, 2004; Fahnestock & Shekari, 2019; R. Lee et al., 2001; Masoudi et al., 2009). Overall, our findings suggest that a promising therapeutic avenue to pursue to prevent AD-related BFCN degeneration could involve a two-pronged approach targeting oxidative stress reduction and $p75^{NTR}$ antagonism. Additional considerations and limitations regarding this collective body of work are discussed below.

6.2 Limitations and Future Directions

The goal of this work was to understand how and why BFCNs degenerate in the aging and AD brain. However, it is important to keep in mind that embryonic tissue was used in all the experiments outlined above. The use of embryonic tissue to study diseases of aging, while not ideal, is necessary when studying neurons due to the great difficulty involved in culturing neurons from adult animals (Moutin et al., 2020). This limitation was partially addressed in Chapter 3 by utilizing an *in vitro* aging model. This model served as an invaluable tool and allowed the investigation of age-related changes in cultured neurons. It was instrumental to the success of the foundational experiments outlined in Chapters 3 and 4. With a foundation now set, consideration must be given to improving the external validity of this model with respect to studying age-related neurodegeneration.

Transitioning from the use of murine embryonic primary neurons to human induced human pluripotent stem cells (iPSCs) and direct-induced neurons (iNs) represents a promising avenue to pursue to increase the translatability of this work to diseases of

aging in humans. Techniques relating to the differentiation of iPSCs to specific neuronal lineages have advanced greatly in the past decade (Chang et al., 2020). These advances have made the *in vitro* study of human neurons not only possible, but relatively straightforward (Chang et al., 2020; Mertens et al., 2018). Protocols have also been established for the differentiation and maintenance of iPSCs in microfluidic culture (Kane et al., 2019). However, up until very recently, the differentiation of iPSCs to TrkA-expressing cholinergic neurons was technically challenging and involved using non-adherent (floating) cultures that are incompatible with microfluidic culture (Bissonnette et al., 2011). Thankfully, protocols outlining the differentiation of iPSCs to adherent BFCNs have become available in the past year (Muñoz et al., 2020). These protocols do not involve nucleofection-based cell sorting and other technically challenging techniques that were previously required to achieve BFCN differentiation (Bissonnette et al., 2011; Muñoz et al., 2020). These techniques allow for the generation of a highly pure, differentiated neuronal population that produces acetylcholine and expresses all relevant markers of BFCN lineage, including VAChT, ChAT, and TrkA at both the RNA and protein level (Muñoz et al., 2020). Transitioning from using murine embryonic primary neurons to fully differentiated human neurons is critical for determining the applicability of our findings to diseases of aging in humans.

While the microfluidic culture of iPSC-derived BFCNs is now achievable, the embryonic reprogramming required to generate iPSCs poses a challenge to their use in studying diseases of aging. Inducing pluripotency of human somatic cells via overexpression of Yamanaka transcription factors OCT4, KLF4, SOX2, and C-MYC triggers a developmental reset that reverts cells back to an embryonic-like state (Mertens et al., 2018; Studer et al., 2015). This embryonic reversion, while instrumental in the ability to differentiate these cells to any desired lineage, is problematic when studying diseases of aging, as embryonic reversion has been shown to rejuvenate cells at the level of epigenetic modification, mitochondrial function, and telomere length, key indicators of cellular aging (Frobel et al., 2014; Lapasset et al., 2011; Lo Sardo et al., 2017; Marion et al., 2009; Ocampo et al., 2016).

This problem can be mitigated by using iNs, neurons that are derived from the direct reprogramming of terminally differentiated cells without reversion to the pluripotent stage (Graf & Enver, 2009; Mertens et al., 2018). Direct reprogramming, a relatively new and ground-breaking technique in the field of *in vitro* science, involves forcing lineage transition in differentiated cells via the overexpression of specific genes and micro RNAs (miRNA) (Graf & Enver, 2009). The overexpression of transcription factors BRN2, ASCL1, and MYTL1 (collectively referred to as BAM), along with miR-124 and miR-9 is commonly employed to transform human fibroblasts to neurons without the need for embryonic reversion (Pang et al., 2011; Vierbuchen et al., 2010). While iN technology is extremely promising, current technical considerations limit their utility with respect to this work. Unfortunately, the only known method for obtaining cholinergic neurons from differentiated cells involves the use of neonatal tissue (M.-L. Liu et al., 2013). Additionally, protocols for the generation of iNs in microfluidic culture, cholinergic phenotype notwithstanding, have not been developed. These limitations point

to iPSCs, at least for the time being, as the most promising model to improve the validity of this work with respect to human disease.

Utilizing iPSC-derived BFCNs would allow us to determine if the mechanisms outlined in this work are applicable to humans. Translatability to humans is especially critical when studying AD, as the disorder does not natively occur in rodents – murine Aβ isoforms lack neurotoxicity and are far less prone to aggregation (Esquerda-Canals et al., 2017; Lv et al., 2013; Ueno et al., 2014). The use of human neurons would also allow for the treatment of BFCNs with scFvs-45, a human-specific PTP1B antibody that stabilizes PTP1B in its oxidated, inactivated state (Haque et al., 2011). These experiments would allow us to further validate the role of oxidation mediated PTP1B inactivation in TrkA downregulation and proNGF transport loss in BFCNs. iPSCs also allow for our proposed mechanism to be studied in fully differentiated, mature neurons. This is especially critical to our work, as the role of PTP1B in TrkA trafficking has only been studied in the context of embryonic development (Yamashita et al., 2017).

Without the mention of the canonical benefits of using iPSCs, such as the ability to study tissue derived directly from individuals with AD, iPSC-derived BFCNs already strike a promising balance between technical accessibility and the ability to answer key questions pertaining to the applicability of this work to human disease. While aging is difficult to study using this model due to embryonic rejuvenation, models of cellular aging in iPSC-derived neurons, most of which involve inducing oxidative stress, have recently been developed (Nguyen et al., 2011; Seibler et al., 2011). Until cholinergic neurons, like other neuron types, can be directly transformed from adult somatic cells, iPSC-derived BFCN microfluidic culture represents the most promising avenue to explore the applicability of this work in the context of human aging (Mertens et al., 2018).

The transition to iPSC microfluidic culture, while promising, represents a drastic methodological shift that likely requires significant optimization time. To maximize efficiency, consideration must also be given to experiments within the current model while this transition takes place. The work exploring Rab conversion and pathological changes in 3xTg-AD BFCNs outlined in Chapter 4 is largely preliminary and would benefit the most from additional experiments during the transition.

With respect to Rab conversion, a key limitation of these experiments was the use of epifluorescent microscopy to capture images. These images lack data pertaining to depth and prevent the quantification of colocalization. Conventional colocalization experiments utilize confocal microscopy in order to gather data in the z-axis in addition to the standard x and y plane to ensure true colocalization (Dunn et al., 2011). Thankfully, the immunocytochemical techniques outlined in Chapter 4 are fully compatible with confocal microscopy. The Rab conversion experiments outlined in Chapter 4 can be easily repeated using confocal microscopy to ensure the validity of our preliminary results.

Another limitation of the Rab conversion experiments lies in the use of fixed neurons. Reports of the sequential recruitment of both Rab5 and Rab7 GEFs to the NGF signaling endosome coupled with the controversial observations surrounding its Rab identity suggest that Rab conversion is a highly dynamic and temporally graded process (Harrington & Ginty, 2013; H. Horiuchi et al., 1997; Marlin & Li, 2015; Rink et al.,

2005). The analysis of fixed neurons may not be the most productive approach given the potentially dynamic nature of Rab conversion in BFCNs. Visualization of Rab proteins in live cells in conjunction with QD-labelled proNGF would allow for the Rab identity of proNGF particles to be assessed in real time over the duration of transport. This can be achieved via baculoviral transfection of BFCNs with DNA coding for Rab5 and Rab7 GFP/RFP fusion constructs (available from ThermoFisher Scientific). As a proof of concept, BFCNs have been successfully transfected with Rab5a-GFP (Supplementary Figure 1). Co-transfection of Rab5 and Rab7 fluorescent constructs has been successfully used to observe Rab conversion using live cells *in vitro* (Rink et al., 2005). The analysis of Rab5 to Rab7 conversion in live cells using these fluorescent constructs is critical to our understanding of the potential role Rab conversion plays in proNGF transport in BFCNs.

Rab5 and Rab7 are among the most highly expressed and thus most widely studied members of the Rab superfamily (Mignogna & D'Adamo, 2018; Stenmark, 2009; Wandinger-Ness & Zerial, 2014). However, the contribution of other, lesser known, Rab proteins in the context of proNGF retrograde transport should not be ignored. Another promising Rab target in this context is Rab22. Rab22 is a member of the Rab5 subfamily and, like Rab5, plays a role in mediating endocytosis (Marlin & Li, 2015; Pereira-Leal & Seabra, 2000). Along with Rab5, Rab22 has been found to associate with NGF-TrkA signaling endosomes (L. Wang et al., 2011). However, unlike Rab5, Rab22 does not promote the activation of Rab7 (Magadán et al., 2006). Instead, Rab22 mediates the sorting of endocytic cargoes into recycling endosomes, organelles responsible for the delivery of endocytosed cargoes back to cell membrane (Goody et al., 2005; Magadán et al., 2006; Weigert et al., 2004). The differential recruitment of Rab22 and Rab5 to proNGF signaling complexes may contribute to the stalling of proNGF particles within axonal projections due to the inability of Rab22 to trigger Rab conversion. However, the role of Rab22 in neurotrophin trafficking has only been studied in cell lines. Repeating the Rab colocalization experiments outlined in Chapter 4 using commercially available Rab22 antibodies represents an exciting avenue to explore its function in the context of proNGF trafficking in the CNS.

Another promising Rab protein that may play a role in proNGF trafficking is Rab11. Rab11 has been observed to co-localize with TrkA-positive endosomes (Harrington et al., 2011). The recruitment of Rab11 to these endosomes is critical for the delivery of newly synthesized TrkA receptors to the axonal membrane (Ascaño et al., 2009). Rab11 functions mainly as a mediator of anterograde transport and recruits kinesin-family proteins to membrane-bound cargoes (Schonteich et al., 2008; G. C. Simon & Prekeris, 2008). However, Rab11 can also recruit the dynein motor protein to the cargoes with which it associates (Horgan et al., 2010a, 2010b). The ability of Rab11 to recruit both anterograde and retrograde-directed motors suggests it plays a key role in determining the directionality of proNGF transport. However, the role of Rab11 in mediating proNGF transport is currently unknown. The experiments in Chapter 3 can be easily repeated using commercially available Rab11 antibodies to determine if Rab11 colocalizes with proNGF-QD particles.

Chapter 4 also included experiments observing proNGF transport impairments in BFCNs derived from 3xTg-AD mice. This work was preliminary and would benefit from additional experiments to validate our conclusions. While we observed that oxidative stress reduction improved neurotrophin transport in 3xTg-AD BFCNs, the absolute levels of oxidative stress in these neurons was not quantified. Thankfully, protocols for the quantification of oxidative stress in BFCNs have been established since the completion of these experiments and are outlined in Chapter 5. While the levels of lipid peroxidation, a marker of oxidative stress, are increased in the brains of 3xTg-AD mice compared to controls, reports of ROS load in neurons derived from 3xTg-AD mice are absent from the literature (Resende et al., 2008). Experiments quantifying ROS levels in these neurons and comparing them to wild type levels is critical to supporting the notion that increased oxidative stress underlies the neurotrophin transport deficits we observe in 3xTg-AD mice.

The experiments in Chapter 4 involving the manipulation of oxidative stress using L-NAME suggest that impaired anterograde TrkA trafficking contributes to the impairment of proNGF retrograde transport. However, no assays that directly manipulate or measure TrkA were completed. Repeating the proNGF-KKE uptake experiments outlined in Chapter 5 would allow us to confirm that axonal TrkA trafficking is impaired in 3xTg-AD BFCNs. Determining proNGF-KKE uptake following L-NAME administration would similarly allow us to determine if the partial rescue of proNGF transport that we observed was indeed due to the increased anterograde trafficking of TrkA to the axon terminal.

Interestingly, the rescue of proNGF retrograde transport via L-NAME may be mediated by the activity of PTP1B. PTP1B was the focus of Chapter 5 where a deliberate switch was made from targeting nitric oxide using L-NAME to superoxide using antioxidant deprivation. We initially focused on nitric oxide due to the ability of nitrative species to impact amyloid cleavage and secretion, a process that is impaired in 3xTg-AD neurons due to the *APP* and *PSEN1* mutations present in this model (Belfiore et al., 2019; Guix et al., 2012). Correspondence with the lab of Dr. Scott Ryan (University of Guelph, Ontario, Canada) regarding the ability of L-NAME to rescue axonal transport *in vitro* further solidified our focus on nitric oxide (Stykel et al., 2018). However, reports outlining the novel role of PTP1B in TrkA trafficking necessitated the switch to focusing on superoxide, as the inactivation of PTP1B by superoxide is well documented (Haque et al., 2011; Londhe et al., 2020; Salmeen et al., 2003; van Montfort et al., 2003; Yamashita et al., 2017). However, PTP1B can also be inactivated by peroxynitrite, a highly reactive molecule formed in the presence of excess nitrogen radicals (Takakura et al., 1999). This suggests that the reduced nitrative inactivation of PTP1B following L-NAME treatment may contribute to the rescue of proNGF transport. Experiments determining if proNGF retrograde transport can be rescued in 3xTg-AD BFCNs following the administration of PTP1B-reducing enzymes thioredoxin-1 and thioredoxin reductase would help determine the validity of this hypothesis. Determining if the antagonism of PTP1B (as described in Chapter 5) attenuates the rescue of proNGF transport following L-NAME treatment would further shed light on this potential mechanistic link.

While the potential contribution of PTP1B in 3xTg-AD BFCNs is promising, its inactivation is likely not the sole contributor to the rescue of axonal transport following L-NAME treatment. The presence of excess nitrative species triggers the non-specific post translational modification of many proteins and lipids, culminating in widespread cellular damage (Cobb & Cole, 2015). Paramount amongst these in the context of this work is the peroxynitrite-mediated nitration of tyrosine residues. Tyrosine nitration results in the formation of tyrosyl radicals (Radi, 2013). Tyrosyl radicals increase steric hindrance around tyrosine residues and inhibit their ability to be phosphorylated (Radi, 2013). Formation of tyrosyl radicals has been shown to decrease the phosphorylation and downstream signaling of TrkA via PI3K (Ali et al., 2008; Radi, 2013). PI3K activation is required for the internalization of the NGF signaling endosome (Bodmer et al., 2011; Harrington et al., 2011; Kuruvilla et al., 2000; Marlin & Li, 2015). Based on these reports, the increased proNGF uptake we observed following L-NAME treatment may be the result of reduced tyrosine nitration and subsequent increased activation of PI3K by TrkA. Determining if the inhibition of PI3K (using commercially available pharmacological inhibitor HS-173, Sigma Aldrich) attenuates the restorative effect of L-NAME would allow us to confirm the possible contribution of nitration-mediated TrkA signaling failure to proNGF transport deficits in 3xTg-AD BFCNs (Son et al., 2013).

Nitrative stress may also affect proNGF transport by modifying proteins that can interact with TrkA. A promising protein in this context is JNK, a known mediator of axonal transport whose activity is increased following nitrative post-translational modification (Go et al., 1999). JNK activation triggers the dissociation of cargo from Kinesin-1, the motor protein responsible for the anterograde delivery of TrkA to the axon terminal (D. Horiuchi et al., 2007; Tanaka et al., 2016). While the role of JNK in TrkA trafficking specifically has not been explored, based on these reports it is likely that its increased activity reduces TrkA trafficking (and therefore proNGF transport). Interestingly, JNK activation has been shown to increase the retrograde transport of BDNF by $p75^{NTR}$ (Escudero et al., 2019). The potential opposing influence of JNK activation on proNGF and BDNF transport may explain why L-NAME treatment selectively rescues proNGF transport in 3xTg-AD BFCNs. The role of JNK and other potential contributions of nitration to neurotrophin transport impairment are topics of active investigation in our lab.

The neurotrophin transport impairments observed in 3xTg-AD BFCNs are accompanied by a significant impairment in axonal outgrowth. We surmised that these impairments are largely due to the expression of tau-P301L, as this point mutation reduces both the microtubule binding affinity and stabilizing ability of tau (Dayanandan et al., 1999; Hutton et al., 1998). However, experiments assaying and manipulating the microtubule integrity of 3xTg-AD BFCNs were not completed. Thankfully, protocols for the staining and visualization of tubulin in BFCNs cultured in microfluidic chambers have been established since the completion of these experiments and are outlined in Chapter 5. Additionally, microtubule stability can be manipulated pharmacologically *in vitro* using the stabilizing agent epothilone-D and destabilizing agent colchicine (Fanale et al., 2015). Interestingly, treatment with epothilone-D has been shown to improve cognition in both AD and tauopathy mouse models (Barten et al., 2012; Fernandez-Valenzuela et al., 2020).

Determining the effect of epothilone-D treatment on axonal outgrowth and neurotrophin transport in 3xTg-AD BFCNs is critical to determine the contribution of tau-mediated microtubule instability to the impairments we observe. Recapitulating these impairments in wild type BFCNs following colchicine treatment would further support this notion.

It is important to keep in mind that, in addition to proNGF, BDNF transport deficits were also observed in both 3xTg-AD BFCNs and aged wild type BFCNs. However, mechanisms explaining these impairments were not established. BDNF was observed to accumulate in large, stationary aggregates in 3xTg-AD axon projections. In aged wild type BFCNs, BDNF particles were less motile and paused more often. These observations suggest that mechanisms related to the retrograde procession of BDNF via dynein contributes to these deficits. The retrograde procession of dynein is facilitated by its interaction with dynactin. Dynactin is a large, multi-subunit complex that mediates both the movement and cargo binding ability of dynein (J.-J. Liu, 2017). In the absence of dynactin, dynein possesses a low retrograde processivity and often takes lateral steps along the microtubule lattice, resulting in little to no minus-end directed movement (Reck-Peterson et al., 2006; Ross et al., 2006). The binding of dynactin to dynein aligns its microtubule binding domains to the microtubule lattice, greatly enhancing its retrograde processivity (Ayloo et al., 2014; K. Zhang et al., 2017). Based on these reports, impaired dynactin recruitment may contribute to the impaired retrograde movement of BDNF.

Dynactin recruitment is partially mediated by Hook proteins, a small family of proteins characterized by the presence of a highly conserved N-terminal domain with a hook-like structure (Schroeder & Vale, 2016). The binding of Hook proteins to the first light intermediate chain of dynein greatly increases both dynactin binding and retrograde processivity (Olenick et al., 2016; Schroeder & Vale, 2016). Interestingly, the knockdown of the Hook protein Hook1 in primary hippocampal neurons greatly decreases the retrograde processivity of BDNF (Olenick et al., 2019). This transport impairment is cargo-dependent and only affects BDNF, suggesting that dynactin recruitment via Hook1 is critical for BDNF retrograde transport specifically. Interestingly, Hook protein expression is reduced in the AD brain, suggesting it may play a role in the transport deficits we observed (Herrmann et al., 2015). Performing BDNF-Hook1 colocalization experiments (using commercially available Hook1 antibodies, ThermoFisher Scientific) would allow us to determine if reduced Hook1 expression mediates the BDNF retrograde transport impairments observed in Chapters 3 and 4. BDNF-dynactin colocalization experiments should be completed alongside these to confirm that the any transport impairments observed are mediated by the recruitment of dynactin via Hook1. Recapitulating BDNF transport deficits in young BFCNs following Hook1 siRNA knockdown would further support this notion.

Like BDNF, mechanisms underlying the transport impairment of proNGF-9/13 were not explored. In Chapter 5, we observed proNGF-9/13 transport failures that were concomitant with significant axonal degeneration. The ability (or lack thereof) of proNGF to be retrogradely transported exclusively via $p75^{NTR}$ could not be determined due to this degeneration. Understanding the transport dynamics of proNGF-9/13 would further our knowledge of the mechanisms that govern axonal transport in BFCNs.

The axonal degeneration that accompanies $p75^{NTR}$-mediated transport must be attenuated to study the axonal transport of proNGF-9/13. $p75^{NTR}$-mediated apoptotic signaling involves the activation of multiple signaling pathways that converge on the phosphorylation and activation of JNK (Kraemer et al., 2014). JNK activation triggers the activation of multiple apoptosis-triggering substrates including Bag-1L, c-JUN, and BAD, among others (Dhanasekaran & Reddy, 2008). Based on these reports, inhibiting JNK prior to the administration of proNGF-9/13 will likely attenuate its apoptotic ability, allowing the transport of proNGF-9/13 to be assayed. Repeating the proNGF-9/13 transport assays described in Chapter 5 following treatment of BFCNs with the JNK inhibitor CC-401 (a second generation version of the commonly used SP600125 inhibitor that is less toxic *in vitro*, available from Sigma Aldrich) would allow for the receptor dependency of proNGF transport in BFCNs to be further characterized (Q. Wu et al., 2020).

The receptor dependency of proNGF, along with all other aspects of neurotrophin transport outlined in this collective body of work, have only been observed in an *in vitro* context. This focus was chosen due to the largely foundational nature of this work. While many foundational questions still remain, consideration must also be given to validating our findings *in vivo*. The work outlined in Chapter 5 determining the effects of oxidative stress and PTP1B antagonism on proNGF transport would likely benefit the most from validation *in vivo*. A brief overview of promising *in vivo* models and assays in the context of oxidation mediated PTP1B-depdendent TrkA loss are discussed below.

Oxidative stress is often studied *in vivo* through the induction of mitochondrial damage. The most commonly used model of mitochondrial damage is the mitochondrial mutator mouse. These mice accumulate mtDNA mutations at an accelerated rate due to a loss-of-function mutation in the proofreading domain of mitochondrial DNA polymerase γ (Edgar & Trifunovic, 2009). While these mice show significant increases in markers of oxidative stress in many organs, including the brain, they also develop many confounding abnormalities including impaired B-cell function and anemia (Ahlqvist et al., 2012; M. L. Chen et al., 2009). Numerous antioxidant knockout mouse lines have also been generated to study oxidative stress *in vivo*, however most models suffer from complications including lung dysfunction, allergic asthma, and cataracts that interfere with performance on cognitive assays (Hamilton et al., 2012). Alternatively, behavioral models like caloric restriction manipulate ROS *in vivo* by reducing mitochondrial ROS output instead of increasing it. Caloric restriction (CR) involves reducing *ad libitum* caloric intake by 30-40% in the absence of malnutrition (Amigo et al., 2017; Walsh et al., 2014). Mitochondria isolated from CR mice produce significantly less ROS compared to age-matched animals fed *ad libitum* (Desai et al., 1996; Feuers, 1998; Lanza et al., 2012). Calorically restricted animals subsequently develop significantly less oxidative damage in their tissues compared to age-matched controls (Lanza et al., 2012; Trepanowski et al., 2011; Walsh et al., 2014). Reductions in oxidative damage are most consistently observed in the brain compared to other organs (Walsh et al., 2014). CR has also been shown to be protective against both age-related cognitive decline and AD-related neurodegeneration (Means et al., 1993; Patel et al., 2005; J. Wang et al., 2005; Witte & Fobker, 2009). These

findings suggest that CR is a promising *in vivo* model for the study of age-related oxidative damage on BFCN neurotrophin transport.

In addition to oxidative stress, PTP1B must also be manipulated *in vivo* to determine the physiological relevance of our proposed mechanism. This can be achieved via intraperitoneal injection of C57BL/6 mice with the blood brain barrier permeant PTP1B inhibitor trodusqemine (available from Sigma Aldrich) (Ricke et al., 2020). Alternatively, selective neuronal PTP1B ablation can be achieved by crossing $PTP1B^{flx/flx}$ mice with Camk2α-CRE mice (both available from the Jackson Laboratory). Using these transgenic mice avoids the potential confounding effects of systemic PTP1B inhibition. However, the generation of a transgenic mouse colony is both time consuming and expensive. Additionally, trodusqemine has been shown to improve both cognitive deficits and hippocampal neuron loss in an AD mouse model (Ricke et al., 2020). This coupled with its relatively cheap cost, simple administration route, and established compatibility with a commonly used mouse line point to trodusqemine intraperitoneal injection as an accessible and promising model for the study of PTP1B manipulation *in vivo*.

Finally, the levels of TrkA must also be manipulated to determine the effect of its loss on BFCN proNGF transport *in vivo*. TrkA manipulation is usually done at the genetic level due to the poor selectivity of TrkA inhibitors (Jiang et al., 2021). Homozygous TrkA knockout mice do not live past 2-3 weeks of age – heterozygous TrkA knockout lines are the only viable model available for the study of TrkA loss in adult animals (Smeyne et al., 1994). The magnitude of TrkA loss in these animals is highly disease-relevant in the context of AD as TrkA levels are reduced by around 50% in the AD basal forebrain compared to healthy controls (Boissiere et al., 1997; Counts et al., 2004; E. J. Mufson et al., 2000). This model is also very accessible to our lab as we have already established a colony of TrkA heterozygous knockout mice thanks to the generous donation of breeder mice from Dr. Lino Tessarollo (National Cancer Institute, Maryland, USA).

Our lab is very well versed in the techniques required to assay BFCN neurotrophin transport and neuronal health *in vivo*. Paramount amongst these is the determination of retrograde neurotrophin transport via the injection of radiolabelled I^{125}-NGF into BFCN target fields (discussed in Chapter 1). Neurotrophin transport can also be assessed via Western blot by measuring neurotrophin immunoreactivity in basal forebrain nuclei and neocortical target areas (Fahnestock et al., 2001; Perez et al., 2011). Neurotrophin receptor levels can be similarly assayed via Western blot to determine the effects of PTP1B inhibition (trodusqemine-treated mice) and oxidative stress (CR mice) on TrkA levels *in vivo* (Perez et al., 2011). BFCN neuronal health can be determined by the immunohistochemical staining of rostral-to-caudal sections of the medial septum with antibodies against VAChT and ChAT (Jaffar et al., 2001; Perez et al., 2007, 2011).

Our lab also has experience performing behavioural assays like the Morris Water Maze (MWM) to determine the effect of our *in vivo* manipulations on cognition. In fact, the cognitive ability of a cohort of TrkA heterozygous knockout mice has already been assayed using the MWM and is currently being analyzed by members of our lab. These assays were performed on aged (18-20 months old) mice to determine the effect of TrkA loss on cognition in an aging context (Flurkey et al., 2007). Completion of the

biochemical assays outlined above on this cohort will allow us to determine if neurotrophin transport loss and BFCN degeneration underlie any observed cognitive deficits. The same aging paradigm should be adopted when assaying CR mice, as reductions in brain oxidative stress become more pronounced with age (Trepanowski et al., 2011). However, biochemical and behavioural assays of trodusqemine-injected animals should be completed using younger mice (between 3-6 months old) to isolate the effect of PTP1B inhibition on any observed changes. The completion of the biochemical and behavioural assays outlined above are critical to determine the translatability of our *in vitro* findings to cognition and BFCN neurotrophin transport *in vivo*.

6.3 Final Remarks

This body of work represents a thorough examination of BFCN neurotrophin transport in the context of age-related neurodegeneration. First, protocols for the accurate quantification of neurotrophin transport involving the microfluidic culture of BFCNs were established. These protocols were used to determine that the transport of the neurotrophins BDNF and proNGF declined with age in BFCNs. Next, the contributions of Rab proteins and classical AD pathological hallmarks Aß and tau to these impairments were explored. Finally, a specific molecular mechanism contributing to these impairments was established by demonstrating that oxidative stress impairs proNGF axonal transport in BFCNs via the PTP1B-mediated loss of TrkA.

The bulk of this work was focused on oxidative stress due to its longstanding role as a mediator of both aging and AD pathogenesis (Tramutola et al., 2017). Oxidative stress likely plays a bigger role in the age-related degeneration of the brain compared to other tissues due to the extremely high metabolic rate of neurons (Chamberlain & Sheng, 2019; Misgeld & Schwarz, 2017). Paradoxically however, neurons have relatively underdeveloped antioxidant systems to deal with oxidative stress compared to other cell types (Ahlgren-Beckendorf et al., 1999; P. S. Baxter & Hardingham, 2016). To account for this deficiency, neurons are heavily reliant on glial cells for antioxidant support (P. S. Baxter & Hardingham, 2016; Y. Chen et al., 2020). While factors relating to glial support are beyond the scope of this work, it is important to keep in mind that the precipitating insults pertaining to the increase in oxidative stress that accompanies aging and AD likely involve glial cell dysfunction.

Our work highlights the importance of understanding the contribution of neurotrophin transport impairments to BFCN degeneration in aging and AD. BFCNs have long been known to be critical for the modulation of hippocampal and cortical circuit dynamics that underlie learning, memory, and attention (Ballinger et al., 2016). In recent years, the role of BFCNs in mediating other functions including hippocampal neurogenesis and neural inflammation, two newly established contributors to AD pathogenesis, has also been established (Maurer & Williams, 2017). It seems that as time goes on, the importance of BFCNs to overall brain health only becomes more apparent. Understanding how and why these neurons degenerate is critical for the prevention of age-associated cognitive dysfunction. We hope that the work outlined here contributes to this understanding.

References

Ahlgren-Beckendorf, J. A., Reising, A. M., Schander, M. A., Herdler, J. W., & Johnson, J. A. (1999). Coordinate regulation of NAD(P)H:quinone oxidoreductase and glutathione-S-transferases in primary cultures of rat neurons and glia: Role of the antioxidant/electrophile responsive element. *Glia*, *25*(2), 131–142.

Ahlqvist, K. J., Hämäläinen, R. H., Yatsuga, S., Uutela, M., Terzioglu, M., Götz, A., Forsström, S., Salven, P., Angers-Loustau, A., Kopra, O. H., Tyynismaa, H., Larsson, N. G., Wartiovaara, K., Prolla, T., Trifunovic, A., & Suomalainen, A. (2012). Somatic progenitor cell vulnerability to mitochondrial DNA mutagenesis underlies progeroid phenotypes in polg mutator mice. *Cell Metabolism*. https://doi.org/10.1016/j.cmet.2011.11.012

Ali, T. K., Matragoon, S., Pillai, B. A., Liou, G. I., & El-Remessy, A. B. (2008). Peroxynitrite mediates retinal neurodegeneration by inhibiting nerve growth factor survival signaling in experimental and human diabetes. *Diabetes*, *57*(4), 889–898. https://doi.org/10.2337/db07-1669

Amigo, I., Menezes-Filho, S. L., Luévano-Martínez, L. A., Chausse, B., & Kowaltowski, A. J. (2017). Caloric restriction increases brain mitochondrial calcium retention capacity and protects against excitotoxicity. *Aging Cell*. https://doi.org/10.1111/acel.12527

Ascaño, M., Richmond, A., Borden, P., & Kuruvilla, R. (2009). Axonal targeting of Trk receptors via transcytosis regulates sensitivity to neurotrophin responses. *The Journal of Neuroscience: The Official Journal of the Society for Neuroscience*, *29*(37), 11674–11685. https://doi.org/10.1523/JNEUROSCI.1542-09.2009

Ayloo, S., Lazarus, J. E., Dodda, A., Tokito, M., Ostap, E. M., & Holzbaur, E. L. F. (2014). Dynactin functions as both a dynamic tether and brake during dynein-driven motility. *Nature Communications*, *5*, 4807. https://doi.org/10.1038/ncomms5807

Ballinger, E. C., Ananth, M., Talmage, D. A., & Role, L. W. (2016). Basal Forebrain Cholinergic Circuits and Signaling in Cognition and Cognitive Decline. *Neuron*, *91*(6), 1199–1218. https://doi.org/10.1016/j.neuron.2016.09.006

Barten, D. M., Fanara, P., Andorfer, C., Hoque, N., Wong, P. Y. A., Husted, K. H., Cadelina, G. W., Decarr, L. B., Yang, L., Liu, V., Fessler, C., Protassio, J., Riff, T., Turner, H., Janus, C. G., Sankaranarayanan, S., Polson, C., Meredith, J. E., Gray, G., … Albright, C. F. (2012). Hyperdynamic microtubules, cognitive deficits, and pathology are improved in tau transgenic mice with low doses of the microtubule-stabilizing agent BMS-241027. *The Journal of Neuroscience: The Official Journal of the Society for Neuroscience*, *32*(21), 7137–7145. https://doi.org/10.1523/JNEUROSCI.0188-12.2012

Baxter, P. S., & Hardingham, G. E. (2016). Adaptive regulation of the brain's antioxidant defences by neurons and astrocytes. *Free Radical Biology & Medicine*, *100*, 147–152. https://doi.org/10.1016/j.freeradbiomed.2016.06.027

Belfiore, R., Rodin, A., Ferreira, E., Velazquez, R., Branca, C., Caccamo, A., & Oddo, S. (2019). Temporal and regional progression of Alzheimer's disease-like pathology

in 3xTg-AD mice. *Aging Cell*, *18*(1), e12873. https://doi.org/10.1111/acel.12873

Bissonnette, C. J., Lyass, L., Bhattacharyya, B. J., Belmadani, A., Miller, R. J., & Kessler, J. A. (2011). The Controlled Generation of Functional Basal Forebrain Cholinergic Neurons from Human Embryonic Stem Cells. *STEM CELLS*, *29*(5), 802–811. https://doi.org/10.1002/stem.626

Bodmer, D., Ascaño, M., & Kuruvilla, R. (2011). Isoform-Specific Dephosphorylation of Dynamin1 by Calcineurin Couples Neurotrophin Receptor Endocytosis to Axonal Growth. *Neuron*, *70*(6), 1085–1099. https://doi.org/10.1016/j.neuron.2011.04.025

Boissiere, F., Faucheux, B., Ruberg, M., Agid, Y., & Hirsch, E. C. (1997). Decreased TrkA gene expression in cholinergic neurons of the striatum and basal forebrain of patients with Alzheimer's disease. *Experimental Neurology*, *145*(1), 245–252. https://doi.org/10.1006/exnr.1997.6443

Chamberlain, K. A., & Sheng, Z. (2019). Mechanisms for the maintenance and regulation of axonal energy supply. *Journal of Neuroscience Research*, *97*(8), 897–913. https://doi.org/10.1002/jnr.24411

Chang, C.-Y., Ting, H.-C., Liu, C.-A., Su, H.-L., Chiou, T.-W., Lin, S.-Z., Harn, H.-J., & Ho, T.-J. (2020). Induced Pluripotent Stem Cell (iPSC)-Based Neurodegenerative Disease Models for Phenotype Recapitulation and Drug Screening. *Molecules*, *25*(8). https://doi.org/10.3390/molecules25082000

Chen, M. L., Logan, T. D., Hochberg, M. L., Shelat, S. G., Yu, X., Wilding, G. E., Tan, W., Kujoth, G. C., Prolla, T. A., Selak, M. A., Kundu, M., Carroll, M., & Thompson, J. E. (2009). Erythroid dysplasia, megaloblastic anemia, and impaired lymphopoiesis arising from mitochondrial dysfunction. *Blood*. https://doi.org/10.1182/blood-2008-08-169474

Chen, Y., Qin, C., Huang, J., Tang, X., Liu, C., Huang, K., Xu, J., Guo, G., Tong, A., & Zhou, L. (2020). The role of astrocytes in oxidative stress of central nervous system: A mixed blessing. *Cell Proliferation*, *53*(3). https://doi.org/10.1111/cpr.12781

Cobb, C. A., & Cole, M. P. (2015). Oxidative and Nitrative Stress in Neurodegeneration. *Neurobiology of Disease*, *84*, 4–21. https://doi.org/10.1016/j.nbd.2015.04.020

Counts, S. E., Nadeem, M., Wuu, J., Ginsberg, S. D., Saragovi, H. U., & Mufson, E. J. (2004). Reduction of cortical TrkA but not p75NTR protein in early-stage Alzheimer's disease. *Annals of Neurology*, *56*(4), 520–531. https://doi.org/10.1002/ana.20233

Dayanandan, R., Van Slegtenhorst, M., Mack, T. G., Ko, L., Yen, S. H., Leroy, K., Brion, J. P., Anderton, B. H., Hutton, M., & Lovestone, S. (1999). Mutations in tau reduce its microtubule binding properties in intact cells and affect its phosphorylation. *FEBS Letters*, *446*(2–3), 228–232. https://doi.org/10.1016/s0014-5793(99)00222-7

Desai, V. G., Weindruch, R., Hart, R. W., & Feuers, R. J. (1996). Influences of age and dietary restriction on gastrocnemius electron transport system activities in mice. *Archives of Biochemistry and Biophysics*. https://doi.org/10.1006/abbi.1996.0375

Dhanasekaran, D. N., & Reddy, E. P. (2008). JNK signaling in apoptosis. *Oncogene*, *27*(48), 6245–6251. https://doi.org/10.1038/onc.2008.301

Dunn, K. W., Kamocka, M. M., & McDonald, J. H. (2011). A practical guide to evaluating colocalization in biological microscopy. *American Journal of Physiology - Cell Physiology*, *300*(4), C723–C742. https://doi.org/10.1152/ajpcell.00462.2010

Edgar, D., & Trifunovic, A. (2009). The mtDNA mutator mouse: Dissecting mitochondrial involvement in aging. *Aging*.

Escudero, C. A., Cabeza, C., Moya-Alvarado, G., Maloney, M. T., Flores, C. M., Wu, C., Court, F. A., Mobley, W. C., & Bronfman, F. C. (2019). C-Jun N-terminal kinase (JNK)-dependent internalization and Rab5-dependent endocytic sorting mediate long-distance retrograde neuronal death induced by axonal BDNF-p75 signaling. *Scientific Reports*, *9*(1), 6070. https://doi.org/10.1038/s41598-019-42420-6

Esquerda-Canals, G., Montoliu-Gaya, L., Güell-Bosch, J., & Villegas, S. (2017). Mouse Models of Alzheimer's Disease. *Journal of Alzheimer's Disease*, *57*(4), 1171–1183. https://doi.org/10.3233/JAD-170045

Fahnestock, M., & Shekari, A. (2019). ProNGF and neurodegeneration in Alzheimer's disease. In *Frontiers in Neuroscience* (Vol. 13, Issue FEB). https://doi.org/10.3389/fnins.2019.00129

Fahnestock, M., Yu, G., & Coughlin, M. D. (2004). ProNGF: a neurotrophic or an apoptotic molecule? In *Progress in Brain Research* (pp. 101–110). https://doi.org/10.1016/S0079-6123(03)46007-X

Fahnestock, Michalski, B., Xu, B., & Coughlin, M. (2001). The precursor pro-nerve growth factor is the predominant form of nerve growth factor in brain and is increased in Alzheimer's disease. *Molecular and Cellular Neuroscience*, *18*(2), 210–220. https://doi.org/10.1006/mcne.2001.1016

Fanale, D., Bronte, G., Passiglia, F., Calò, V., Castiglia, M., Di Piazza, F., Barraco, N., Cangemi, A., Catarella, M. T., Insalaco, L., Listì, A., Maragliano, R., Massihnia, D., Perez, A., Toia, F., Cicero, G., & Bazan, V. (2015). Stabilizing versus Destabilizing the Microtubules: A Double-Edge Sword for an Effective Cancer Treatment Option? *Analytical Cellular Pathology*, *2015*, e690916. https://doi.org/10.1155/2015/690916

Fernandez-Valenzuela, J. J., Sanchez-Varo, R., Muñoz-Castro, C., De Castro, V., Sanchez-Mejias, E., Navarro, V., Jimenez, S., Nuñez-Diaz, C., Gomez-Arboledas, A., Moreno-Gonzalez, I., Vizuete, M., Davila, J. C., Vitorica, J., & Gutierrez, A. (2020). Enhancing microtubule stabilization rescues cognitive deficits and ameliorates pathological phenotype in an amyloidogenic Alzheimer's disease model. *Scientific Reports*, *10*(1), 14776. https://doi.org/10.1038/s41598-020-71767-4

Feuers, R. J. (1998). The effects of dietary restriction on mitochondrial dysfunction in aging. *Annals of the New York Academy of Sciences*. https://doi.org/10.1111/j.1749-6632.1998.tb09902.x

Flurkey, K., M. Currer, J., & Harrison, D. E. (2007). Chapter 20—Mouse Models in Aging Research. In J. G. Fox, M. T. Davisson, F. W. Quimby, S. W. Barthold, C.

E. Newcomer, & A. L. Smith (Eds.), *The Mouse in Biomedical Research (Second Edition)* (pp. 637–672). Academic Press. https://doi.org/10.1016/B978-012369454-6/50074-1

Frobel, J., Hemeda, H., Lenz, M., Abagnale, G., Joussen, S., Denecke, B., Sarić, T., Zenke, M., & Wagner, W. (2014). Epigenetic rejuvenation of mesenchymal stromal cells derived from induced pluripotent stem cells. *Stem Cell Reports*, *3*(3), 414–422. https://doi.org/10.1016/j.stemcr.2014.07.003

Go, Y. M., Patel, R. P., Maland, M. C., Park, H., Beckman, J. S., Darley-Usmar, V. M., & Jo, H. (1999). Evidence for peroxynitrite as a signaling molecule in flow-dependent activation of c-Jun NH(2)-terminal kinase. *The American Journal of Physiology*, *277*(4), H1647-1653. https://doi.org/10.1152/ajpheart.1999.277.4.H1647

Goody, R. S., Rak, A., & Alexandrov, K. (2005). The structural and mechanistic basis for recycling of Rab proteins between membrane compartments. *Cellular and Molecular Life Sciences CMLS*, *62*(15), 1657–1670. https://doi.org/10.1007/s00018-005-4486-8

Graf, T., & Enver, T. (2009). Forcing cells to change lineages. *Nature*, *462*(7273), 587–594. https://doi.org/10.1038/nature08533

Guix, F. X., Wahle, T., Vennekens, K., Snellinx, A., Chávez-Gutiérrez, L., Ill-Raga, G., Ramos-Fernandez, E., Guardia-Laguarta, C., Lleó, A., Arimon, M., Berezovska, O., Muñoz, F. J., Dotti, C. G., & De Strooper, B. (2012). Modification of γ-secretase by nitrosative stress links neuronal ageing to sporadic Alzheimer's disease. *EMBO Molecular Medicine*, *4*(7), 660–673. https://doi.org/10.1002/emmm.201200243

Hamilton, R. T., Walsh, M. E., & Van Remmen, H. (2012). Mouse Models of Oxidative Stress Indicate a Role for Modulating Healthy Aging. *Journal of Clinical & Experimental Pathology*, *Suppl 4*. https://doi.org/10.4172/2161-0681.S4-005

Haque, A., Andersen, J. N., Salmeen, A., Barford, D., & Tonks, N. K. (2011). Conformation-Sensing Antibodies Stabilize the Oxidized Form of PTP1B and Inhibit Its Phosphatase Activity. *Cell*, *147*(1), 185–198. https://doi.org/10.1016/j.cell.2011.08.036

Harrington, A. W., & Ginty, D. D. (2013). Long-distance retrograde neurotrophic factor signalling in neurons. *Nature Reviews Neuroscience*, *14*(3), 177–187. https://doi.org/10.1038/nrn3253

Harrington, A. W., St. Hillaire, C., Zweifel, L. S., Glebova, N. O., Philippidou, P., Halegoua, S., & Ginty, D. D. (2011). Recruitment of Actin Modifiers to TrkA Endosomes Governs Retrograde NGF Signaling and Survival. *Cell*, *146*(3), 421–434. https://doi.org/10.1016/j.cell.2011.07.008

Herrmann, L., Wiegmann, C., Arsalan-Werner, A., Hilbrich, I., Jäger, C., Flach, K., Suttkus, A., Lachmann, I., Arendt, T., & Holzer, M. (2015). Hook Proteins: Association with Alzheimer Pathology and Regulatory Role of Hook3 in Amyloid Beta Generation. *PLoS ONE*, *10*(3). https://doi.org/10.1371/journal.pone.0119423

Horgan, C. P., Hanscom, S. R., Jolly, R. S., Futter, C. E., & McCaffrey, M. W. (2010a). Rab11-FIP3 links the Rab11 GTPase and cytoplasmic dynein to mediate transport

to the endosomal-recycling compartment. *Journal of Cell Science*, *123*(Pt 2), 181–191. https://doi.org/10.1242/jcs.052670

Horgan, C. P., Hanscom, S. R., Jolly, R. S., Futter, C. E., & McCaffrey, M. W. (2010b). Rab11-FIP3 binds dynein light intermediate chain 2 and its overexpression fragments the Golgi complex. *Biochemical and Biophysical Research Communications*, *394*(2), 387–392. https://doi.org/10.1016/j.bbrc.2010.03.028

Horiuchi, D., Collins, C. A., Bhat, P., Barkus, R. V., DiAntonio, A., & Saxton, W. M. (2007). Control of a kinesin-cargo linkage mechanism by JNK pathway kinases. *Current Biology : CB*, *17*(15), 1313–1317. https://doi.org/10.1016/j.cub.2007.06.062

Horiuchi, H., Lippé, R., McBride, H. M., Rubino, M., Woodman, P., Stenmark, H., Rybin, V., Wilm, M., Ashman, K., Mann, M., & Zerial, M. (1997). A Novel Rab5 GDP/GTP Exchange Factor Complexed to Rabaptin-5 Links Nucleotide Exchange to Effector Recruitment and Function. *Cell*, *90*(6), 1149–1159. https://doi.org/10.1016/S0092-8674(00)80380-3

Hutton, M., Lendon, C. L., Rizzu, P., Baker, M., Froelich, S., Houlden, H., Pickering-Brown, S., Chakraverty, S., Isaacs, A., Grover, A., Hackett, J., Adamson, J., Lincoln, S., Dickson, D., Davies, P., Petersen, R. C., Stevens, M., de Graaff, E., Wauters, E., … Heutink, P. (1998). Association of missense and 5′-splice-site mutations in tau with the inherited dementia FTDP-17. *Nature*, *393*(6686), 702–705. https://doi.org/10.1038/31508

Jaffar, S., Counts, S. E., Ma, S. Y., Dadko, E., Gordon, M. N., Morgan, D., & Mufson, E. J. (2001). Neuropathology of mice carrying mutant APP(swe) and/or PS1(M146L) transgenes: Alterations in the p75(NTR) cholinergic basal forebrain septohippocampal pathway. *Experimental Neurology*, *170*(2), 227–243. https://doi.org/10.1006/exnr.2001.7710

Jiang, T., Wang, G., Liu, Y., Feng, L., Wang, M., Liu, J., Chen, Y., & Ouyang, L. (2021). Development of small-molecule tropomyosin receptor kinase (TRK) inhibitors for NTRK fusion cancers. *Acta Pharmaceutica Sinica B*, *11*(2), 355–372. https://doi.org/10.1016/j.apsb.2020.05.004

Kane, K. I. W., Moreno, E. L., Hachi, S., Walter, M., Jarazo, J., Oliveira, M. A. P., Hankemeier, T., Vulto, P., Schwamborn, J. C., Thoma, M., & Fleming, R. M. T. (2019). Automated microfluidic cell culture of stem cell derived dopaminergic neurons. *Scientific Reports*, *9*(1), 1796. https://doi.org/10.1038/s41598-018-34828-3

Kraemer, B. R., Yoon, S. O., & Carter, B. D. (2014). The biological functions and signaling mechanisms of the p75 neurotrophin receptor. *Handbook of Experimental Pharmacology*, *220*, 121–164. https://doi.org/10.1007/978-3-642-45106-5_6

Kuruvilla, R., Ye, H., & Ginty, D. D. (2000). Spatially and Functionally Distinct Roles of the PI3-K Effector Pathway during NGF Signaling in Sympathetic Neurons. *Neuron*, *27*(3), 499–512. https://doi.org/10.1016/S0896-6273(00)00061-1

Lanza, I. R., Zabielski, P., Klaus, K. A., Morse, D. M., Heppelmann, C. J., Bergen, H. R., Dasari, S., Walrand, S., Short, K. R., Johnson, M. L., Robinson, M. M., Schimke,

J. M., Jakaitis, D. R., Asmann, Y. W., Sun, Z., & Nair, K. S. (2012). Chronic caloric restriction preserves mitochondrial function in senescence without increasing mitochondrial biogenesis. *Cell Metabolism*. https://doi.org/10.1016/j.cmet.2012.11.003

Lapasset, L., Milhavet, O., Prieur, A., Besnard, E., Babled, A., Aït-Hamou, N., Leschik, J., Pellestor, F., Ramirez, J.-M., De Vos, J., Lehmann, S., & Lemaitre, J.-M. (2011). Rejuvenating senescent and centenarian human cells by reprogramming through the pluripotent state. *Genes & Development*, *25*(21), 2248–2253. https://doi.org/10.1101/gad.173922.111

Lee, R., Kermani, P., Teng, K., & Hempstead, B. (2001). Regulation of Cell Survival by Secreted Proneurotrophins. *Science*, *294*(5548), 1945–1948. https://doi.org/10.1126/science.1065057

Liu, J.-J. (2017). Regulation of dynein-dynactin-driven vesicular transport. *Traffic (Copenhagen, Denmark)*, *18*(6), 336–347. https://doi.org/10.1111/tra.12475

Liu, M.-L., Zang, T., Zou, Y., Chang, J., Gibson, J., Huber, K. M., & Zhang, C.-L. (2013). Small Molecules Enable Neurogenin 2 to Efficiently Convert Human Fibroblasts to Cholinergic Neurons. *Nature Communications*, *4*, 2183. https://doi.org/10.1038/ncomms3183

Lo Sardo, V., Ferguson, W., Erikson, G. A., Topol, E. J., Baldwin, K. K., & Torkamani, A. (2017). Influence of donor age on induced pluripotent stem cells. *Nature Biotechnology*, *35*(1), 69–74. https://doi.org/10.1038/nbt.3749

Londhe, A. D., Bergeron, A., Curley, S. M., Zhang, F., Rivera, K. D., Kannan, A., Coulis, G., Rizvi, S. H. M., Kim, S. J., Pappin, D. J., Tonks, N. K., Linhardt, R. J., & Boivin, B. (2020). Regulation of PTP1B activation through disruption of redox-complex formation. *Nature Chemical Biology*, *16*(2), 122–125. https://doi.org/10.1038/s41589-019-0433-0

Lv, X., Li, W., Luo, Y., Wang, D., Zhu, C., Huang, Z. X., & Tan, X. (2013). Exploring the differences between mouse mAβ1-42 and human hAβ1-42 for Alzheimer's disease related properties and neuronal cytotoxicity. *Chemical Communications*. https://doi.org/10.1039/c3cc40779a

Magadán, J. G., Barbieri, M. A., Mesa, R., Stahl, P. D., & Mayorga, L. S. (2006). Rab22a regulates the sorting of transferrin to recycling endosomes. *Molecular and Cellular Biology*, *26*(7), 2595–2614. https://doi.org/10.1128/MCB.26.7.2595-2614.2006

Marion, R. M., Strati, K., Li, H., Tejera, A., Schoeftner, S., Ortega, S., Serrano, M., & Blasco, M. A. (2009). Telomeres acquire embryonic stem cell characteristics in induced pluripotent stem cells. *Cell Stem Cell*, *4*(2), 141–154. https://doi.org/10.1016/j.stem.2008.12.010

Marlin, M. C., & Li, G. (2015). Biogenesis and Function of the NGF/TrkA Signaling Endosome. In *International Review of Cell and Molecular Biology* (pp. 239–257). https://doi.org/10.1016/bs.ircmb.2014.10.002

Masoudi, R., Ioannou, M. S., Coughlin, M. D., Pagadala, P., Neet, K. E., Clewes, O., Allen, S. J., Dawbarn, D., & Fahnestock, M. (2009). Biological Activity of Nerve Growth Factor Precursor Is Dependent upon Relative Levels of Its Receptors.

Journal of Biological Chemistry, *284*(27), 18424–18433. https://doi.org/10.1074/jbc.M109.007104

Maurer, S. V., & Williams, C. L. (2017). The Cholinergic System Modulates Memory and Hippocampal Plasticity via Its Interactions with Non-Neuronal Cells. *Frontiers in Immunology*, *8*. https://doi.org/10.3389/fimmu.2017.01489

Means, L. W., Higgins, J. L., & Fernandez, T. J. (1993). Mid-life onset of dietary restriction extends life and prolongs cognitive functioning. *Physiology and Behavior*. https://doi.org/10.1016/0031-9384(93)90243-9

Mertens, J., Reid, D., Lau, S., Kim, Y., & Gage, F. H. (2018). Aging in a Dish: IPSC-Derived and Directly Induced Neurons for Studying Brain Aging and Age-Related Neurodegenerative Diseases. *Annual Review of Genetics*, *52*, 271–293. https://doi.org/10.1146/annurev-genet-120417-031534

Mignogna, M. L., & D'Adamo, P. (2018). Critical importance of RAB proteins for synaptic function. *Small GTPases*, *9*(1–2), 145–157. https://doi.org/10.1080/21541248.2016.1277001

Misgeld, T., & Schwarz, T. L. (2017). Mitostasis in Neurons: Maintaining Mitochondria in an Extended Cellular Architecture. *Neuron*, *96*(3), 651–666. https://doi.org/10.1016/j.neuron.2017.09.055

Moutin, E., Hemonnot, A.-L., Seube, V., Linck, N., Rassendren, F., Perroy, J., & Compan, V. (2020). Procedures for Culturing and Genetically Manipulating Murine Hippocampal Postnatal Neurons. *Frontiers in Synaptic Neuroscience*, *12*. https://doi.org/10.3389/fnsyn.2020.00019

Mufson, E. J., Ma, S. Y., Cochran, E. J., Bennett, D. A., Beckett, L. A., Jaffar, S., Saragovi, H. U., & Kordower, J. H. (2000). Loss of nucleus basalis neurons containing trkA immunoreactivity in individuals with mild cognitive impairment and early Alzheimer's disease. *The Journal of Comparative Neurology*, *427*(1), 19–30. https://doi.org/10.1002/1096-9861(20001106)427:1<19::AID-CNE2>3.0.CO;2-A

Muñoz, S. S., Engel, M., Balez, R., Do-Ha, D., Cabral-da-Silva, M. C., Hernández, D., Berg, T., Fifita, J. A., Grima, N., Yang, S., Blair, I. P., Nicholson, G., Cook, A. L., Hewitt, A. W., Pébay, A., & Ooi, L. (2020). A Simple Differentiation Protocol for Generation of Induced Pluripotent Stem Cell-Derived Basal Forebrain-Like Cholinergic Neurons for Alzheimer's Disease and Frontotemporal Dementia Disease Modeling. *Cells*, *9*(9). https://doi.org/10.3390/cells9092018

Nguyen, H. N., Byers, B., Cord, B., Shcheglovitov, A., Byrne, J., Gujar, P., Kee, K., Schüle, B., Dolmetsch, R. E., Langston, W., Palmer, T. D., & Pera, R. R. (2011). LRRK2 mutant iPSC-derived DA neurons demonstrate increased susceptibility to oxidative stress. *Cell Stem Cell*, *8*(3), 267–280. https://doi.org/10.1016/j.stem.2011.01.013

Nixon, R. A. (2017). Amyloid precursor protein and endosomal–lysosomal dysfunction in Alzheimer's disease: Inseparable partners in a multifactorial disease. *The FASEB Journal*, *31*(7), 2729–2743. https://doi.org/10.1096/fj.201700359

Ocampo, A., Reddy, P., Martinez-Redondo, P., Platero-Luengo, A., Hatanaka, F., Hishida, T., Li, M., Lam, D., Kurita, M., Beyret, E., Araoka, T., Vazquez-Ferrer,

E., Donoso, D., Roman, J. L., Xu, J., Rodriguez Esteban, C., Nuñez, G., Nuñez Delicado, E., Campistol, J. M., … Izpisua Belmonte, J. C. (2016). In Vivo Amelioration of Age-Associated Hallmarks by Partial Reprogramming. *Cell*, *167*(7), 1719-1733.e12. https://doi.org/10.1016/j.cell.2016.11.052

Olenick, M. A., Dominguez, R., & Holzbaur, E. L. F. (2019). Dynein activator Hook1 is required for trafficking of BDNF-signaling endosomes in neurons. *The Journal of Cell Biology*, *218*(1), 220–233. https://doi.org/10.1083/jcb.201805016

Olenick, M. A., Tokito, M., Boczkowska, M., Dominguez, R., & Holzbaur, E. L. F. (2016). Hook Adaptors Induce Unidirectional Processive Motility by Enhancing the Dynein-Dynactin Interaction. *The Journal of Biological Chemistry*, *291*(35), 18239–18251. https://doi.org/10.1074/jbc.M116.738211

Pang, Z. P., Yang, N., Vierbuchen, T., Ostermeier, A., Fuentes, D. R., Yang, T. Q., Citri, A., Sebastiano, V., Marro, S., Südhof, T. C., & Wernig, M. (2011). Induction of human neuronal cells by defined transcription factors. *Nature*, *476*(7359), 220–223. https://doi.org/10.1038/nature10202

Patel, N. V., Gordon, M. N., Connor, K. E., Good, R. A., Engelman, R. W., Mason, J., Morgan, D. G., Morgan, T. E., & Finch, C. E. (2005). Caloric restriction attenuates Aβ-deposition in Alzheimer transgenic models. *Neurobiology of Aging*. https://doi.org/10.1016/j.neurobiolaging.2004.09.014

Pereira-Leal, J. B., & Seabra, M. C. (2000). The mammalian Rab family of small GTPases: Definition of family and subfamily sequence motifs suggests a mechanism for functional specificity in the Ras superfamily. *Journal of Molecular Biology*, *301*(4), 1077–1087. https://doi.org/10.1006/jmbi.2000.4010

Perez, S. E., Dar, S., Ikonomovic, M. D., DeKosky, S. T., & Mufson, E. J. (2007). Cholinergic forebrain degeneration in the APPswe/PS1DeltaE9 transgenic mouse. *Neurobiology of Disease*, *28*(1), 3–15. https://doi.org/10.1016/j.nbd.2007.06.015

Perez, S. E., He, B., Muhammad, N., Oh, K.-J., Fahnestock, M., Ikonomovic, M. D., & Mufson, E. J. (2011). Cholinotrophic basal forebrain system alterations in 3xTg-AD transgenic mice. *Neurobiology of Disease*, *41*(2), 338–352. https://doi.org/10.1016/j.nbd.2010.10.002

Radi, R. (2013). Protein tyrosine nitration: Biochemical mechanisms and structural basis of functional effects. *Accounts of Chemical Research*, *46*(2), 550–559. https://doi.org/10.1021/ar300234c

Reck-Peterson, S. L., Yildiz, A., Carter, A. P., Gennerich, A., Zhang, N., & Vale, R. D. (2006). Single-molecule analysis of dynein processivity and stepping behavior. *Cell*, *126*(2), 335–348. https://doi.org/10.1016/j.cell.2006.05.046

Resende, R., Moreira, P. I., Proença, T., Deshpande, A., Busciglio, J., Pereira, C., & Oliveira, C. R. (2008). Brain oxidative stress in a triple-transgenic mouse model of Alzheimer disease. *Free Radical Biology & Medicine*, *44*(12), 2051–2057. https://doi.org/10.1016/j.freeradbiomed.2008.03.012

Ricke, K. M., Cruz, S. A., Qin, Z., Farrokhi, K., Sharmin, F., Zhang, L., Zasloff, M. A., Stewart, A. F. R., & Chen, H.-H. (2020). Neuronal Protein Tyrosine Phosphatase 1B Hastens Amyloid β-Associated Alzheimer's Disease in Mice. *The Journal of*

Neuroscience: The Official Journal of the Society for Neuroscience, *40*(7), 1581–1593. https://doi.org/10.1523/JNEUROSCI.2120-19.2019

Rink, J., Ghigo, E., Kalaidzidis, Y., & Zerial, M. (2005). Rab Conversion as a Mechanism of Progression from Early to Late Endosomes. *Cell*, *122*(5), 735–749. https://doi.org/10.1016/j.cell.2005.06.043

Ross, J. L., Wallace, K., Shuman, H., Goldman, Y. E., & Holzbaur, E. L. F. (2006). Processive bidirectional motion of dynein-dynactin complexes in vitro. *Nature Cell Biology*, *8*(6), 562–570. https://doi.org/10.1038/ncb1421

Salmeen, A., Andersen, J. N., Myers, M. P., Meng, T.-C., Hinks, J. A., Tonks, N. K., & Barford, D. (2003). Redox regulation of protein tyrosine phosphatase 1B involves a sulphenyl-amide intermediate. *Nature*, *423*(6941), 769–773. https://doi.org/10.1038/nature01680

Schonteich, E., Wilson, G. M., Burden, J., Hopkins, C. R., Anderson, K., Goldenring, J. R., & Prekeris, R. (2008). The Rip11/Rab11-FIP5 and kinesin II complex regulates endocytic protein recycling. *Journal of Cell Science*, *121*(22), 3824–3833. https://doi.org/10.1242/jcs.032441

Schroeder, C. M., & Vale, R. D. (2016). Assembly and activation of dynein-dynactin by the cargo adaptor protein Hook3. *The Journal of Cell Biology*, *214*(3), 309–318. https://doi.org/10.1083/jcb.201604002

Seibler, P., Graziotto, J., Jeong, H., Simunovic, F., Klein, C., & Krainc, D. (2011). Mitochondrial Parkin recruitment is impaired in neurons derived from mutant PINK1 induced pluripotent stem cells. *The Journal of Neuroscience: The Official Journal of the Society for Neuroscience*, *31*(16), 5970–5976. https://doi.org/10.1523/JNEUROSCI.4441-10.2011

Simon, G. C., & Prekeris, R. (2008). Mechanisms regulating targeting of recycling endosomes to the cleavage furrow during cytokinesis. *Biochemical Society Transactions*, *36*(Pt 3), 391–394. https://doi.org/10.1042/BST0360391

Smeyne, R. J., Klein, R., Schnapp, A., Long, L. K., Bryant, S., Lewin, A., Lira, S. A., & Barbacid, M. (1994). Severe sensory and sympathetic neuropathies in mice carrying a disrupted Trk/NGF receptor gene. *Nature*, *368*(6468), 246–249. https://doi.org/10.1038/368246a0

Son, M. K., Ryu, Y.-L., Jung, K. H., Lee, H., Lee, H. S., Yan, H. H., Park, H. J., Ryu, J.-K., Suh, J.-K., Hong, S., & Hong, S.-S. (2013). HS-173, a Novel PI3K Inhibitor, Attenuates the Activation of Hepatic Stellate Cells in Liver Fibrosis. *Scientific Reports*, *3*(1), 3470. https://doi.org/10.1038/srep03470

Stenmark, H. (2009). Rab GTPases as coordinators of vesicle traffic. *Nature Reviews. Molecular Cell Biology*, *10*(8), 513–525. https://doi.org/10.1038/nrm2728

Studer, L., Vera, E., & Cornacchia, D. (2015). Programming and Reprogramming Cellular Age in the Era of Induced Pluripotency. *Cell Stem Cell*, *16*(6), 591–600. https://doi.org/10.1016/j.stem.2015.05.004

Stykel, M. G., Humphries, K., Kirby, M. P., Czaniecki, C., Wang, T., Ryan, T., Bamm, V., & Ryan, S. D. (2018). Nitration of microtubules blocks axonal mitochondrial transport in a human pluripotent stem cell model of Parkinson's disease. *The FASEB Journal*, *32*(10), 5350–5364. https://doi.org/10.1096/fj.201700759RR

Takakura, K., Beckman, J. S., MacMillan-Crow, L. A., & Crow, J. P. (1999). Rapid and irreversible inactivation of protein tyrosine phosphatases PTP1B, CD45, and LAR by peroxynitrite. *Archives of Biochemistry and Biophysics*, *369*(2), 197–207. https://doi.org/10.1006/abbi.1999.1374

Tanaka, Y., Niwa, S., Dong, M., Farkhondeh, A., Wang, L., Zhou, R., & Hirokawa, N. (2016). The Molecular Motor KIF1A Transports the TrkA Neurotrophin Receptor and Is Essential for Sensory Neuron Survival and Function. *Neuron*, *90*(6), 1215–1229. https://doi.org/10.1016/j.neuron.2016.05.002

Tramutola, A., Lanzillotta, C., Perluigi, M., & Butterfield, D. A. (2017). Oxidative stress, protein modification and Alzheimer disease. *Brain Research Bulletin*, *133*, 88–96. https://doi.org/10.1016/j.brainresbull.2016.06.005

Trepanowski, J. F., Canale, R. E., Marshall, K. E., Kabir, M. M., & Bloomer, R. J. (2011). Impact of caloric and dietary restriction regimens on markers of health and longevity in humans and animals: A summary of available findings. In *Nutrition Journal*. https://doi.org/10.1186/1475-2891-10-107

Ueno, H., Yamaguchi, T., Fukunaga, S., Okada, Y., Yano, Y., Hoshino, M., & Matsuzaki, K. (2014). Comparison between the aggregation of human and rodent amyloid β-proteins in GM1 ganglioside clusters. *Biochemistry*. https://doi.org/10.1021/bi501239q

van Montfort, R. L. M., Congreve, M., Tisi, D., Carr, R., & Jhoti, H. (2003). Oxidation state of the active-site cysteine in protein tyrosine phosphatase 1B. *Nature*, *423*(6941), 773–777. https://doi.org/10.1038/nature01681

Vierbuchen, T., Ostermeier, A., Pang, Z. P., Kokubu, Y., Südhof, T. C., & Wernig, M. (2010). Direct conversion of fibroblasts to functional neurons by defined factors. *Nature*, *463*(7284), 1035–1041. https://doi.org/10.1038/nature08797

Walsh, M. E., Shi, Y., & Van Remmen, H. (2014). The effects of dietary restriction on oxidative stress in rodents. In *Free Radical Biology and Medicine*. https://doi.org/10.1016/j.freeradbiomed.2013.05.037

Wandinger-Ness, A., & Zerial, M. (2014). Rab Proteins and the Compartmentalization of the Endosomal System. *Cold Spring Harbor Perspectives in Biology*, *6*(11). https://doi.org/10.1101/cshperspect.a022616

Wang, J., Ho, L., Qin, W., Rocher, A. B., Seror, I., Humala, N., Maniar, K., Dolios, G., Wang, R., Hof, P. R., & Pasinetti, G. M. (2005). Caloric restriction attenuates β-amyloid neuropathology in a mouse model of Alzheimer's disease. *The FASEB Journal*. https://doi.org/10.1096/fj.04-3182fje

Wang, L., Liang, Z., & Li, G. (2011). Rab22 controls NGF signaling and neurite outgrowth in PC12 cells. *Molecular Biology of the Cell*, *22*(20), 3853–3860. https://doi.org/10.1091/mbc.E11-03-0277

Weigert, R., Yeung, A. C., Li, J., & Donaldson, J. G. (2004). Rab22a regulates the recycling of membrane proteins internalized independently of clathrin. *Molecular Biology of the Cell*, *15*(8), 3758–3770. https://doi.org/10.1091/mbc.e04-04-0342

Witte, A., & Fobker, M. (2009). Caloric restriction improves memory in elderly adults. *Proceedings of the ….*

Wu, Q., Wu, W., Jacevic, V., Franca, T. C. C., Wang, X., & Kuca, K. (2020). Selective inhibitors for JNK signalling: A potential targeted therapy in cancer. *Journal of Enzyme Inhibition and Medicinal Chemistry*, *35*(1), 574–583. https://doi.org/10.1080/14756366.2020.1720013

Yamashita, N., Joshi, R., Zhang, S., Zhang, Z.-Y., & Kuruvilla, R. (2017). Phospho-Regulation of Soma-to-Axon Transcytosis of Neurotrophin Receptors. *Developmental Cell*, *42*(6), 626-639.e5. https://doi.org/10.1016/j.devcel.2017.08.009

Zhang, K., Foster, H. E., Rondelet, A., Lacey, S. E., Bahi-Buisson, N., Bird, A. W., & Carter, A. P. (2017). Cryo-EM Reveals How Human Cytoplasmic Dynein Is Auto-inhibited and Activated. *Cell*, *169*(7), 1303-1314.e18. https://doi.org/10.1016/j.cell.2017.05.025

Appendix A: Supplementary Material for Chapter 6

Supplementary Figure 1: Basal Forebrain Cholinergic Neurons (BFCNs) Transfected With Rab5-GFP

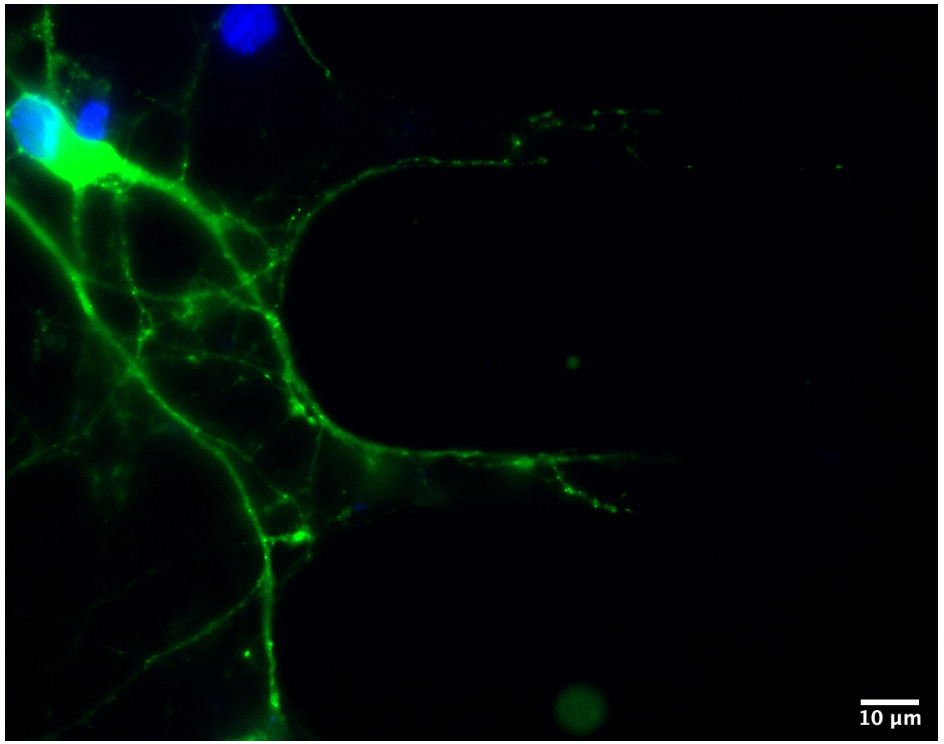

Basal Forebrain Cholinergic Neurons (BFCNs) Transfected With Rab5-GFP. BFCNs transfected with a baculoviral vector containing a Rab5-GFP fusion construct downstream of a cytomegalovirus (CMV) mammalian promoter. Transfected BFCNs express Rab5-GFP at adequate levels for detection with fluorescence microscopy and are robust enough to extend axons within the microgrooves of microfluidic chambers. Rab5-GFP expression within axons is detectable in axonal projections within the microgrooves.